2020

An Investigation into the Application of Raman Spectroscopy for Cervical Cancer Screening

Damien Traynor
Technological University Dublin

An investigation into the application of Raman Spectroscopy for cervical cancer screening

Damien Traynor (B.Sc)

Radiation and Environmental Science Centre (RESC)

School of Physics & Clinical & Optometric Sciences

Technological University Dublin

May 2019

Supervisor: Fiona Lyng

Abstract: An investigation into the application of Raman Spectroscopy for cervical cancer screening

Raman spectroscopy is a powerful tool that has the potential to be, used for cervical cancer screening. It is a label-free, low-cost method providing a biochemical fingerprint of a given sample. The objective of this thesis was to address issues associated with the application of Raman spectroscopy for cervical cancer screening and to demonstrate the potential for triage of HPV positive cases.

The first study investigated hormonal effects due to the menstrual cycle, the use of hormone-based contraceptives (HC) and the onset of menopause on Raman spectra of cervical cells and determined if these changes would affect the ability to successfully identify dyskaryotic cells. Spectral changes were observed depending on the day of the menstrual cycle and on the use of HC. Despite this, high grade (HG) dyskaryotic cells could be discriminated from normal cells regardless of the day on which the sample was taken or the use of HC.

The second study aimed to extend previous work on blood contamination of cervical smear samples and to investigate if excessively bloody samples could be rendered suitable for Raman spectroscopy. ThinPrep liquid based cytology (LBC) specimens were treated by adding hydrogen peroxide directly to the vial before slide preparation. Good discrimination between negative and HG cytology could be achieved for samples with no blood contamination (sensitivity 92%, specificity 93%) and heavy blood contamination (sensitivity 89%, specificity 88%) with poorer classification when samples were combined (sensitivity 82%, specificity 87%). The improved potential of Raman spectroscopy for analysis of ThinPrep specimens regardless of blood contamination was shown.

The third study investigated Raman spectroscopy for screening for histologically confirmed cases of CIN using long term biobanked LBC samples. Classification of CIN was compared using Raman spectra from fresh LBC samples and biobanked LBC samples. Raman spectroscopy was found to effectively discriminate negative from CIN 3 fresh and biobanked LBC samples. In addition, it was found that biobanked LBC samples could be combined with fresh LBC samples and still achieve a similar sensitivity and specificity.

The fourth study investigated the ability of Raman spectroscopy as a triage of HPV positive cases to discriminate between latent HPV infections and persistent HPV infections which are clinically more important. The results showed that Raman spectroscopy could distinguish between patients with latent and persistent HPV infections and a sensitivity and specificity of 90% and 100% respectively was achieved for an unknown test set.

Declaration

I certify that this thesis which I now submit for examination, is entirely my own work and has not been taken from the work of others, save and to the extent that such work has been cited and acknowledged within the text of my work.

This thesis was prepared according to the regulations for graduate study by research of the Technological University Dublin and has not been submitted in whole or in part for another award in any other third level institution.

The work reported in this thesis conforms to the principles and requirements of the Technological University Dublin guidelines for ethics in research.

The Dublin Technological University Dublin has permission to keep, lend or copy this thesis in whole or in part, on the condition that any such use of the material of the thesis be duly acknowledged.

Signed_____ Date _____

Acknowledgements

On the very outset of this report, I would like to extend my sincere and heartfelt thanks to my supervisor Prof Fiona Lyng who took a chance and gave me a job 5 years ago and who has also encouraged me to pursue a PhD. Without her guidance, help and encouragement, I would not have made it this far.

I am extremely thankful to all the staff of FOCAS Hugh Byrne, Aidan Meade, Orla Howe and Luke O Neil for their valuable support and guidance in the completion of this project.

I would like to thank my Cerviva colleagues Dr Cara Martin, Prof John O Leary, Dr Christine White, Stephen Reynolds and Dr. Prerna Tewari for all there help with patient requirement and testing.

I am extremely lucky to have many people in my life both inside and out of work who have helped me through this journey. Grace, Sandra, Mam, Dad, Sarah, Alex, Andrew, Amelia, Ian, Karen, Karen, Garreth, Aisling, Brian, Alex, Maikki, Naomi, Ola, Lucie, Dan, Megan, Jamie Tadhg, Conor, Andrea, Giuliana, T.J, Caroline, Isha, Declan, Drishya ,Neha, Fionn, Emma, Agnes, Ken, Christine, Michelle, Jane, Rory, Ulises.

This research was undertaken as part of CERVIVA, the Irish Cervical Screening Research Consortium and we gratefully acknowledge funding from the Health Research Board Collaborative Applied Research Grant, CARG2012/29, and Enterprise Ireland co-funded by the European Regional Development Fund (ERDF) and Ireland's EU Structural Funds Programme 2007–2013, CF2011 1045.

Abbreviations

ASC	Atypical squamous cells
ASC-H	Atypical squamous cells of undetermined significance but high grade changes can't be ruled out
ASC-U	Atypical squamous cells of undetermined significance
CCD	Charged coupled device
CIN	Cervical Intraepithelial Neoplasia
CWIUH	Coombe Women's and Infants University Hospital
DNA	Deoxyribonucleic acid
GDPR	General Data protection Regulation
H_20_2	Hydrogen Peroxide
HC	Hormone based contraceptive
HG	High grade
HPV	Human Papilloma virus
hrHPV	High risk HPV
HSIL	High grade squamous intraepithelial lesion
IMS	Industrial Methylated Spirits
LSIL	Low grade squamous intraepithelial lesion
LBC	Liquid based cervical cytology
LV	Latent variables
mRNA	Messenger ribonucleic acid
NNLS	Non- negative constrained least squares
Pap	Papanicolaou stain
PCR	Polymerase Chain reaction
PLS-DA	Partial least squares discriminate analysis
SIL	Squamous Intraepithelial lesion
STM	Specimens transport media
TN	True negative
TZ	Transformation zone

Contents

List of Tables

List of figures

1 Introduction

1.1 What is Cervical Cancer?

Cellular maturation is a normal part of a cell's life cycle which involves the growth, ageing and death of cells. This process of maturation is controlled by the cell's own genetic makeup. If a mutation occurs within this genetic makeup, control over the cell's maturation can be lost resulting in abnormal growth and a mass of cells known as a tumour (Fouad and Aanei, 2017).

Cervical Cancer is a cancer of the cells of the cervix. It is a slow progressive form of cancer that has three precancerous stages which are currently screened for via the national cervical cancer screening programme (CervicalCheck, 2013). The aim of CervicalCheck is to screen for and prevent the progression of cervical cancer. It does this through a series of molecular and objective based tests.

1.2 The Female Reproductive System

The female reproductive system is made up of the ovaries, fallopian tubes, uterus and vagina (Figure 1.1). The ovaries and fallopian tubes control the production and release of eggs during a women's menstrual cycle. The vagina allows the passage of a baby and receives the penis and sperm during intercourse. The uterus provides mechanical support for a developing foetus and will expel the foetus by forceful contractions of its smooth muscles. Located at the inferior portion of the uterus is the cervix. The cervix is a 2-4 cm long cylinder shaped tissue that connects the vagina and uterus. The cervix itself is made up of the ectocervix and endocerix, where they meet is called the squamous columnar junction. The ectocervix is the outer portion of the cervix and is lined with stratified non-keratinising squamous epithelium and is in continuation with the endocervix at the external os. The external os is the opening in the centre of the ectocervix which connects the vagina to the uterus. The endocervical canal is located within the cervix between the internal os and the external os which contains glandular

epithelium. The squamous columnar junction is where the squamous and glandular epithelium meet between the endocervix and ectocervix (Koss, 2005).

The site of the squamous columnar junction will change during puberty. This junction is a known site of metaplasia. Metaplasia is the transformation of vulnerable glandular epithelium into protective stratified squamous epithelium. Metaplasia occurs due to the glandular epithelium's exposure to the acidic environment of the vagina. The area of metaplasia close to the original position of the squamous columnar junction is known as the transformation zone. More than 90% of premalignant lesions develop in the transformation zone (Koss, 2005)

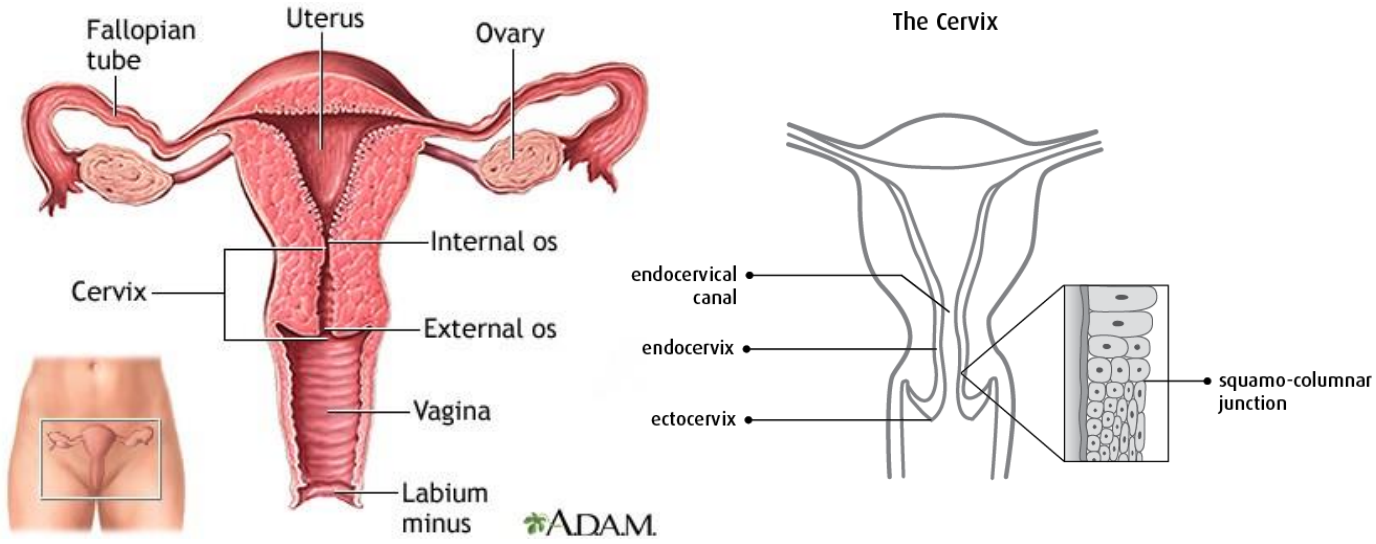

Figure 1.1 Diagram of female reproductive system (*Medlineplus*, 2018)(Canadian Cancer society, 2019)

1.2.1 Stratified squamous epithelium

The stratified squamous epithelium is made up of four cell types, Basal, Parabasal, Intermediate and Superficial cells. Basal cells are immature cells which are parent cells to all cells which make up the epithelium. They are firmly attached to the basement membrane. They are small round cells with oval nuclei, fine chromatin and a high nuclear to cytoplasmic ratio (Figure 1.2 (A)). Parabasal cells lay above the basal cells. Their nuclei occupy about half of the cell's cytoplasm and have a fine chromatin pattern (Figure 1.2 (B)). Intermediate cells are large polygonal cells (Figure 1.2 (C)). They have round to oval vesicular nuclei and have a diameter 2-3 times the size of a Parabasal cell. Superficial cells are large polygonal cells. They have small condensed nuclei, angular cytoplasm and keratohyaline granules (Figure 1.2 (D)) (Koss, 2005).

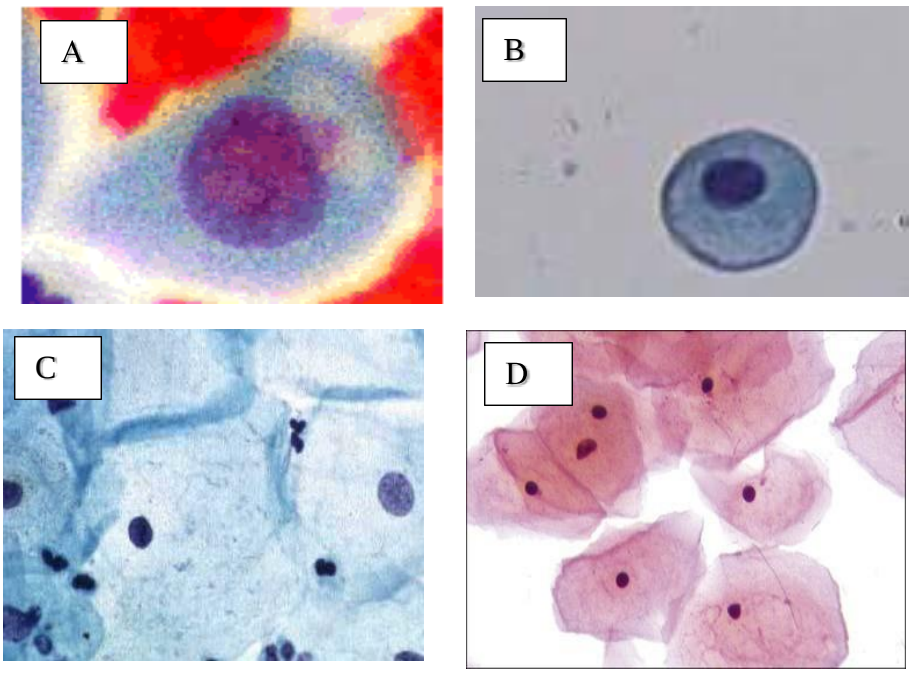

Figure 1.2:Pap stained (A) Basal cell small round cells with oval nuclei, fine chromatin and a high nuclear to cytoplasmic ratio. (B) Small round cells with fine chromatin pattern. (C) Intermediate cells, large polygonal cells which have round to oval vesicular nuclei. (D) Superficial cells, large polygonal cells with a small condensed nuclei, angular cytoplasm and keratohyaline granules (Basicmedicalkey.com, 2016).

1.2.2 The Menstrual cycle

The menstrual cycle (Figure 1.3) is a change that occurs within the female reproductive cycle that makes pregnancy possible (Silverthorn, 2013). It is controlled by the rise and fall of hormones. Each cycle is divided between the ovarian and uterine cycle. The ovarian cycle is made up of the follicular phase, ovulation and luteal phase. The uterine cycle is made up of menstruation, proliferative and secretory phase. The uterine cycle is the most clinically relevant for this study. The proliferative phase averages over 14 days for most women and begins with the start of menstruation. It involves the rapid production of follicle stimulating hormone and luteinizing hormone which stimulate the growth of follicles which in turn produce oestrogen which stimulates the rapid growth of the endometrium. The secretory phase involves the production of progesterone and small amounts of oestrogen which stimulates the shedding of the endometrium if implantation doesn't occur (Boron, 2005).

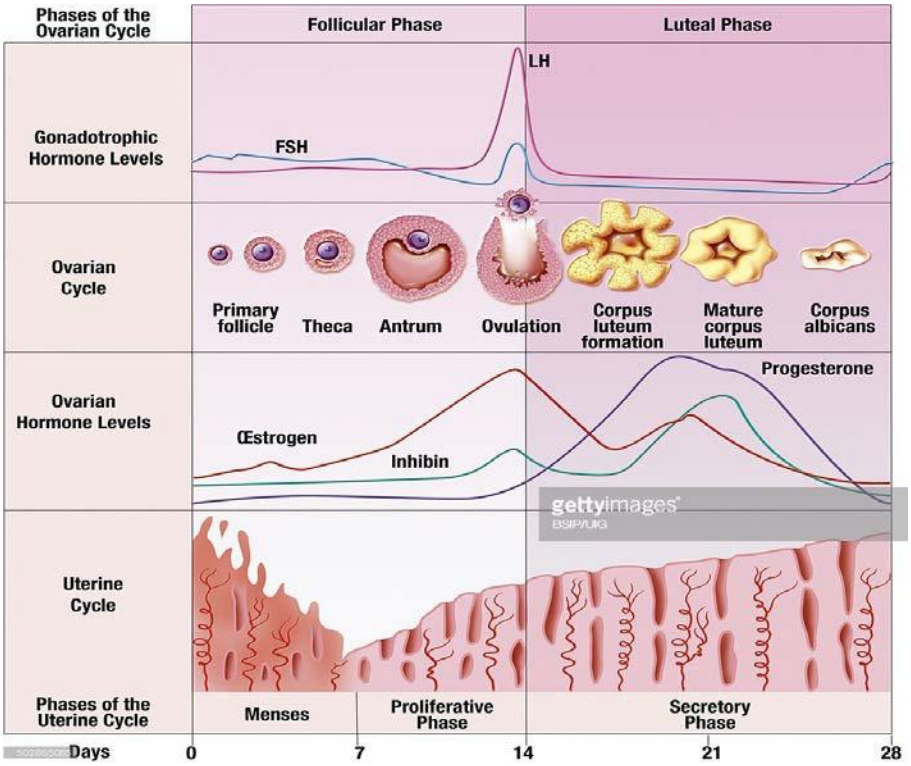

Figure 1.3 Schemmatic illustration of the menstrual cycle over 28 days (Gettyimages, 2018)

1.2.3 Hormonal Contraceptive

Hormonal contraceptive is the most commonly used method of birth control. In the United States over 30% of sexually active women use a form of hormone based contraceptive (HC). There are different forms of contraceptive that are widely available including oestrogen and progesterone based forms and a combination of the two. The contraceptives work by lowering the level of follicle stimulating hormone and luteinizing hormone produced, thereby preventing the growth of the endometrium thus preventing implantation. Progesterone only pills work by causing cervical mucus to thicken thus preventing the sperm penetrating the uterus (Boron, 2005). There is no direct link between the amount of hormone present in the contraceptive and the response of the cervical epithelium. This relationship varies significantly from patient to patient (Koss, 2005)

1.3 Cervical Cancer

There were an estimated 570,000 new cervical cancer cases and 311,000 deaths from cervical cancer worldwide in 2018 (Bray *et al.*, 2018). There are three main types of cervical cancer. Cervical cancer which develops from the squamous epithelium is known as squamous cell carcinoma and accounts for 80-85% of all detected cervical cancers and will be the main topic of this research. Cervical cancer which develops from endocervical cells is known as adenocarcinoma and accounts to approximately 10% to 15% of all invasive cervical cancers (Koss, 2005). Cervical cancer which develops from the ecto or endocervical cells is known as adenosquamous carcinoma and accounts for approx. 3% of all detected cervical cancers (Sahdev, 2010).

1.3.1 Human Papillomavirus

The Human Papillomavirus, is present in 99% of all cervical cancers worldwide and is the main aetiological agent associated with the disease. It is sexually transmitted and affects up to 80% of women at some point in their life (Sahdev, 2010). There are over 100 known HPV types which are classified according to their potential to induce malignant transformations. HPV 16, 18, 31, 35, 39, 45, 50, 51, 53, 55, 56, 58, 59, 64 and 68 are classified as high risk types (Sahdev, 2010). HPV 16 and 18 are found in 70% of all cases of cervical cancer (Sanjosé *et al.*, 2007).

1.3.1.1 HPV Infection

The HPV genome (Figure 1.4) is made up of 8,000 base pairs. It has five early genes E1, E2, E5, E6, E7 and two late genes, L1 and L2 (Fouad and Aanei., 2017). HPV infection is thought to start in the basal layer of cells in the epithelium which it gains access via micro abrasions in the epithelium. The virus first attacks the host cell's DNA where it uses the host cell machinery to transcribe its early genes. Following genome amplification, the virus is maintained in a stable condition via an episome. Viral replication can then begin via the transcription of E1 and E2 (Zheng and Baker, 2006). E1 is responsible for the helicase which allows the E2 viral DNA to bind which results in the helicase binding to the replication associated proteins including DNA polymerase alpha primase. E2 also has a role in the binding of the viral episome to the chromosome undergoing mitosis which allows for segregation of the HPV episome into each progenitor cell (Zheng and Baker, 2006).

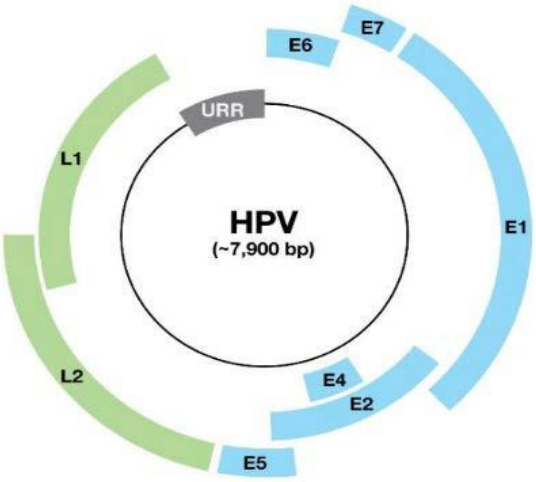

Figure 1.4 Graphical representation of the HPV genome (Semantic Scholar, 2019)

1.3.1.2 Cell Proliferation and Genome Amplification

The increased proliferation of HPV infected cells is a result of the HPV oncogenes E6 and E7 working with E1 and E2. Together these proteins stimulate the progression of the infected cells into the S-phase of its life cycle (Zheng and Baker, 2006). This method of progression is first controlled by E7 which involves the binding and degradation of the retinoblastoma protein (pRb). Under normal conditions the role of pRb is to control the expression of proteins that are required for cell cycle progression. The degradation of pRb results in the release of E2F. E2F is then free to recruit proteins for viral replication and cellular proteins cyclin A and E which control S-phase progression. The role of E6 is to degrade the tumour suppressor protein P53 which is overly produced due to the function of E7. Under normal conditions P53 acts as a regulator of the cell cycle that triggers growth arrest or apoptosis to prevent the replication of damaged DNA. The lack of P53 due to E6 results in the replication of damaged DNA. The complete HPV life cycle involves the expression of both minor and major coat proteins which allow genome packaging. This involves a change in splice site usage which results in a switch from the production from E1^E4, E5 mRNA to E1^E4, L1 transcript which facilities the end of genome amplification and gives way to genome packaging (Johansson , *et al*.,2012, Doorbar .,2005, Milligan *et al.,2007*). Encapsidation of the genome requires the accumulation of E2 and the collection of infectious virions in the nucleus. Virus maturation is then free to occur in superficial cells, which is triggered by a

change from a reducing to an oxidizing environment within the cell (Doorbar .,2005). This change enables the accumulation of disulphide bonds between L1 proteins resulting in the production of infectious HPV virions (Holmgren , *et al*,2005).

1.3.1.3 Possible Outcomes of a HPV infection

HPV DNA can be detected in the epithelial tissues due to its presence as virus particles on the surface of the epithelium. This detection can be misinterpreted as HPV latency. To cause a lesion or to initiate a latent infection, the virus particles have to gain access to the epithelial basal cells at a sufficiently high level. Each type of virus has a specific epithelial site where it can initiate a productive life cycle, as well as sites where the virus entry occurs in the absence of lesion formation. At low titres or at non permissive epithelial sites an asymptomatic infection can occur, in which viral genomes may exist in the basal layer without gene expression or lesion formation. This is a form of latency as it does not trigger an immune response. Certain high risk HPV types at a particular epithelial site can deregulate viral gene expression which has the potential to lead to neoplasia. Persistent high risk HPV infections can lead to the accumulation of genetic errors and the progression to cancer (Zheng and Baker, 2006, Youssef *et al.*, 2016)

1.3.1.4 Persistence

If a HPV infection is not cleared by the host immune system, it can persist over many years resulting in intermittent or constant disease. In order for a persistent infection to occur, HPV must maintain the viral genome in the epithelial stem cell and the host immune system must fail to recognise it and clear the infection (Doorbar *et al.*, 2012).

1.3.1.5 Regression

Persistent infection with high risk HPV is necessary but not sufficient for the development of squamous carcinoma of the cervix or its precursor lesions CIN 1, 2, 3. A CIN 1 lesion represents a chronic HPV infection, in which HPV DNA is episomal and intact viron production and shedding is occurring. In women who are immune competent, many CIN 1 lesions (up to 58% over 24 months) will eventually regress without treatment (Burd, 2003). Only 2% will progress to high grade lesions. High grade lesions are less likely to regress. The risk for progression to invasive cancer at 24 months in women with high–grade lesions is 1-2%. However CIN 1 and CIN 2 regression rates vary due to the subjectivity involved in their diagnosis (Rodriguez *et al.*, 2012). The main reason for over treatment of patients remains the lack of a diagnostic test to directly identify lesions that are likely to progress or regress.

1.4 Cervical Screening

CervicalCheck is the national cervical screening programme for Ireland. It provides a free cervical smear for all eligible women (1.1 million) between the ages of 25 and 60. The purpose of screening is to reduce the incidence and mortality of cervical cancer (CervicalCheck, 2013).

There are four current screening/diagnostic tests currently in use by CervicalCheck for cervical cancer:

1) Papanicolaou test
2) HPV test
3) Colposcopy
4) Histopathology

1.4.1 The Papanicolaou Test

The Papanicolaou test (Pap test) is named after its inventor George Papanicolaou. Papanicolaou's work in cytology involving the female genital tract helped cytology diagnosis gain credibility (Koss, 2005). Since it was introduced in hospitals in the 1940's the Pap test has become the most commonly used method for identifying cervical cancer and its associated pre-cancerous lesions.

Within the last 10 to 15 years conventional cytology has been replaced by liquid based cytology (LBC) such as ThinPrep or SurePath. Conventional cytology and LBC both share them same method of sampling cells from the transformation zone of the cervix with a cervical brush or spatula. In the case of conventional smears, the cells are directly spread onto a glass slide, fixed and stained. In the case of LBC, the cervical brush in rinsed in a vial of preservative fluid and transferred to the lab where a uniform layer of cells on a glass slide is prepared and then fixed and stained (Rozemeijer *et al.,* 2016). The LBC method improves sample quality by producing a more even layer of cells and helps remove unwanted cellular

material such as red blood cells and inflammatory cells (leukocytes). Specimen vials can also be stored allowing an additional smear to be made if necessary and ancillary techniques to be performed on the same sample. The Pap smear generally has a specificity of 96.5% but its sensitivity can vary from 30-85% depending on the prevalence of the disease within the population (Nanda *et al*., 2000). Thinprep (Figure 1.5) is the preferred method of sample processing employed throughout Ireland, hence all samples used in this study will only be processed using the ThinPrep method.

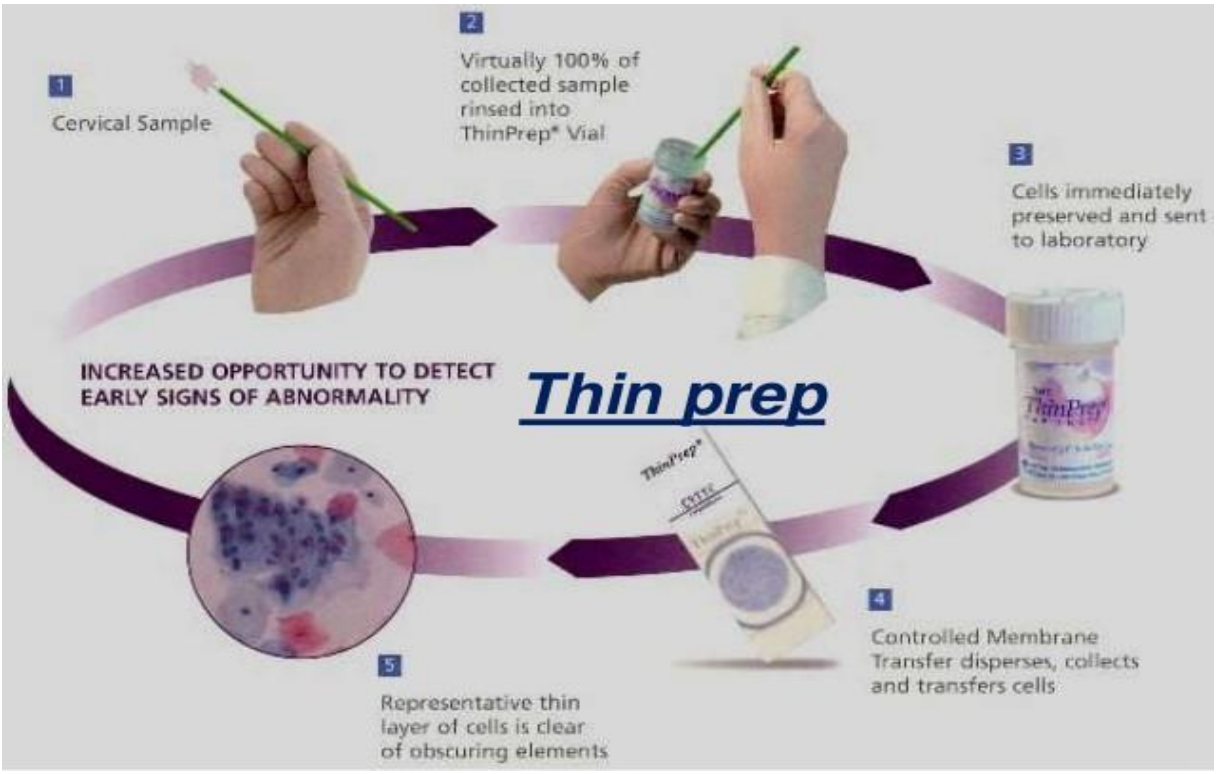

Figure 1.5 Illustration of Thinprep process of sample collection and processing (HeakthDxs,2017)

1.4.1.1 Cytology

Cytology is the study of the microscopic appearance of cells. Cytologists are trained to identify the type of cells that are normally present in different areas of the body. The cells are then screened to detect either changes in the morphology of the cells or the presence of inappropriate cells that are associated with particular conditions.

1.4.1.2 Bethesda Classification for Cytology

CervicalCheck employs the Bethesda Classification system for its terminology of squamous intraepithelial lesions (SIL). This is divided into three categories:

1) Low grade SIL (LSIL) which includes HPV- associated cellular changes and mild dyskaryosis.
2) High grade SIL (HSIL) which includes moderate dyskaryosis and severe dyskaryosis
3) Query squamous cell carcinoma

Cytological changes in squamous cells which are not normal and do not fit the criteria for SIL are classed as atypical squamous cells (ASC). ASC is divided into two subcategories:

1) ASC-US Atypical Squamous cells of undetermined significance.
2) ASC-H Atypical Squamous cells of undetermined significance but high grade changes cannot be ruled out (CervicalCheck 2013).

1.4.1.3 Low grade (LSIL)

The cytological features of LSIL (Figure 1.6) are:

- Abnormal/irregular chromatin pattern
- Irregular nuclear membrane
- Irregular nuclear contours
- Nuclear enlargement
- Hyperchromasia
- Hypochromasia
- Multi-nucleation
- Seen in Intermediate and Superficial cells
- Often seen with Koilocytic changes
- Features correspond to changes in CIN 1
- Nuclear to cytoplasmic ration

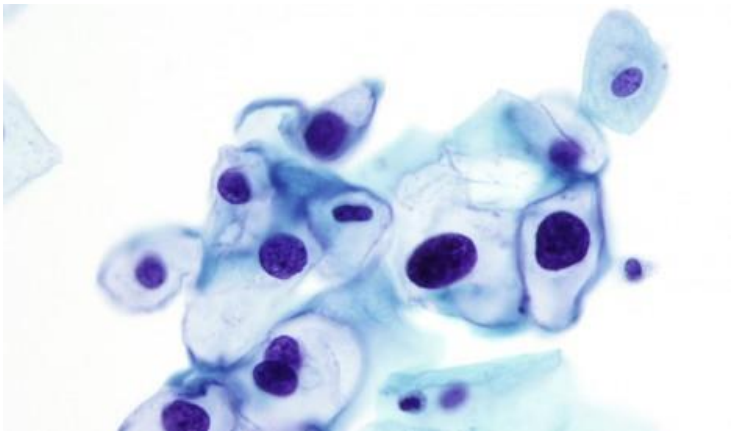

Figure 1.6 Cytological representation of LSIL on Pap smear (CPLmag.com, 2019)

1.4.1.4 High grade (HSIL)

The cytological features of HSIL (Figure 1.7) are:

- Nuclear enlargement
- An increase in the nuclear to cytoplasmic ratio
- Abnormal nuclear morphology
- Nuclear contours
- Seen in immature cells – parabasal and metaplastic

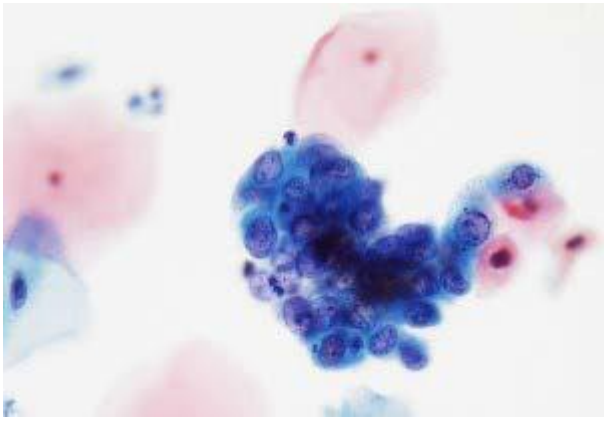

Figure 1.7 Cytological features of HSIL on Pap smear (CPLmag.com, 2019)

1.4.1.5 Squamous Cell Carcinoma

The cytological features of Squamous Cell Carcinoma (Figure 1.8) are:

- Windowing- irregular chromatin distributed causing holes
- Fibre/tadpole/ bizarre cells
- Keratinisation
- Diathesis
- Blood

Invasive squamous cell carcinoma can't be diagnosed on cervical cytology, but these features can suggest invasion.

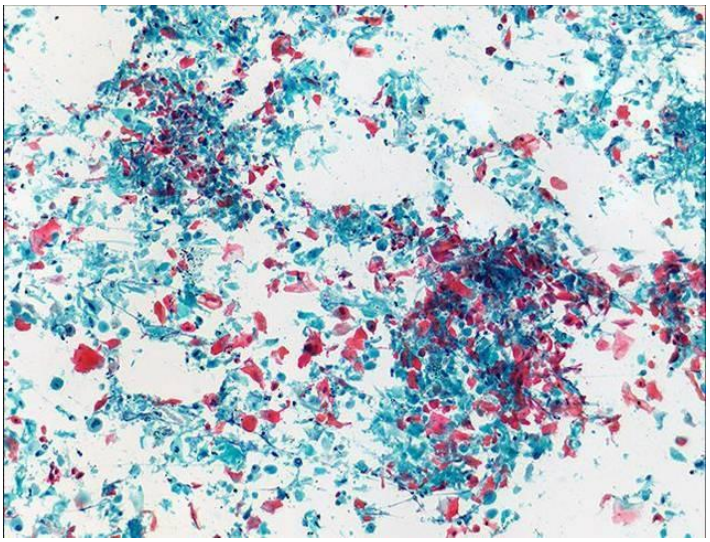

Figure 1.8 Cytological features of Squamous Cell Carcinoma on Pap smear (eurocytology.eu, 2019)

1.4.1.6 Inflammation Vs Dyskaryosis

Cells are susceptible to injury. The response of tissues or cells to injury is known as inflammation. When inflammation occurs in the cervix the condition is called cervicitis (Figure 1.9). Inflammatory smears usually contain abundant polymorphs and histiocytes. If the inflammation persists lymphocytes, plasma cells and multinucleated histiocytes may be seen. A dirty background may be seen. Epithelial cells are not involved in the process of inflammation but they do react to it via a process of degeneration and regeneration (Shambayati.,2011)

Nuclear changes associated with inflammation are:

- Wrinkling of nuclear membrane
- Condensation of chromatin
- Nuclear death
- Nuclear enlargement
- Course but regular granulation of chromatin
- Prominent nucleoli
- Multi-nucleation

Cytoplasmic changes associated with inflammation are:

- Vacuolisation
- Perinuclear halo
- Altered staining pattern
- Dense cytoplasm
- Cytoplasmic projections

There are many cytological similarities between inflammation and dyskaryosis. However, dyskaryosis will usually show coarse chromatin granularity with uneven distribution and irregular nuclear membranes with contours. The causes of inflammation can vary but could be related to the use of intrauterine devices, radiation, cytotoxic drugs, hormones or infection (Shambayati., 2011).

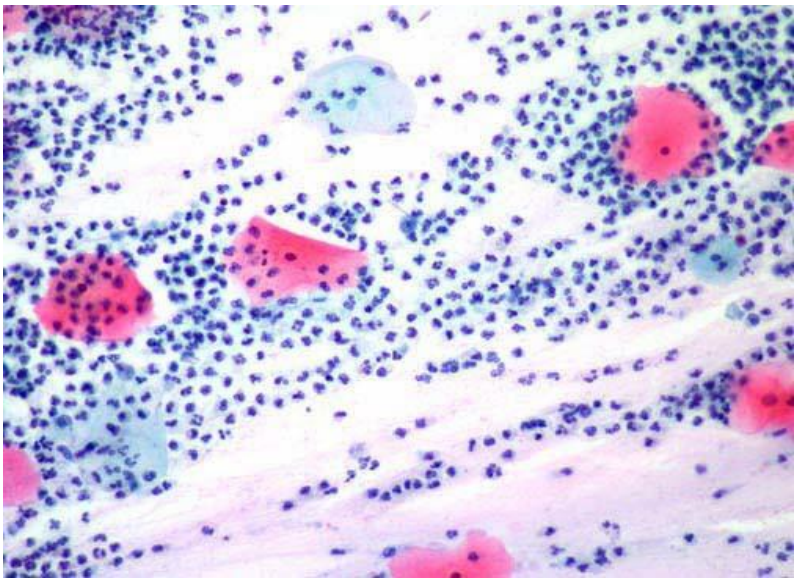

Figure 1.9 The cytological presentation of cervicitis on Pap smear. Note the high level of polymorphs (General cytopathology, 2016)

1.4.2 HPV Testing

HPV testing has been incorporated in most cervical cancer screening programmes and can be applied in three ways

1. Primary screening
2. Management and triage
3. Test of cure

At present HPV testing is currently only being used by Cervical Check as a triage test for Pap smears graded as LSIL on cytology and as a test of cure following treatment at colposcopy. HPV testing will be discussed in more detail in the section on current screening practice (section 1.1.31).

1.4.3 Colposcopy

As of 2013 there are currently 15 colposcopy services available as part of CervicalCheck.

Women can be referred to colposcopy for a number of reasons:

- Abnormal vaginal bleeding
- Suspicious cervix
- Abnormal cytology referral
- HPV result

The CervicalCheck guidelines (CervicalCheck, 2013) state that 90% of women with a high grade cytological abnormality should be offered an appointment for colposcopy within four weeks of the result being issued. All women with low grade cytological abnormalities should be offered an appointment within eight weeks.

1.4.3.5 Diagnosis at Colposcopy

Colposcopy plays an important role in the evaluation of women with suspected cervical abnormalities. It allows the identification of the site of the abnormality as well as an estimation of the grade of abnormality including the presence or absence of features which are suggestive of invasive cancer. As a procedure used alone however, it has diagnostic limitations with a lack of correlation between the colposcopic and histological diagnosis, lack of reproducibility and difficulties in assuring the optimum site (transformation zone) and the quality of any biopsies taken (Powers, 2011).

1.4.3.6 Colposcopy Process

A speculum is used to spread apart the walls of the vagina before dilute acetic acid is applied to the cervix under direct vision (Figure 1.10). The diagnosis is made using visual recognition. The acetic acid interacts with the cell's protein structure. Abnormal tissue will show up as a white area (Figure 1.11). The intensity of the colour change as well as the sharpness of the margins helps discriminate between grades of abnormality. (low or high grade). New blood vessel formation often accompanies high grade on the cervix. Invasive cancer often presents with abnormal blood vessel formation (CervicalCheck, 2013) A review of colposcopy services demonstrated sensitivity and specificity levels for discrimination between high and low grades of disease to be 96% and 48% respectively (CervicalCheck, 2013). The performance of colposcopy increases with the severity of the lesion. However a study showed that colposcopy had a detection accuracy of only 52% for high grade lesions (Zuchna *et al.*, 2010) which confirms that some lesions may be difficult to detect and highlights the risk of a false-negative biopsy result. When compared to the identification of glandular lesions at colposcopy the sensitivity of colposcopy for glandular lesions drops to 9.8% (Ullal.A et al., 2009) which again highlights the difficulty in identifying areas of abnormality.

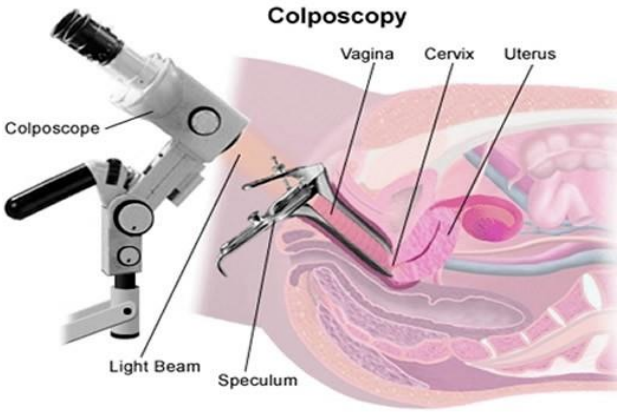

Figure 1.10 A graphical representation of the Colposcopy process (manhattancenterforgynecology, 2019)

Figure 1.11 (A) Visual appearance of a normal cervix. (B) visual appearance of CIN 1 after the application of acetic acid to the cervix (Shekinah Medical Centre, 2017)

1.4.3.7 Biopsy Methods

A histological diagnosis can be obtained by taking one or more diagnostic punch biopsies using a tissue sampling forceps, small loop biopsy or by complete removal of the atypical area using an excisional biopsy via a large loop excision of the transformation zone (LLETZ) (Figure 1.12). The aim when taking a biopsy is to sample an area which is indicative of the most abnormal area of cervical tissue to provide confirmation of the colposcopic impression. The accuracy of the biopsy is dependent on the target site chosen by the colposcopist. There are two types of biopsy that can be taken during colposcopy - punch or cone biopsy. Punch biopsies are small pieces of tissue a few millimetres in diameter that are removed from the cervical mucosa. Cone biopsies/excision biopsies are made up of cone shaped portions if cervical tissue and taken with the aim of removing all the pathological tissue on the cervix. This is both diagnostic and therapeutic (Bulten *et al.*, 2011).

There are certain situations where a diagnostic biopsy must be performed:

- If the cytology shows HSIL.
- If there is evidence of significant atypia (irregularity) on the transformation zone.
- If there is a completely visible normal TZ and confirmed low grade cytological abnormality.

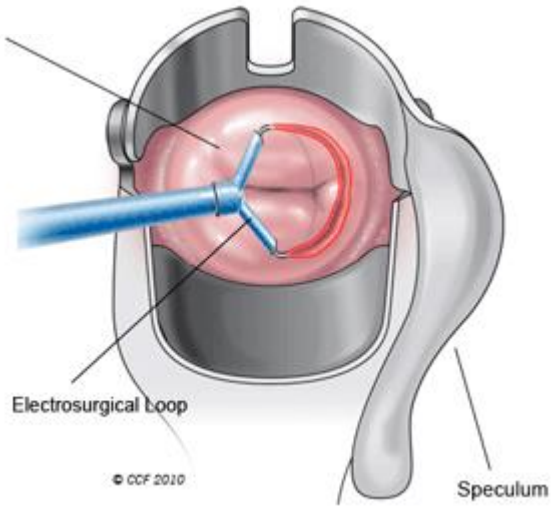

Figure 1.12 Graphical representation of Large loop excision of the transformation zone (LLETZ) process of biopsy collection(Clinic, 2014)

1.4.4 Histopathology Examination

Histopathology refers to the examination of stained tissue sections under a microscope for the presence of abnormality. It is referred to as the gold standard in cancer diagnosis. Once a biopsy is taken it is immediately placed into a fixative and processed into a paraffin wax block. Sections from this block are then cut, placed on to a glass slide, stained and reviewed under a light microscope by a pathologist. The terminology for reporting disease in histopathololology is cervical intraepithelial neoplasia (CIN) rather than SIL which is used for cytology.

A judgement of whether or not a cervical tissue specimen reveals CIN, and to what degree, is dependent on the histological features concerned with differentiation, maturation and

stratification of cells and nuclear abnormalities. The proportion of the thickness of the epithelium showing mature and differentiated cells is used for grading CIN. More severe degrees of CIN are likely to have a greater proportion of the thickness of epithelium composed of undifferentiated cells, with only a narrow layer of mature, differentiated cells on the surface.

Nuclear abnormalities such as enlarged nuclei, increased nuclear-cytoplasmic ratio, and increased intensity of nuclear staining (hyperchromasia), nuclear polymorphism and variation in nuclear size (anisokaryosis) are assessed when a diagnosis is being made. There is often a strong correlation between the proportion of epithelium revealing maturation and the degree of nuclear abnormality. As the severity of CIN increases, the number of mitotic figures also increases; these may be seen in the superficial layers of the epithelium. The less differentiation in an epithelium, the higher the level at which mitotic figures are likely to be seen (Bulten *et al.*, 2011).

1.4.4.5 CIN histological features

In CIN 1 there is good maturation with minimal nuclear abnormalities and few mitotic figures, undifferentiated cells are confined to the deeper layers (lower third) of the epithelium. Cytopathic changes due to HPV infection may be observed in the full thickness of the epithelium (Figure 1.13(A)). CIN 2 is characterized by dysplastic cellular changes mostly restricted to the lower half or the lower two-thirds of the epithelium, with more marked nuclear abnormalities than in CIN1. Mitotic figures may be seen throughout the lower half of the epithelium (Figure 1.13(B)). In CIN 3 differentiation and stratification may be totally absent or present only in the superficial quarter of the epithelium with numerous abnormal mitotic figures. Nuclear abnormalities extend throughout the thickness of the epithelium.

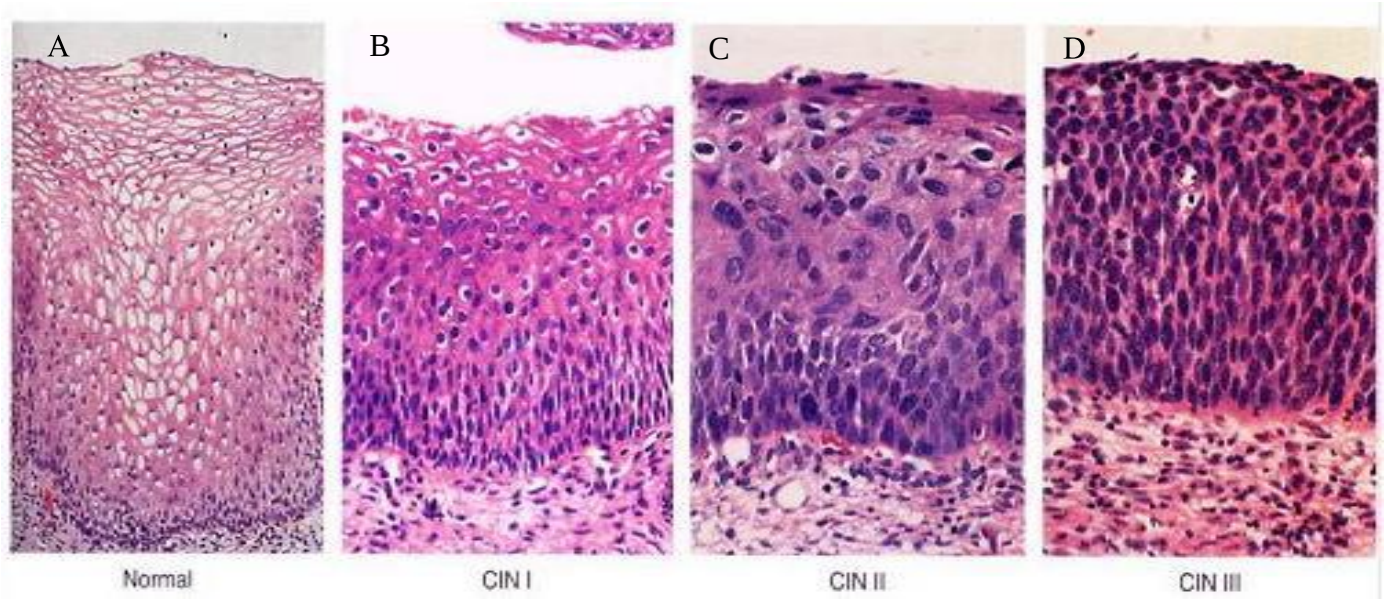

Figure 1.13 Histological representation of normal (A),CIN I (B), CIN II (C), and CIN III (D) of H&E stained cervical tissue (Medicoapps.org ,2019)

1.4.4.6 Principles of treatment

Not all women who attend colposcopy will require treatment. If the colposcopist is able to identify a high grade lesion and can clearly identify its limits, then immediate treatment is possible. This is known as a see and treat approach (CervicalCheck, 2013). If the colposcopist assessment or biopsy reports a low grade lesion then the decision to treat is a clinical one. Treatment is not mandatory in such cases. The colposcopist will make a decision based on the likelihood that the lesion will regress, the age of the patient and if the patient is willing to return for future appointments.

The aim of treating a CIN lesion is to remove the whole of the transformation zone to prevent the development of invasive disease. There are different methods available. Options include laser or cryotherapy (ablation) or diagnostic excision. Laser treatment uses a high energy beam of light to heat the intracellular water of the target cells, thus killing them. Cryotherapy works by freezing target cells resulting in irreversible cellular damage and death. LLETZ treatment works by cutting away the whole of the transformation zone with a wire loop that has been heated (Shambayati, 2011). All have similar treatment outcomes for the eradication

of CIN. Physical risks associated with colposcopy include lower abdominal pain, cramps, fainting and vaginal discharge (Sankaranarayanan *et al*., 2003).

1.4.4.7 False positives and unnecessary referral to colposcopy

From the 1st of September 2012 to the 31st of August 2013 in Ireland, 702 patients were referred to colposcopy based on an ASCUS cytology result, 146 based on an ASC-H and 799 based on a LSIL result, all of which were reported as having a negative biopsy after colposcopy (CervicalCheck, 2013). The colposcopic biopsy is regarded as the gold standard on which a final result will be issued. However histological examination is by no means perfect. Arbyn *et al.* (2007) reported that factors related to colposcopy biopsy, sampling and interpretation errors were the most common cause of discrepancy between the cytology result and the corresponding histology result. Zuchna *et al.(*2010) found that the sensitivity of colposcopic-directed biopsy for the detection of CIN 2 was 52%, which confirms that many lesions may be difficult to detect. Another possible source of error that could account for the high volume of negative biopsies could be the number of false positive HPV DNA results. If the HPV infection is newly acquired the infection will likely resolve in the first 6 months (Adams *et al.*, 2006).

1.4.5 Risk of Psychological Harm

For women, the receipt of an abnormal smear test frequently leads to a higher level of anxiety (Gray *et al.*, 2006). Often a result of an abnormal smear leads to fear on the part of the women that she has cancer. Gray *et al.* (2006) reported a high prevalence of anxiety among women with a low grade smear despite attempts to improve the way abnormal smear results are communicated. They determined that those who are at the highest risk of anxiety tend to be younger, have children, be smokers and have a high level of physical activity.

1.4.6 Vaccination

There are two clinical approaches for the prevention of cervical cancer. The first is mass screening and treatment for pre-cancer, the second approach is vaccination to prevent infection of HPV. In 2010, two licensed HPV vaccines became available in Ireland, Cervarix and Gardasil. Cervarix is a bivalent vaccine against HPV types 16, 18 while Gardasil is a quadrivalent vaccine against HPV 6, 11, 16, 18. The efficacy of the HPV vaccine has been demonstrated in multiple studies (Baldur-Felskov *et al.*, 2014, Munoz *et al.*, 2010, Adams *et al.*, 2006, Garland *et al.*, 2016). All have shown a significant reduction in the rate of high grade histological abnormalities. Vaccination is a preventive approach as it is used with the intention of preventing HPV infection from occurring. Given the link between HPV and developing cervical cancer, women who have been vaccinated will have a reduced risk of developing the disease, however these women will still have to be screened, as vaccination does not cover all forms of the virus and may not be effective for women exposed to the virus prior to vaccination (Garland *et al.*, 2016).

1.4.7 Current and future screening practice

Liquid based cytology (LBC) was introduced in the 1990's as a means of replacing conventional cytology to improve cytology test performance. A LBC sample will be sent to the lab where it will be processed using either the Thinprep or Surepath™ methods. These two methods while similar involve different sample processing techniques. Thinprep uses a cell filtration system to remove unwanted cells (red and white blood cells). Surepath™ uses a density gradient centrifugation to remove unwanted cells. Both result in a circular monolayer of cells on a glass slide. In 2008 automated image analysis was introduced which allowed cytologist to be shown an area of interest on the slide that most likely contained abnormal cells. This resulted in a quick screening time for each sample and a reduced detection error (Arbyn *et al*., 2008).

In 2012 HPV testing was introduced by CervicalCheck as a test of cure following treatment at colposcopy. There are over 100 different types of HPV, 12 of which have been identified as carcinogenic and associated with a higher risk of progression to malignancy. The HPV virus/genome can be identified in exfoliated cells which allows for HPV testing to be performed on LBC samples. There are two common methods employed for HPV testing. The first is a nucleic acid amplification method and the second is a signal amplification method. Nucleic acid amplification involves the targeting and amplification of a particular HPV gene. Signal amplification involves the use of RNA probes to hybridise viral DNA. These RNA/DNA hybrids are then identified by a secondary structure. The Hybrid Capture 2 (HC2) HPV DNA assay from Qiagen was the first HPV test to become commercially available. It can identify 13 HPV types (16, 18, 31, 33, 35, 39, 45, 51, 52, 56, 58, 59 and 68) (Wong *et al.*, 2012). The Aptima E6 and E7 mRNA HPV test employs nucleic acid sequence base amplification for E6 and E7 viral oncoproteins. The over expression of E6 and E7 mRNA is associated with increased severity of disease (Haedicke *et al.*, 2016). While these two tests can provide information on the patient's HPV status they do not provide information on which types of HPV are present. The ability to identify which type of HPV is present allows for further risk stratification in HPV positive patients due to the risk posed by the various types of HPV. HPV 16 and 18 are associated with a higher risk of developing disease (Garland *et al.*, 2016). The Roche Cobas 4800 HPV test is specifically designed to identify HPV 16 and 18 while also detecting the presence of HPV 31, 33, 35, 39, 45, 51, 52, 56, 58, 59, 66 and 68 (Poljak *et al.*, 2016).

In 2015 HPV testing was utilised by CervicalCheck as part of a triage when low grade cytological abnormalities were detected on primary liquid based cytology screening. Women who present with LSIL but who are negative for HPV are at a very low risk of developing cervical cancer within the next 5 years and should return to routine screening. Women with

HSIL are at a higher risk of developing the disease and would be directly referred to colposcopy. The HPV test that has recently been introduced into the screening programme has high sensitivity values but low specificity values (Cobas test, 95.2% sensitivity, 24% specificity (Dillner *et al.*, 2008, Rozemeijer *et al.*, 2016)). The high sensitivity has led to HPV testing being considered as a primary screening replacement for cytology. Despite this high sensitivity there remains a low specificity as HPV is widespread in under 35 year olds. While the HPV DNA tests currently available as part of a screening programme can indicate the presence and specific genotype of HPV they cannot distinguish between the transient and acute infection of minor clinical relevance and a transforming infection which is clinically more significant. If used as a primary screening tool, HPV DNA testing could result in a high proportion of women being unnecessarily being referred to colposcopy.

Molecular biomarkers have the potential to be used for the management of women who test positive for HPV. $P16^{INK4a}$ is seen as a biomarker that could be used to identify a transforming infection. The activation of E6 and E7 can be detected indirectly by the accumulation of $P16^{INK4a}$ protein within the exfoliated cells. $P16^{INK4a}$ is not currently being used as part of any screening programme, however it does have the potential to be used as a primary screening test, in combination with or as a replacement for other triage tests (HPV testing). A recent study (Garland *et al.*, 2016) reported sensitivity rates based on initial pathologist reviews of 76.4% to 80.01%.

1.4.7.5 Triage Tests

The aim of a primary screening test is to identify patients most at risk, not to provide a diagnosis. At present the Pap test is the primary screening test followed by HPV testing followed by diagnosis on histology. Most of these tests are still subjective and a result is largely based on who is screening the sample. There are plans to adopt HPV testing as the primary screening method to identify patients most at risk. However, the identification of HPV does not correlate with the presence of disease as the infection is often transient. The application of primary HPV screening will require a high sensitivity for the detection of all high risk HPV types which will result in a reduction in specificity as it will include all the weaker carcinogenic HPV genotypes thus increasing the burden of hrHPV positive women needing follow up (Arbyn et al.,2009). To address this, additional triage tests are still required.

The use of cytology as a triage test is one possibility. Cytology has proven itself to be an effective primary screening method for cervical cancer with a specificity of 96.5% but a sensitivity of between 30- 85% (Nanda *et al*., 2000)

Biomarkers which are widely expressed in transforming infections could be used as a triage test. The PALMS study conducted a large scale clinical trial to assess whether p16/ki-67 dual stained cytology could provide high sensitivity for CIN2+ in screening while maintaining high specificity. The report concluded that p16/ki-67 dual-stained cytology had superior sensitivity and non-inferior specificity over the Pap test for the detection of CIN2+ and could help with the limitations for primary HPV screening (Ikenberg *et al.*, 2013).

Other methods based on optical spectroscopy could represent a new approach for cervical cancer screening and this is the main topic of this PhD thesis.

1.5 Vibrational Spectroscopic techniques

Vibrational spectroscopic techniques are potential tools for the non-invasive, label free investigation of biological samples at a molecular level (Bellisola *et al*., 2012,Downes et al., 2010). Vibrational spectroscopy is a fast developing discipline that is showing a strong potential in the field of cervical cancer screening and was first proposed by Wong *et al.* (1991). Vibrational spectroscopy (FTIR and Raman) analyses vibrations within a molecule; these vibrations are characteristic of the molecular structure, resulting in a spectroscopic fingerprint (Lyng *et al.*, 2015).

1.5.1 Raman Spectroscopy

Raman spectroscopy was named in honour of its inventor C.V. Raman along with K.S. Krishnan. Raman spectroscopy is based on the Raman Effect/ Raman scattering which is used to detect and measure the presence of certain molecules. Raman scattering occurs when the vibrational state of a molecule is changed after its interaction with a photon which results in a change in the frequency of the photon. Raman scattering can be further broken down into two types Stokes and anti-Stokes Raman scattering (Figure 1.14)

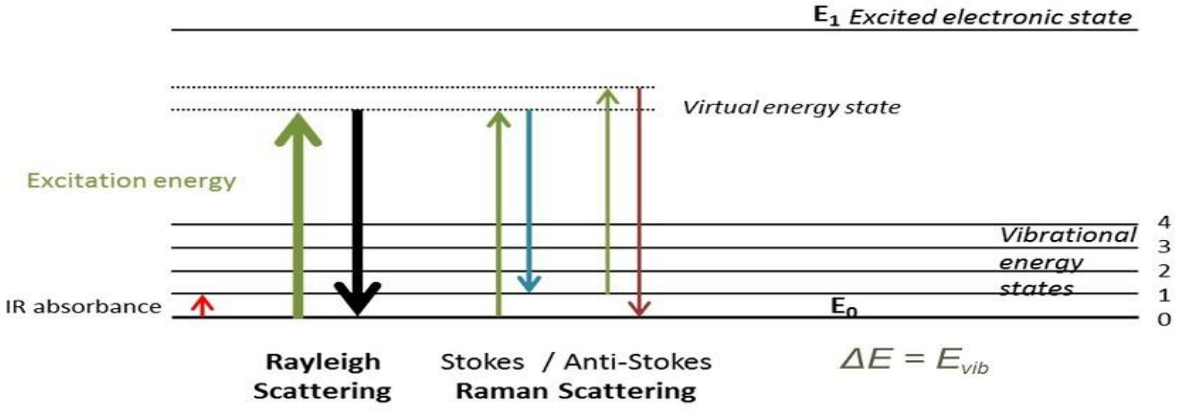

Figure 1.14 Jablonski diagram showing the change in vibrational energy of a molecule upon interaction with a photon. In Rayleigh scattering, the predominate form of light scattering, the electrons are excited to a virtual state before returning to the original vibrational energy level. In Stokes and Anti-Stokes Raman scattering, the electrons are excited to a virtual energy state, before returning to a higher and lower energy state (with respect to the original energy state) respectively (Biomed.tamu.edu. 2016)

In order for Stokes scattering to occur a molecule needs to be excited to a virtual energy level that comprises a distortion of an electron cloud so when it then returns to the first excited vibrational state, a photon with a lower energy (longer wavelength) is emitted. The energy difference between the incident and emitted photon excite the molecule to a higher vibrational state (Gauglitz et al. 2003; Ball 2001).

In anti-Stokes scattering the molecule is in a higher vibrational energy level so when subsequently excited to a virtual energy level, relaxes, and returns to the ground vibrational state. In this case, the energy difference between emitted and excited photon is converted to radiant energy and a vibrational quantum has been annihilated (Gauglitz et al. 2003; Ball 2001).

For a molecular vibration to be Raman active, a change in net molecular polarizability must occur. The polarizability (α) represents the ability of an applied electric field, *E*, to induce a dipole moment, μ_0, in an atom or molecule; a process represented mathematically by the equations below (Ball 2001):

$$\mu_o = \alpha E$$

Equation 1.1 Dipole moment.

At the molecule's nuclear geometry equilibrium the polarizability has a value, α_0. In case of displacement, Δr, away from the molecule's equilibrium geometry, the instantaneous polarization α is given by:

$$\alpha = \alpha_o + \left[\frac{\partial \alpha}{\partial r}\right] \Delta r$$

Equation 1.2 Instantaneous polarization at equilibrium displacement where $\left[\frac{\partial \alpha}{\partial r}\right]$ represents the change in polarizability as a function of displacement.

If the molecule is vibrating in a sinusoidal fashion, Δr can be written as a sinusoidal function in terms of the frequency of the vibration, ν_s, and the time, t:

$$\Delta rr = r_{mmmmm}\ ccccc(2\pi\pi\pi\pi\pi)$$

Equation 1.3 Equilibrium displacement when the molecule vibrates in a sinusoidal fashion where r_{max} is the maximum vibrational amplitude.

Light of a particular frequency, ν_o, has an associated electric field, E, which also has sinusoidal behaviour:

$$E = E_{\max} \cos\left(2\pi \nu_0 t\right)$$

Equation 1.4 Electric field where E_{max} is the maximum electric field frequency.

Equations 1.1 to 1.4 can thus be written into equation 1.5 so that the first term represents the scattered phenomenon of a photon with the same intensity as the incident photon – Rayleigh scattering. The second term represents the Raman scattering of frequency $\nu_0+\nu_s$ (anti-Stokes scattering) when the frequency of the scattered photon increases by molecular motion, ν_s; and $\nu_0-\nu_s$ (Stokes scattering) when the frequency decreases.

$$\mu_0 = \alpha_0 E_{0\,max} \cos(2\pi\upsilon t) + E_{0\,max} r_{max} \left\lceil \frac{d\alpha}{dr} \right\rceil \cos(2\pi\upsilon t)\cos(2\pi\upsilon t) \Leftrightarrow$$

$$\Leftrightarrow \mu_o = \alpha_o E_{o\,max} \cos(2\pi\nu t) + \frac{E_{max} r_{max} \left\lceil \frac{\partial\alpha}{\partial r} \right\rceil}{2} \cos\left(2\pi t(\nu_o + \nu_s)\right) + \cos\left(2\pi t(\nu_o - \nu_s)\right)$$

Equation 1.5 Scattered light component frequencies by oscillating polarization in which v_0 is the frequency of incident light and v_s is the frequency of the scattered molecular motion.

1.5.2 The Raman Spectrum

The Raman spectrum of cells and tissues is made up of a superposition of many biochemical components including DNA, RNA, proteins, lipids and carbohydrates. A Raman plot is the intensity of the scattered light which is measured in arbitrary units vs. the Raman shift which is measured in wavenumbers (cm^{-1}). The shift provides information on the vibrational, rotational and other low frequency transitions in a given sample. The full spectral range extends from 400-3500cm^{-1}. The fingerprint region extends from 400-1800 cm^{-1} and the high wavenumber region extends from 2800-3500 cm^{-1} (Figure 1.15).

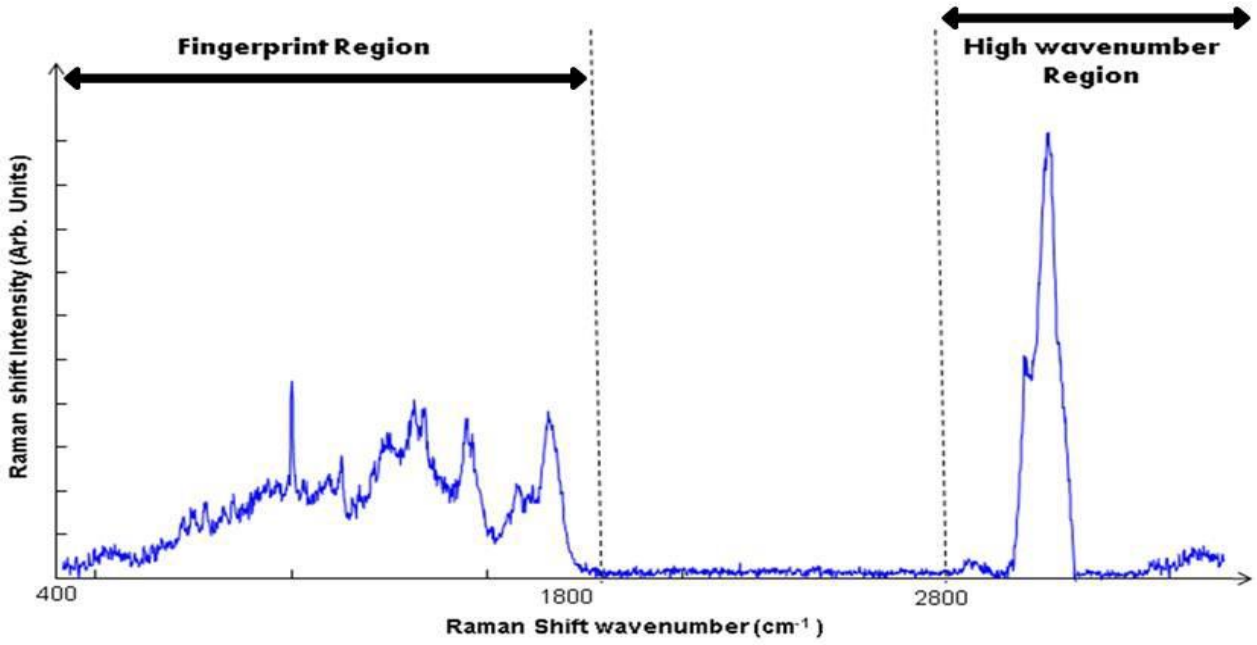

Figure 1.15 Raman spectrum of cervical cancer CaSki cell line. The variation of Raman shift wavelength is expressed in wavenumbers (cm^{-1}) and can be observed along the X-axis whilst the intensity is represented along the Y-axis. The fingerprint and the high wavenumber (HW) regions of the spectrum are indicated by the arrows.

Biological studies typically focus on the fingerprint region of the spectrum between wavenumbers 400cm^{-1} to 1800cm^{-1} (Figure 1.16). It is important to note that Raman peaks representing the Raman active molecules often overlap and can obscure one another. Some are narrow bands whereas others are broader. A tentative assignment of Raman peaks is presented in Table 1.1.

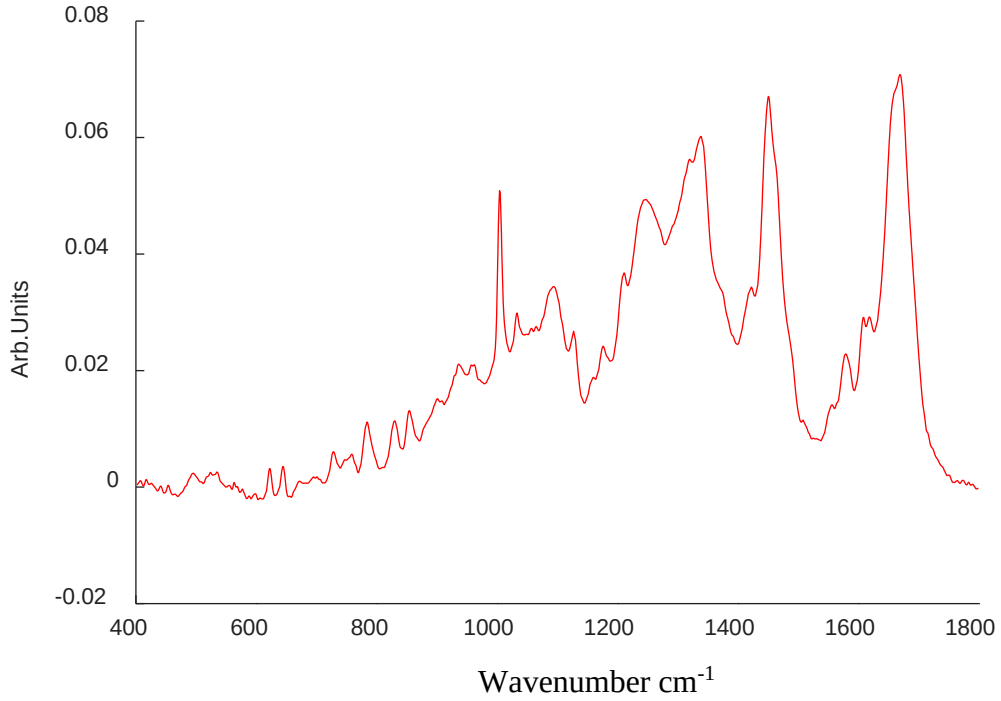

Figure 1.16 Raman spectra of a cervical Intermediate cell recorded in the fingerprint region 400-1800cm^{-1}.

Table 1.1Tentative Peak Assignments for Raman spectra of cells and tissues (Movasaghi et al. 2007)

Raman peak position [cm^{-1}]	Proteins	Lipids	Carbohydrates	Nucleic acids
482			Glycogen	
577			Glycogen	
622	C-C twist Phe			
643	C-C twist Tyr			
727	CH2 def	C-C head		A
752	Sym br. Trp			
781				U,C,T ring br
826	Out of Plane ring br.Tyr			PO2 a.str
851	Ring br. Tyr,C-C str. Pro			
852			Glycogen	
937			Glycogen	
985		C-C head		
1002	Sym. Ring br. Phe			
1033	C-H in plane Phe, C-C str			
1044			Glycogen	
1060	C-N str			

1082	C-N str	Chain C-C str	C-O str, Glycogen	
1096		Chain C-C str	C-C str	
1106			Glycogen	
1123	C-N str	Chain C-C str	C-O str	
1152	C-N str			
1207	C-C6H5 str. Phe, Trp			
1238	C-N str, Amide III			
1261			Glycogen	
1334			Glycogen	
1338	Trp			G
1366		Sym. Str. CH3		
1381			Glycogen	
1450	CH2 def	CH2 def		
1458			Glycogen	
1487	CH2 def			G,A
1560	Tyr, Trp			
1575				A,G ring br
1584	C=C str, C=C bend. Trp, Phe			
1605	C=C Phe, Tyr			

1642	C=O str, C=C sym. Str.			
1669	C=O str. Amide I			

1.5.3 Raman Instrumentation

The Raman microspectrometer used in this study (Labram XploRA™ Raman spectrometer) (Figure 1.17 (A)) consists of a Raman spectrometer joined to an optical microscope which facilitates focusing of the Raman laser on particular areas of interest in the cells. A 532 nm green Argon ion laser (Figure 1.17 (B)) was used and focused through an x100 objective lens. The objective lens also allows for the collection of the Raman scattered light. The scattered light is then dispersed by the diffraction grating onto a charged coupled device, which converts it into an electrical signal which is projected as a spectrum. The grating used will determine the spectral resolution via the groove density of the grating. Typically 300-1800 grooves/mm are used. The presence of a notch filter prevents the elastically scattered light (Rayleigh scattering) from reaching the detector (Figure 1.18).

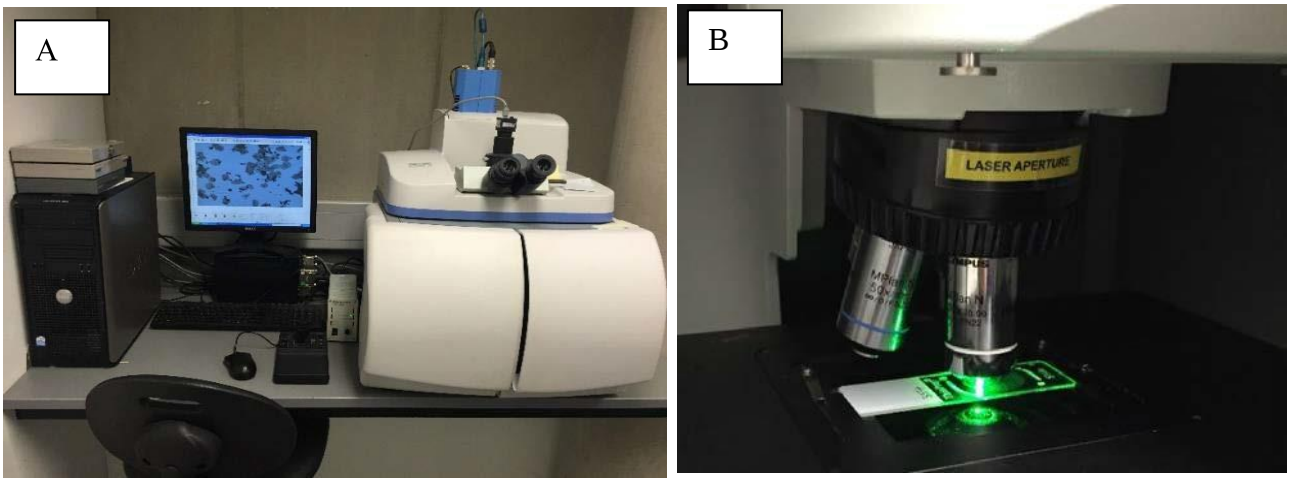

Figure 1.17(A) Labram XploRATM Raman spectrometer. The spectrometer is linked to a confocal microscope, which allows the user to view the sample surface and direct the laser accordingly. Figure 1.17 (B) A 532 nm green Argon ion laser focused through an x100 microscope objective.

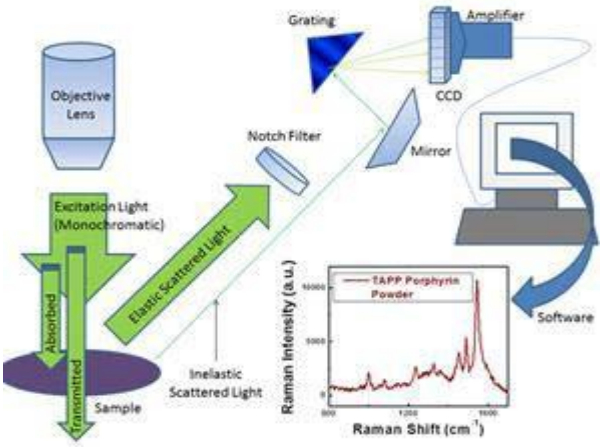

Figure 1.18 Basic Schematic of Raman spectrometer. The argon ion laser is deflected by a series of mirrors onto the sample surface. Scattered light is collected by the objective lens and sent through a filter onto a holographic grating and finally onto a CCD (*Laboratory,T.P.K. Spectroscopic Characterization*, 2012)

1.5.4 Raman Spectroscopy in Cancer Research

Raman spectroscopy has the potential to play an important role in diagnostic cytology, histology, biopsy targeting, surgical targets, treatment monitoring and drug studies (Baker *et al.*, 2018). A study conducted by Pirro et al used fibre based Raman spectroscopy for intra-operative guidance of brain surgery aiming to minimise the amount of brain tissue removal by identifying brain cancer (glioma) from normal brain tissue. They concluded that Raman spectroscopy could accurately differentiate normal brain from dense cancer and normal brain invaded by cancer cells, with a sensitivity of 93% and a specificity of 91% (Pirro *et al.*, 2017).

A study conducted by Brozek-Pluska et al, attempted to use Raman spectroscopy for imaging as well as diagnosis of breast cancer based on paraffin embedded tissue sections that were cancerous and non-cancerous from the same patient. They concluded that Raman bands associated with carotenoids, proteins and lipids dominated the spectra obtained from cancerous tissue when compared to non-cancerous tissue (Brozek-Pluska *et al.*, 2012).

Biofluids are an up and coming trend in the field of spectroscopy. Given the ease of collection and general acceptance by patients, biofluidscan give an accurate snap shot of a patient's health (Baker *et al.*, 2018). A recent study conducted by (Medipally *et al.*, 2017) aimed to develop a high throughput Raman spectroscopy method for rapid screening of liquid blood plasma from prostate cancer patients. Sample preparation parameters were investigated, with the aim of identifying a combination that would reduce the overall acquisition time for spectra from peripheral blood plasma, reduce the complexity of sample preparation and retain the classification accuracy from Raman spectroscopic diagnostics. They identified spectral differences in the region around 1155 and 1523 cm^{-1} that were highly expressed in healthy volunteers compared to prostate cancer patients. Control versus cancer cases could be classified with similar discriminating features using both 785 and 532 nm laser lines and the discriminating features were resonant at 532 nm. A sensitivity and specificity of 96.5% and 95% respectively was achieved (Medipally *et al.*, 2017).

A recent study conducted by Behl et al, attempted to standardise the protocol for Raman spectroscopy for oral cancer screening. Testing various collection methods the study was able to record high quality spectra from cells obtained from both the ventral side of the tongue and the buccal mucosa. The study utilised the Thinprep method of sample preparation cells were recorded on a glass substrate (Behl *et al.*, 2017).

1.5.5 Raman Spectroscopy in Cervical Cancer Research

In 1998, MahadevanJansen. *et al* (1998) developed an in vivo fiberoptic probe for the clinical diagnosis of cervical pre-cancers. They determined that an acquisition time of 90 seconds was required to obtain adequate spectra of the cervix however if they increased the power of the excitation source they could reduce that acquisition time to less than 20 seconds. Longer acquisition times increase signal to noise ratio however too long of an acquisition can result in burning of the sample resulting in a spectrum with ill-defined Raman bands not suitable for analysis.

Another clinical trial by the same group (Utzinger, *et al.,* 2001) showed that in vivo Raman spectra resemble ex vivo cervix tissue. This study was also completed using acquisition times of 60-180 seconds which is longer than is clinically accepted.A study conducted by Robichaux-Viehoever *et al.* (2007) utilized clinically feasible acquisition times of 5 seconds. The study concluded by stating that they were able to distinguish between benign and high grade dysplasia with a sensitivity and specificity of 89% and 81% respectively. A probe based study investigated the effect of race, ethnicity, body mass index, parity and social economic status on Raman spectra from patients with a normal cervix and determined that only body mass index and parity resulted in significant variation within the spectral profile (Vargis *et al.*, 2011). A study conducted by Krishna et al. (2006) used formalin fixed cervical tissues using Raman and FTIR spectroscopy. They reported the ability to distinguish between normal and malignant tissues based on differences in protein, lipids, and nucleic acid peaks and stronger amide III assignments, indicating disorder, helical secondary-protein structure in malignant conditions. A recent study Kanter *et al.* (2009) categorized the spectra according to the menstrual cycle and menopausal status and histopathological classification as determined by the pathologist. The results showed that incorporating the women's hormonal status and particular point in the menstrual cycle and menopausal state resulted in a classification

accuracy of 94%. Kamemoto *et al.* (2010) reported the ability to distinguish normal cervical tissue from invasive cervical cancer tissue using frozen tissue sections. The discrimination was mainly based on collagen and CH stretching bands. A study conducted by Rashid *et al.* (2014) attempted to utilise formalin fixed paraffin embedded cervical tissue sections for Raman spectroscopy analysis. They concluded that they were effectively able to distinguish negative/normal tissues from pre-cancer tissue based on a reduction in glycogen and an increase in nucleic acids. The pre-cancer tissue loses differentiation with increased proliferation which resulted in reduced levels of glycogen while the cells that make up the normal tissue accumulated glycogen as they matured. Most Raman studies investigating cervical cancer fail to incorporate HPV into their analysis. Jess *et al.* (2007) outlined the clinical importance of Raman spectroscopy for identification of HPV infection. Fixed and live cell lines were recorded which included PHK cells that express the E7 gene of HPV 16 and CaSki cells which are a HPV 16 containing cervical carcinoma derived cell line. The results demonstrated a change in the Raman peaks most likely associated with DNA and protein which are consistent with an active HPV infection and changes associated with neoplasia. Ostrowska *et al.* (2010) used Raman and FTIR spectroscopy to study cervical cancer cell lines. HPV-negative (C33a) and low HPV copy number (SiHa) cell lines were investigated. Both cell lines were found to be biochemically similar but different when compared to mid (HeLa) and high (CaSki) HPV copy number cervical cancer cell lines. They reported variations in protein, nucleic acid and lipid bands. Using partial least squares regression analysis with HPV copy number as a target, the spectral profile of the cells could be used to evaluate the degree of HPV infection. Vargis *et al.* (2012) utilised both cell lines and cytology samples to investigate the potential of Raman microspectroscopy to detect the presence of HPV. They achieved discrimination between HPV negative normal human keratinocytes (NHEK), HPV negative cervical cancer cell line (C33a) and HPV positive

cervical cancer cell lines (HeLa and SiHa) with an accuracy of 89-93%. A study conducted by Rubina *et al*. (2013) used Raman spectroscopy to identify negative cervical cytology samples from cervical cancer samples. The results showed that the spectra were contaminated with blood and removal of this blood with the use of a red blood cell lysing agent, however, failed to improve the sensitivity values of 79%. Bonnier et al outlined the crucial need to adapt Raman spectroscopy protocols to reach suitable reproducibility for screening a large cohort of patients (Bonnier *et al.*, 2014). The study demonstrated the use of H_2O_2 and industrial methylated spirits to remove contaminating blood residue which contributed to variability in the spectroscopic data sets. This was achieved without altering cell morphology or spectral features. Ultimately this work further demonstrated the potential of Raman spectroscopy to be used as a cervical cancer screening method based on improved sample preparation. A study conducted by (Duraipandian et al.,2018) outlined Raman spectroscopy ability to detect high-grade cervical cytology using morphologically normal appearing cells. They reported high rates of sensitivity and specificity for classifying HSIL cases based on intermediate and superficial cells. They also reported that intermediate and superficial cells could be mixed when recording and still be used for HSIL diagnosis as the biochemical difference between negative and HSIL samples were more than the biochemical differences between intermediate and superficial cells. A recent study defined the Raman spectral signatures of cervical exfoliated cells present in liquid-based cytology Pap test specimens and compared the signature of high-grade dysplastic cells to each of the normal cell types (Kearney *et al.*, 2017). The study demonstrated that Raman spectroscopy can identify biochemical signatures associated with the most common cell types seen in liquid-based cytology samples; superficial, intermediate, and parabasal cells. In addition, biochemical changes associated with high grade dysplasia could be identified suggesting that Raman spectroscopy could be used to aid current cervical screening tests.

1.6 CERVIVA

This body of work was performed as a continuation of on-going research on the application of Raman spectroscopy into cervical cancer screening which was conducted under the direction of the CERVIVA consortium (www.cerviva.ie).

CERVIVA is an Irish research consortium that was founded in 2005 by Prof John O'Leary and Dr Cara Martin. The aim of CERVIVA is to provide research in the field of HPV associated diseases while supporting CervicalCheck and national agencies. CERVIVA is funded by the HRB, The Irish Cancer Society, and Friends of the Coombe and works closely with universities, government health agencies and biotechnology companies.

1.7 Research Question and Hypothesis

- Research Question:

  Can Raman spectroscopy be used as a tool for cervical cancer screening?

- Hypothesis

  We hypothesise that Raman spectroscopy can be used to differentiate between normal and abnormal cervical cytology smear samples.

1.8 Aims and Objectives

- To conduct a study of variability due to hormonal effects in cervical Pap smear samples using Raman spectroscopy
- To conduct a study on the removal of contaminating blood from cervical Pap smear samples and the implications for cervical cancer screening using Raman spectroscopy
- To assess the utility of frozen biobanked samples for cervical cancer screening using Raman spectroscopy
- To assess the utility of Raman spectroscopy as a triage test for cervical cancer screening

Chapter 2

Materials and Methods

2 Materials and Methods

2.1 Sample Cohort1 and 2

Samples were obtained from patients attending the colposcopy department of the Coombe Women's and Infants University Hospital (CWIUH). The inclusion criteria for patient recruitment was for first time colposcopy patients who had no previous history of disease and recruitment took place over a four year period (2014-2018).These patients made up sample cohort 1. Each patient was informed verbally and in writing on the purpose of the study and given the opportunity to opt in or out. Upon agreeing to take part in the study, written consent was obtained from each patient. Two copies of the same consent form were signed by the patient, one was kept with the patient's clinical details, and the other was kept by CERVIVA at CWIUH. Each patient was assigned a random sample number to maintain patient confidentiality which is in keeping with general data protection regulation (GDPR). Upon receipt of the patient's consent form, a nurse colposcopist would take the smear according to the standard operating procedure. Each patient was followed up for their corresponding histology result and monitored for a period of 12 months.'

Sample Cohort 2 was made up of LBC biobank samples provided by the National HPV Archive HPV research group, University of Edinburgh. The samples had been stored at -25ºC for an unknown period of time. All clinical details outlining the patient's cytology, HPV, colposcopy and histology status were provided.All biobank LBC samples were stored at -25^0C and shipped to the lab on dry ice. The samples were gradually allowed to come up to room temperature and then processed in the same way as non biobanked samples outlined in section 2.3. Numbers of samples for each study are detailed in the results chapters 3-6.

The number of samples selected and overall number of spectra recorded for each chapter was determined by the availability of samples recruited from CWIUH and the National HPV Archive HPV research group while ensuring that the same number of spectra was recorded for each category. This helped to ensure no bias with regards to leave one patient out cross validation and model prediction. As this was a pilot study and sample numbers were limited, power calculations were not applicable.

2.2 HPV Testing

2.2.1 Cobas^{R} 4800 HPV DNA Test

The Cobas 4800 (Roche Diagnostics) is an automated system for the extraction of HPV DNA and the detection by real time PCR of 14 different high risk HPV types (16, 18 , 31,33, 35, 39, 45, 51, 52, 56, 58, 59, 66 and 68) with the ability to genotype for HPV 16 and 18. The system consists of two parts, the first is a sample extraction and preparation instrument (X480) and the second is an analyser (z480) which carries out real time PCR on the processed samples (Figure 2.1).

The system starts once the samples are loaded and a barcode is assigned to each sample. After sample loading, the reagents (SDS magnetic glass particles, wash buffer, lysis buffer positive control, negative control, PCR master mix, Proteinase K, Magnesium ions) and consumables (96 well plate, deep well plate, 1000 µl tips and reagent reservoirs) are scanned. The rest of the process is automated, which involves 400 µl of the LBC samples being collected and digested under denaturing conditions at elevated temperatures, before the cells are lysed by a chaotropic reagent which results in the release of HPV nucleic acids. These nucleic acids are negatively charged and will bind to the positively charged magnetic glass particles, which are held in place with a magnetic plate. The nucleic acids are then washed and separated from the glass particles before they are amplified and detected by real time

PCR. Approximately 200 nucleotides are targeted by the primers for the PCR reaction which are located within the L1 region of the HPV genome. The master mix contains primers designed for 14 different high risk genotypes (16, 18, 31, 33, 35, 39, 45, 51, 52, 56, 58, 59, 66 and 68). Fluorescent oligonucleotides probes will then bind to the sequences within these primers during PCR. A meta-analysis of 23 industrialised countries using the Hybrid Capture 2 (HC2) HPV assay indicate that the pooled sensitivity of primary HPV screening in the detection of CIN 2+ and CIN 3+ was 95.2% (95% CI: 92.5% to 97.1%) and 98.2% (95% CI: 96.7% to 99.1%). The specificity reported in detecting CIN 2+ was 88% and CIN 3+ was 87.6% (HIQA,2017).

Figure 2.1The Cobas® x480 instrument and z480 analyser. The cobas® x480 (left) is an automated system that extracts DNA from ThinPrep cervical cytology specimens. The z480 analyser (right) then amplifies and detects the presence of 14 different high risk HPV genotypes.

2.2.2 Aptima HPV mRNA test

The Aptima assay (Hologic Gen-Probe, san Diego, Ca, USA) is an automated target amplification assay that detects the presence of E6/E7 mRNA from 14 high risk HPV types with the entire process being automated and carried out by a dedicated system, the Panther instrument (figure 2.2).

Figure 2.2 Panther instrument which runs the Aptima HPV assay, and detects HPV mRNA from 14 high risk HPV types. All samples as well as assay reagents and consumables were loaded into the Panther system prior to beginning an assay run. Panther functions were controlled through the use of the on board computer, shown to the right of the main instrument.

The first step involves the transfer of 1 ml of the test sample into transport media (STM) which causes the cells to lyse and prevents RNA degradation. The STM tubes are then placed into the sample racks and placed into the Panther instrument. HPV amplification reagents, HPV enzyme reagents, HPV internal control reagent and HPV selection reagents are loaded into the instrument. Positive and negative calibrators are present within the system. The samples are then run. mRNA is isolated using capture oligomers which are bound to magnetic micro particles. The oligomers bind to the target sequences in the mRNA target, before the complex is removed from the solution using magnets while the supernatant is

aspirated. The complex is then washed before the mRNA is amplified through the use of an MMLV reverse transcriptase and T7 RNA polymerase. The reverse transcriptase is used to generate a DNA copy of the target mRNA sequence containing a promoter sequence for T7 RNA polymerase. T7 RNA polymerase produces multiple copies of RNA amplicon from the DNA copy template. Detection of the amplicon is achieved by HPA using single-stranded nucleic acid probes with chemiluminescent labels that are complementary to the amplicon

which are detected through an illuminometer. The detection step is completed by the software which analyses the signal in order to produce the assay results.

2.3 ThinPrep slide preparation

A slide was prepared for each sample using a ThinPrep 2000 processor (Hologic Inc; Marlborough, MA 01752, America). The Thin Prep processor starts by homogenizing the sample by spinning the filter, creating shear forces in the fluid that are strong enough to disaggregate randomly joined material, break up blood, mucus and non-diagnostic debris. The cells are then collected onto the membrane of the filter and transferred onto a glass slide to create a circular monolayer deposit of cells 20 mm in diameter and a few microns in thickness. The slide is then ejected automatically into a fixative bath of 95% ethanol.

2.4 H_2O_2 treatment

LBC samples can contain varying levels of blood according to a blood scale index (0-3). Blood can also be present even though it may not be visible to the human eye, however it has previously been shown that Raman spectroscopy can detect these low levels of hemoglobin present (Bonnier *et al.*, 2014) thus blood is deemed a limiting factor and should be removed. An in house method of utilizing H_2O_2 for the removal of blood was applied to all samples regardless of whether there was visual evidence of blood present in the LBC samples or not (Bonnier *et al.*, 2014). The H_2O_2 method works by oxidizing the hemoglobin present within the blood. The ThinPrep slides were covered in H_2O_2 for 30 seconds before washing in 70%

industrial methylated spirits (IMS) for 3 minutes, followed by multiple dips in 100% IMS to remove any remaining H_2O_2. The slides were then allowed to air dry and ready for spectroscopic analysis.

2.5 Raman Measurements

All samples used as part of this study were recorded on a HORIBA Jobin Yvon XploRA^{TM} system (Villeneuve d'Asq, France), which is connected to an Olympus microscope Bx41 equipped with a X10 and X100 objectives (MPlanN, Olympus). The equipped laser is a 532 nm green argon ion laser with a spot size of 1-2 μm. The power of the laser was set at 100%. The confocal hole and slit was set at 100 μm with a 1200 lines/mm grating. The 1200 grating gives a spectral resolution of 3 cm^{-1} per pixel.

The Raman spectrometer was calibrated to the spectral line of silicon, 520 cm^{-1}. The dark current, the reference spectrum of polystyrene and of the NIST standard and the daily laser intensity were recorded. A CCD detector (Andor, 1024x256 pixels) was used and Labspec v6.0 software (Horiba Jobin Yvon) was used to operate the Raman spectrometer. One Raman spectrum was recorded from the nucleus of each cell for 30 seconds and averaged over two accumulations. This helps to increase the intensity of the scattered photons and reduces noise. The number of cells recorded from each sample depended on the quality of the cells present on the slide. A suitable cell would present on the slide as a single cell not obscured by surrounding material with the nucleus and cytoplasm being well defined. As all the cells recorded (Superficial and Intermediate) were morphologically normal, they were consistent in their size and shape and overall appearance (section 1.2.1). A good quality Pap smear would allow 25 cells to be recorded per sample. The coordinates of each cell was recorded in each sample and saved using the Labspec software. A typical slide could take between 35-40 minutes to complete recording. Chapter 3 involved the recording of dyskaryotic cells from 15 HPV positive, high grade dyskaryotic samples. As these cells were not morphologically

normal and could be present in low numbers it took additional time (20-30 minutes) to screen for these abnormal cells. Samples were also recorded randomly (ie. not recorded in batches according to any biological class) across a four year time period. This helped avoid any batch effects in our recording.

2.6 Pap stain

The Pap stain was carried out on each ThinPrep slide after Raman spectral recording. The protocol was carried out in the following manner. Each slide was soaked in a bath of equal parts distilled water and glycerol for 10 minutes. The slides were then washed in distilled water for 2 minutes. The slides were then submerged in hematoxylin for 2 minutes and washed in running hot tap water for 2 minutes. 1 % acetic was then added and washed off in distilled water for 1 minute. The slides were then submerged in 70% and 95% industrial methylated spirits (IMS), followed by 3 minutes in OG6. The slides were then washed in 100% IMS for 2 minutes followed by Xylene for 1 minute. The slides were then mounted in Coverquick and cover slipped. The Pap stain was only performed once the spectroscopic analysis was complete.

2.7 Raman Spectral Processing

All sample data was pre-processed regardless of when or how the samples were recruited to avoid bias. Data was normalised and analysed using Matlab software (Mathworks) and specific scripts developed and adapted for uploading of the spectra and their pre-processing, including smoothing (Savitzky-Golay K=5, K=13) baseline correction (Rubberband) , vector normalization and glass subtraction

2.7.1 Smoothing

Smoothing is employed for the removal of high frequency components. Savitzky- Golay filtering is a common technique employed (Gautam *et al.*, 2015). The goal of smoothing is to

remove rough changing components of the spectra and to highlight slow changes in intensity so that it's easier to see trends in data.

2.7.2 Base Line Correction

A common problem when using Raman spectroscopy is fluorescence. When a sample fluoresces the fluorescing photons can be detected by the photon detector thereby distorting the Raman spectrum obtained from the test sample resulting in an elevation of intensity which can obscure biological peaks particularly those in the fingerprint region. Rubberband baseline correction is employed to correct this change in intensity. First the spectrum is divided up into a given number of ranges. The lowest point in each range is determined, then the initial baseline is built out of those points. All the points on the spectrum are then drawn down by the difference between the lowest point on the baseline.

2.7.3 Vector normalization

Raman spectra can exhibit a change in intensity levels even when recording the same sample due to different Raman conditions such as a change in laser alignment or power levels. Raman spectra from the same sample could have different intensity levels. Normalization is the process that corrects for this change in intensity by making sure the intensity of a given band (1004 cm^{-1}) of the same material is similar across all the spectra recorded under slightly different conditions. Vector normalisation involves calculating the norm which is defined as the square root of the sum of the squared intensities of the spectrum. Each of the Raman intensities corresponding to a Raman shift is divided by the norm to obtain the normalized spectrum (Gautam *et al.*, 2015).This is a standard operating procedure for all Raman spectroscopic analysis.

2.7.4 Glass subtraction

Glass is the only substrate used in cytopathology as it is inexpensive and allows the processing of hundreds of samples a day. Its use in Raman spectroscopy, however, is hampered by the fact that glass exhibits broad peaks at 550 and 1100cm^{-1} which overlap with the biological spectra in the fingerprint region thus resulting in the need for the spectra to be corrected for glass background.

There are two ways that the contribution of glass to the spectra can be reduced. The first involves the fine focus of the laser on the target cell's nucleus. Focusing the laser on the upper portion of the nucleus to increase the distance between the laser and the glass slide reduces the glass contribution to the spectra. The second involves the use of an in house developed algorithm based on non-negativity constrained least squares (NNLS). In NNLS, the coefficients are not allowed to become less than zero. Using a matrix of 300 glass spectra (Figure 2.3), and a set of cellular components (nucleic acids, proteins, and carbohydrates), a non-negative vector is found that estimates the contributions of the cellular components and glass to the recorded cell spectrum. This vector is then multiplied by the glass matrix and cell components, before being subtracted from the original recorded cell spectrum (Figure 2.4).

After these pre-processing steps, the data was mean centered and subjected to partial least squares discriminant analysis (PLSDA). It is possible to use other forms of substrate such as calcium fluoride which don't require subtraction, as this does not contribute a Raman signal to the spectrum in the fingerprint region. This substrate is very expensive, however, and as it is thicker than a glass slide, Thinprep technology cannot be used for slide preparation.

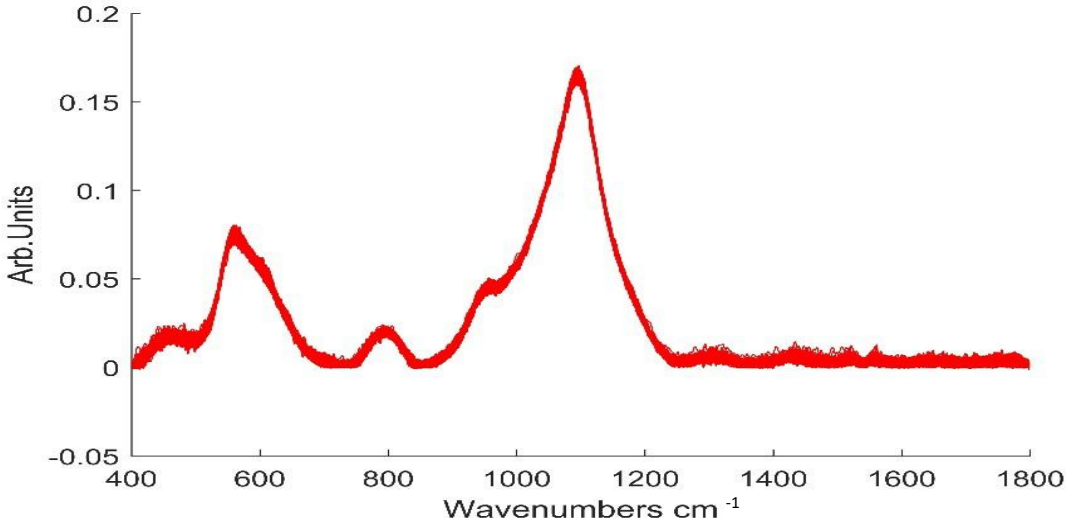

Figure 2.3 300 glass spectra recorded in the fingerprint region 400-1800cm^{-1}

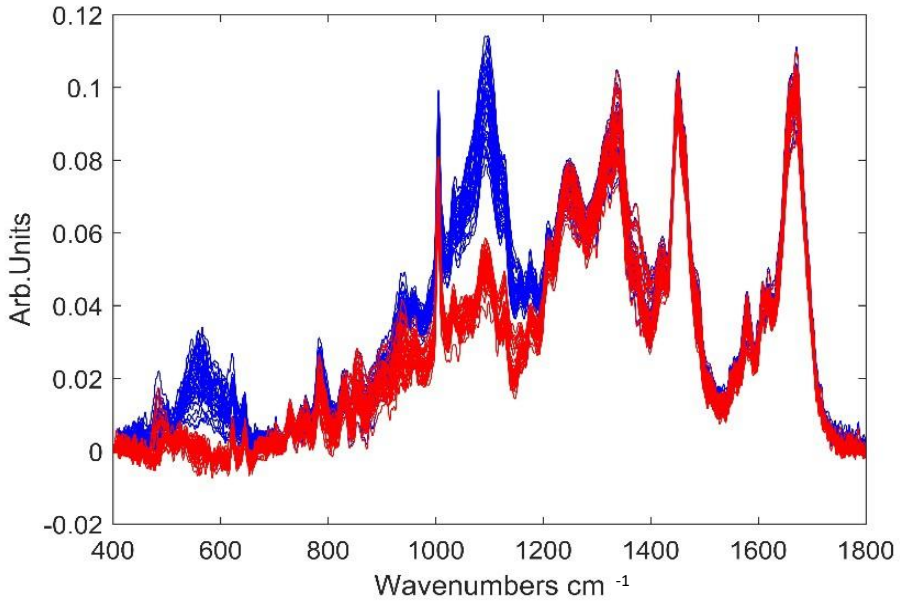

Figure 2.4 100 Intermediate cell spectra before (blue) and after (red) pre-processing for glass removal.

2.8 Partial least squares discriminant analysis (PLSDA)

Partial least squares discriminant analysis (PLSDA) is a chemometric technique used to optimise the separation between different groups of samples. It is a supervised form of multivariate analysis which works as a linear classifier. Its aim is to maximise the variance between groups and to minimise the variation within each group. The loadings/latent variables (LVs) can be plotted to give information on the source of the variation between groups. PLSDA was chosen over multivariate techniques for a number of reasons. The first being that it can analyse data with numerous variables and it works well on data that is noisy. The limitations of PLSDA can be, that it can over fit a model meaning that it can classify training data well but not new data. This can be corrected for by using a validation data set or a method of cross validation (Ballabio *et al*., 2013). Mean centering (dividing all the variables by the mean) was performed on the pre-processed spectra before PLSDA modelling to adjust for the variance between large and small unit variables, leaving the relevant variance (between the samples) for analysis.

2.9 Cross –Validation

Cross-validation is a model validation technique used to assess how results will generalize to a new dataset. It is mainly used to determine prediction (how well a model will predict in practice). The main reason for using cross validation instead of conventional validation is that conventional validation requires a 70:30 split of the data. 70% for training and 30% for testing (Dobbin K et al., 2011). However in most cases there isn't enough data available to separate out 70% for training and 30% for testing without losing modelling or test capability, hence the use of cross validation (Kohavi., 1995). Cross validation is performed by dividing samples into validation groups. Each group is then removed from the training set one at a time. The model is then calibrated on the remaining training samples and is then used to predict samples of the cross validation group (Ballabio *et al.*, 2013). In this study one methods of cross validation was performed.

Leave one patient out = A test set is determined by leaving out each patient sample one at a time and comparing it to the training set. Every sample is tested. This helps ensures bias is avoided.

Chapter 3

A study of hormonal effects in cervical smear samples using Raman spectroscopy.

Adapted from: Traynor D, Kearney P, Ramos I, Martin CM, O'Leary JJ, Lyng FM. A study of hormonal effects in cervical smear samples using Raman spectroscopy. *J. Biophotonics*. 2018;e201700240.

3.1 Introduction:

Until recently the primary method for cervical screening was based on the Papanicolaou test (Pap test). The Pap test requires cells to be scraped from the cervix, fixed to a glass slide, stained and reviewed by a trained cytologist. Cellular abnormalities are identified by the cytologist based on cellular morphology and staining characteristics and classified according to the degree of dysplasia (Low grade or High grade). The advantage of the Pap test is that it is a widely accepted screening based test with a high specificity of 95-98% and a sensitivity of 74-96% (Kitchener *et al.*, 2011). The variability in the rates of sensitivity can be due to sampling technique; the subjectivity of the cytology based screening and can result in a high rate of gynaecological referral and patient recall which adds to cost and patient stress. Persistent infection with high risk human papillomavirus (HPV), such as HPV types 16, 18, is accepted as the major cause of cervical pre-cancer and cancer (Walboomers *et al.*, 1999). HPV DNA testing has a higher sensitivity (>95%) but lower specificity (~ 84%) than the Pap test (Cuzick *et al.*, 2013) and these tests are expensive, time-consuming and provide no information on cervical cytopathology. Current gold standard methods for detection of cervical cancer and pre-cancer are therefore limited and there is an unmet clinical need for new objective screening or diagnostic tests. Optical spectroscopic techniques, such as Raman or infrared spectroscopy, are label-free, non-invasive and have several advantages over traditional approaches, including objectivity, speed and cost. These methods can provide quantitative information based on the spectroscopic signature of the biochemical components of the sample allowing diagnosis to be based on biochemical changes rather than on morphological changes. The focus of the present study is on Raman spectroscopy, which is based on inelastic light scattering. The coupling of the light generates vibrations within the material and these vibrations are characteristic of the chemical structure, the energy of the scattered light is reduced by an amount equal to the vibrational energy and from this a rapid, label free, non-destructive measurement of the

complete biochemical fingerprint of a biological sample can be obtained. Over the past 15 years, the potential of Raman spectroscopy together with multivariate statistical analysis has been demonstrated for the detection of a variety of cancers, including cervical cancer (Diem *et al.*, 2013, Lyng *et al.*, 2015). In initial infrared spectroscopy studies on cervical cytopathology samples (González-Solís *et al.*, 2013, Wong *et al.*, 1991), spectra were recorded from cell pellets rather than from single cells and the presence of metaplastic cells, endocervical columnar cells, polymorphs, blood, cervical mucus and debris were all identified as confounding factors (Wong et al., 2002, Chiriboga *et al.*, 1998, Cohenford *et al.*, 1997, Diem *et al.*, 2002, Wood *et al.*, 1998). Recent studies by Ramos *et al.* (2016) and Bonnier *et al.* (2014) addressed the variability in Raman spectra from cervical smear samples and reported a new method to clear blood residue contamination before Raman spectroscopy based on pre- treatment of the slides with hydrogen peroxide. This method significantly minimised variability and resulted in the collection of highly reproducible data and was employed in this study to reduce variability based on the presence of blood residue. Physiological factors such as hormonal changes during the menstrual cycle or during menopause may also be potential sources of variability in the normal cervix.

The cellular make up of an individual woman's smear is dependent on which day during the menstrual cycle the sample was taken. Days 1-4 are classed as the menstruation phase of the cycle when bleeding will occur and smear samples are generally not taken during this phase. Days 5-13 are classified as the proliferative phase. During this phase oestrogen levels reach their peak resulting in complete maturation of the squamous epithelium and the cervical smear will present with a higher ratio of superficial cells to intermediate cells. Days 14-28 are classified as the secretory phase where progesterone production reaches its peak and prevents complete maturation of the epithelium. The cervical smear will present with a higher ratio of intermediate cells to superficial cells. During menopause, levels of both oestrogen and

progesterone will drop dramatically and there is a gradual arrest of the maturation of the squamous epithelium. This results in the loss of superficial and intermediate cells leading to the final atrophic stage where the squamous epithelium is composed entirely of parabasal cells.

The use of hormone based contraceptives (HC) will affect the natural hormone mediated maturation process of the cervical epithelium. A study by Romeo *et al.* (2002) used infrared spectroscopy to investigate hormonal influences on cervical cells throughout the menstrual cycle and showed spectral changes such as increases in the 1200-1000 cm^{-1} region due to glycogen increases around ovulation (mid cycle). Cervical cells from women on HC did not show the same degree of spectral changes as cells from women not on HC. Despite the variability throughout the menstrual cycle, principal component analysis (PCA) showed good discrimination between high grade dysplasia and normal samples collected at different phases of the menstrual cycle.

A more recent study by Kanter *et al*,(2009) has shown that hormonal differences due to the menstrual cycle can influence the Raman spectra acquired from the cervix *in vivo*. Spectra were divided into four groups, pre-menopausal proliferative phase (days 1-14), pre-menopausal secretory phase (day 15-28+), peri-menopausal and post-menopausal. Spectral differences were mainly observed at 1250, 1300 and 1320 cm^{-1}, most likely due to changes in the proteins collagen and elastin (Movasaghi *et al.*,2007). Incorporating hormonal status into their dysplasia classification algorithm increased the classification accuracy from 88% to 94%. The main objective of our study was to investigate hormone associated changes in the Raman spectra of cytologically negative ThinPrep cervical smear samples related to; (1) the menstrual cycle, (2) the onset of menopause and (3) the use of hormone based contraceptives. A further objective was to determine if any changes observed would interfere with the ability to discriminate normal and high grade dyskaryotic cervical smear samples caused by HPV infection.

3.2 Materials and methods

3.2.1 Sample collection and ThinPrep slide preparation

Cervical smear samples collected in PreservCyt solution were obtained from the Cytology Department at the Coombe Women and Infants University Hospital (CWIUH), Dublin, Ireland (recruitment period 2014-2018), after routine cytological screening had been performed. Ethical approval for use of encoded samples for the study was granted by the CWIUH Research Ethics Committee (no. 28-2014). Clinical data which was recorded relating to the samples included cytology result, date of last menstrual period, age at time of smear test and reported use of hormonal based contraceptives. No information on smoking status was available. A total of 60 cervical smear samples, 45 confirmed as cytology negative and 15 confirmed high grade dyskaryosis (high grade squamous intraepithelial lesion (HSIL)) samples, were used for this study. A slide was prepared for each sample as outlined in section 2.3 and 2.4.

3.2.2 HPV Testing

HPV testing was carried out as outlined in section 2.2.1

3.2.3 Raman Microspectroscopy

Raman recording was carried out as outlined in section 2.5-2.6. 25 cells were recorded from each cytologically confirmed negative test sample and 35 dyskaryotic cells were recorded in total from the 15 confirmed HSIL samples.

3.2.4 Data Pre-Processing and Analysis

Data Pre-processing and analysis was preformed as outlined in section 2.7-2.9

From the data provided by the patient about their last menstrual period and the day on which the sample was taken, the day of the menstrual cycle the smear was taken was calculated. It was assumed that each patient follows the standard 28 day cycle. Samples were only available from days 7-24 of the cycle. Table 3.1 shows the sample details including day of the menstrual cycle, menopausal status and use of hormone based contraceptive (HC).

Table 3.1 Sample details including day of the menstrual cycle, menopausal status and use of hormone based contraceptive

Sample number	Cytology Result	Day of cycle	Postmenopausal	HPV Result	Contraceptive
1	Negative	7	No	Negative	None
2	Negative	9	No	Negative	None
3, 4, 5, 6, 7	Negative	10	No	Negative	None
8, 9	Negative	11	No	Negative	None
10, 11, 12, 13, 14	Negative	12	No	Negative	None
15, 16, 17, 18, 19, 20, 21, 22	Negative	13	No	Negative	None
23, 24	Negative	16	No	Negative	None
25, 26	Negative	20	No	Negative	None
27	Negative	21	No	Negative	None
28	Negative	24	No	Negative	None
29, 30, 31, 32, 33, 34, 35	Negative	Not applicable	Postmenopausal	Negative	None
36, 37, 38, 39, 40, 41, 42, 43, 44, 45	Negative	Not applicable	No	Negative	Hormone based Contraceptive
46, 47, 48, 49, 50, 51, 52, 53, 54, 55, 56, 57, 58, 59, 60	High Grade	Not applicable	No	Positive	None

3.3 Results

3.3.1 Proliferative and Secretory Phase and Postmenopausal Cellular Presentation on Pap smear.

The proliferative and secretory phase presentation of a Pap smear are shown in Figure 3.1(A) and Figure 3.1(B) respectively. A higher ratio of superficial (pink stained) to intermediate (blue stained) cells in the proliferative phase compared to a higher ratio of intermediate (blue stained) to superficial (pink stained) cells in secretory phase can be observed. A postmenopausal Pap smear is shown in Figure 3.1(C). A lack of cellular material, mucus and cellular debris can be observed which caused difficulties in recording good quality spectra.

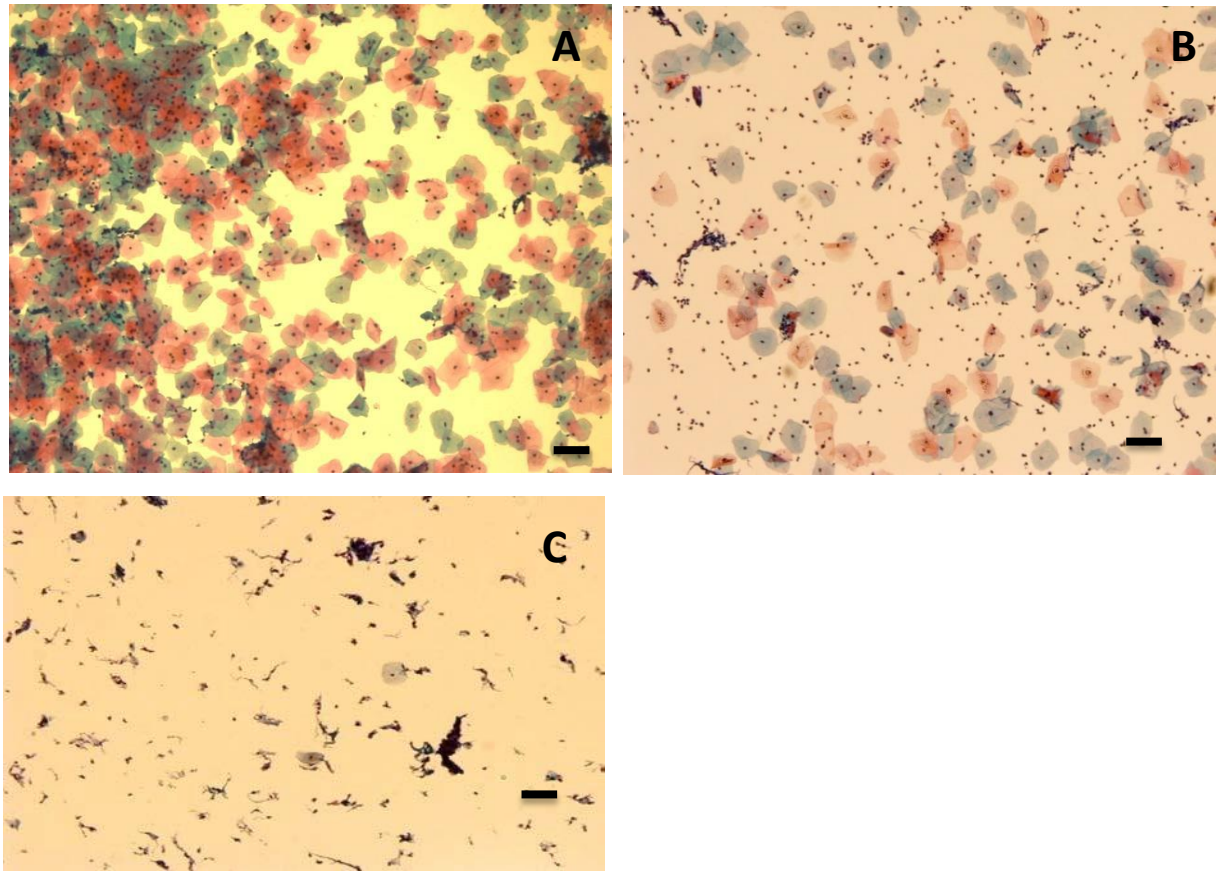

Figure 3.1 (A) Proliferative phase presentation of a Pap smear. Note the higher ratio of superficial (pink stained) to intermediate (blue stained) cells, (B) Secretory phase presentation of a Pap smear. Note the higher ratio of intermediate (blue stained) to superficial (pink stained) cells, (C) Postmenopausal presentation of a Pap smear. Note the lack of cellular material, mucus and cellular debris. Bar = 35 μm.

3.3.2 Raman signature of Proliferative Phase Vs Secretory Phase

The spectral data from the Pap smears was divided up according to the day of the menstrual cycle the sample was taken on. Figure 3.2(A) shows the mean Raman spectra of cells from days 7 to 24 of the menstrual cycle. Increases in the Amide I (1640-1650 cm^{-1})(see Table 1.1), Phenylalanine and Tyrosine (1605-1610 cm^{-1}) and glycogen (480 cm^{-1}) bands over time were observed. The latent variables (LV) scores scatter plot Figure 3.2(B) shows reasonable separation between the proliferative phase (blue) and the secretory phase (red). Some overlapping is observed which is most likely due to the fact that each woman will differ slightly between the days of the menstrual cycle and the levels of oestrogen and progesterone present. The LV1 loadings shown in Figure 3.2(C) highlight areas similar to those highlighted in the mean Raman spectra Figure 3.2(A). The discrimination is mainly based on glycogen (480, 937, 1381, 1458 cm^{-1}) which is more present in the secretory samples (red) due to the higher levels of progesterone which promotes sub nuclear glycogen accumulation (Nair *et al.*, 2010) and proteins (CH_2 def, 1450 cm^{-1}) and Amide I (1669 cm^{-1}) which are higher in samples collected from the proliferative phase of the cycle. The prediction plot from the PLSDA model Figure 3.2(D) shows reasonably good classification of menstrual cycle phase (proliferative phase or secretory phase) with sensitivity of 83% and specificity of 86%.

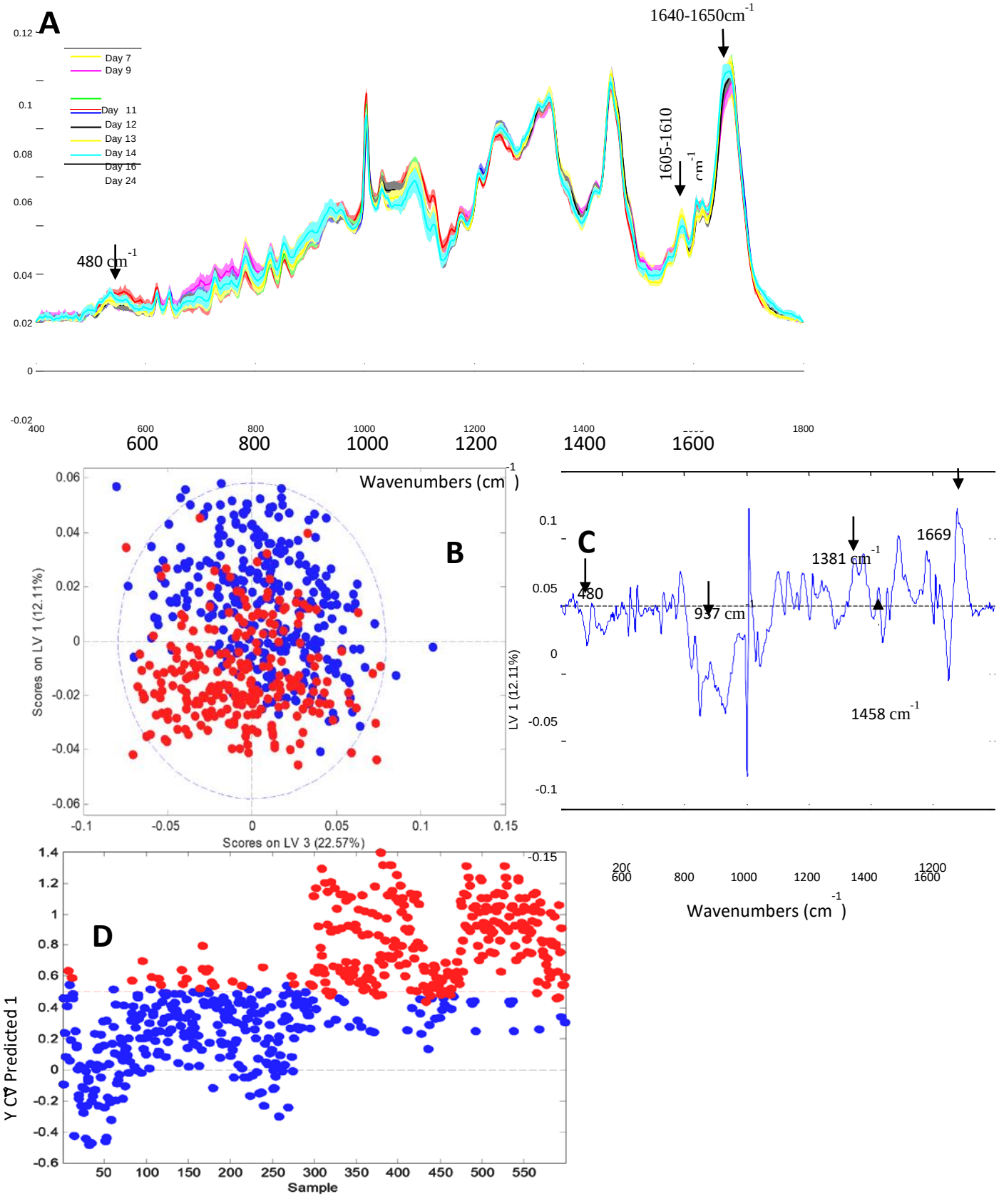

Figure 3.2 (A) Mean Raman spectra of intermediate and superficial cells from days 7 to 24. Shading denotes the standard deviation. Glycogen (480 cm^{-1}), Amide I (1640-1650 cm^{-1}), Phenylalanine and Tyrosine (1605-1610 cm^{-1}) show increases in intensity over time (B) LV scores scatter plot of Proliferative Phase, Days 7-14 (Blue) Vs Secretory Phase, Days 15-24 (Red), (C) LV1 loadings show that discrimination is based on based on glycogen (480, 937, 1381, 1458 cm^{-1}) and proteins (CH_2 def, 1450 cm^{-1}) and Amide I (1669 cm^{-1}) , (D) PLSDA prediction

plot which has a sensitivity of 83% and specificity of 86%.

3.3.3 Raman signature of postmenopausal samples

Most women are generally screened for cervical cancer up until the age of 65. Between the ages of 48-55 most women are said to be menopausal. Hence it is important to determine if Pap smears collected from postmenopausal women will have a similar Raman signature to non-postmenopausal women. Mucus and cellular debris present on postmenopausal samples obscure the little cellular material that is present on the slide and make it very difficult to obtain good spectra hence the number of spectra recorded is severely reduced and it is difficult to draw any firm conclusions. Figure 3.3(A) shows the mean and standard deviation spectra of the 22 postmenopausal cells recorded. Figure 3.3(B) shows good discrimination between the two sample types. The loadings shown in Figure 3.3(C) shows that the discrimination is based on glycogen (852, 1106, 1138 cm^{-1}) and nucleic acids (781 cm^{-1}) proteins (1450 cm^{-1}) and Amide I (1669 cm^{-1}). Figure 3.3(D) shows the PLSDA prediction plot which has a sensitivity of 100% and specificity of 95%.

Atrophic samples were not available as part of this study. No firm conclusions can be drawn from this data set except that postmenopausal samples can represent a problem for Raman based screening based on their Pap smear presentation due to mucus, cellular debris and lack of cellular material.

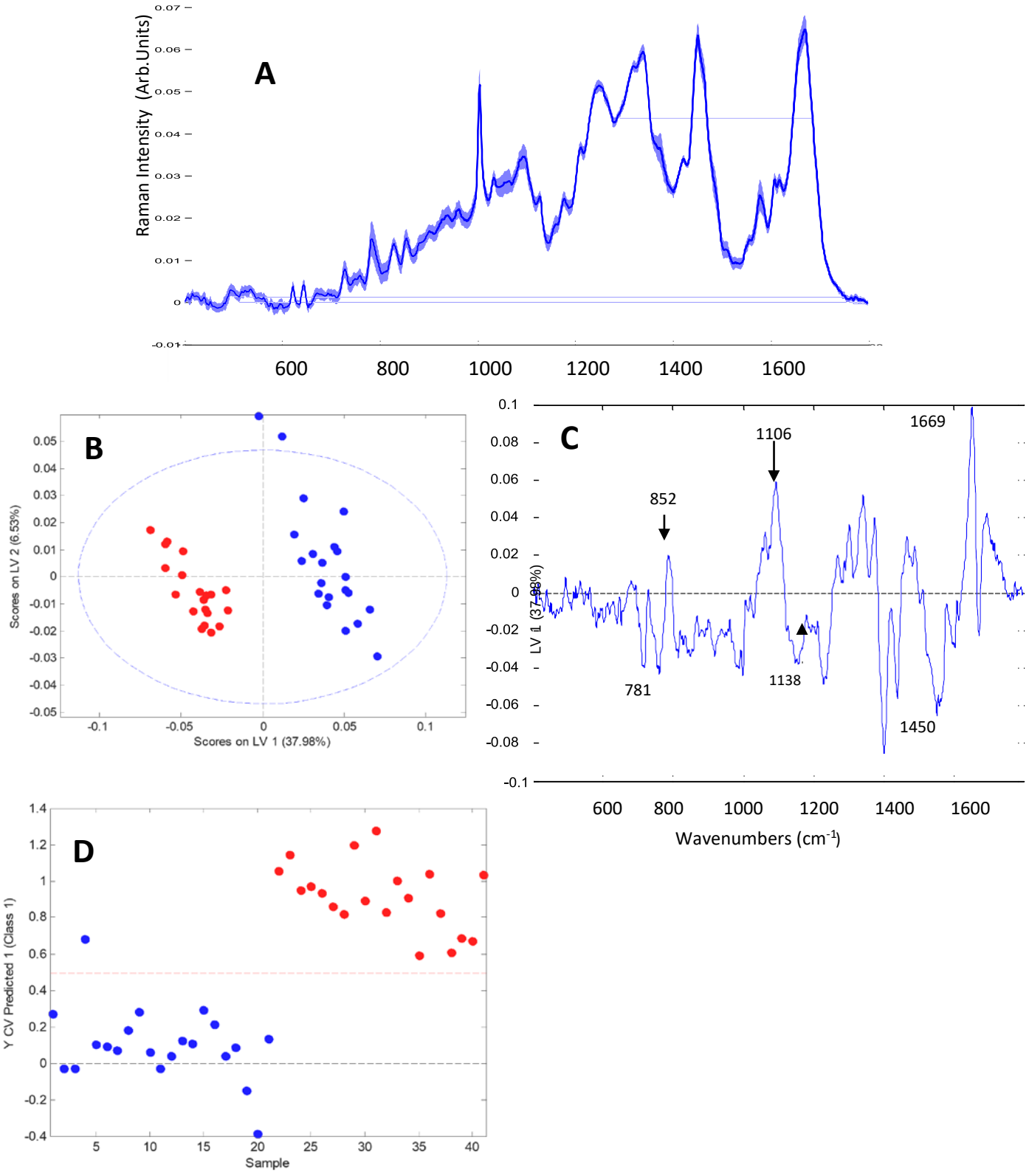

Figure 3.3 (A) Mean Raman spectra from postmenopausal samples. Shading denotes the standard deviation, (B) LV scatter scores plot of postmenopausal (blue) and non-menopausal (red), (C) LV1 loadings, (D) PLSDA prediction plot

3.3.4 Raman signature associated with women on hormone based contraceptives.

The clinical details obtained indicated if the patient was on some form of hormone based contraceptive (HC). However information on which type of contraceptive they are currently on was not included. The aim of this part of the study was to determine if Pap smears collected from women on HC will have a similar Raman signature to women who are not on HC. Figure 3.4(A) shows that the levels of glycogen (482 cm^{-1} and 855-939 cm^{-1}) in the HC positive samples are lower when compared to the controls. The controls were made up of the samples collected throughout the menstrual cycle which were HC negative. Tryptophan and Phenylalanine at peak position (1584-1605 cm^{-1}) and Amide I at peak (1669 cm^{-1}) are higher in HC samples compared to the control. The lower levels of glycogen in the HC samples could be linked to lower levels of progesterone due to its role in promoting sub-nuclear glycogen accumulation. The same could be said for the higher levels of proteins detected (Phenylalanine, Tryptophan, and Amide I). There is also a consistent change in the shoulder of Amide I, which is a change in Amide I protein position and folding between HC positive and negative samples. Overall protein synthesis may be increased due to the constant level of hormones present.

The LV scores scatter plot Figure 3.4(B) shows good separation between HC positive samples and HC negative samples. There is a small amount of overlapping which could be due to a number of factors. Multiple types of contraceptive are available which contain different types and levels of hormones, including implants, injectable contraceptive, progesterone pills, oestrogen and progesterone pills, combined oral and the patch all of which work by maintaining a constant level of hormones in the body thus preventing the rise and fall of oestrogen and progesterone. Hence they may work differently and individual patients will also respond differently to the levels of hormones present. The loadings 3.4(C) from LV1 show that glycogen (483 and 1386 cm^{-1}) and proteins and lipids (1146, 1450, 1566 cm^{-1}) and Amide I (1669 cm^{-1}) are the main discriminating factors between HC positive and HC negative samples

The PLSDA prediction plot Figure 3.4(D) shows excellent classification with a sensitivity of 100% and specificity of 100%.

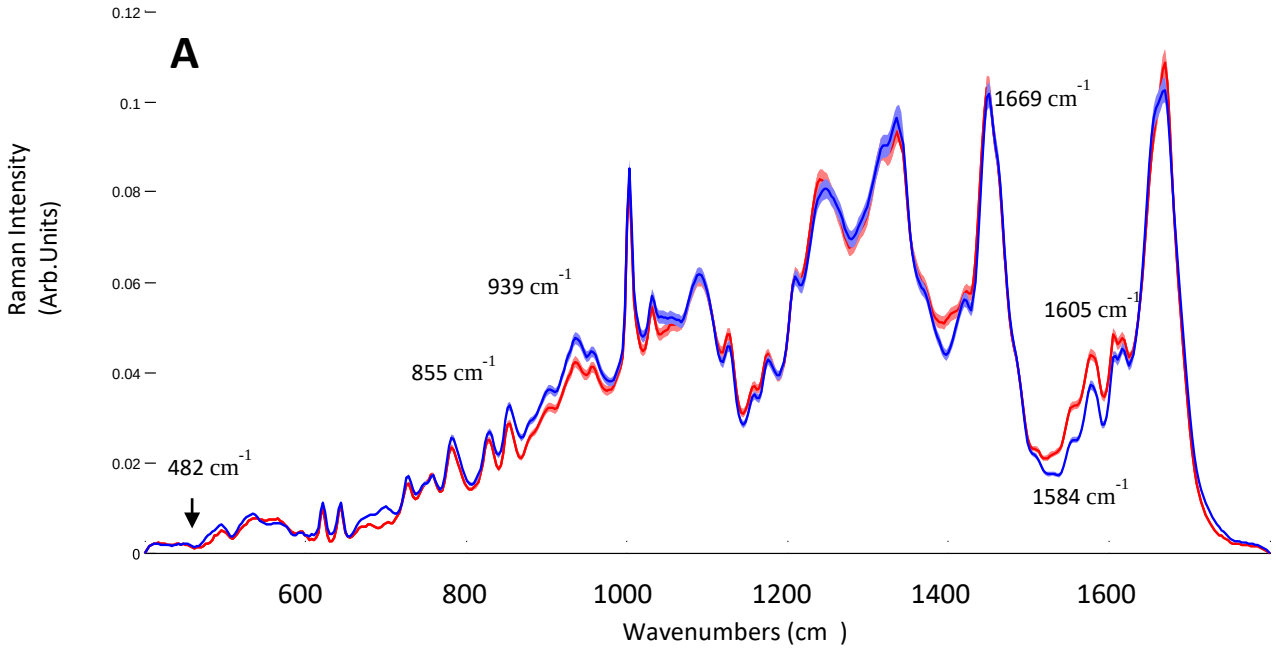

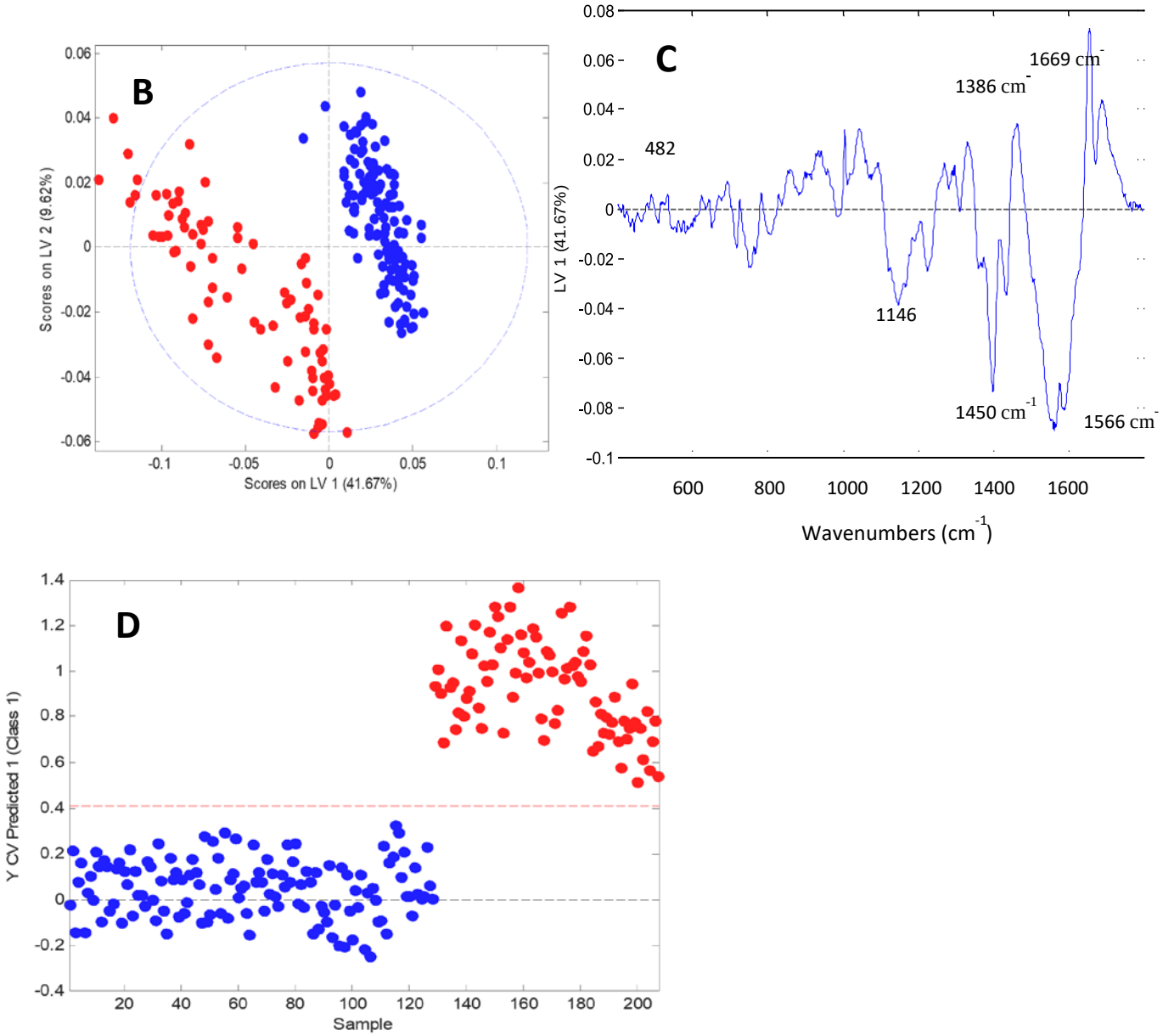

Figure 3.4 (A) Mean Raman spectra from HC positive and HC negative cells. Shading denotes the standard deviation, (B) LV scatter scores plot of HC negative (blue) and HC positive (red), (C) LV1 loadings, (D) PLSDA prediction plot.

3.3.5 Phase of Menstrual Cycle vs High Grade Dyskaryosis

It is important to determine if the changes observed throughout the menstrual cycle as seen in Figure 3.2(A) would affect the ability of Raman spectroscopy to discriminate HSIL from normal cells affected by the normal maturation of the cervical epithelium controlled by both the rise and fall of progesterone and oestrogen. For this part of the study, spectra from HSIL cells Figure 3.5(A) were recorded from 15 HPV positive, high grade dyskaryotic samples and compared to an equivalent number of spectra from negative samples from days 7-21 of the menstrual cycle, all of which were HPV negative. Figure 3.5(B) shows the mean spectra from negative samples from days 7-21 of the menstrual cycle and spectra recorded from HSIL cells. The LV scores scatterplot in Figure 3.5(C) shows that HSIL cells separate well from normal cells on the first LV. This shows that regardless of when a sample is taken during day 7-21 of the menstrual cycle, HSIL cells can still be effectively discriminated from cytology negative cells using Raman spectroscopy. Spectral changes due to the hormonal influence of oestrogen and progesterone seem to be less than the spectral changes due to the biochemical changes in the dyskaryotic cells. The loadings from LV1 in Figure 3.5(D) show that glycogen (495, 1080, 1120, 1380, 1458 cm^{-1}), nucleic acids (780 and 1487 cm^{-1}), Amide III and Amide I proteins (1239 cm^{-1} and 1669 cm^{-1} respectively) and tryptophan and phenylalanine (1605 cm^{-1}) mainly contribute towards the discrimination between normal and HSIL cells. As the HSIL cells are a result of a high risk HPV infection, the biochemical difference in glycogen, proteins and nucleic acids can be attributed to the downstream effects of the HPV infection. The predictions plot Figure 3.5(E) from the PLSDA model shows excellent classification of the negative samples (all menstrual cycle phases) and the dyskaryotic samples with sensitivity of 98% and a specificity of 97%. However even with a high sensitivity and specificity between the menstrual cycle and dyskaryotic cells, recording from dyskaryotic cells is not efficient for Raman spectroscopy due to the minimal number of dyskaryotic cells present per sample and the difficulty in locating and recording from them.

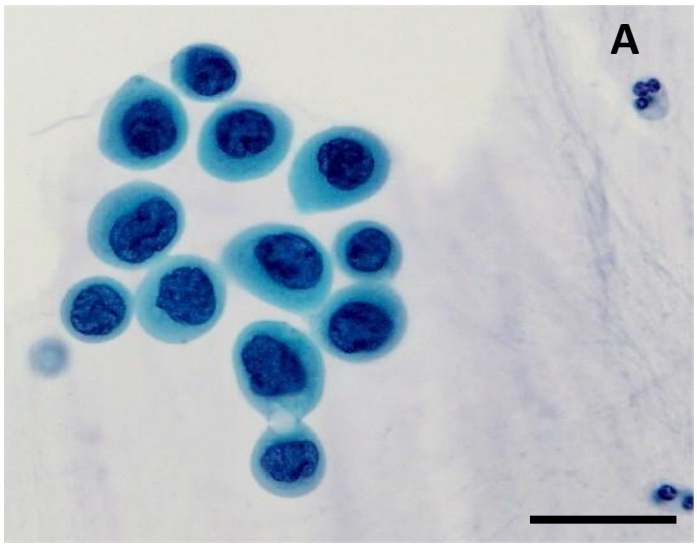
A

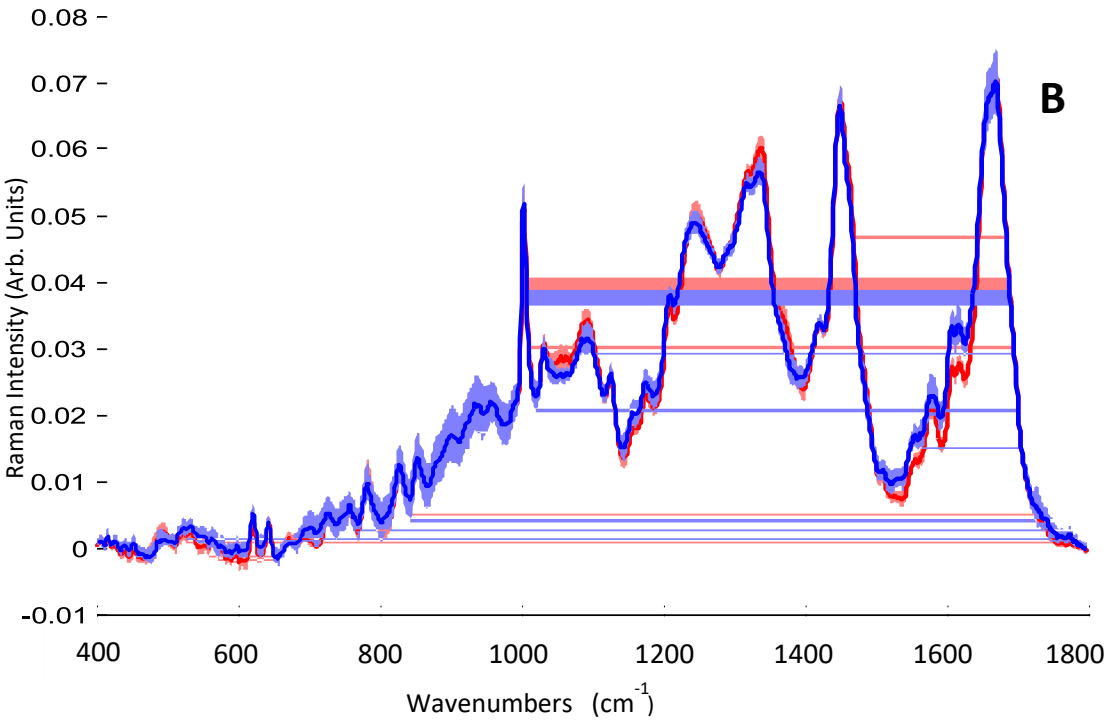
B
Raman Intensity (Arb. Units)
0.08
0.07
0.06
0.05
0.04
0.03
0.02
0.01
0
-0.01
400
600
800
1000
1200
1400
1600
1800
Wavenumbers (cm-1)

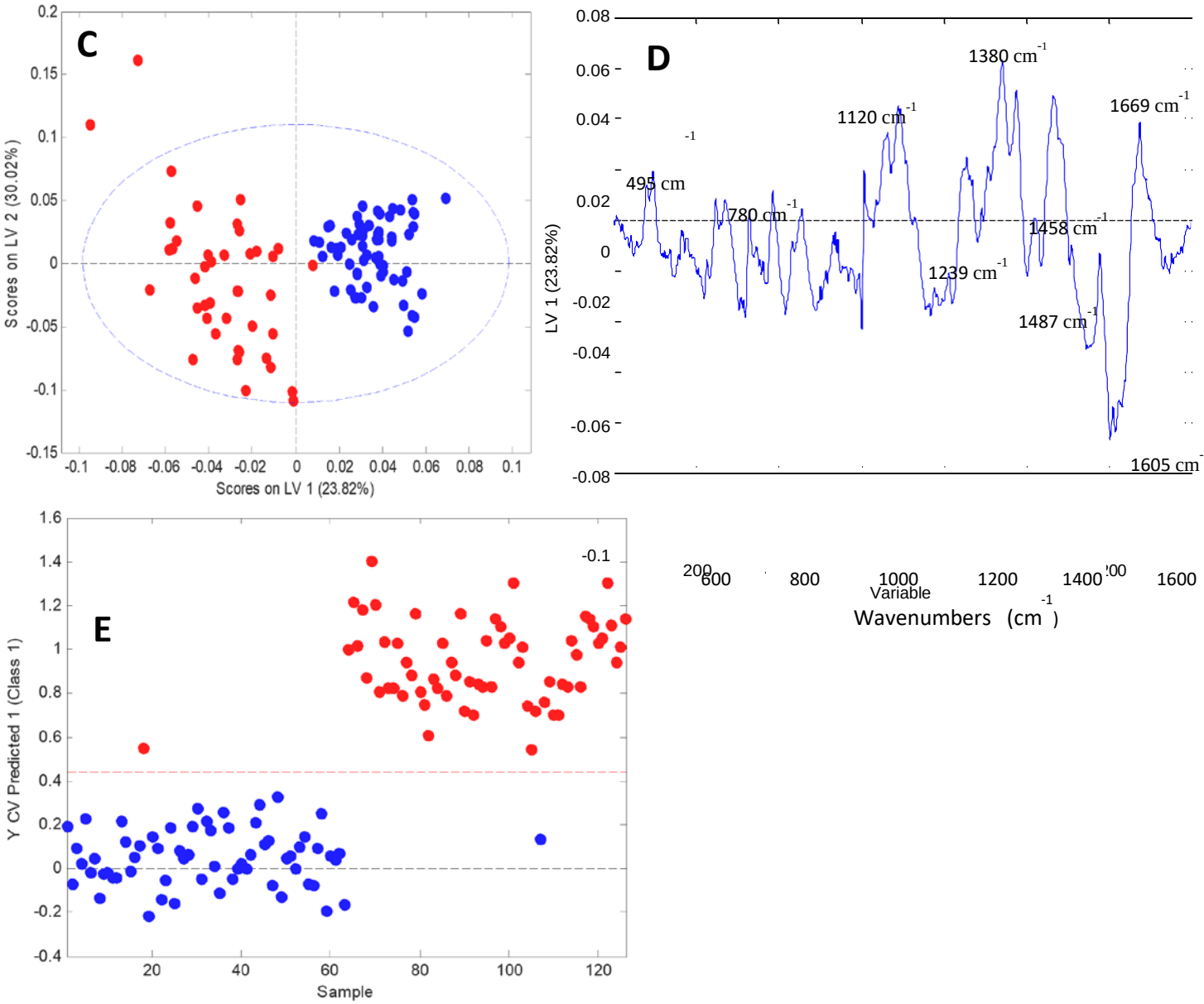

Figure 3.5 (A) Pap stained HSIL cells. Bar = 35 µm, (B) Mean Raman spectra from negative samples from days 7-21 of the menstrual cycle (red) and spectra from HSIL positive samples (blue). Shading denotes the standard deviation, (C) LV scores scatter plot of HSIL positive samples (red) and negative samples (blue), (D) LV1 loadings, (E) PLSDA prediction plot.

3.3.6 HC positive samples vs High Grade Dyskaryosis

It is important to determine if the use of HC will also affect the ability of Raman spectroscopy to discriminate normal HC positive cells from HSIL cells. Figure 3.6(A) shows the mean Raman spectra of HC positive negative samples and spectra from HSIL cells. The LV scores scatterplot in Figure 3.6(B) shows that spectra from HC positive samples separate from spectra from HSIL cells from high grade dyskaryotic samples on the first LV component with minimal overlap. Figure 3.6(C) shows the LV1 loadings which indicate that the main differences between the HC positive cells and HSIL cells are very similar to those found for the HC negative and high grade dyskaryotic samples. Glycogen (482, 1261 and 1381 cm^{-1}), nucleic acids (781 cm^{-1}), and proteins (1450, 1560 and 1669 cm^{-1}) again contribute towards the discrimination. As before, it appears that the overtaking of the host cell machinery by HPV causes more of a biochemical change within the cell than the biochemical changes associated with the use of HC. Our results are backed up by a study conducted by (Daniel et al., 2017) which used a linear combination of non-negative least squares from the main biochemicals associated with tissue and cell composition and confirmed that nucleic acids, glycogen and protein were the main discriminating factors between negative and HSIL.

The predictions plot from the PLSDA model shows excellent classification of the negative samples (HC positive) and the HSIL cells from high grade dyskaryotic samples Figure 3.6(D) with sensitivity of 96% and specificity of 98%.

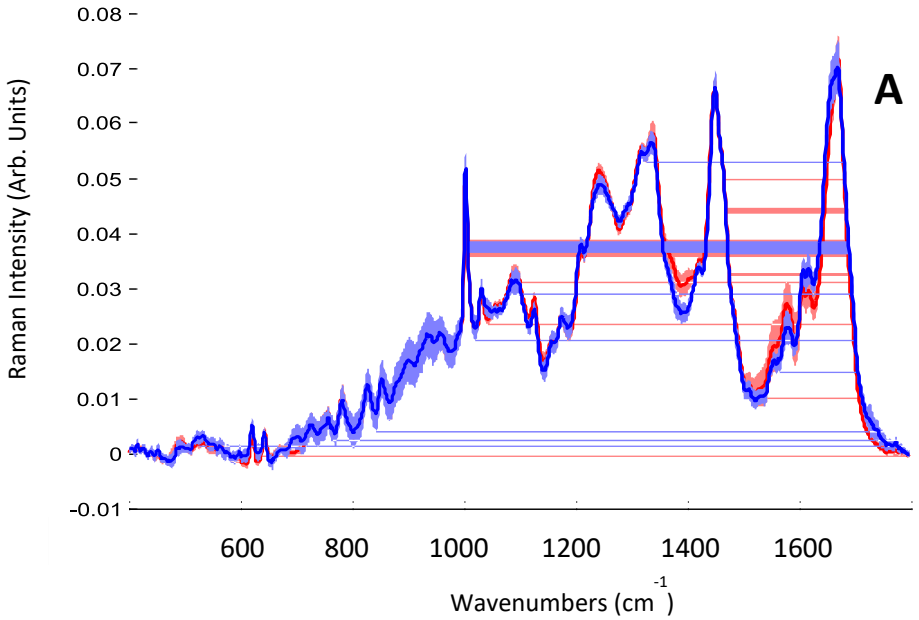

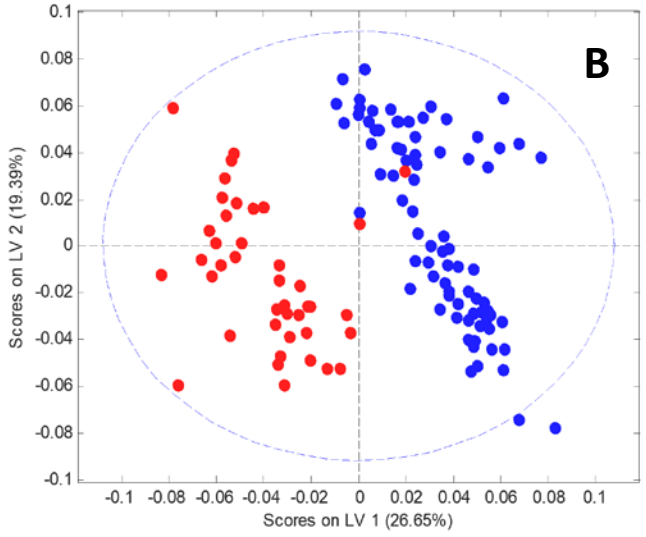

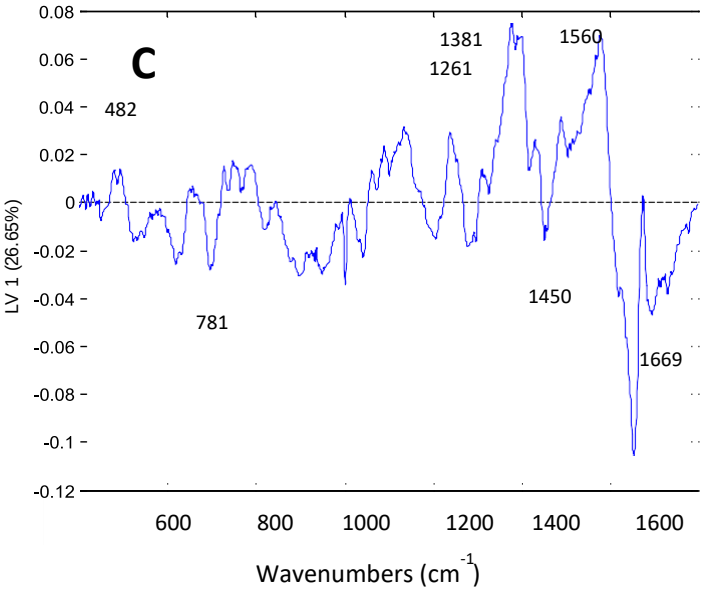

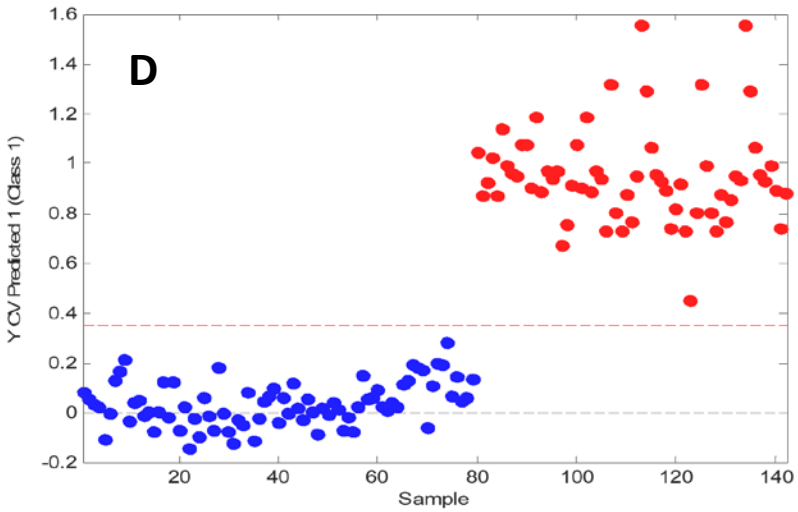

Figure 3.6 (A) Mean Raman spectra from negative HC positive samples (red) and spectra from HSIL cells (blue). Shading denotes the standard deviation, (B) LV scores scatter plot of HSIL samples (red) and negative HC positive samples (blue), (C) LV1 loadings, (D) PLSDA prediction plot.

3.4 Discussion

This study has shown that the day a Pap smear is taken during days 7-21 of the menstrual cycle will have an effect on the spectra with regard to the level of glycogen and proteins. It should be noted, however, that this study assumes that each patient recruited follows the standard 28 day cycle, and that the patient details recorded for each sample were correct. It is possible for women have a longer or shorter cycle, hence this variation may have influenced our analysis. Postmenopausal samples represent a problem for Raman based screening due to their lack of cellular material and presence of cellular debris and mucus.

The use of HC causes the most variability. Further study would be required to determine which hormone is causing the discrimination between HC positive and HC negative samples. These findings suggest that the use of oral contraceptives and the day on which the Pap smear was taken during the menstrual cycle should be incorporated into the data analysis to reduce variability between patient samples. Incorporating this effect into our model would require us to establish a standard effect of the various types of HC used within the population to identify any specific changes associated with a particular type/brand. For example a pure oestrogen and a pure progesterone based HC might produce different effects particularly related to the level of glycogen present within the cells as progesterone promotes sub-nuclear glycogen accumulation. Once the standard effect of all HC was established it would then be used to set a new baseline for the various molecular components (glycogen, Amide I etc) that could be used to distinguish normal from dyskaryotic cells. Our results can be backed up by other studies (Kanter *et al.,* 2009) which showed that hormonal status influences Raman spectra from the cervix *in vivo* and that incorporating hormonal status into their classification algorithm increased the accuracy from 88% to 94%. Despite this, however, the variability between days of the menstrual cycle or use of HC did not hinder the ability of Raman spectroscopy to discriminate cytology negative cells from HSIL cells. The biochemical changes induced in HSIL cells due to an active HPV infection were more pronounced than the biochemical changes

due to the menstrual cycle or the use of hormone based contraceptives. This makes sense given that that a chronic HPV infection alters cell cycle regulation, transcribes viral oncogenes and is producing and shedding HPV virons (Johansson C *et al.*, 2012) thus altering the biochemical signature of the infected cells when compared to normal/negative cells. However, going forward, it would not be practical to try and record spectra from these HSIL cells due to time constraints and the minimal number of cells present per sample.

3.5 Conclusion

This study highlights the scope of Raman spectroscopy for cervical screening despite the presence of biochemical changes associated with the menstrual cycle and the use of HC. It is acknowledged that the study is limited in focussing only on HSIL positive samples and a further study would be required to include low grade (LSIL) samples.

Chapter 4

Improved removal of blood contamination from Thinprep cervical cytology samples for Raman spectroscopic analysis

Adapted from: Traynor D, Kearney P, Ramos I, Martin CM, O'Leary JJ, Lyng FM. Improved removal of blood contamination from Thinprep cervical cytology samples for Raman spectroscopic analysis *J. Biomed. Opt.* **23**(5), 055001 (2018)

4.1 Introduction

The most common method for cervical screening is based on the Papanicolaou test (Pap test) which is designed to screen for signs of pre-cancer and cancer of the cervix. The Pap test requires cells to be scraped from the cervix, fixed to a glass slide, stained and reviewed by a trained cytologist. Cellular abnormalities are identified based on cellular morphology and staining characteristics and classified according to the degree of dysplasia. The ThinPrep liquid based cytology method involves the patient's cells being transferred into a specimen vial containing PreservCyt transport medium. PreservCyt is an alcohol based solution that preserves cell morphology and breaks down biological components such as mucin and blood. The normal smear pattern is made up of epithelial and non-epithelial components (Figure 4.1(A)). The epithelial cell components include parabasal cells, intermediate cells, superficial cells, endocervical and endometrial cells. Non-epithelial cell components include red blood cells, lymphocytes, histiocytes, polymorphs, mucus and bacteria. Red blood cells are 7-8 μm in size and stain red or pink with the Pap stain. They are often found in cervical samples, either due to menstruation or inflammation and their presence can also be used as an indicator of disease (pre-cancer)(Kitchener *et al.*, 2011). A patient's cervix with a high grade lesion will often bleed on contact with the cervical brush and as a result the smear becomes contaminated with blood. The presence of blood in the sample will often dilute diagnostic cells, cover and surround cell groups, increase screening time and make microscopic interpretation difficult (Figure 4.1(B)). PreservCyt contains a lysis agent for mucus and red blood cells but excessive blood in the sample vial will prevent a satisfactory smear being produced. High volumes of red blood cells will prevent the collection of epithelial cells onto the polycarbonate filter membrane during processing resulting in a ringed halo effect with red blood cells deposited mostly around the edges of the smear with very few epithelial cells present (Figure 4.1(C)).

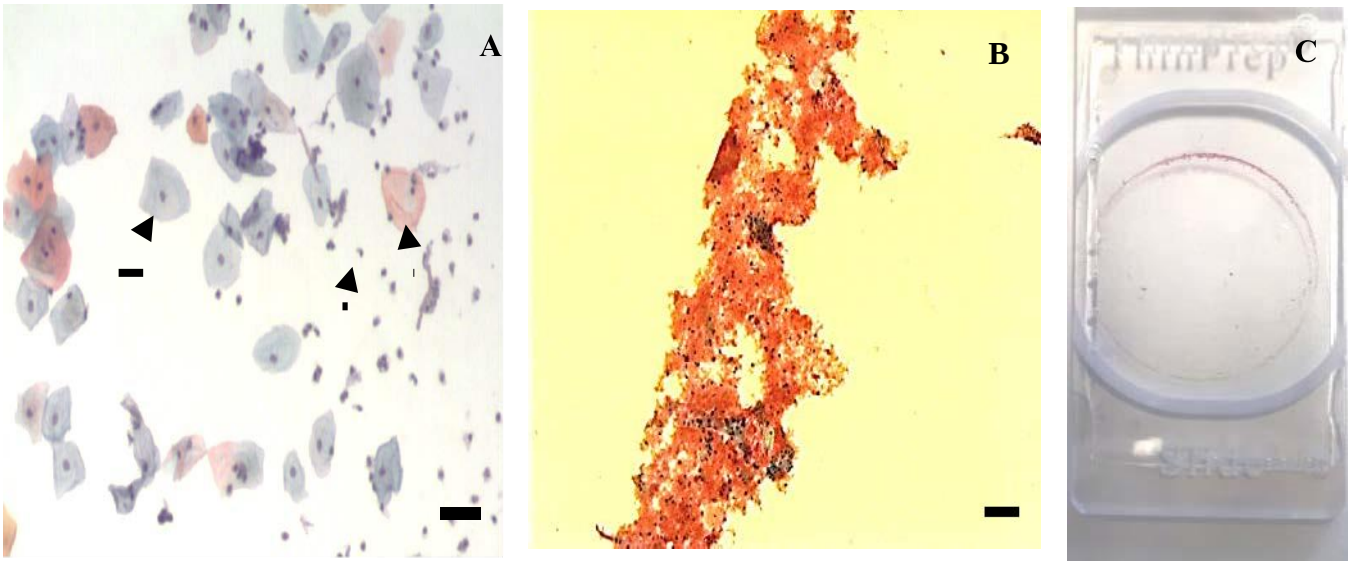

Figure 4.1 (A) Pap smear after staining. Note the presence of intermediate (blue), superficial (pink) cells and lymphocytes (indicated by arrows), (B) Bloody smear pattern with red blood cells, obscuring diagnostic cells. Bar = 35 μm. (C) Pap smear contaminated with blood showing ringed halo effect.

Cytology laboratories often annotate Pap smears according to a blood scale index whereby 0 indicates no visible evidence of blood present and 3 indicates an extremely bloody sample (Figure 4.2). Samples presenting as a 2 or 3 on the blood scale are often either rejected as being unsatisfactory or treated with a wash solution to lyse more of the red blood cells to increase the number of epithelial cells present on the slide. This blood scale grading is subjective and is only based on a visual appearance of a sample. The advantage of the Pap test is that it is a widely accepted screening based test. However, despite a high specificity of 96.5%, a lower sensitivity of 85% can be due to sampling, technical and inter-observer errors associated with the subjectivity of the test (Kitchener *et al.*, 2011). Over the past 20 years, Raman spectroscopy has shown potential for the diagnosis of cervical cancer both *in vivo* and *ex vivo* (Utzinger *et al.*, 2001, Mahadevan-jansen, 2010, Mo *et al.*, 2009, Duraipandian *et al.*, 2012, Kong *et al.*, 2015,Santos, et al 2017). Raman spectroscopy is based on inelastic light scattering in which a sample is illuminated by monochromatic laser light and interactions between the incident photons and molecules in the sample result in the scattering of the light. The coupling of the light generates vibrations within the sample which are characteristic of the chemical structure.

The energy of the scattered light is reduced by an amount equal to the vibrational energy which is called the Raman shift. This means that the position, peaks and shape of the Raman bands carry information about the molecular makeup of the sample. The Raman spectrum of cells and tissues is made up of contributions from many biochemical components including DNA, RNA, proteins, lipids and carbohydrates (Santos et al 2017) To date, most likely due to confounding factors such as blood contamination, there have been relatively few studies on Raman spectroscopy of cervical smear samples (Lyng *et al.*, 2015, Diem *et al.*, 2013, Vargis *et al.*, 2012, Rubina et al, 2013, Bonnier *et al.*, 2014, Ramos, et al 2015, Kearney *et al.*, 2017). Rubina et al described the influence of blood on the Raman spectra of cervical cell pellets and how this might lead to false interpretations. Classification efficiency of 86% and 84% was reported for normal and abnormal samples respectively and this decreased to 78% and 79% after samples were treated with red blood cell lysis buffer to reduce blood contamination. A previous study by our group (Bonnier *et al.*, 2014) addressed many of the issues involved in recording Raman spectra from liquid based cytology (ThinPrep) samples and described a new method to remove blood contamination before Raman spectroscopy based on pre-treatment of the slides with hydrogen peroxide. This was shown to minimise variability and to result in the collection of highly reproducible data with excellent discrimination between negative and high grade samples. However, only blood scale 0 and blood scale 1 samples were used for this study as the treatment was not found to be effective for excessively contaminated blood scale 2 and 3 samples. (Kerr et al.,2016) investigated the effect of blood contamination on Raman spectra of urine cytology samples. They determined that spectra recorded from samples with a low level of blood appeared free from contamination due to the effective removal of many of the red blood cells using the lysing agent CytoLyt. However, for excessively bloody samples several additional Raman peaks associated with blood were observed leading to the conclusion that excessively bloody samples are not suitable for diagnostics with Raman micro-spectroscopy. The aim of

the present study was to extend our previous study (Bonnier *et al.*, 2014) to samples annotated as blood scale 2-3 which would have previously been excluded, to investigate if these excessively bloody samples could be treated to render them suitable for Raman spectroscopy.

Figure 4.2ThinPrep vials graded according to the blood scale index. 0 indicates no visible evidence of blood and 3 indicates an extremely bloody sample

4.2 Materials and Methods

4.2.1 Samples and blood treatment

The Coombe Women and Infants University Hospital (CWIUH), Dublin Ireland, for spectroscopic analysis with the final clinical report prepared by the cytologist and / or pathologist, provided cervical liquid based cytology (LBC) samples. This study was approved by the Research Ethics Committee at the Coombe Women and Infants University Hospital. A set of 30 samples were selected, 15 high grade intraepithelial neoplasia (HG) samples which received a cervical intraepithelial neoplasia (CIN) 2 or CIN 3 result on their associated biopsy from pathology and 15 negative samples (TN) which received a negative result from cytology. All cytology samples were evaluated by eye according to the blood scale index and annotated as being either a grade 0, 1, 2 or 3. All samples were tested for HPV as outlined in section 2.2.1-2.2.2. All negative samples (TN) tested negative for the presence of HPV DNA and mRNA. All HG samples tested positive for both HPV DNA and mRNA.

HeLa cervical cancer cells were also prepared and fixed as for Thinprep samples in PreservCyt. These samples were seeded with blood to mimic excessively bloody cytology samples. This was achieved by adding blood to the samples until they visually represented a blood scale 2-3 index sample.

Each Thinprep sample vial was mixed for 3 minutes to break up cellular clumps. The sample was then poured into a 50 ml centrifuge tube and centrifuged for 5 minutes at 300 rpm. The supernatant was removed and 1 ml of H_2O_2 was added and mixed for 30 seconds. 20 ml of PreservCyt was added to neutralise the H_2O_2. The sample was then centrifuged for 5 minutes at 600 rpm. Most of the supernatant was removed. The cell pellet was re-suspended multiple times with a 1ml pipette to break up cell clumps. 20ml of PreservCyt was then added and the contents poured back into the original vial.

4.2.2 Thinprep slide preparation

The samples were then prepared as outlined in section 2.3

4.2.3 Raman spectroscopy

All Raman analysis was performed as outlined in sections 2.5 and 2.7

4.2.4 Data pre-processing and analysis

All Raman data was pre-processed and analyzed as outlined in sections 2.7.-2.9

4.3 Results/ Discussion

Figure 4.3(A) shows an untreated Pap smear, blood scale 3. The slide was coated in blood and cellular debris. Figure 4.3(B) shows Raman spectra recorded from 5 cells present on the slide. Overall very few cells were present and often burned on contact with the laser. A high background was observed together with Raman bands associated with blood at 754, 1311, 1374, 1398, 1588, 1640 cm^{-1}. The high background can be attributed to the cellular debris or a sub unit of the oxidized hemoglobin on the surface of the cell nuclei which has a weak fluorescence signal. When a sample fluoresces the fluorescing photons can be detected by the photon detector in the Raman spectrometer overwhelming the weaker Raman signal and obscuring the Raman peaks. Figure 4.3(C) shows the same sample from Figure 4.3(A) after undergoing the blood removal method. Any blood residue has been oxidised with the H_2O_2 treatment and cellular debris has been reduced allowing for high quality spectra to be recorded as demonstrated in Figure 4.3(D).

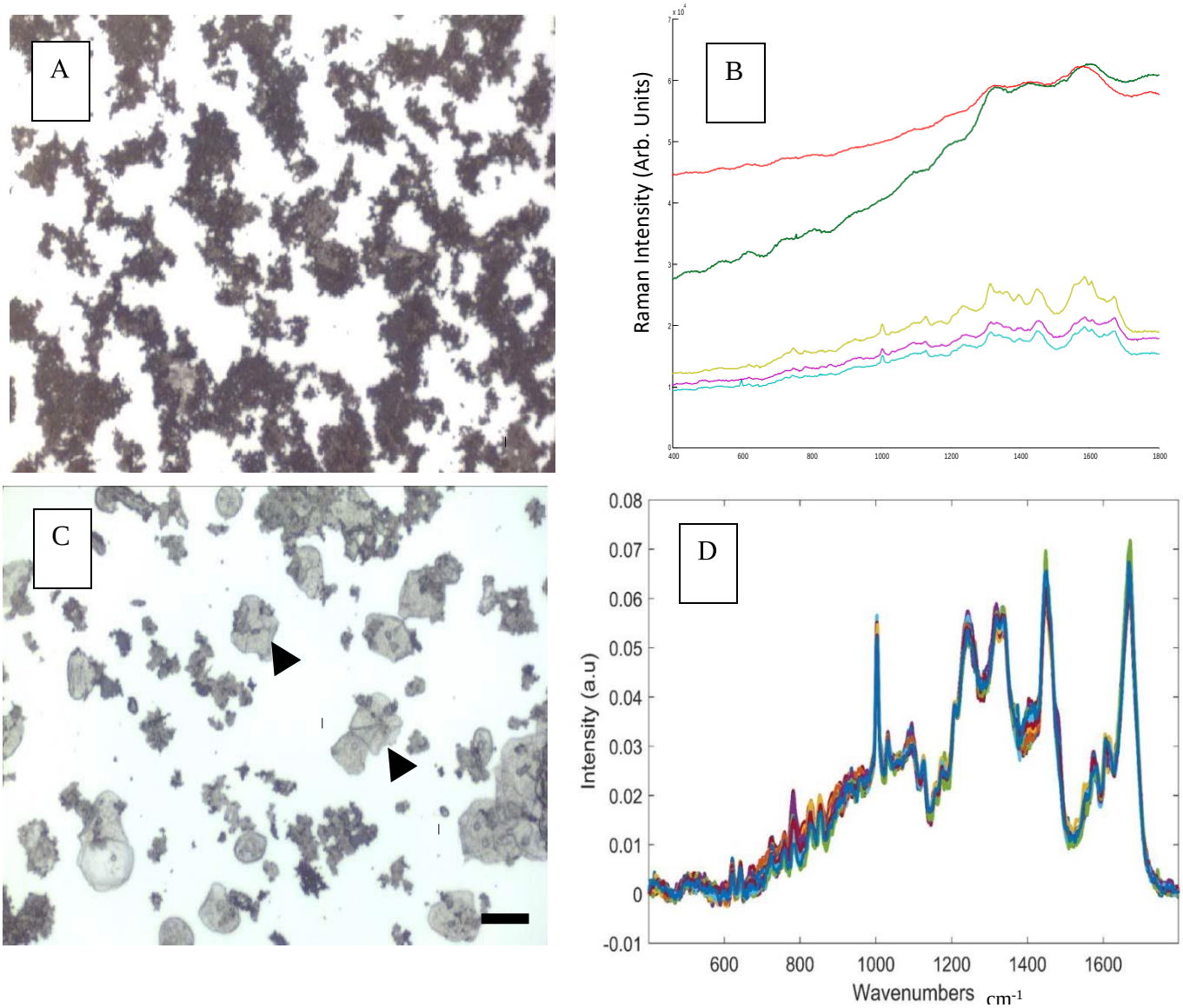

Figure 4.3 (A) Untreated Pap smear, blood scale 3 shows blood and cellular debris masking diagnostic cells. Bar = 35 μm, (B) Raw Raman spectra recorded from five cells (each colored spectrum is from an individual cell) from a untreated Pap smear (C) Treated Pap smear. Arrows indicate Intermediate cells and Superficial cells . Bar = 35 μm. (D) 25 Raman spectra recorded from individual cells (each colored spectrum is from an individual cell) on a treated Pap smear.

In order to determine if the Raman specific method of blood removal using H_2O_2 had any effect on the spectra recorded without any external confounding factors such as inflammation, HPV infection etc, the protocol was performed on HeLa cervical cancer cells. HeLa cells were seeded with blood to mimic cytology samples with blood scale index 2-3 and HeLa cells with no added blood acted as controls. Both sample types were treated with H_2O_2 and slides prepared as for the ThinPrep cytology samples. Figure 4.4(A) shows the mean Raman spectra recorded from 30 HeLa cells with and without blood contamination (blood scale 2-3) and treated with H_2O_2. The mean spectra display strong similarities with only minor changes at 1242 cm^{-1} (Amide III), 1350 cm^{-1} (DNA/RNA, CH def. in proteins and carbohydrates), 1430 cm^{-1} (protein, lipids), and 1669 cm^{-1} (Amide I). Figure 4.4(B) shows the mean Raman spectra of negative cytology samples (TN) with and without blood contamination (blood scale 2-3) and treated with H_2O_2. The mean spectra display strong similarities with small changes at 1242 cm^{-1}, 1350 cm^{-1}, 1430 cm^{-1} and 1669 cm^{-1} as observed for the HeLa cells. These small changes in the spectra were consistent throughout all samples tested including the HG samples (Figure 4.4(C)).

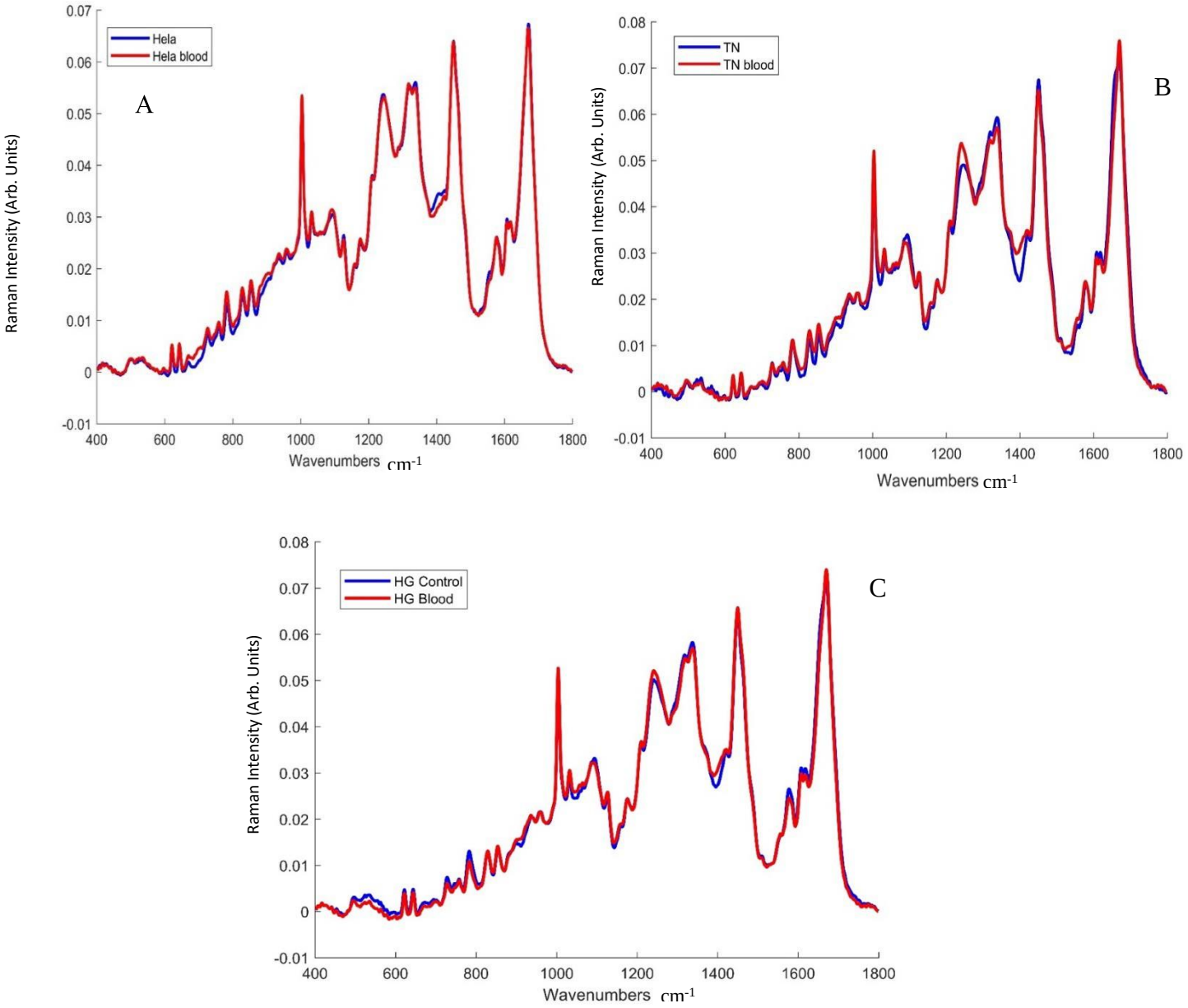

Figure 4.4 (A) Mean Raman spectra of HeLa cervical cancer cells treated with blood (blood scale 2-3) and subsequently treated with H_2O_2 (red) and HeLa cervical cancer cells not treated with blood but treated with H_2O_2 (blue), (B) Mean Raman spectra of true negative samples (TN), blood scale 2-3, treated with H_2O_2 (red) and blood scale 0, treated with H_2O_2, (C) Mean Raman spectra of high grade (HG) samples, blood scale 2-3 treated with H_2O_2 (red) and blood scale 0, treated with H_2O_2.

PLSDA classification of negative cytology samples and high grade cytology samples, blood scale index 0, is shown in figure 5. Figure 4.5(A) is a latent variables (LV) scores scatter plot of LV1 and LV2 which shows good discrimination along LV1. The loadings shown in figure 4.5(B), show that the discrimination is based around Raman peaks at 482, 851, 936, 1128, 1338, 1449, 1572, 1655 and 1669 cm^{-1} which are mainly related to DNA, proteins and glycogen. Figure 4.5(C) is a PLSDA prediction plot showing good classification of negative and high grade samples with a sensitivity of 92% and a specificity of 93% (Table 4.1).

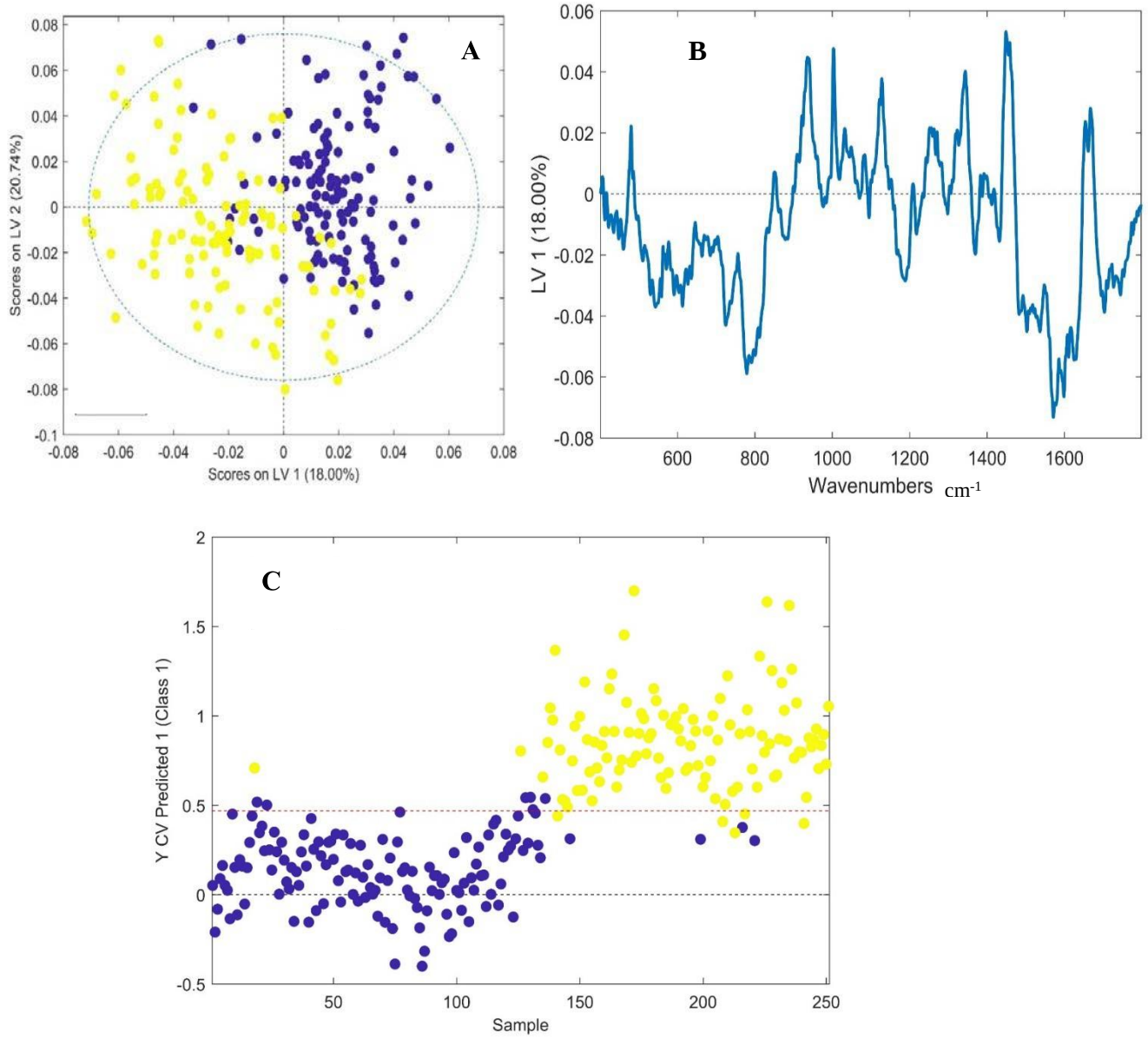

Figure 4.5 (A) LV score scatter plot of 136 spectra acquired from 15 TN samples and 136 spectra acquired from 15 HG samples (blood scale index 0), (B) LV 1 loadings, (C) PLSDA prediction plot showing good discrimination between TN (blue) and HG (yellow) ThinPrep cytology samples.

PLSDA classification of TN and HG cytology samples, blood scale index 2-3, is shown in Figure 4.6. Both negative and high grade samples have undergone the Raman specific blood removal method. Figure 4.6(A) is a LV scores scatter plot of treated TN and HG samples which show overlap between the samples. The LV1 loadings shown in figure 4.6(B), shows that the discrimination is based around Raman peaks at 482, 549, 851, 936, 1145, 1182, 1237, 1338, 1449,1576, and 1669 cm^{-1} and are similar to the loadings shown in figure 4.5(B). The PLSDA prediction plot is shown in figure 4.6(C) and has a sensitivity of 89% and a specificity of 88% (Table 4.1).

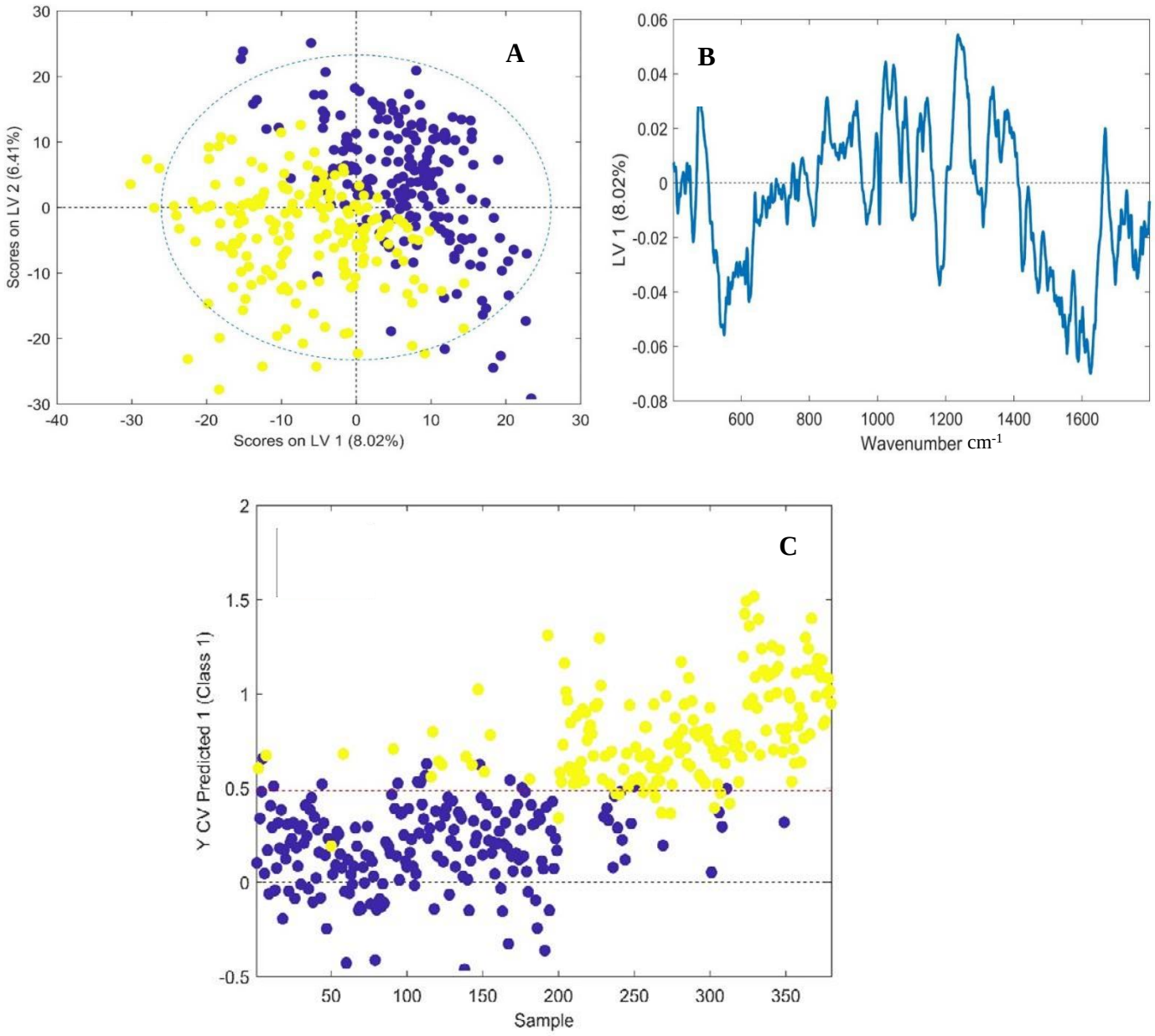

Figure 4.6 (A) LV score scatter plot of 185 spectra acquired from 15 TN cytology and 185 spectra acquired from 15 HG cytology samples (blood scale index 2-3), (B) LV1 loadings. (C) PLSDA prediction plot showing some discrimination between TN (blue) and HG (yellow) Thinprep cytology samples, blood scale 2-3 and treated with H_2O_2.

In order to determine if excessively bloody samples could be treated the same way as non-bloody samples in terms of data analysis, the Raman spectral data from the two groups (blood scale 0 and blood scale 2-3) was combined. Figure 4.7(A) shows the LV scores scatter plot which highlights decreased discrimination between TN and HG cytology. However the loadings shown in Figure 4.7(B) remain similar to the loadings shown in figure 4.5(B) and 4.6(B) with Raman peaks at 482, 851, 1129, 1184, 1251, 1338, 1449, and 1669 cm^{-1}. The PLSDA prediction plot is shown in Figure 4.7(C) and has a sensitivity of 82% and a specificity of 87% (Table 4.1).

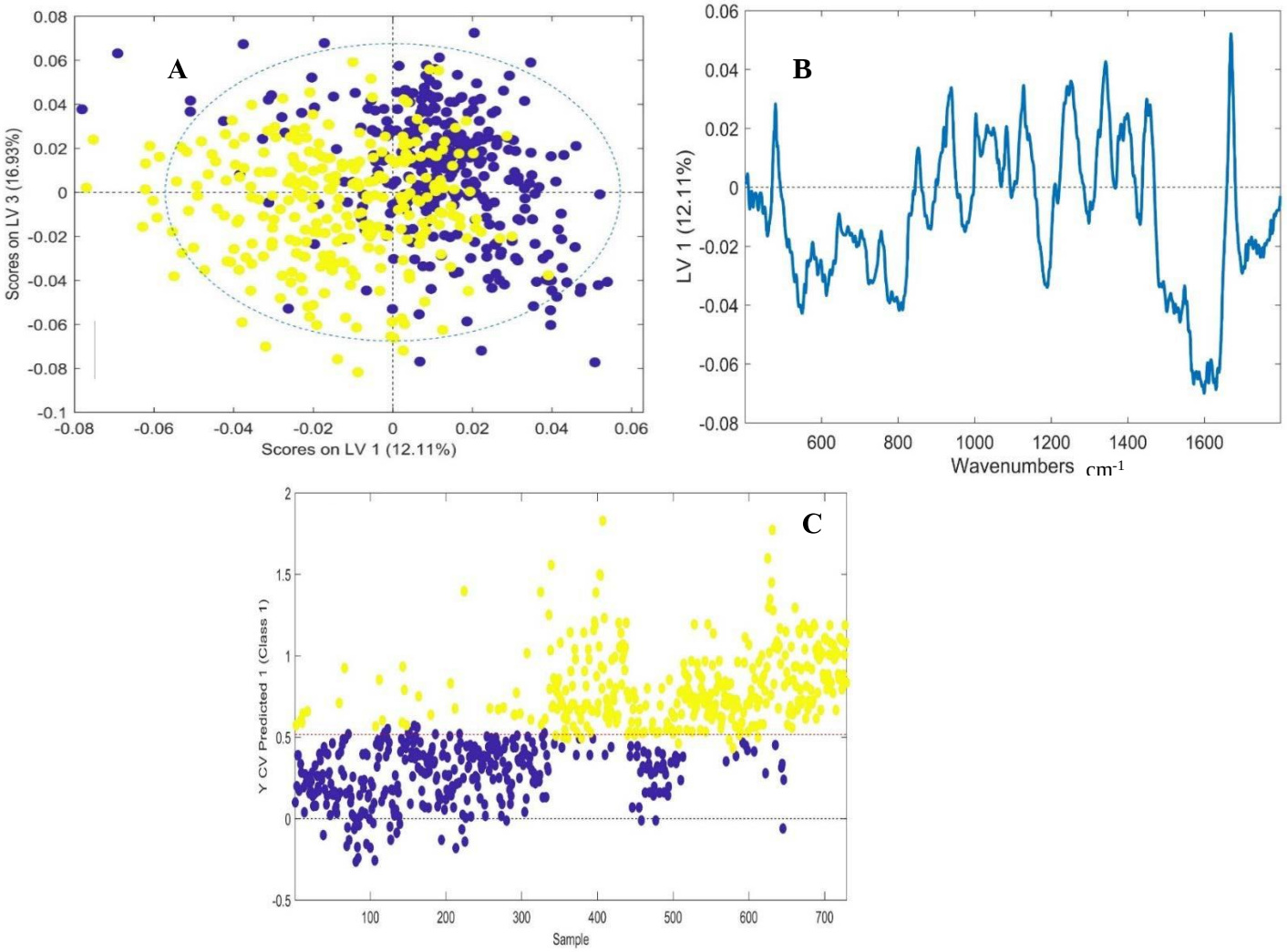

Figure 4.7 (a) LV score scatter plot of 321 spectra from TN cytology and 321 spectra HG cytology samples (combined blood scale 0 and blood scale 2-3), (b) LV1 loadings. (c) PLSDA prediction plot showing some discrimination between TN (blue) and HG (red) Thinprep cytology samples, combined blood scale 0 and blood scale 2-3 and treated with H_2O_2

Table 4.1 Sensitivity and specificity from PLSDA classification of TN and HG cervical cytology samples with and without blood contamination and combined.

	Sensitivity	Specificity
Negative Vs High Grade (blood scale 0)	92%	93%
Negative Vs High Grade (blood scale 2-3)	89%	88%
Combined (blood scale 0 and 2-3)	82%	87%

Interestingly, the loadings (482, 851, 936, 1149, 1338 and 1669 cm^{-1}) remain almost the same between all three data sets, blood scale 0, blood scale 2-3 and combined, confirming that glycogen, DNA and proteins are the main discriminating features between negative cytology and high grade cytology samples regardless of blood contamination. As previously stated, HPV can integrate its viral DNA into the host cell's DNA located in the cell nucleus resulting in the transcription of its viral oncogenes and control over the cell's life cycle. This results in increased proliferation which would alter protein, glycogen and nucleic acid levels present within the cell. However, as mentioned earlier, some spectral features undergo minor changes following the blood removal method. As these features overlap with the discriminating features, this results in a reduction in classification efficiency when excessively bloody (blood scale index 2-3) samples and non-bloody samples (blood scale index 0) samples are combined for analysis. Comparing sensitivity and specificity of the test groups shows that blood scale 0 samples with no blood contamination performed best with a sensitivity of 92% and specificity of 93% when compared to excessively bloody blood scale 2-3 samples which had a sensitivity of 89% and specificity of 88%. Combining the blood scale 0 and blood scale 2-3 samples for analysis resulted a sensitivity of 82% and specificity of 87%. The high specificity indicates a good ability to accurately exclude negative samples (few false positives), however the reduction in sensitivity indicates a reduced ability to accurately detect high grade samples and an increased likelihood of false negatives.

Despite the reduction in classification efficiency, the values are higher than previously reported for samples with blood contamination. Rubina *et al*. (2013) reported a classification efficiency of 78% and 79% for normal and abnormal bloody samples treated with red blood cell lysis buffer. As far as it is reported this study did not attempt to combine both treated and non-treated samples together to improve their sensitivity and specificity. In addition, Kerr *et al.* (2016) concluded that excessively bloody samples were not suitable for diagnostics with Raman spectroscopy.

4.4 Conclusion

This study demonstrates for the first time that excessively bloody (blood scale 2-3) Thinprep cervical smear samples can be used for diagnostics with Raman spectroscopy following a hydrogen peroxide treatment in the collection vial. However, the presence of excessive blood contamination (blood scale index 2-3) did result in reduced in sensitivity and specificity for classification of negative and high grade samples. A higher sensitivity and specificity could be achieved by keeping excessively bloody samples separate from non-bloody samples for analysis. Although this study has focused only on cervical cytology samples, thyroid, urine and serous fluid cytology samples may also benefit from such an approach for Raman spectroscopic analysis. Serous fluid for cytological examination are often contaminated with a high level blood (pericardium, pleura and peritoneum fluids) and often require additional treatment methods such a density gradient technique to remove red blood cells which can result in a loss of diagnostic cellular material. The application of our blood treatment method would prevent this loss of material and allow Raman spectroscopy to be performed.

While these results are promising for the development of Raman spectroscopy for cervical cancer screening, Raman spectroscopy in its current form does not have the ability to replace cytology for cervical cancer screening However it could be used to supplement the Pap test or as a possible new triage test after HPV testing.

Chapter 5

The potential of biobanked liquid based cytology samples for cervical cancer screening using Raman spectroscopy.

Adapted from: Traynor, D. (2019)The potential of biobanked liquid based cytology samples for cervical cancer screening using Raman spectroscopy- J. Biophotonics.;12:e201800377.

5.1 Introduction

Every year millions of cervical Pap tests are performed throughout the world in countries for purposes of cervical screening. Most Pap tests are performed through use of liquid based cytology (LBC) where cervical cells are collected before deposition into a volume of liquid preservative. As not all the material is required for cytological assessment, the surplus, which would ordinarily be discarded, can be stored within tissue biobanks with due process of governance. Biobanks constitute a valuable source of material which may support a number of studies including those on the natural history of disease, evaluation of screening practices, vaccination effectiveness or the development of new technologies to support screening and disease management (Fox et al., 2017, Marquez-Curtis et al., 2017, Peakman et al.,2010).

Different collection media for liquid based cytology exist however one of the more common media is PreservCyt (Hologic). PreservCyt is a methanol based solution that preserves cell morphology via fixation. Fixation is routinely employed as it allows a "snapshot" of a cell's physical and biochemical state to be assessed; methanol is an organic solvent that preserves cells through dehydration and precipitation of proteins (Troiano et al., 2009). Fixation is important given that sample collection and assessment is not performed concurrently. In addition to supporting routine screening, fixation of cells also supports long term storage of residual material in biobanks.

Current methods for detection of cervical cancer and pre-cancer (CIN) are limited and there is an unmet clinical need for new screening or diagnostic tests. Recently Raman spectroscopy has shown potential as a tool for screening and diagnosis of cervical lesions and cancer (Lyng et al., 2015, Ramos et al., 2016 Rubina et al., 2015).

Due to confounding factors such as sample collection, blood contamination and sample variability, few studies have been performed using Raman spectroscopy on cervical cytology

samples and none to our knowledge have investigated the potential of utilising biobanked LBC samples. The aim of this feasibility study was to assess the utility and performance of Raman spectroscopy for the detection of CIN using biobanked LBC samples. Samples stored at -80^{o}C and -25^{o}C were assessed and the ability of Raman spectra to delineate disease from no disease was determined. Additionally, Raman spectroscopy was assessed in un-banked LBC samples as a comparator.

5.2 Methods

5.2.1 Sample collection

Two classes of samples were used for the study, classed as disease and no disease. Samples with no disease were defined as cytology negative and HPV negative whereas samples with disease were those associated with a cytological HSIL result and a histologically confirmed CIN3 result and HPV positivity according to HPV DNA and mRNA status. All samples were recruited from patients presenting at a colposcopy clinic for the first time, and had no prior history of disease. Samples were collected from each patient according to the standard operating procedure issued by Cervical Check, Ireland's national cervical cancer screening programme, and the NHS Scottish cervical screening programme. Both procedures are similar and all samples were biobanked using the same methodology.

133 samples were used in total for this study of which 64 were LBC biobanked samples; 32 with no disease (cytology negative) and 32 with disease (HSIL). Biobanked samples were provided by the Scottish HPV Archive, a research tissue biobank set up to facilitate HPV associated research.

Ethical approval for use of the samples was obtained from the East of Scotland Research Ethics Service - Tayside committee. Biobanked LBC samples used for this study had been sedimented with the cellular pellet transferred into a 4.5 ml vial for long term storage in

PreservCyt. After transit, samples were re-constituted to a volume of 20 ml fresh PreservCyt solution to resemble the original LBC specimen from which the sample was derived.

A further 64 non biobanked "fresh" LBC samples, 32 with no disease (cytology negative) and 32 with disease (HSIL), were collected in PreservCyt solution from the Coombe Women and Infants University Hospital (CWIUH), Dublin, Ireland, as part of routine cytological screening. Ethical approval for use of coded samples for the study was granted by the CWIUH Research Ethics Committee (no. 28-2014). A further 5 fresh LBC samples with disease (HSIL) were collected and split into two separate vials. One vial from each sample underwent the standard biobanking process and was stored for 3 weeks, while the other was stored at room temperature.

5.2.2 ThinPrep

The samples were prepared as outlined in section 2.3 and 2.4

5.2.3 Raman spectroscopy

All Raman analysis recorded as outlined in section 2.5-2.6 with 25 cells recorded from each sample. Cell selection was performed as outlined in section 2.5 Raman measurements.

5.2.4 Data pre-processing and analysis

Data was pre-processed and analysed as outlined in section 2.7-2.9

5.3 Results

5.3.1 -25°C Vs -80°C biobanked LBC samples

The samples stored at -25°C presented with intact cellular morphology (Figure 5.1(A)) and allowed for high quality spectra to be recorded (Figure 5.1(B)). The samples stored at -80°C presented with cell lysis, cellular debris and very little cellular material which prevented the recording of spectra (Figure 5.1(C)). One possible explanation for this, is the freeze thaw effect which is commonly used to lyse bacteria and mammalian cells. Storing cells at -80 °C in PreservCyt without any Dimethyl Sulfoxide and bring up to room temperature can cause the cells to contract during the thawing process resulting in cell lysis. As a result, only biobanked samples previously stored at -25°C were used for this study.

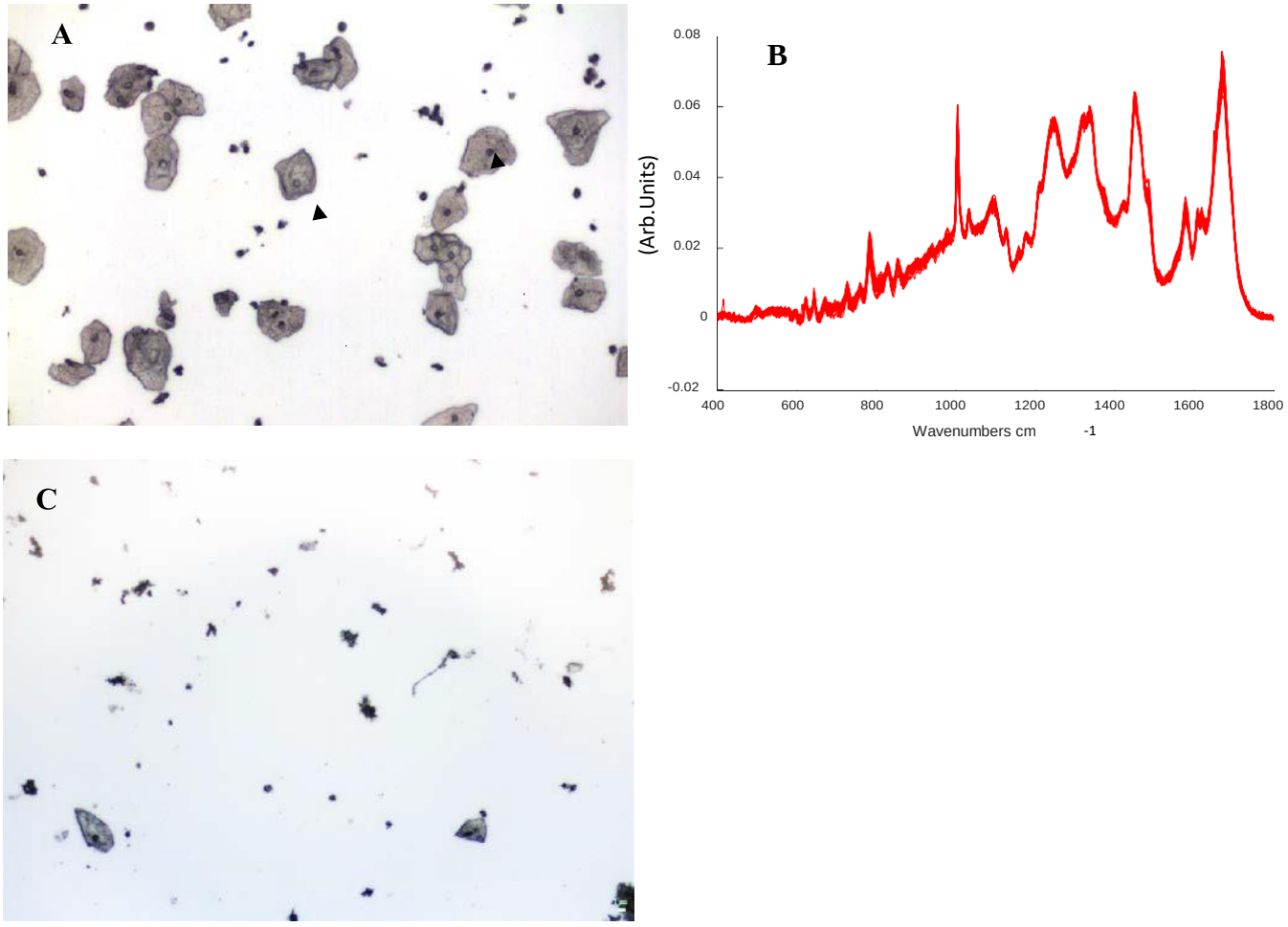

Figure 5.1 (A) Pap smears stored at -25°C present with intact cellular morphology. Note the presence of superficial and intermediate cells (arrows) on the unstained slide which were selected for Raman spectral recording. (B) High quality spectra recorded from 25 morphologically normal intermediate and superficial cells in the spectral range 400-1800cm^{-1}. (C) Pap smears stored at -80°C. Note lack of cellular material and presence of cellular debris.

5.3.2 Negative Vs HSIL (fresh LBC samples) Model

In order to determine if biobanked LBC samples could be used to discriminate no disease (cytology negative) from disease (HSIL) using Raman spectroscopy, fresh (non biobanked) LBC samples were first examined as a control. Figure 5.2(A) shows mean spectra of Negative (Red) Vs HSIL (Blue). Figure 5.2(B) is a latent variables (LV) scores scatter plot of LV1 (Blue) and LV2 (Orange) which shows good discrimination along LV1 and LV2. The loadings shown in Figure 5.2(C), show that the discrimination is based around Raman peaks at 484 (glycogen), 575 (glycogen), 881 (nucleic acids), 1004 (proteins Phenylalanine), 1139, 1238 (proteins Amide III), 1487 (proteins), 1575 (nucleic acids), 1605 (proteins) and 1669 cm^{-1} (proteins Amide I). The LV2 loadings show discrimination is based around 1238 (proteins), 1381 (glycogen), 1450 (proteins and lipids), 1642 (proteins) and 1669cm^{-1} (proteins) (see table 1.1) (Movasaghi et al.,2007). The PLSDA prediction plot shown in Figure 5.2(D) and has a sensitivity of 86% and a specificity of 90% for HSIL. Comparing these results to the results from chapter 3 section 3.3.5, which reported a sensitivity of 98% and a specificity of 97%, a slight reduction. This is mainly due to a change in cell selection. In chapter 3, spectra were recorded from morphologically abnormal cells while in chapter 5, spectra were recorded from morphologically normal cells. Abnormal cells would have a different biochemical signature due to a chronic HPV infection that cause morphological change in the cell. However, given the difficulty in locating unstained abnormal cells as previously discussed, this slight reduction in sensitivity and specificity is acceptable.

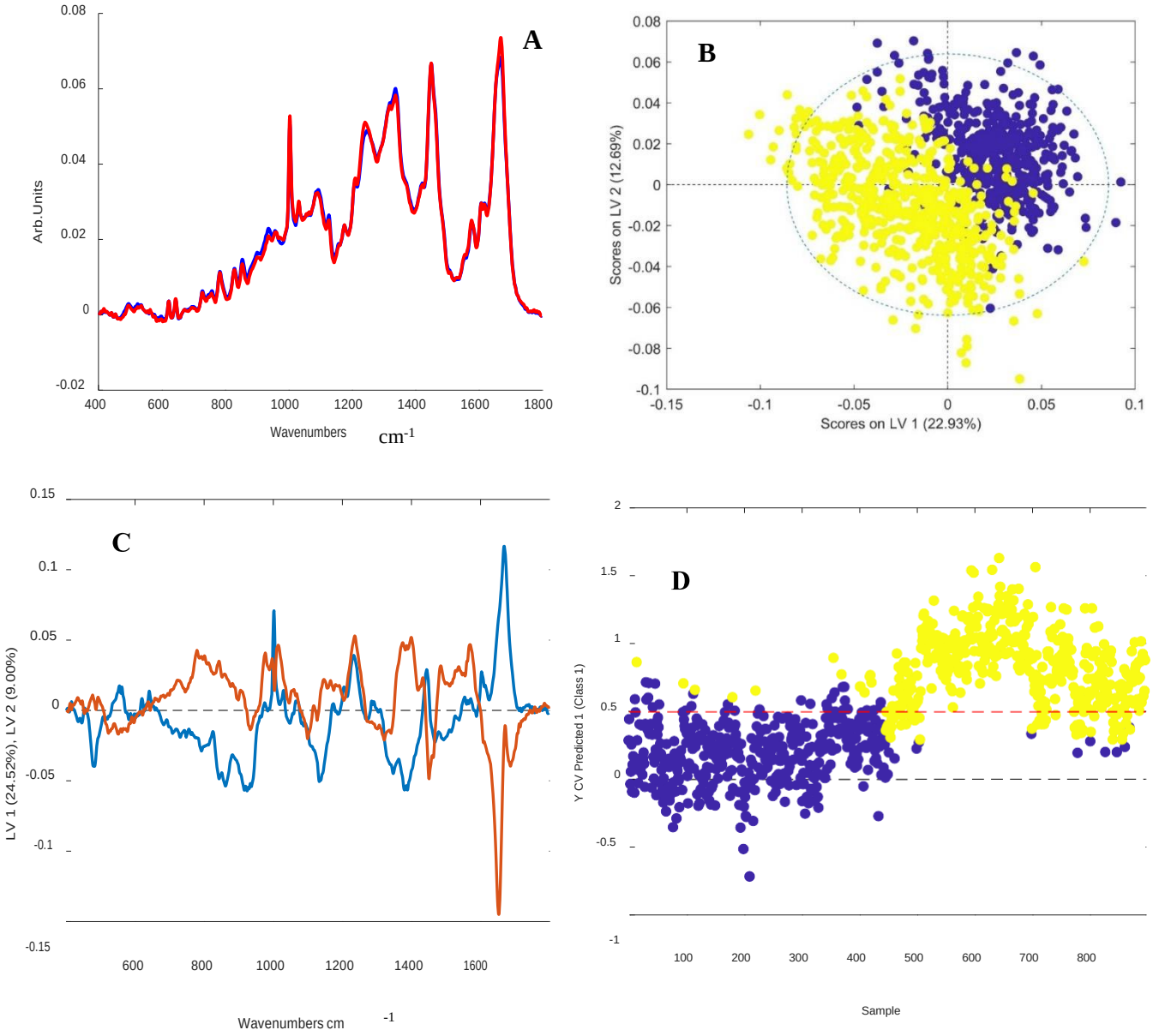

Figure 5.2 (A) mean spectra of fresh Negative (red) Vs HSIL (blue). (B) latent variables (LV) scores scatter plot of LV1 and LV2, Negative (yellow) Vs HSIL(blue). (C) LV1 (blue) and LV2 (orange) loadings (D) PLS_DA prediction plot HSIL (blue), negative (yellow) . Note some slight overlap between HSIL and Negative categories. This could be due to some **inconsistencies** in Raman recording or due to the fact that not all cells are exhibiting the biochemical signature associated with a HPV infection.

5.3.3 Negative Vs HSIL (Biobanked LBC samples) Model

In order to determine if the biobanked samples can be used in a similar fashion to the fresh samples, negative and HSIL biobanked samples were compared. Figure 5.3(A) shows the mean spectra of biobanked Negative samples Vs HSIL. Figure 5.3(B) is a latent variables (LV) scores scatter plot of LV1 and LV2 which shows good discrimination along LV1 and LV2.The loadings from LV1 are shown in Figure 5.3(C) and show that discrimination is based around Raman peaks, 622 (proteins), 640 (proteins),775 (proteins), 850 (proteins), 1122 (proteins),1152 (proteins), 1207 (proteins), 1450 (proteins), 1560 (proteins), 1605 (proteins), 1642 (proteins) and 1669 cm^{-1} (proteins). LV2 loadings show discrimination is based on 1123 (proteins, lipids, carbohydrates), 1338 (proteins) and 1605 cm^{-1} (proteins) Raman peaks assigned to phenylalanine 1004 cm^{-1} show a slight shift between 1003-1004 cm^{-1} which is most likely attributed to the methanol based fixation method which suggests a change in the conformation of the phenylalanine protein (Meade et al.,(2010). The PLSDA prediction plot shown in Figure 5.3(D) and has a sensitivity of 91% and a specificity of 92% for HSIL.

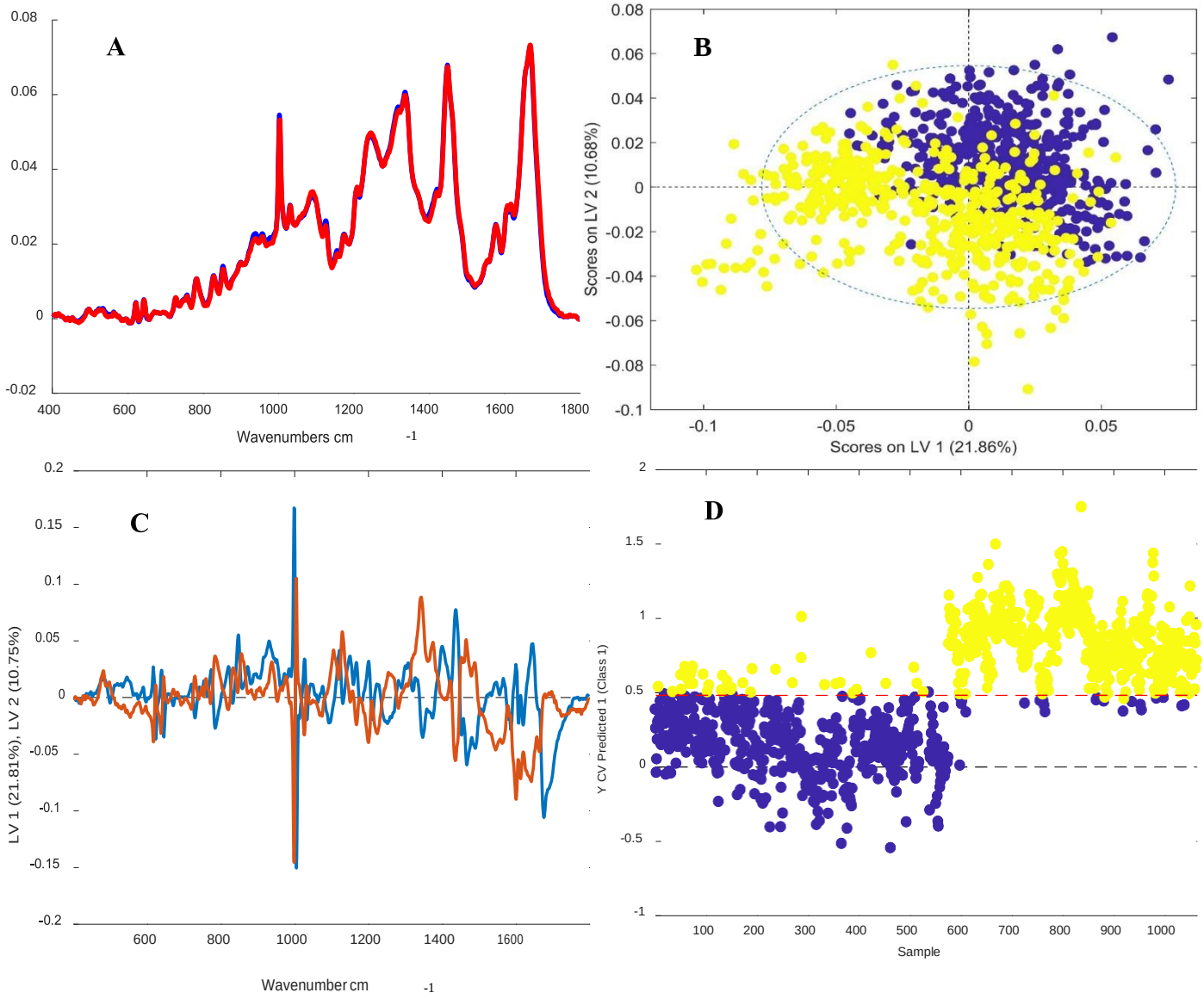

Figure 5.3 (A) mean spectra of biobanked Negative (red) Vs HSIL (blue). (B) latent variables (LV) scores scatter plot of LV1 and LV2, TN (yellow) Vs HSIL (blue). (C) LV1 (blue) LV2 (orange) .(D) PLS_DA prediction plot HSIL (blue), negative (yellow) .

5.3.4 Biobanked Vs non-Biobanked samples

Five fresh HSIL patient samples were split into two separate vials. One vial from each sample was frozen as described earlier and the other stored at room temperature. Figure 5.4(A) show the mean spectra for biobanked HSIL samples and the same samples kept at room temperature for 3 weeks after collection. The mean spectra appear identical. There does not appear to be a difference between the fresh and biobanked samples. While the mean spectra appear very similar, PLSDA can maximize the separation between the two groups and present the discrimination in the form of loadings, as outlined in section 2.8. The latent variable scatter scores plot (Figure 5.4(B)) shows slight discrimination between the sample types which is most likely due to internal sample variability (Serafin-Higuera et al., 2016) (LBC samples are variable by nature) and the low number of spectra recorded (60 for room temperature/biobanked). The PLSDA prediction plot (Figure 5.4(C)) has a sensitivity of 29% and specificity of 88% for biobanked samples indicating poor discrimination between the two groups. The low sensitivity highlights that the model was not able to separate between positive samples (biobanked) and negative samples (non-biobanked) samples. A loadings plot was not included as this would only show the internal sample variability and not any biochemical changes associated with the biobanking process. A limiting factor on this study is the low sample number, this is due to the fact that this section was performed last and no additional non frozen HSIL samples were available to record.

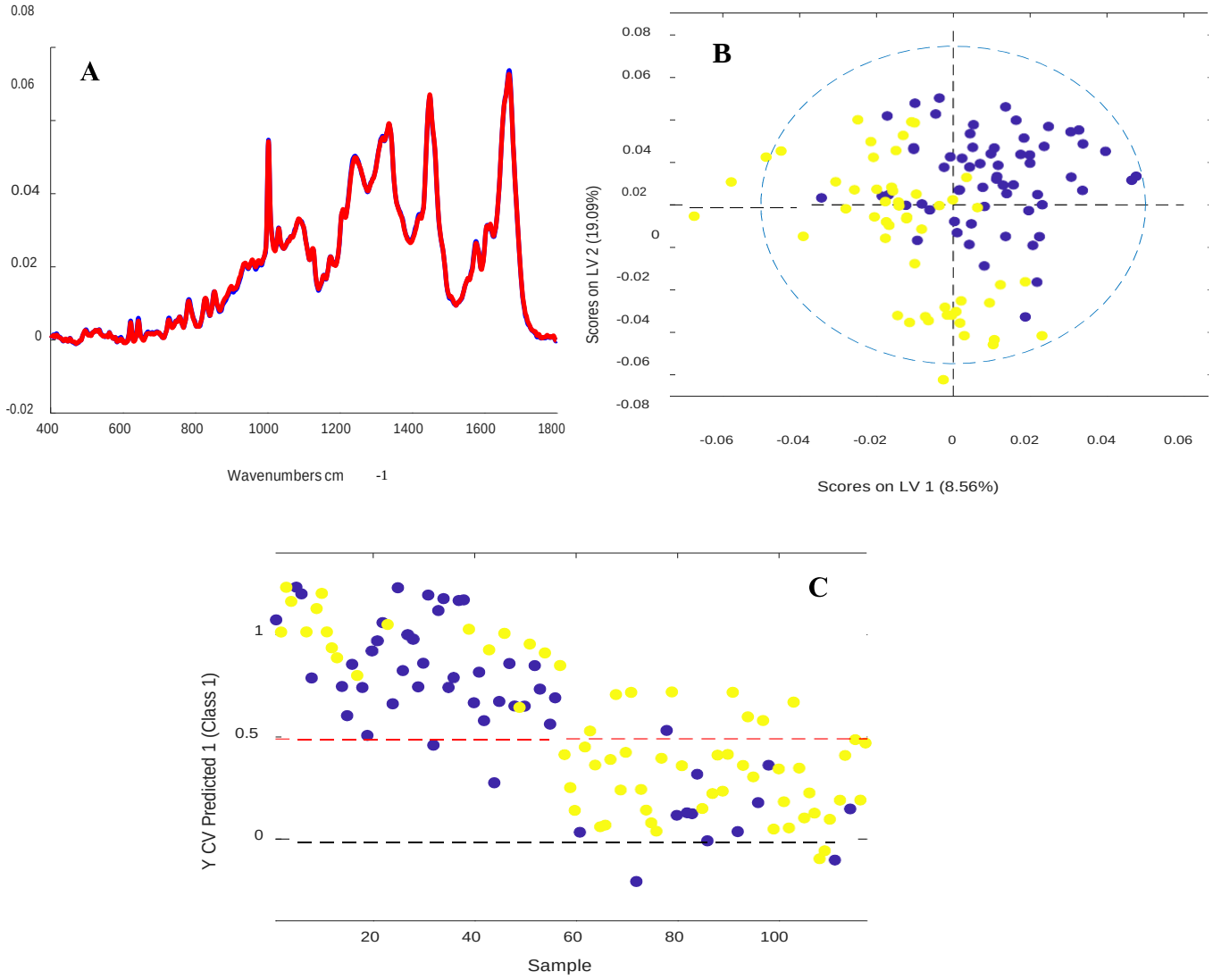

Figure 5.4 (A) mean spectra of fresh HSIL (blue) vs biobanked HSIL (red). (B) latent variables (LV) scores scatter plot of LV1 and LV2, fresh HSIL (yellow) Vs biobanked HSIL.(C) PLSDA prediction plot biobanked HSIL (blue) vs fresh HSIL (yellow).

5.3.5 Mixed Model

In order to determine if we could mix fresh and biobanked samples together and still achieve a sensitivity and specificity similar to the fresh and biobanked models, 15 biobanked HSIL samples were mixed with 15 fresh HSIL samples and compared with 15 negative biobanked/ 15 fresh negative samples. The samples were recorded individually (ie. not mixed) and the spectra from fresh and biobanked samples were pooled into negative and HSIL categories for analysis. Figure 5.5(A) shows the latent variable scatter scores plot of the model and we can see clear discrimination between the sample types across LV1 and LV2. The LV1 loadings (Figure 5.5(B)) show that discrimination is based on 482, (glycogen), 1443 (proteins, lipids) 1487 (proteins), 1605 (proteins) 1669cm^{-1} (proteins) while LV2 shows the discrimination is based around 486 (glycogen), 851 (proteins), 1152 (proteins), 1381 (glycogen), 1450 (proteins/lipids), 1575 (nucleic acids) and 1669 cm^{-1} (proteins). The loadings show similarities to both the fresh and biobanked loadings, but overall show that glycogen and proteins are the main discriminating factor between negative and HSIL samples. PLSDA prediction plot has a sensitivity of 94% and a specificity of 95% for CIN 3 (Figure 5.5(C)).

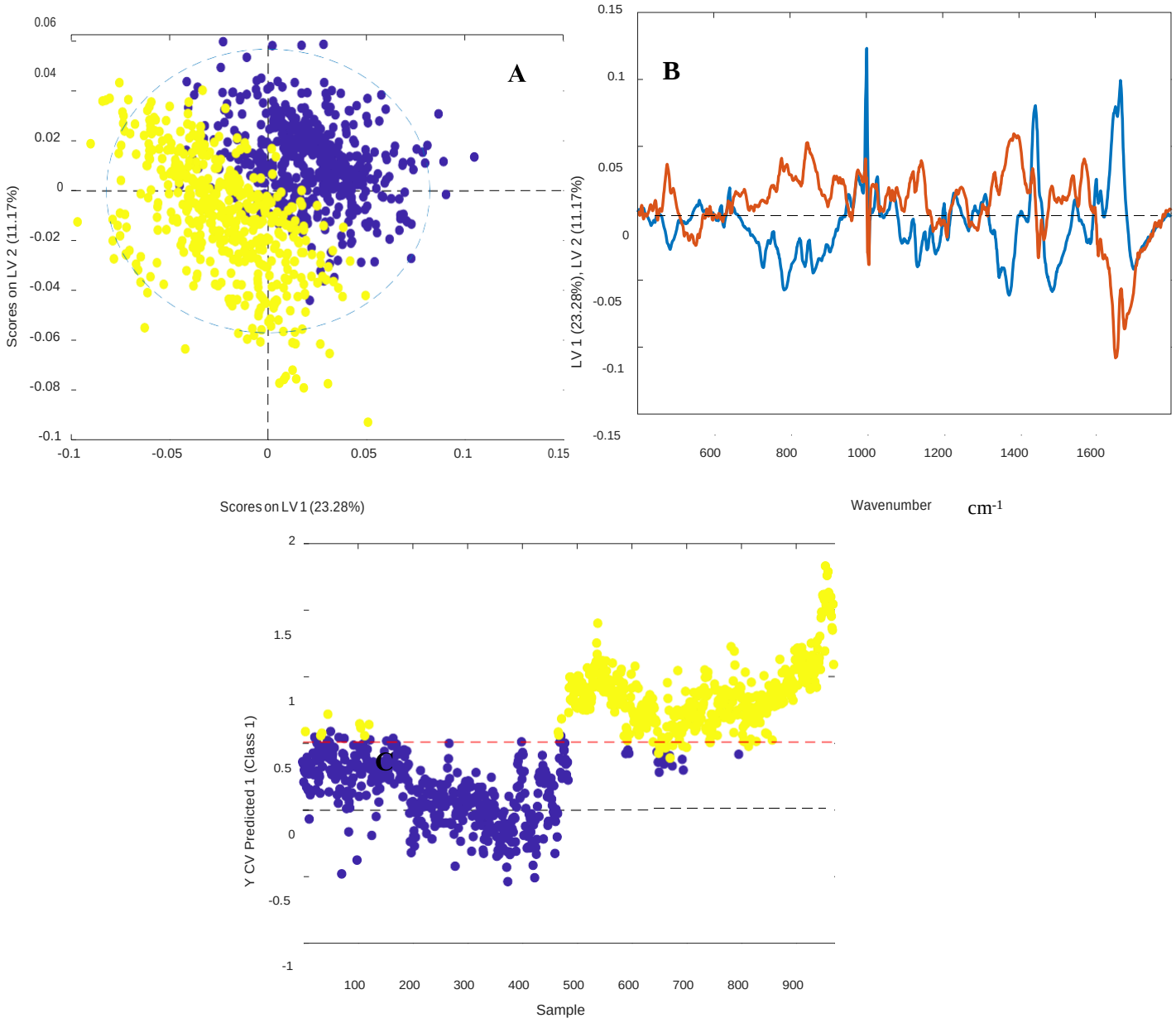

Figure 5.5 (A) latent variables (LV) scores scatter plot of LV1 and LV2, TN (yellow) Vs HSIL (blue). (B) LV1 loadings (blue) and LV2 loadings (orange). (C) PLSDA prediction plot HSIL (blue), negative (yellow)

5.4 Discussion

From the results it is clear that samples biobanked at -80^{o}C are not suitable for screening using Raman spectroscopy due to a lack of cellular material and the presence of cellular debris. The samples biobanked at -20^{o}C provided high quality smears with intact cellular material and no cellular debris which made them suitable for Raman spectroscopic analysis.

Spectral differences between fresh negative and HSIL samples were observed with regards to glycogen, nucleic acids and proteins. HSIL cells often contain little to no glycogen, hence the use of dilute acetic acid to visualize abnormal cells in colposcopy (CervicalCheck., 2013). The discrimination associated with changes in proteins and DNA is consistent with the neoplastic changes that occur in HSIL supported by persistent HPV infection such as increased cell cycling with coincident increase in replication and levels of nucleic acids (Serafin-Higuera et al.,2016). The PLSDA prediction plot gives a sensitivity of 86% and a specificity of 90% for HSIL.

Negative Vs HSIL biobanked sample results showed that discrimination was driven solely by proteins. Raman peaks associated with nucleic acids/ DNA are not as strongly present as they are in the non-biobanked samples. Long term storage of biobanked samples is likely to have led at least to an element of nucleic acids degradation which would explain why nucleic acid is not discriminatory between negative and HSIL samples. Negative Vs HSIL (non-biobanked) showed that discrimination was based on Proteins, glycogen and nucleic acids which included negative cells, the same category of negative cells from our biobanked samples. Therefore, the lack of nucleic acids as a discriminatory factor cannot be associated with the recording of negative cells.

However the PLSDA prediction plot (Figure 3(D)) does show slightly higher sensitivity (91%) and specificity (92%) rates when compared to fresh samples (86% sensitivity and 90%

specificity) indicating that biobanking at -20ºC does not preclude discrimination of negative and HSIL samples on Raman spectroscopy.

The same patient samples that had been split in two with half biobanked and the other half stored at room temperature showed no discrimination between the samples. Hence the 3 week period of biobanking at -20ºC had no detrimental effects on the physical or biochemical properties of the samples. The mixed model showed that biobanked and fresh LBC samples could be combined with an improved sensitivity of 94% and specificity of 95%. A limitation of this study is the inability to use biobanked LBC samples stored at -80^{0}C for Raman spectroscopic analysis as most biobanks will have samples stored at -80^{0}C for long term storage hence the true potential of using biobanks as a source of patient samples could be lost. Further research in this area should involve the use of different biobanked specimens (bronchial and thyroid fine needle aspirations) to investigate any detrimental effects the biobanking process may have on cytological specimens (Al-Abbadi et al.,2013,O'Dea et al., 2018).

5.5 Conclusion

Raman spectroscopy can effectively discriminate disease free cervical LBC samples from those with disease (HSIL) and this is possible using biobank cervical LBC samples stored at -25ºC. Pooling samples stored at -25 ºC with fresh samples does not affect the sensitivity and specificity of Raman spectroscopy for the discrimination of disease. This study demonstrates that biobanks of cervical LBC samples are a useful resource for future Raman spectroscopy studies and will facilitate the further assessment of this technology which shows highly encouraging performance for the detection of cervical disease.

Chapter 6

The potential application of Raman spectroscopy to be used as a triage test for cervical cancer in a primary HPV screening environment.

6.1 Introduction

The current primary method for cervical screening employed by CervicalCheck (Ireland's national screening program) is the Papanicolaou test (Pap test) and reflex HPV testing (HIQA, 2017). The Pap test is a widely accepted screening based test with a high specificity of 95-98% and a sensitivity of 74-96% (Kitchener *et al.*, 2011).The aetiological role of HPV infection among women with cervical cancer is clearly established (Petry *et al.*, 2017,Youssef *et al.*, 2016, De Vincenzo *et al.*, 2014). HPV is a double stranded DNA virus that infects the skin, mucous membrane and the anogenital tract (Zheng and Baker, 2006). It is an extremely common sexually transmitted infection that occurs in most sexually active men and women. It is estimated that 80% of all sexually active women will become infected with HPV (Winer *et al.*, 2003) There are over 100 known HPV types which are classified according to their potential to induce malignant transformations. HPV 16, 18, 31, 35, 39, 45, 50, 51, 53, 55, 56, 58, 59, 64, and 68 are classified as high risk type HPV (hrHPV). HPV 16, 18, 31, and 45 account for 80% of all cervical cancers (Schiffman *et al.*, 2009). The HPV genome is made up of 8,000 base pairs. It has five early genes E1, E2, E5, E6, E7 and two late genes, L1 and L2 (Fouad and Aanei, 2017). The target cells for the initial HPV infection are the immature basal cells of the epithelium. The virus gains entry through micro-abrasions in the epithelium. The initial number of copies of the HPV genome in the nucleus of the immature basal cells is low with a low level of viral proteins being produced. At this stage there is no morphological change within the nucleus of these infected basal cells hence the infection is now referred to as a latent infection (Zheng and Baker, 2006). A latent infection would result in a positive HPV DNA result however there would be no cytological abnormality present and no lesion to see or treat at colposcopy. As infected basal cells differentiate and move up the epithelium viral transcription increases which eventually results in the release of the virus as the infected differentiated cells are shed from the epithelium. In most cases patients will develop

immunity against the HPV virus after a period of months or years destroying the virus in the process (Youssef *et al.,* 2016). These patients will eventually become HPV DNA negative. A situation can arise where the virus presents at a non-permissive epithelial site in which viral genomes exist as particles on the surface of the epithelium and this prevents genome transcription thereby preventing the development of disease. This would still result in a HPV DNA positive test result due to the presence of HPV nucleic acids. In this situation and in the case of a latent infection both would represent a non-transcriptionally active HPV infection.

If a patient fails to remove the infection it can become persistent. Persistent infection with high risk HPV is required for the development of HSIL. Failure to destroy the infection can result in a rapid increase in the production of E6/ E7 messenger RNA (mRNA) transcripts (Zheng and Baker, 2006). E6/E7 proteins will disrupt normal cell cycle regulation, control over apoptosis mechanisms and genetic instability (McGrath *et al.*, 2017). Genetic instability will result in distorted chromosome distribution and structure and eventually result in a change in DNA content, therefore genetic instability is critical for the development of cervical cancer, hence it is not the HPV virus itself that causes disease but the presence of E6/E7 mRNA viral proteins. Hence this persistent form of infection can be termed a transcriptionally active HPV infection. This implies that a test designed to detect the over expression of E6 and E7 mRNA could be more accurate than a test that only detects the presence of viral DNA (Poljak *et al.*, 2016). Since the association between infection by high risk HPV types and high grade cervical cancer precursors and cervical cancer is so strong, HPV testing was introduced by CervicalCheck in 2012 (HIQA, 2017). The HPV virus/genome can be identified in exfoliated cells which allows for HPV testing to be performed on liquid based cytology (LBC) samples. Since April 2015 CervicalCheck employs reflex HPV DNA testing on all cytologically confirmed cases of LSIL, in order to identify patients that are hrHPV positive and more likely to develop disease (Figure 6.1). Patients who test positive will be referred to colposcopy for

further examination and treatment. Any patients who test negative will be returned to routine screening despite the initial low grade cytology result as they are at a very low risk of developing disease in the next five years (HIQA, 2017). In a European study it was confirmed that hrHPV based primary screening (Figure 6.2) provides better protection against cervical cancer than cytology (Ronco *et al.*, 2014). It works by initially removing all hrHPV DNA negative patients and returning them to routine screening, thus only patients with an increased risk of disease will go onto cytological evaluation. This reduces the number of negative samples a cytologist would have to screen thereby reducing the associated workload of mass screening. If the cytologist then identifies an abnormality and classifies it as LSIL/HSIL that patient will then be referred to colposcopy. hrHPV testing used as a primary screening tool has limitations in that it can't differentiate between transcriptionally active and non transcriptionally active forms of the virus.. This inability to distinguish between the different forms of HPV infection will result in a larger number of samples requiring additional tests and an increase in the number of patients referred to colposcopy. This underlines the need for more specific triage tests which could include Raman spectroscopy. The main objective of this study was to assess the ability of Raman spectroscopy to be used as a triage test in a primary HPV screening environment (Figure 6.3).

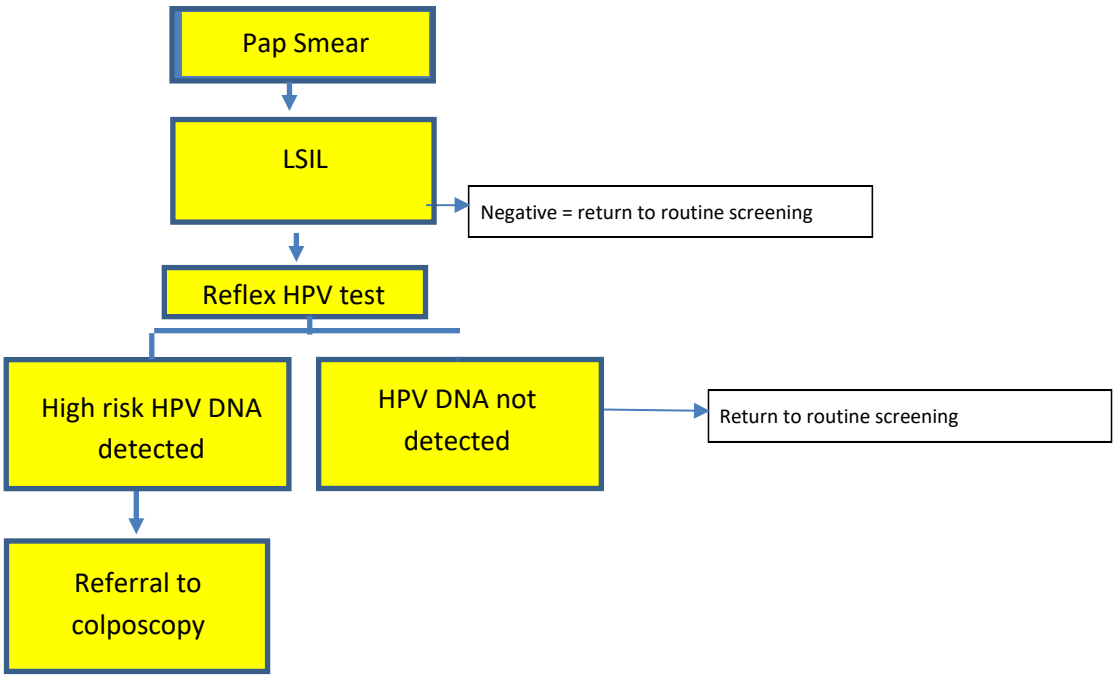

Figure 6.1 Process flowchart for HPV reflex testing. Patients will start with an initial Pap smear. If LSIL is detected the patient samples will automatically undergo a HPV DNA test to help rule out a false positive result. If the patient then tests positive for hrHPV DNA they will be refereed to colposcopy.

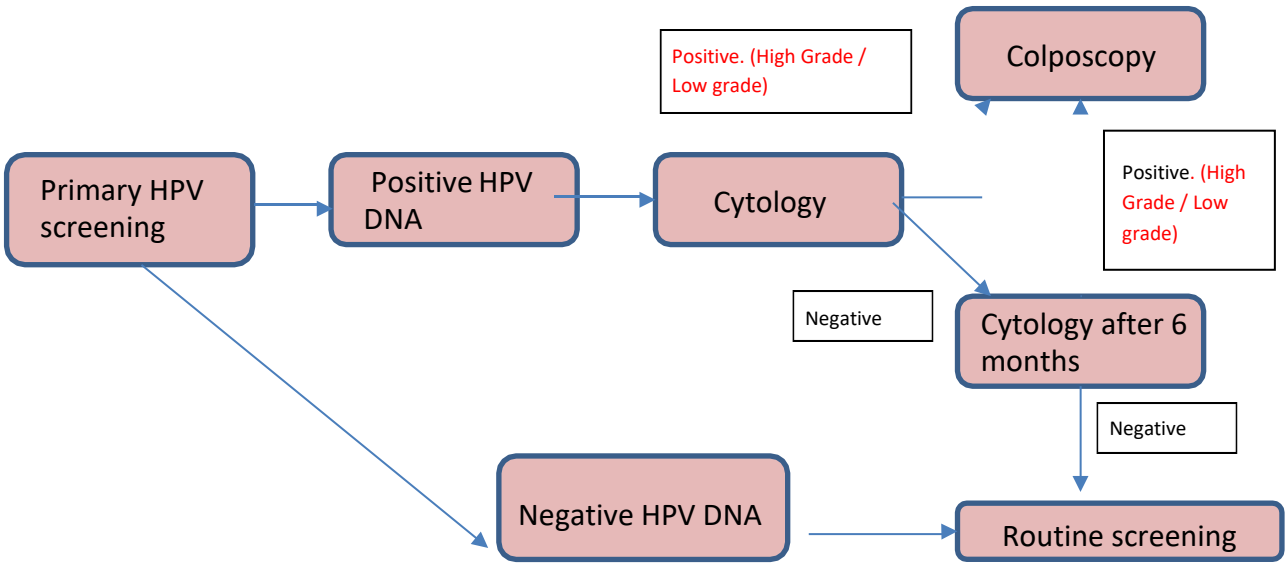

Figure 6.2 Process flowchart for hrHPV primary testing. Patient samples will be initially tested for the presence for hrHPV. All negative samples will be returned to routine screening while positive samples will undergo cytological evaluation. If LSIL/HSIL is reported the patient will be referred to colposcopy. All negative samples will receive a repeat smear in 6 months and eventually be returned to routine screening.

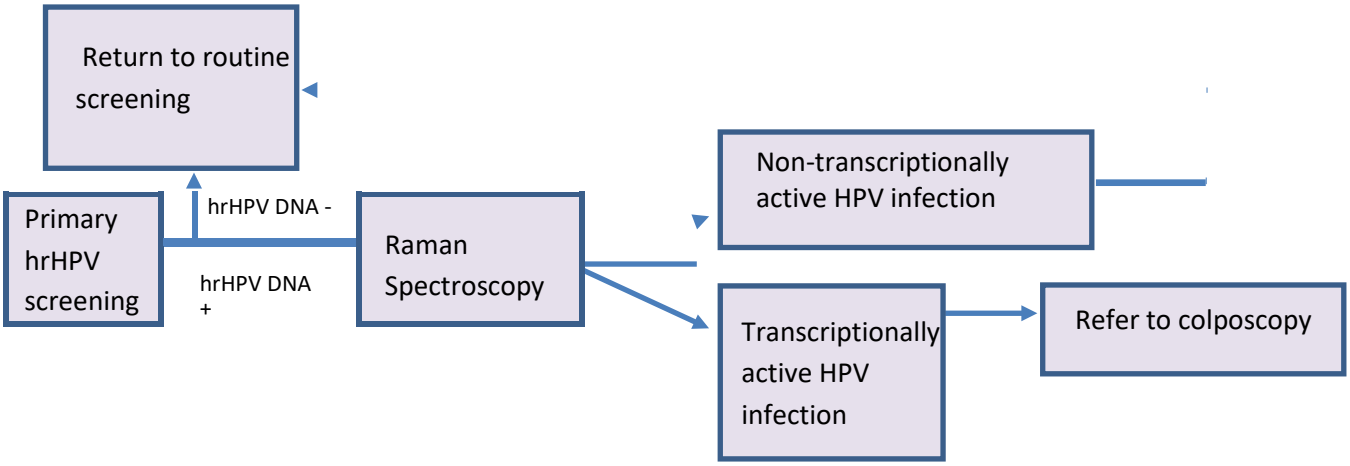

Figure 6.3 Process flow chart for Raman Spectroscopy as a triage to primary HPV screening. Patient samples will be initially tested for hrHPV. Patients that test negative will return to routine screening. Patients that test positive will undergo Raman spectroscopic analysis to identify patients with a transcriptionally active HPV infection and refer them to colposcopy, Patients identified with a non-transcriptionally active HPV infection will be returned to routine screening.

6.2 Methods

30 HPV DNA and mRNA positive LBC samples and 30 HPV DNA positive and mRNA negative LBC samples were collected in PreservCyt solution from the Coombe Women and Infants University Hospital (CWIUH), Dublin, Ireland, after routine cytological screening and HPV testing had been performed. Ethical approval for use of encoded samples for the study was granted by the CWIUH Research Ethics Committee (no. 28-2014). HPV DNA/mRNA positive samples represent the transcriptionally active form of infection and HPV DNA positive mRNA negative samples represented the non-transcriptionally active form. A further 14 encoded samples were recruited to validate the classification model which were made up of a mixture of non-transcriptionally active and transcriptionally active sample types.

6.2.1 ThinPrep

The samples were then prepared as per section 2.3 and 2.4

6.2.2 Raman spectroscopy

All Raman analysis recorded as outlined in section 2.5-2.6 .In order to discriminate transcriptionally active samples from non-transcriptionally active samples, a classification model was developed from known samples. 30 transcriptionally active samples and 30 non transcriptionally active samples were recorded (see table 6.1) with 520 cell nuclei being recorded in total for each sample type with approx. 30 nuclei per sample.

6.2.3 Data pre-processing and analysis

All data was pre-processed as outlined in section 2.7-2.9

6.2.4 Prediction

Since PLSDA is a supervised technique meaning prior knowledge of a sample's HPV status is known to build the model, it is important to also include a test set to further validate the model. The test set was made up of 14 coded samples (transcriptionally active/ non transcriptionally active). Two methods were employed to validate the model. The first tested all sample spectra individually to identify how well the model predicts the coded samples, the second method involved getting the mean of each sample and identifying how well the model predicts the mean of each sample. Samples with transcriptionally active HPV infection acted as the positive class as the aim of screening is to identify patients most at risk and who will require further treatment. Samples with non-transcriptionally active HPV infection acted as a negative class as they are deemed to be at a lower risk of developing cervical cancer in the next 5 years and can return to routine screening.

6.3 Results and Discussion

6.3.1 Transcriptionally Active Vs Non-Trancriptionally Active

Figure 6.4 (A) shows the mean spectra for non-transcriptionally active samples and transcriptionally active samples. While both samples appear very similar there are differences at Raman peak positions 782 cm^{-1} (nucleic acids) and 1238cm^{-1} and 1670cm^{-1} (Proteins Amide I, Amide III) (table 1.1). Figure 6.4(B) shows latent variables (LV) scores scatter plot of LV1 and LV2 which shows good discrimination along LV1.The loadings from LV1 are shown in figure 6.4 (C) and show that discrimination is based around Raman peaks, 483 (glycogen), 727 (Proteins-CH_2 def), 782 (nucleic acids- U,C,T, ring br), 851 (proteins-ring br. Tyr, C-C str), 937 (glycogen), 1002-1004 (Proteins- phenylalanine), 1121 (proteins C-N str, lipids-Chain C-C str, Carbohydrates- C-O str, 1204 (proteins-C-C_6H_5 str, Phe, Trp), 1335 (glycogen), 1443 (proteins- CH_2 def) 1450 (proteins -CH_2 def, lipids CH_2 def), 1642 (C=O str, C=C sym. Str) and 1670 cm^{-1} (C=O str. Amide I). The PLSDA prediction plot shown in Figure 6.4 (D) has a sensitivity of 88% and a specificity of 88%. The results show that it is possible for Raman spectroscopy to distinguish non-transcriptionally active forms of the HPV infection from the transcriptionally active forms. The LV1 loadings show that discrimination is mostly based around glycogen and proteins. Glycogen is often found to be lower in malignant tissue when compared to normal tissue. The high rate of proliferation in malignant tissue caused by the HPV infection prevents the accumulation of glycogen within the cell (Lyng *et al.*, 2015). In the regions assigned to proteins there is a marked difference. Raman peaks assigned to phenylalanine 1004 cm^{-1} show a slight shift between 1003-1004 cm^{-1}, which is most likely attributed to the methanol based fixation method which suggests a change in the conformation of the phenylalanine protein (Meade et al 2010). This shift appears to occur at random and is not sample specific. Overall protein seems to be the main discriminating factor between the non- transcriptionally active and transcriptionally active

samples. This is most likely down to the altered protein expression due to the persistent HPV infection taking control of the host cell machinery resulting in the over expression of E6/ E7 viral proteins

Table 6.1 Non-transcriptionally active Vs Transcriptionally active patient summary

Sample Number	HPV DNA	HPV mRNA
1,2,3,4,5,6,7,8,9,10,11,12,13,14,15,16, 17,18,19,20,21,22,23,24,25,26,27,28,29,30	Positive	Negative
31,32,33,34,35,36,37,38,39,40,41,42,43,44 45,46,47,48,49,50,51,52,53,54,55,56,57,58,59,60	Positive	Positive

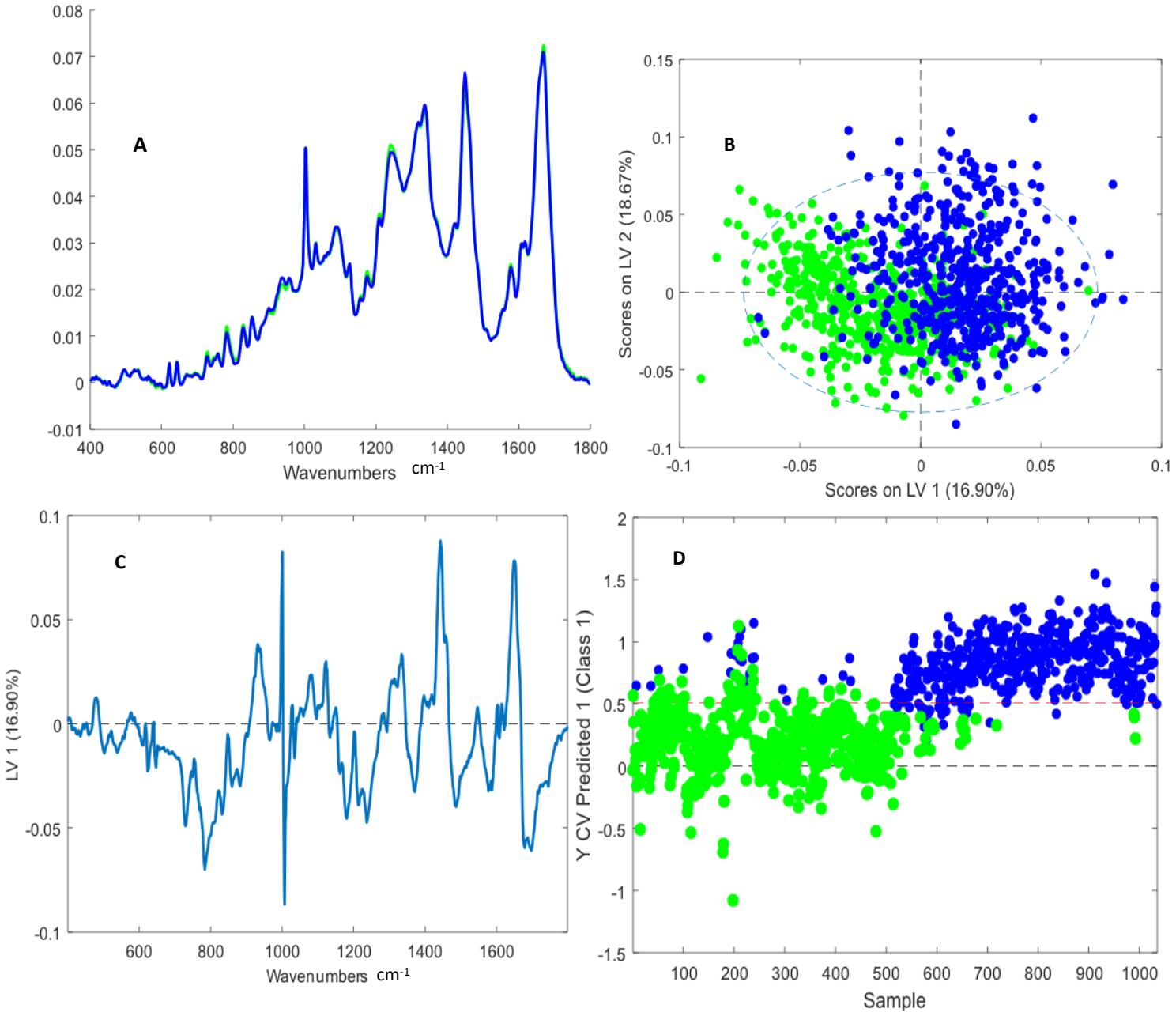

Figure 6.4 (A) Mean spectra of samples with non transcriptionally active HPV infection (green) Vs samples with transcriptionally active HPV infection (blue). B) Latent variables (LV) scores scatter plot of LV1 and LV2 of samples with non-transcriptionally active HPV infection (green) and transcriptionally active HPV infection (blue). C) LV1 loadings. (D) The PLSDA prediction plot.

6.3.2 Prediction

6.3.2.1 Method 1

Table 6.2 Result of Prediction Method 1 showing how Raman spectroscopy predicted each cell between non-transcriptionally active and transcriptionally active categories along with the correct classification.

Sample Number	Model prediction (Non-Transcriptionally active cells)	Model prediction (Transcriptionally active)	Correct Classification
001	0	16	Transcriptionally active
002	15	16	Transcriptionally active
003	1	12	Transcriptionally active
004	4	33	Transcriptionally active
005	7	25	Transcriptionally active
006	0	19	Transcriptionally active
007	2	17	Transcriptionally active
008	3	16	Transcriptionally active
009	4	44	Transcriptionally active
010	10	6	Transcriptionally active
011	29	0	Non-transcriptionally active
012	26	3	Non-Transcriptionally active
013	21	3	Non-transcriptionally active
014	22	2	Non-Transcriptionally active

Sensitivity	85%
Specificity	92%

6.3.2.2 Method 2

Table 6.3 Result of Prediction Method 2 showing how Raman spectroscopy predicted the mean values of each sample between non-transcriptionally active and transcriptionally active categories along with the correct classification.

Sample Number	Model prediction (Non-transcriptionally active Mean Cells)	Model prediction (transcriptionally active Mean Cells)	Correct Classification
001	0	1	Transcriptionally active
002	0	1	Transcriptionally active
003	0	1	Transcriptionally active
004	0	1	Transcriptionally active
005	0	1	Transcriptionally active
006	0	1	Transcriptionally active
007	0	1	Transcriptionally active
008	0	1	Transcriptionally active
009	0	1	Transcriptionally active
010	1	0	Transcriptionally active
011	1	0	Non-transcriptionally active
012	1	0	Non-transcriptionally active
013	1	0	Non-transcriptionally active
014	1	0	Non-transcriptionally active

Sensitivity	90%
Specificity	100%

6.3.2.3 Comparison of Raman classification, Cytology result, Histology result and HPV status .

Table 6.4 *Raman classification, Cytology result, Histology result and HPV status for the independent test set*

Sample Number	Raman Classification	Cytology	Histology	Cobas HPV DNA Test	Aptima HPV mRNA Test
001	Transcriptionally active	HSIL	CIN 2	Positive	Positive
002	Transcriptionally active	HSIL	CIN3	Positive	Positive
003	Transcriptionally active	HSIL	CIN 3	Positive	Positive
004	Transcriptionally active	HSIL	CIN 2	Positive	Positive
005	Transcriptionally active	HSIL	CIN1	Positive	Positive
006	Transcriptionally active	HSIL	CIN2	Positive	Positive
007	Transcriptionally active	HSIL	CIN2	Positive	Positive
008	Transcriptionally active	HSIL	CIN3	Positive	Positive
009	Transcriptionally active	HSIL	CIN2	Positive	Positive
010	Non Transcriptionally active	LSIL	CIN1	Positive	Positive
011	Non-transcriptionally active	LSIL	Negative	Positive	Negative
012	Non-transcriptionally active	Negative	Negative	Positive	Negative
013	Non-transcriptionally active	LSIL	Negative	Positive	Negative
014	Non-transcriptionally active	Negative	Negative	Positive	Negative

From the prediction results it is clear that both method 1 and 2 provided successful validation of the classification model. Method 1 shows that 9 out of 10 samples with transcriptionally active HPV infection were successfully predicted and 4 out of 4 samples with a non-transcriptionally active HPV infection were predicted correctly. Sample 010 was the only sample to be wrongly predicted. 10 out of 16 cells were predicted to be non-transcriptionally active when they were from a transcriptionally active sample. Sample 002 also highlights the need to record multiple spectra from the same sample. Even though the sample was classified correctly via method 1 there was only 1 cell in the difference between non-transcriptionally active and transcriptionally active. This demonstrates that not all the cells within a given sample may classify correctly. This could be down to a number of factors such as sampling technique, and the size of the infected area and the presence of HPV mRNA in every cell tested. One possible way to address this issue is to predict the independent test set samples using the mean spectra from each sample thereby reducing the variability within the data. If the mean spectra show the biochemical changes associated with the transcriptionally active infection then correct classification should be achieved . Overall this method gave the model a sensitivity and specificity of 85% and 92% respectively. It is not possible to know from this study if the level of abnormality (LSIL/HSIL) affects the number of cells predicting into each category as all transcriptionally active samples tested were reported as HSIL. Future work would involve testing LSIL samples that are reported as transcriptionally active to see if this would affect the number of cells correctly predicted between the two groups.

Method 2 showed an improved result with a sensitivity of 90% and a specificity of 100% The mean spectra were used for each sample rather than individual cell spectra. This reduced the variability within the dataset resulting in the increase in sensitivity and specificity. However sample 010 was again misclassified. A limitation of this study is the relatively low

number of latent samples used for prediction. As the main source of sample recruitment was a colposcopy clinic, most patient referrals were based on HSIL hence most patients had a transcriptionally active HPV infection so it was difficult to recruit patients who had a non-transcriptionally active infection.

Table 6.4 shows the Raman classification, cytology result, histology result and HPV DNA/ mRNA status for the independent test set samples. Samples 001-009 show a strong correlation between Cytology, Histology and HPV testing which are backed up by the Raman classification result of transcriptionally active. Sample 010's cytology and histology result report a LSIL or CIN1 lesion. The positive Aptima mRNA test result indicates that this patient has a transcriptionally active infection meaning that this patient would be at a higher risk of developing disease in the next 3-5 years. Given the Raman classification of a negative result (non transcriptionally active) and all other tests indicate a transcriptionally active infection, it suggests that this Raman result is a false negative. Samples 011-014 were all classified as a non-transcriptionally active by Raman spectroscopy which is backed up by the histology and HPV mRNA tests. The cytology LSIL result could be down to false positives caused by an inflammatory condition or the regression of a non-transcriptionally active HPV infection. Either way these patients are at a lower risk of developing cancer in the next 3-5 years and should be returned to routine screening. Apart from sample 010, Raman spectroscopy was successful in identifying transcriptionally active and non -transcriptionally active HPV infections which is backed up by the standard screening approach of cytological, histological and HPV DNA/mRNA testing.

6.4 Conclusion

The advantage of employing Raman spectroscopy as a triage test in a primary hrHPV screening environment is that it would prevent the unnecessary referral of patients with a non-transcriptionally active HPV infection for cytological evaluation while ensuring that patients with an increased risk of disease are referred to colposcopy. All analysis could be performed on the same initial Pap test thereby reducing costs and preventing unnecessary additional sample collection and delays. Raman spectroscopy can provide a cheap rapid non-destructive method to identify patients most at risk without subjectivity. Future work on this subject should involve using a primary screening cohort of samples which would provide a larger sample base of non-transcriptionally active samples for testing compared to colposcopy based recruitment.

Chapter 7

Conclusions and Future Work

7.1 Conclusions

Cervical cancer remains one of the most common cancers affecting women worldwide. Most developed countries operate a cervical screening programme, which are based on the cytological evaluation of cervical cells. While this method generally operates with a high specificity (96.5%), it suffers from a variability in its sensitivity rates (30-85%) (Nanda *et al.*, 2000). The variability in sensitivity is mainly due to the subjectivity of the associated test. New technology is, therefore, needed. HPV testing has been incorporated into most cervical cancer screening programmes as either a form of management and triage or as a test of cure. Currently, there are plans to introduce HPV screening as a primary method of screening in Ireland for cervical cancer. This clearly indicates that cervical cancer screening programmes are attempting to move away from tests based on visual interpretation, which are prone to subjectivity and human error and more towards molecular tests which are more objective.

The overall goal of cervical screening research is to create new triage tests that identify women who are HPV positive but who are also at a higher risk of developing cervical cancer. The triage tests should also be able to identify women who are HPV positive but also at a lower risk of developing cervical cancer in the next five years and return them to routine screening. Costs should be reduced and the rates of sensitivity and specificity for disease should increase.

The research question of this thesis was to assess the potential of Raman spectroscopy as a new test for cervical cancer screening by investigating the potential hurdles associated with the disease and technology. Chapter 1 acts as an introduction to the thesis and outlines the natural history of the disease, the clinical aspects of screening and introduces the Raman spectroscopy technology. Chapter 2 outlines the materials and methods which were employed for this thesis.

Chapter 3 investigated potential hormonal effects in cervical smear samples using Raman spectroscopy. The findings from this chapter suggest that the menstrual cycle will have an effect on the Raman spectra recorded with regards to the levels of glycogen and proteins. Postmenopausal samples proved to be problematic for Raman spectroscopy due to a lack of cellular material and the presence of cellular debris. The use of hormone-based contraceptives resulted in the most variability within the spectra. However all these hormone based changes did not hinder the ability of Raman spectroscopy to discriminate cytology negative cells from HSIL cells. Overall, this study highlighted the scope of Raman spectroscopy for cervical cancer screening despite the presence of biochemical changes associated with the menstrual cycle and the use of hormone-based contraceptives. Previous work published by Kanter *et al* (2009) showed that hormonal differences due to the menstrual cycle can influence the Raman spectra acquired from the cervix *in vivo*. Our study reports similar findings, however our study also addressed the use of hormone based contraceptives, and if these hormone induced changes will hinder the ability of Raman spectroscopy to identify dyskaryotic cells, which is the primary goal when developing a screening test for cervical cancer.

Chapter 4 outlines a study which aimed to improve on our previous published work (Bonnier et al. 2014) on a method for removal of blood contamination from Thinprep cervical cytology samples for Raman spectroscopic analysis. Liquid based cytology Thinprep specimens were treated by adding hydrogen peroxide directly to the vial followed by a process of centrifugation and pipetting. Good quality Raman spectra were recorded from negative and high-grade cytology samples which initially presented with heavy blood contamination. This study demonstrated for the first time the improved potential of Raman spectroscopy for analysis of ThinPrep specimens regardless of blood contamination. This technique is a continuation of our previous work (Bonnier et al 2014), however it is novel in that it is not restricted to blood

scale 0-1 samples and can be applied to all samples on the blood scale index (blood scale 0-4).

Chapter 5 assessed the potential of using biobanked liquid based cytology samples for cervical cancer screening using Raman spectroscopy. The aim of this study was to assess the ability of Raman spectroscopy to screen for histologically confirmed cases of CIN using biobanked (LBC) samples. Two temperatures for long-term storage were assessed, -80^{o}C and -25^{o}C. The utility of Raman spectroscopy for the detection of CIN was compared for fresh LBC samples and biobanked LBC samples. Two groups of samples were used for the study with one group associated with disease (CIN3) and the other associated with no disease (cytology negative). The data indicated that samples stored at -80^{o}C are not suitable for assessment by Raman spectroscopy due to a lack of cellular material and the presence of cellular debris. However, the technology can be applied to fresh LBC samples and those stored at -25^{o}C and is effective in the discrimination of negative samples from those where CIN 3 has been confirmed. This study demonstrates for the first time that cervical cytology samples stored within biobanks at temperatures that preclude cell lysis can act as a useful resource for Raman spectroscopy and will facilitate research and translational studies in this area. To our knowledge, this is the first study of its kind to investigate the application of biobanked LBC samples for Raman spectroscopy analysis.

Chapter 6 investigated the potential application of Raman spectroscopy as a triage test for cervical cancer screening in a primary HPV screening environment. This study outlined the two possible outcomes of a HPV infection and divided samples into two separate categories, non-transcriptionally active and transcriptionally active. The latent stage of infection represents an initial low level of viral proteins being produced, which would still result in a positive HPV DNA based test even though there would be no cytological abnormality present and no lesion to see or treat at colposcopy, hence this would result in an unnecessary patient

referral. In most cases, a patient would develop immunity against the HPV virus and clear the virus in the process. If the patient fails to remove the infection, it can result in the rapid expression of E6 and E7 mRNA transcripts resulting in a transcriptionally active infection. At this stage, a patient would test positive for both HPV DNA and mRNA and should be referred to colposcopy for treatment. The aim for this chapter was to determine if Raman spectroscopy could identify individuals with a transcriptionally active HPV infection in a primary HPV screening environment to prevent unnecessary referral of those with a non transcriptionally active HPV infection. In a blind validation study, the results showed that Raman spectroscopy could successfully identify transcriptionally active samples with a sensitivity of 90% and a specificity of 100%. A number of previous works (Vargis et al., 2012 Ostrowska et al., 2010 ,Jess et al., 2007) investigated the ability of Raman spectroscopy to identify HPV infection. However, most of these studies utilised HPV infected cell lines rather than 'real world' cytology samples. With the current trend of HPV molecular testing taking over as a primary method of cervical cancer screening it is not sufficient to just detect the presence of HPV, additional information is required on whether the infection is non-transcriptionally active or transcriptionally active. If Raman spectroscopy is to be considered as a possible triage test for cervical screening. Our study advances the Raman spectroscopy technique for cervical cancer screening but also highlights the potential of Raman spectroscopy to advance screening technology beyond conventional methods in a cost effective, label free and non-destructive manner.

Previous studies involving Raman spectroscopy for cervical cancer diagnosis (Rashid et al.,2014, Krishna at al., 2006, Kamemoto et al., 2010 and Tan et al 2010) all utilised fixed tissue sections for their studies however tissue sections are not suitable for a screening based test given the invasive nature of obtaining an excision biopsy.

A study conducted by Rubina et al. (2013) utilised patient cytology samples in a cell pellet form but was not able to report a sensitivity higher than 79% for disease detection due to confounding factors such as blood which have been addressed in this thesis. Numerous studies (Mahadevan-Jansen.,et al 1998, Utzinger.,et al 2001 and Robichaux-Viehoever et al.,2007) employed a Raman probe for sample recording with the latter reporting a sensitivity and specificity of 89% and 81% respectively between negative and HSIL. While this represents a higher sensitivity/specificity rate compared to other studies involving Raman spectroscopy, it fails to account for long acquisition times of 60-180 seconds or more and the ability for a clinician to locate and hold the Raman probe against an area of interest on the cervix. While this probe based method shows potential, the studies reported in this thesis obtained sensitivity rates between 86-90% and specificity rates of 95-100% for disease across multiple studies with a larger sample base.

An advantage of this study over others is that it utilises an already established processing method (Thinprep) for Raman spectroscopic analysis. The technology/ processing method is already established in all cytology labs, and therefore requires no alterations or additional costs with regards to sample processing. This means that the Raman spectroscopy method can fit easily into the current routine workflow. An added benefit of using the Thinprep method is that after completion of the Raman spectral screening of a given sample, the same slide could be stained and screened by a cytologist, which could act as a failsafe or as an additional triage test. Interestingly, in all the studies described in this thesis, Raman spectra were recorded from morphologically normal intermediate and superficial cells on Thinprep Pap smears. It was not necessary to find the morphologically abnormal cells on each slide as is required for cytological screening.

Therefore, this study is unique in that it does not require abnormal cells for screening, it can utilise an already validated sample processing method (Thinprep), it is non-destructive which

allows additional tests to be performed on the same Thinprep slide used for Raman spectroscopy and would be a cheaper alternative to HPV testing (Cobas/Aptima).

Overall, this study has confirmed our hypothesis that Raman spectroscopy can be utilised for cervical cancer screening. We have investigated hormonal effects, removal of contaminating blood from cervical Pap smear samples, utility of frozen biobanked samples for cervical cancer screening using Raman spectroscopy and the utility of Raman spectroscopy as a triage test for cervical cancer screening.

7.2 Future Work

There is currently a lot of interest in using Raman spectroscopy as a diagnostic aid as the technique makes it possible to extract information about a given sample non-invasively, non-destructively and in a label free manner. Spectra can be accumulated, corrected for un-wanted signal (glass), processed and analysed rapidly. Raman spectroscopy can currently satisfy many of the criteria required for transforming a vibrational spectroscopic technique into a diagnostic clinical based test. However, there are limitations with the current Raman spectroscopy technology. The Raman spectrometer is comprised of three separate components, which include a light source, light delivery system with collection and a dispersive element and a detector all of which will have to become robust, compact and be able to operate efficiently within a lab or clinical based setting. This project was completed manually, which involved lining up the laser with the centre of the selected cell nucleus and recording a Raman spectrum. For a clinical based setting or future studies, this process should become automated. In order for the Raman method to become automated, a standard operating procedure would have to be established which would be based on a series of algorithms that allow for the highest quality spectra with high signal to noise ratio to be recorded. These algorithms would have to account for variations in sample quality and cell type. An automated cell recognition routine would also have to be developed which could

work in tandem with the Raman spectroscopy routine to identify specific cell nuclei and align the target nuclei with the Raman laser source. The test samples would have to consist of a monolayer of cells free of debris and blood contamination.

In the studies presented in this thesis, sample recruitment was based at a colposcopy clinic and limited to patients with no previous history of disease; future studies should involve a larger more comprehensive sample base, which includes patients with a previous history of disease. Also future samples should be recruited from a screening population. Given the introduction of the HPV vaccine with the first round participants about to enter the screening programme, future studies should also incorporate this demographic.

This body of work was performed as a continuation of on-going research on the application of Raman spectroscopy into cervical cancer screening which was conducted under the direction of the CERVIVA consortium (www.cerviva.ie) and the Technological University Dublin. All findings from this thesis are being used to implement a clinical utility study of the Raman technology using 1,000 patient samples, funded by the Health Research Board.

Chapter 8

References and Publications

8.1References

Adams, A. L. et al. (2006) 'Negative Colposcopic Biopsy After Positive Human Papilloma Virus (HPV) DNA Testing', American Journal of Clinical Pathology, 125(May), pp. 413–418.

Al-Abbadi MA. Basics of cytology. Avicenna J Med. 2011;1(1) pp. 18-28.

Arbyn M, et al (2008) 'Liquid compared with conventional cervical cytology: a systematic review and meta-analysis', Obstet Gynecol, 111(1), pp. 167–77.

Arbyn, M. et al. (2007) 'Burden of cervical cancer in Europe: Estimates for 2004', Annals of Oncology, 18(10), pp. 1708–1715.

Arbyn, M. and Ronco, G. (2009) 'How to evaluate emerging technologies in cervical cancer screening', Journal of Cancer, 125(11), pp. 2489–2496.

Baker, M. J. et al. (2018) 'Clinical applications of infrared and Raman spectroscopy: state of play and future challenges', The Analyst. Royal Society of Chemistry 143(8),pp.1735-1757

Baldur-Felskov, B. et al. (2014) 'Early impact of human papillomavirus vaccination on cervical neoplasia - Nationwide follow-up of young danish women', Journal of the National Cancer Institute, 106(3).

Ballabio, D Consonni, V. (2013) 'Classification toold in chemistry.Part 1: Linear models. PLSDA', royal society of chemsitry, 5, pp. 3790–3798.

Ball, D.W., 2001. Theory of Raman Spectroscopy. Spectroscopy, 16(11).

Basicmedicalkey.com
https://basicmedicalkey.com/cervical-benign-and-non-neoplastic-conditions. (accessed Feburary 10, 2016)

Behl, I. et al. (2017) 'Development of methodology for Raman microspectroscopic analysis of oral exfoliated cells', Analytical Methods. Royal Society of Chemistry, 9, pp. 1–22.

Bellisola, G. Sorio, C. (2012) 'Infrared spectroscopy and microscopy in cancer research and diagnosis.', American journal of cancer research, 2(1), pp. 1–21.

Biomed.tamu.edu
http://biomed.tamu.edu/obsl/OBSL/Research%20Projects/SERS_biosensor.htm (accessed October ,2016)

Bonnier, F. et al. (2014) 'Processing ThinPrep cervical cytological samples for Raman spectroscopic analysis', Anal. Methods, 6(19), pp. 7831–7841.

Boron, W. F Medical physiology. 3rd edn. Elsevier Ltd 2005. p851-854.

Bosch, F. X. et al. (2002) 'The causal relation between human papillomavirus and cervical cancer.', Journal of Clinical Pathology, 55(4), pp. 244–65.

Bray,Freddie. et al (2018) 'Gobal Cancer statistics 2018. Globocan estimates of incidence and mortality worldwide for 36 cancers in 185 countries'.; CA CANCER J CLIN; 68 pp.394–424.

Brozek-Pluska, B. et al. (2012) ‘Raman spectroscopy and imaging: applications in human breast cancer diagnosis’, The Analyst, 137(16), p. 3773.

Bulten, J. et al. (2011) ‘European guidelines for quality assurance in cervical histopathology’, Acta Oncologica, 50(5), pp. 611–620.

Burd, E. et al (2003) ‘Human papillomavirus and cervical cancer’, Clin Microbiol Rev, 16(1), pp. 1–17.

Canadian Cancer Society
https://www.cancer.ca/en/cancer-information/cancer-type/cervical/cervical-cancer/the-cervix/?region=on (accessed September 20, 2019)

CervicalCheck (2013) Organisational and Clinical Guidance for Quality Assured Colposcopy Services.

Chiriboga, L. et al. (1998) ‘Infrared spectroscopy of human tissue. I. Differentiation and maturation of epithelial cells in the human cervix’, Biospectroscopy, 4(1), pp. 47–53.

Clinic, C.
http://www.clevelandclinic.org/health/healthinfo/docs/0600/0642.asp?index=4711 (accessed September 20,2019)

Cohenford, M. a et al. (1997) ‘Infrared spectroscopy of normal and abnormal cervical smears: evaluation by principal component analysis.’, Gynecologic oncology, 66(1), pp. 59–65.

Cplmag.com
http://www.clpmag.com/2019/06/reducing-cervical-cancer (accessed September,2019).

Cuzick, J. et al. (2013) ‘Comparing the performance of six human papillomavirus tests in a screening population’, British Journal of Cancer, 108(4), pp. 908–913.

Daniel,A et al (2018) 'Near-infrared Raman spectroscopy for estimating biochemical changes assoicated with different pathological conditions of the cervix’,Spectrochimica Acta Part A:Molecular and Biochemcial Spectroscopy, 190,pp 409-416.

De Vincenzo, R. et al. (2014) ‘Long-term efficacy and safety of human papillomavirus vaccination’, International Journal of Women’s Health, 6, pp. 999–1010.

Diem, M. et al. (2002) ‘IR spectra and IR spectral maps of individual normal and cancerous cells’, Biopolymers - Biospectroscopy Section, 67(4–5), pp. 349–353.

Diem, M. et al. (2013) ‘Molecular pathology via IR and Raman spectral imaging’, Journal of Biophotonics, 6(11–12), pp. 855–886.

Dillner, J. et al. (2008) ‘Long term predictive values of cytology and human papillomavirus testing in cervical cancer screening: joint European cohort study’, Bmj, 337, pp. 1754–1754.

Dobbin K, Simon RM (2011). 'Optimally splitting cases for training and testing high dimensional classifiers'. BMC Med Genomics,4(31).

Doorbar J (2005). 'The papillomavirus life cycle'. Journal of Clinical Virology; 32, pp. 7-15

Doorbar, J. et al. (2012) ‘The biology and life-cycle of human papillomaviruses’, Vaccine. Elsevier Ltd, 30, pp. 55–70.

Downes, A, Elfick, A. (2010) ‘Raman spectroscopy and related techniques in biomedicine’, Sensors, 10(3), pp. 1871–1889.

Duraipandian.S et al., (2012). “Simultaneous fingerprint and high-wavenumber confocal Raman spectroscopy enhances early detection of cervical precancer in vivo,” Anal. Chem. 84, pp.5913–5919.

Duraipandian, S. et al. (2013) ‘Integrated fingerprint and high wavenumber confocal Raman spectroscopy for in vivo diagnosis of cervical precancer’, Analytical Chemistry, 84(14), p. 85720Z.

Duraipandian, S. et al. (2018) 'Raman spectroscopic detection of high grade cervical cytology: Using morphologically normal appearing cells' SCI Rep 8:15048 |

Eurocytology.eu
https://www.eurocytology.eu/en/course/843 (accessed September 20, 2019)

Ferlay.J et al., (2015). “Cancer incidence and mortality worldwide: sources, methods and major patterns in GLOBOCAN 2012,” Int. J. Cancer 136, pp.359–386.

Fouad, Y. A., Aanei, C. (2017) ‘Revisiting the hallmarks of cancer’, American Journal of Cancer Research, 7(5), pp. 1016–1036.

Fox, J. M. et al. (2017) ‘Methodology for reliable and reproducible cryopreservation of human cervical tissue’, Cryobiology. Elsevier Ltd, 77, pp. 14–18.

Garland, S. M. et al. (2016) ‘Impact and effectiveness of the quadrivalent human papillomavirus vaccine: A systematic review of 10 years of real-world experience’, Clinical Infectious Diseases, 63(4), pp. 519–527.

Gauglitz, G. & Vo-Dinh, T,. Handbook of Spectroscopy , WILEY-VCH,(2003) pp.43.

Gautam, R. et al. (2015) ‘Review of multidimensional data processing approaches for Raman and infrared spectroscopy’, EPJ Techniques and Instrumentation. EPJ Techniques and Instrumentation, 2(1), p. 8.

General cytopathology.
http://pathology.jhu.edu/cytopath/masterclass/general/1gen16.htm. (accessed September 21, 2016)

Gettyimages
https://www.gettyimages.ie/detail/illustration/menstrual-cycle-illustration-stock-graphic/502865065 (accessed January 12, 2018)

González-Solís, J. L. et al. (2013) ‘Cervical cancer detection based on serum sample Raman spectroscopy’, Lasers in Medical Science, 29(3), pp. 979–985.

Gray, N. M. et al. (2006) ‘Psychological effects of a low-grade abnormal cervical smear test result: Anxiety and associated factors’, British Journal of Cancer, 94(9), pp. 1253–1262.

Haedicke, J. and Iftner, T. (2016) ‘A review of the clinical performance of the Aptima HPV assay’, Journal of Clinical Virology, 76, pp. S40–S48.

HealthDxS.
https://healthdxs.com/en/thinprep/.(accessed June 13,2017)

HIQA (2017) ‘Health technology assessment of human papillomavirus testing as the primary screening method for prevention of cervical cancer’, Health Information and Quality Authority, (May), pp. 1–347.

Holmgren SC, et al (2005). The minor capsid protein L2 contributes to two steps in the human papillomavirus type 31 life cycle. Journal of Virology; **79**(7): 3938– 3948.

Ikenberg, H. et al. (2013) ‘Screening for cervical cancer precursors with p16/Ki-67 dual-stained cytology: Results of the PALMS study’, Journal of the National Cancer Institute, 105(20), pp. 1550–1557.

Jess, P. R. T. et al. (2007) ‘Early detection of cervical neoplasia by Raman spectroscopy’, International Journal of Cancer, 121(12), pp. 2723–2728.

Johansson C, et al (2012). HPV-16 E2 contributes to induction of HPV-16 late gene expression by inhibiting early polyadenylation. The EMBO Journal 2012; 31(14) pp. 3212–3227.

Kamemoto, L. E. et al. (2010) ‘Near-infrared micro-Raman spectroscopy for in vitro detection of cervical cancer’, Appl Spectrosc, 64(3), pp. 255–261.

Kanter, E. M. et al. (2009) ‘Application of Raman spectroscopy for cervical dysplasia diagnosis’, Journal of Biophotonics, 2(1–2), pp. 81–90.

Kanter. E.M et al., (2009). “Effect of hormonal variation on Raman spectra for cervical disease detection,” Am. J. Obstet. Gynecol. 200, pp 512 –512.

Kearney, P. et al. (2017) ‘Raman spectral signatures of cervical exfoliated cells from liquid-based cytology samples.’, Journal of biomedical optics, 22(10), pp. 1–10.

Kerr.L.T et al., (2016). “Methodologies for bladder cancer detection with Raman based urine cytology,” Anal. Methods 8, pp.4991–5000.

Kitchener, H. C. et al. (2011) ‘MAVARIC - A comparison of automation-assisted and manual cervical screening: A randomised controlled trial’, Health Technology Assessment, 15(3), pp. 1–176.

Kohavi, R. (1995) ‘A Study of Cross-Validation and Bootstrap for Accuracy Estimation and Model Selection 2 Methods for Accuracy Estimation’, Proc. of IJCAI, (2)pp. 1137–1145.

Kong.K et al., (2015). “Raman spectroscopy for medical diagnostics—from in- vitro biofluid assays to in-vivo cancer detection,” Adv. Drug Delivery Rev. 89, pp.121–134.

Koss, L. G. (2005) Diagnostic Cytology and Its Histopathologic Bases. 5th edn, Volume 5.

5th edn. Edited by L. G.Koss. Lippincott Williams & Wilkins.

Krishna, C. M. et al. (2006) 'Vibrational Spectroscopy Studies of Formalin-Fixed Cervix Tissues Vibrational Spectroscopy Studies of Formalin-Fixed Cervix Tissues', Biopolymers, 85(3), pp. 214–221.

Laboratory,T.P.K. Spectroscopic Characterization https://www3.nd.edu/kamatlab/facilities_spectroscopy.html (accessed December 12, 2016)

Lyng, F,et al. (2015) 'Raman spectroscopy for cytopathology of exfoliated cervical cells', Analytical and Bioanalytical Chemistry, 407(27), pp. 8279–8289.

Lyng, F. et al. (2015) 'Vibrational Microspectroscopy for Cancer Screening', Applied Sciences, 5, pp.23-35.

Mahadevan-jansen, A. (2010) 'Disease Detection', Arn J Obstet Gynecol., 200(5), pp. 1–13.

Mahadevan-Jansen, et al (1998) 'Development of a Fiber Optic Probe to Measure NIR Raman Spectra of Cervical Tissue In Vivo', Photochem Photobiol, 68, pp. 427–31.

manhattancenterforgynecology. https://manhattancenterforgynecology.com/colposcopy/(accessed September 20,2019)

Marquez-Curtis, L. A., McGann, L. E. and Elliott, J. A. W. (2017) 'Expansion and cryopreservation of porcine and human corneal endothelial cells', Cryobiology. Elsevier Ltd, 77, pp. 1–13.

McGrath, C. J. et al. (2017) 'Role of p16 testing in cervical cancer screening among HIV-infected women', Plos one, 12(10), pp. 1–9.

Meade, A. et al (2010) 'Studies of Chemical fixation effects in Human cell lines using Raman Mircrospectroscopy', Bioanalytical chemistry, 369(5), pp. 1781–1791.

Medicoapps.org https://medicoapps.org/m-cervical-intraepithelial-neoplasia-cin/(accessed September 23, 2019)

Medipally, D. K. R. et al. (2017) 'Development of a high throughput (HT) Raman spectroscopy method for rapid screening of liquid blood plasma from prostate cancer patients', The Analyst. Royal Society of Chemistry, 142(8), pp. 1216–1226.

Medlineplus https://medlineplus.gov/ency/imagepages/19263.htm (accessed March 14, 2018).

Milligan SG, et al (2007). Analysis of novel human papillomavirus type 16 late mRNAs in differentiated W12 cervical epithelial cells. Virology; **360**(1) pp. 172– 181.

Mo, J. et al. (2009) 'High wavenumber Raman spectroscopy for in vivo detection of cervical dysplasia', Anal. Chem, 81(21), pp. 8908–8915.

Movasaghi, Z., Rehman, S., U., R. I. (2007) 'Raman spectroscopy of biological tissues.', Applied Spectroscopy Reviews, 42, pp. 493–541.

Munoz, N. et al. (2010) 'Impact of Human Papillomavirus (HPV)-6/11/16/18 Vaccine on All HPV-Associated Genital Diseases in Young Women', Journal of the National Cancer Institute, 102(5), pp. 325–339.

Nair.A, H. T. (2010) A Case Based, Clinical Guide. Edited by S. Science+ and B. (Genevieve N.-P. Media. New York: Contemporary Endocrinology.

Nanda K.et al. (2000) 'Accuracy of the Papanicolaou Test in Screening for and Follow-up of Cervical Cytologic Abnormalities', Ann Intern Med, 132, pp. 810–819.

Ostrowska, K. M. et al. (2010) 'Investigation of the influence of high-risk human papillomavirus on the biochemical composition of cervical cancer cells using vibrational spectroscopy', The Analyst, 135(12), pp. 3087.

O'Dea, D. et al. (2018) 'Raman spectroscopy for the preoperative diagnosis of thyroid cancer and its subtypes: An in vitro proof-of-concept study', Cytopathology, 30(1) pp. 51-60.

Peakman, T. and Elliott, P. (2010) 'Current standards for the storage of human samples in biobanks', Genome Medicine, 2(10), pp. 2–4.

Petry, K. U. et al. (2017) 'A model to evaluate the costs and clinical effectiveness of human papilloma virus screening compared with annual papanicolaou cytology in Germany', European Journal of Obstetrics Gynecology and Reproductive Biology. Elsevier Ireland Ltd, 212, pp. 132–139.

Pirro, V. et al. (2017) 'Intraoperative assessment of tumor margins during glioma resection by desorption electrospray ionization-mass spectrometry', Proceedings of the National Academy of Sciences, 114(26), pp.6459.

Poljak, M. et al. (2016) 'Commercially available molecular tests for human papillomaviruses (HPV): 2015 update', Journal of Clinical Virology, 76, pp.3–13

Ramos.I, Malkin.A, and Lyng.F, (2015). "Current advances in the application of Raman spectroscopy for molecular diagnosis of cervical cancer," BioMed Res. Int. 9,pp 1–9.

Ramos, I. R. et al. (2016) 'Raman spectroscopy for cytopathology of exfoliated cervical cells', in Faraday Discuss., pp. 187–198.

Rashid, N. et al. (2014) 'Raman microspectroscopy for the early detection of pre-malignant changes in cervical tissue', Experimental and Molecular Pathology. Elsevier Inc., 97(3), pp. 554–564.

Robichaux-Viehoever.A. et al (2007) 'Characterization of Raman Spectra Measured in Vivo for the Detection of Cervical Dysplasia', Applied Spectroscopy, Vol 61(9), pp. 986–993.

Rodriguez, E. F. et al. (2012) 'Atypical squamous cells of undetermined significance in patients with HPV positive DNA testing and correlation with disease progression by age group: An institutional experience', International Journal of Clinical and Experimental Pathology, 5(5), pp. 428–435.

Romeo, M. J., Quinn, M. A., Burden, F. R., McNaughton, D (2002) 'Influence of benign cellular changes in diagnosis of cervical cancer using IR microspectroscopy'. Biopolymers 67, pp.362–366.

Romeo.M, Romeo.M.J, Wood B.R. (2002)'Observing the cycling changes in cervical epithelium using infrared microspectroscopy', Vibrational Spectroscopy, 28, pp167-175.

Ronco, G. et al. (2010) 'Efficacy of human papillomavirus testing for the detection of invasive cervical cancers and cervical intraepithelial neoplasia: a randomised controlled trial', The Lancet Oncology, 11(3), pp. 249–257.

Ronco, G. et al. (2014) 'Efficacy of HPV-based screening for prevention of invasive cervical cancer: Follow-up of four European randomised controlled trials', The Lancet, 383(9916), pp. 524–532.

Rozemeijer, K. et al. (2016) 'Comparing SurePath, ThinPrep, and conventional cytology as primary test method: SurePath is associated with increased CIN II+detection rates', Cancer Causes and Control, 27(1), pp. 15–25.

Rozenberg.S et al (2001)'Clinical evidence supporting the rationale for constant oestrogen, intermittent progestogen hormone replacement therapy'.Eur J Obstet Gynecol Reprod Biol. Jan;94(1) pp.86-91.

Rubina.S, M. S. Vidyasagar, and C. M. Krishna, (2013). "Raman spectroscopic study on prediction of treatment response in cervical cancers,Innovative Opt. Health Sci. 6, 1350014

Rubina.S, C, Murali, K. (2015) 'Raman spectroscopy in cervical cancers: An update', Journal of cancer research and therapeutics, 11(1), pp. 10–17.

Vargis.E et al., (2011). "Effect of normal variations on disease classification of Raman spectra from cervical tissue," Analyst 136, pp 2981–2987.

Vargis.E et al., (2012). "Near-infrared Raman microspectroscopy detects high- risk human papillomaviruses," Transl. Oncol. 5, pp 172–179.

Winer, R. L. et al. (2003) 'Genital human papillomavirus infection, incidence and risk factors in a cohort of female university students', American Journal of Epidemiology, 157, pp. 218–226.

Sahdev,A et al. (2010)'Cervical tumours',Seminars in Ultrasound, CT and MRI Elsevier Inc., 31(5), pp399-413.

Sanchez-Rojo et al. (2016)'Cervical cancer detection based on serum sample surface enhanced Ramannspectroscopy', Rev Mex Fis,62, pp. 213-218.

Sankaranarayanan R, S. J. (2003) Colposcopy and Treatment of Cervical Intraepithelial Neoplasia., World Health Organization - International Agency for Research on Cancer (IARC)

Santos, I.P, Barroso, E.M (2017) 'Raman spectroscopy for cancer detection and cancer surgery guidance: translation to the clinics', Analyst, 142, pp. 3025–3047.

Sanjosé, S. et al. (2007) 'Worldwide prevalence and genotype distribution of cervical HPV in women with normal cytology', Lancet Infect, 7(7), pp. 453–459.

Schiffman, M., Clifford, G. and Buonaguro, F. M. (2009) 'Classification of weakly carcinogenic human papillomavirus types: Addressing the limits of epidemiology at the borderline', Infectious Agents and Cancer, 4(1), p. 8.

Semantic Scholar
https://www.semanticscholar.org/paper/Rethinking-Human-Papillomavirus-Vaccine-for-Oral-Yu/284f533e2e16c97bd8fe06015bba1af62560e67a (accessed September 20, 2019)

Shambayati, B. (2011) Cytopathology. 1st edn. Oxford University Press p1-25.

Serafïn-Higuera, I. et al. (2016) 'Differential proteins among normal cervix cells and cervical cancer cells with HPV-16 infection, through mass spectrometry-based Proteomics in women from Southern Mexico', Proteome Science. Proteome Science, 14(1), pp. 1–9.

Shekinah medical
https://shekinahmedical.com/f5/fliers/flierbase.php?title=Colposcopy&graphic=colposcope.jpg&text=colposcopy (accessed November 21, 2017)

Silverthorn, D. U. Human Physiology: An integrated Approach. 6th edn. Edited by I. Glenview. Pearson Education. (2013) pp 236-238.

Torre, L. A. et al. (2015) 'Global Cancer Statistics, 2012', CA: a cancer journal of clinicians., 65(2), pp. 87–108.

Troiano, N. W., Ciovacco, W. A. and Kacena, M. A. (2009) 'The Effects of Fixation and Dehydration on the Histological Quality of Undecalcified Murine Bone Specimens Embedded in Methylmethacrylate', Journal of Histotechnology, 32(1), pp. 27–31.

Ullal, A. Roberts M, Bulmer JN et al. The role of cervical cytology and colposcopy in detecting cervical glandular neoplasia. Cytopathology, 20(6): pp.359-366

Utzinger.U et al., (2001). "Near-infrared Raman spectroscopy for in vivo detection of cervical precancers," Appl. Spectrosc. 55, pp. 955–959.

Walboomers, J. M. M. et al. (1999) 'Human papillomavirus is a necessary cause of invasive cervical cancer worldwide', Journal of Pathology, 189(1), pp. 12–19.

Wong, P. T. et al. (1991) 'Infrared spectroscopy of exfoliated human cervical cells: evidence of extensive structural changes during carcinogenesis.', Proceedings of the National Academy of Sciences of the United States of America, 88(24), pp. 10988–10992.

Wong, P. T. et al. (2002).'Detailed account of confounding factors in interpretation of FTIR spectra of exfoliated cervical cells',Biopolymers, 67: 376-386.

Wong, A. A. et al. (2012) 'Comparison of the hybrid capture 2 and cobas 4800 tests for detection of high-risk human papillomavirus in specimens collected in PreserVcyt medium', Journal of Clinical Microbiology, 50(1), pp. 25–29.

Wood, B. R. et al. (1998) 'FTIR Microspectroscopic Study Of Cell Types And Potential Confounding Variables In Screening For Cervical Malignancies', Biospectroscopy, 4(2), pp. 75–91.

Youssef, M. A. et al. (2016) ‘Prevalence of human papilloma virus (HPV) and its genotypes in cervical specimens of Egyptian women by linear array HPV genotyping test’, Infectious Agents and Cancer. Infectious Agents and Cancer, 11(1), pp. 1–10.

Zheng, Z.-M. and Baker, C. C. (2006) ‘Papillomavirus genome structure, expression, and post-transcriptional regulation.’, Frontiers in bioscience : a journal and virtual library, 11, pp. 2286–302

Zuchna, C. et al. (2010) ‘Diagnostic accuracy of guided cervical biopsies: A prospective multicenter study comparing the histopathology of simultaneous biopsy and cone specimen’, American Journal of Obstetrics and Gynecology. Elsevier Inc., 203(4), p. 321-321

8.2 Publications

- European Patent – Cervical Sample preparation for reduced variability in Raman spectra.
- Traynor, D. (2019)The potential of biobanked liquid based cytology samples for cervical cancer screening using Raman spectroscopy- J. Biophotonics.;12:e201800377.
- Traynor, D. (2018) Improved removal of blood contamination from Thinprep cervical cytology samples for Raman spectroscopic analysis *J. Biomed. Opt.* **23**(5), 055001.
- Traynor, D. (2017) A study of variability due to hormonal effects in cervical smear samples using Raman spectroscopy. J. Biophotonics.;e201700240

Received: 25 August 2017 | Revised: 31 October 2017 | Accepted: 5 December 2017
DOI: 10.1002/jbio.201700240

Journal of BIOPHOTONICS

FU LL ARTICLE

A study of hormonal effects in cervical smear samples using Raman spectroscopy

Damien Traynor[1]* | Padraig Kearney[1] | Ines Ramos[1] | Cara M. Martin[2] | John J. O'Leary[2] | Fiona M. Lyng[1]

[1]DIT Centre for Radiation and Environmental Science, Focas Research Institute, Dublin Institute of Technology (DIT), Dublin, Ireland

[2]Department of Pathology, Coombe Women & Infants University Hospital, Dublin, Ireland

*Correspondence
Damien Traynor, DIT Centre for Radiation and Environmental Science, Focas Research Institute, Dublin Institute of Technology, Kevin Street, Dublin 8, Ireland.
Email: damien.traynor@dit.ie

Raman spectroscopy is a powerful tool that has the potential to be used as a screening method for cervical cancer. It is a label-free, low-cost method providing a biochemical fingerprint of a given sample. The objective of this study was to address patient-to-patient variability contributed by hormonal effects due to the menstrual cycle, the use of hormone-based contraceptives (HC) and the onset of menopause, and to determine if these changes would affect the ability to successfully identify dyskaryotic cells. Raman spectra were recorded from unstained ThinPrep cervical samples (45 cytology negative and 15 high-grade dyskaryosis (high-grade squamous intraepithelial lesion, HSIL) samples using a HORIBA Jobin Yvon XploRA system. HPV DNA testing was also performed. Clinical data collected included date of the last menstrual period, the use of HC and/or menopausal status. Spectral changes were observed depending on the day of the menstrual cycle and on the use of HC. Despite this, HSIL could be discriminated from normal cells regardless of the day on which the sample was taken or the use of HC.

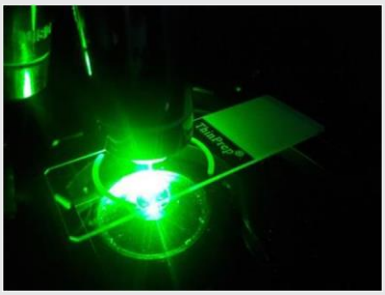

KEYWORDS
contraceptive, cytology, hormones, menstrual cycle, Raman spectroscopy, ThinPrep

1 | INTRODUCTION

There were an estimated 527 600 new cervical cancer cases and 265 700 deaths from cervical cancer worldwide in 2012 [1]. Until recently, the primary method for cervical screening was based on the Papanicolaou test (Pap test). The Pap test requires cells to be scraped from the cervix, fixed to a glass slide, stained and reviewed by a trained cytologist. Cellular abnormalities are identified by the cytologist based on cellular morphology and staining characteristics and classified according to the degree of dysplasia (low grade or high grade). The advantage of the Pap test is that it is a non-invasive and widely accepted screening based test with a high specificity of 95% to 98% and a sensitivity of 74% to 96% [2]. The variability in the rates of sensitivity can be due to sampling technique; the subjectivity of the cytology- based screening and can result in a high rate of gynaecolo- gical referral and patient recall, which adds to cost and patient stress. Persistent infection with high-risk human papillomavirus (HPV), such as HPV types 16 and 18, is accepted as the major cause of cervical pre-cancer and can- cer [3, 4]. HPV DNA testing has a higher sensitivity (>95%) but lower specificity (~84%) than the Pap test [5] and these tests are expensive, time-consuming and provide no information on cervical cytopathology. Current gold standard methods for detection of cervical cancer and pre-

cancer are, therefore, limited and there is an unmet clinical need for new objective screening or diagnostic tests. Optical spectroscopic techniques, such as Raman or infrared spectroscopy, are label-free, non-invasive and have several advantages over traditional approaches, including objectivity, speed and cost. These methods can provide quantitative information based on the spectroscopic signature of the biochemical components of the sample allowing diagnosis to be based on biochemical changes rather than on morphological changes. The focus of the present study is on Raman spectroscopy, which is based on inelastic light scattering. The coupling of the light generates vibrations within the material and these vibrations are characteristic of the chemical structure, the energy of the scattered light is reduced by an amount equal to the vibrational energy and from this a rapid, label-free, non-destructive measurement of the complete biochemical fingerprint of a biological sample can be obtained. Over the past 15 years, the potential of Raman spectroscopy together with multivariate statistical analysis has been demonstrated for the detection of a variety of cancers, including cervical cancer [6, 7]. In initial infrared spectroscopy studies on cervical cytopathology samples [8–10], spectra were recorded from cell pellets rather than from single cells and the presence of metaplastic cells, endocervical columnar cells, polymorphs, blood, cervical mucus and debris were all identified as confounding factors [11–16]. Recent studies by Ramos et al. [17] and Bonnier et al. [18] addressed the variability in Raman spectra from cervical smear samples and reported a new method to clear blood residue contamination before Raman spectroscopy based on pretreatment of the slides with hydrogen peroxide. This method significantly minimised variability and resulted in the collection of highly reproducible data and was used in this study to reduce variability based on the presence of blood residue. Physiological factors such as hormonal changes during the menstrual cycle or during menopause may also be potential sources of variability in the normal cervix.

The cellular make up of an individual woman's smear is dependent on which day during the menstrual cycle the sample was taken [19]. Days 1 to 4 are classed as the menstruation phase of the cycle when bleeding will occur and smear samples are generally not taken during this phase. Days 5 to 13 are classified as the proliferative phase. During this phase, oestrogen levels reach their peak resulting in complete maturation of the squamous epithelium and the cervical smear will present with a higher ratio of superficial cells to intermediate cells. Days 14 to 28 are classified as the secretory phase where progesterone production reaches its peak and prevents complete maturation of the epithelium. The cervical smear will present with a higher ratio of intermediate cells to superficial cells. During menopause, levels of both oestrogen and progesterone will drop dramatically and there is a gradual arrest of the maturation of the squamous epithelium. This results in the loss of superficial and intermediate cells leading to the final atrophic stage where the squamous epithelium is composed entirely of parabasal cells.

The use of hormone-based contraceptives (HC) will affect the natural hormone mediated maturation process of the cervical epithelium. A study by Romeo et al. [20] used infrared spectroscopy to investigate hormonal influences on cervical cells throughout the menstrual cycle and showed spectral changes such as increases in the 1200 to 1000 cm^{-1} region due to glycogen increases around ovulation (mid cycle). Cervical cells from women on HC did not show the same degree of spectral changes as cells from women not on HC. Despite the variability throughout the menstrual cycle, principal component analysis (PCA) showed good discrimination between high-grade dysplasia and normal samples collected at different phases of the menstrual cycle.

A more recent study by Kanter et al. [21] has shown that hormonal differences due to the menstrual cycle can influence the Raman spectra acquired from the cervix in vivo. Spectra were divided into 4 groups, namely, pre-menopausal proliferative phase (days 1-14), pre-menopausal secretory phase (day 15-28+), peri-menopausal and post-menopausal. Spectral differences were mainly observed at 1250, 1300 and 1320 cm^{-1}, most likely due to changes in the proteins collagen and elastin [22]. Incorporating hormonal status into their dysplasia classification algorithm increased the classification accuracy from 88% to 94%.

The main objective of our study was to investigate hormone-associated changes in the Raman spectra of cytologically negative ThinPrep cervical smear samples related to: (1) the menstrual cycle, (2) the onset of menopause and (3) the use of HC. A further objective was to determine if any changes observed would interfere with the ability to discriminate normal and high-grade dyskaryotic (high-grade squamous intraepithelial lesion, HSIL) cervical smear samples caused by HPV infection.

2 | MATERIALS AND METHODS

2.1 | Sample collection and ThinPrep slide preparation

Cervical smear samples collected in PreservCyt solution were obtained from the Cytology Department at the Coombe Women and Infants University Hospital (CWIUH), Dublin, Ireland, after routine cytological screening had been performed. Ethical approval for use of anonymised samples for the study was granted by the CWIUH Research Ethics Committee (no. 28-2014). Clinical data which were recorded relating to the samples included cytology result, date of last menstrual period, age at time of smear test and reported use of HC. No information on smoking status was available. A total of 60 cervical smear samples,

TABLE 1 Sample details including day of the menstrual cycle, menopausal status and use of HC

Sample number	Cytology result	Day of cycle	Postmenopausal	HPV result	Contraceptive
1	Negative	7	/	Negative	None
2	Negative	9	/	Negative	None
3, 4, 5, 6, 7	Negative	10	/	Negative	None
8, 9	Negative	11	/	Negative	None
10, 11, 12, 13, 14	Negative	12	/	Negative	None
15, 16, 17, 18, 19, 20, 21, 22	Negative	13	/	Negative	None
23, 24	Negative	16	/	Negative	None
25, 26	Negative	20	/	Negative	None
27	Negative	21	/	Negative	None
28	Negative	24	/	Negative	None
29, 30, 31, 32, 33, 34, 35	Negative	/	Postmenopausal	Negative	/
36, 37, 38, 39, 40, 41, 42, 43, 44, 45	Negative	/	/	Negative	HC
46, 47, 48, 49, 50, 51, 52, 53, 54, 55, 56, 57, 58, 59, 60	High grade	/	/	Positive	None

45 confirmed as cytology negative and 15 confirmed HSIL samples, were used for this study.

A slide was prepared for each sample using a ThinPrep 2000 processor (Hologic Inc., Marlborough, Massachusetts). The Thin Prep processor starts by homogenising the sample by spinning the filter, creating shear forces in the fluid that are strong enough to disaggregate randomly joined material, break up blood, mucus and non-diagnostic debris. The cells are then collected onto the membrane of the filter and transferred onto a glass slide to create a circular monolayer deposit of cells 20 mm in diameter and a few microns in thickness. The slide is then ejected automatically into a fixative bath of 95% ethanol.

The presence of blood residues on ThinPrep slides is a limiting factor that needs to be removed in order to collect data with minimal variability [19]. Therefore, the slides were treated with a 30% solution of H_2O_2 at room temperature for 3 min. The slides were then placed into a 70% solution of industrial methylated spirits (IMS) for 3 min followed by multiple dips into 100% IMS to remove any remaining cellular debris and H_2O_2. The slide was then air dried.

2.2 | HPV testing

One millilitre of the remaining test sample was tested for HPV using the Cobas 4800 HPV test. The Cobas 4800 test is an automated extraction and real-time PCR system that is capable of identifying 14 different high-risk HPV types as well as the ability to genotype for HPV 16/18. The Cobas 4800 test starts by first collecting 400 μL of the test sample and heating it up to start the denaturing process. The cells are then lysed by a chaotropic reagent. The lysis step releases the HPV nucleic acids. These nucleic acids are negatively charged which bind to positively charged magnetic glass particles that are held in place by a magnetic plate. The nucleic acids are then washed and separated from the glass particles, before they are amplified and detected by RT-PCR. Sequences of approximately 200 nucleotides are targeted by primers for the PCR reaction. The nucleotides are located within the L1 region of the HPV genome, with the master mix containing the primers designed for 14 different high- risk HPV genotypes (16, 18, 31, 33.35, 39, 45, 51, 52, 56, 58, 59, 66 and 68). Fluorescent oligonucleotides are then added which can bind to the sequences within these primers during the PCR. The detection of these fluorescent oligonucleotides will give either a positive or negative result.

2.3 | Raman microspectroscopy

Raman studies were performed using a HORIBA Jobin Yvon XploRA system (Villeneuve d'Ascq, France) which incorporates the Olympus microscope Bx41. As source, a 532 nm laser of ~12 mW power was focused onto the sample using a 100× objective (MPlan; Olympus, NA = 0.9) giving a spot size of 1 to 2 μm. The confocal hole was set at 100 μm for all measurements, the specified settings for confocal operation. The system was pre-calibrated to the 520.7 cm^{-1} spectral line for silicon. The 1200 lines per mm grating was used. The backscattered light was measured using an air-cooled CCD detector (Andor, 1024-256 pixels). The spectrometer was controlled by Labspec V5.0 software (Villeneuve d'Ascq, France). For each cell, one spectrum was recorded from the nucleus for 2 accumulations of 30 seconds in the spectral range of 400 to 1800 cm^{-1}. Spectra were recorded only from the cell nucleus as these have been found to be more reproducible and consistent than spectra from the cell cytoplasm [23]. On average, 30 cells were recorded from each sample (superficial and intermediate cells). The *x*,*y* co-ordinates of each cell were recorded on the Raman microscope. After Raman acquisition was complete and following Pap staining, each cell could be re-visited and assigned as superficial or intermediate. The 15 HSIL smears were screened for HSIL cells and spectra recorded accordingly.

2.4 | Data pre-processing and analysis

Data were normalised and analysed using Matlab software (Mathworks, Natick, Massachusetts, USA) and specific scripts

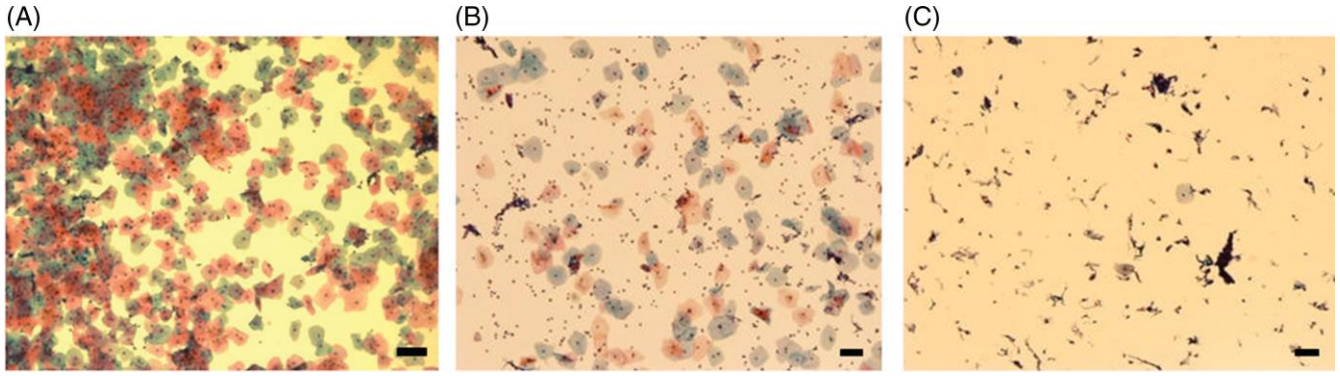

FIGURE 1 (A) Proliferative phase presentation of a Pap smear. Note the higher ratio of superficial (pink stained) to intermediate (blue stained) cells, (B) secretory phase presentation of a Pap smear. Note the higher ratio of intermediate (blue stained) to superficial (pink stained) cells, (C) postmenopausal presentation of a Pap smear. Note the lack of cellular material, mucus and cellular debris. Bar = 35 μm

developed and adapted for uploading of the spectra and their pre-processing, including smoothing (Savitzky-Golay $K = 5$, $K = 13$), baseline correction (rubberband) and vector normalisation. An in house method for glass removal based on non-negativity constrained least squares was used to remove the spectral features of glass [23]. The algorithm weights the values of glass as well as cell components in the acquired spectra from the cell and further subtracts the glass from the cell spectra applying non-negative constraints.

Classification methods find mathematical models that are able to recognise the membership of each sample to its appropriate class on the basis of a set of measurements.

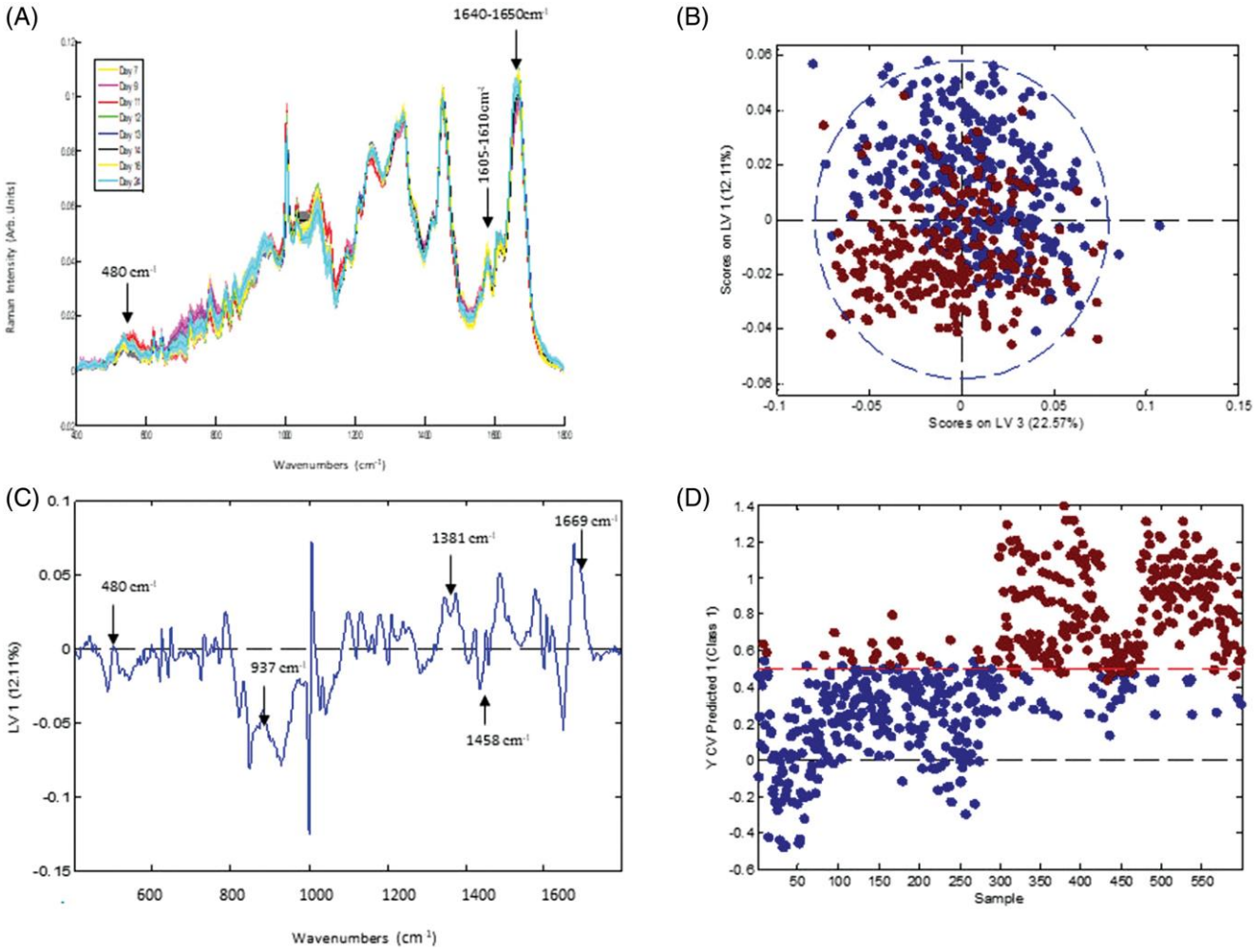

FIGURE 2 (A) Mean Raman spectra of intermediate and superficial cells from days 7 to 24. Shading denotes the SD, (B) LV scores scatter plot of proliferative phase, days 7 to 14 (blue) vs secretory phase, days 15 to 24 (red), (C) LV1 loadings, (D) PLS-DA prediction plot

TABLE 2 Tentative peak assignments [22]

Raman shift (cm^{-1})	Proteins	Lipids	Carbohydrates	Nucleic acids
482			Glycogen	
577			Glycogen	
622	C–C twist Phe			
643	C–C twist Tyr			
727	CH2 def	C–C head		A
752	Sym br. Trp			
781				U,C,T ring br
826	Out of plane ring br. Tyr			PO2 a.Str
851	Ring br. Tyr, C–C str. Pro			
852			Glycogen	
937			Glycogen	
985		C–C head		
1002	Sym. Ring br. Phe			
1033	C–H in plane Phe, C–C str			
1044			Glycogen	
1060	C–N str			
1082	C–N str	Chain C–C str	C–O str, glycogen	
1096		Chain C–C str	C–C str	
1106			Glycogen	
1123	C–N str	Chain C–C str	C–O str	
1152	C–N str			
1207	C–C6H5 str. Phe, Trp			
1238	C–N str, amide III			
1261			Glycogen	
1334			Glycogen	
1338	Trp			G
1366		Sym. Str. CH3		
1381			Glycogen	
1450	CH2 def	CH2 def		
1458			Glycogen	
1487	CH2 def			G,A
1560	Tyr, Trp			
1575				A,G ring br
1584	C–C str, C–C bend. Trp, Phe			
1605	C–C Phe, Tyr			
1642	C–O str, C–C sym. Str.			
1669	C–O str. Amide I			

When the classification model has been calibrated, the membership of unknown samples to one of the defined classes can be predicted. Although PCA-LDA is the standard method used to maximise the variations in the X direction, PLS-DA by rotating both the *X* and *Y* axes allows even small variations to be captured. This was necessary to identify the normal biochemical changes associated with the menstrual cycle. Partial least squares discriminant analysis (PLS-DA) was used to build classification models in this study together with leave-one patient-out cross-validation. PLS-DA analysis was performed using the PLS toolbox (Eigenvector Research, Washington, USA) in the Matlab (Mathworks Inc.) environment.

From the data provided by the patient about their last menstrual period and the day on which the sample was taken, the day of the menstrual cycle the smear was taken was calculated. It was assumed that each patient follows the standard 28 -day cycle. Samples were only available from days 7 to 24 of the cycle. Table 1 shows the sample details including day of the menstrual cycle, menopausal status and use of HC.

3 | RESULTS AND DISCUSSION

3.1 | Proliferative and secretory phase and postmenopausal cellular presentation on pap smear

The proliferative and secretory phase presentation of a Pap smear are shown in Figure 1A,B, respectively. A higher ratio of superficial (pink stained) to intermediate (blue

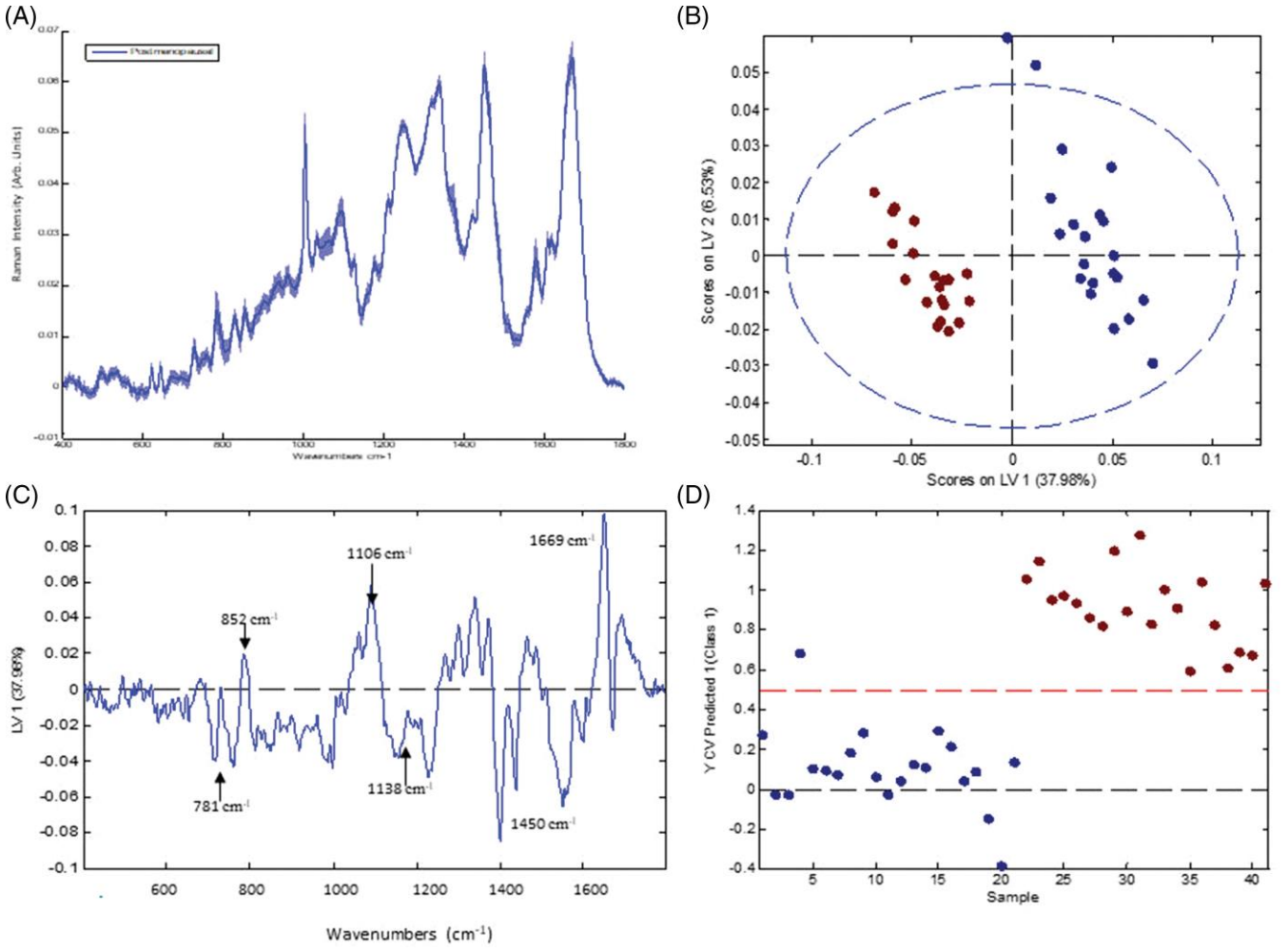

FIGURE 3 (A) Mean Raman spectra from postmenopausal samples. Shading denotes the SD, (B) LV scatter scores plot of postmenopausal (blue) and non-menopausal (red), (C) LV1 loadings, (D) PLS-DA prediction plot

stained) cells in the proliferative phase compared to a higher ratio of intermediate (blue stained) to superficial (pink stained) cells in secretory phase can be observed. A post-menopausal Pap smear is shown in Figure 1C. A lack of cellular material, mucus and cellular debris can be observed which caused difficulties in recording good quality spectra.

3.2 | Raman signature of proliferative phase vs secretory phase

The spectral data from the Pap smears were divided up according to the day of the menstrual cycle the sample was taken on. - Figure 2A shows the mean Raman spectra of cells from days 7 to 24 of the menstrual cycle. Increases in the Amide I (1640-1650 cm^{-1}) (see Table 2), Phenylalanine and Tyrosine (1605-1610 cm^{-1}) and glycogen (480 cm^{-1}) bands over time were observed. The latent variables (LV) scores scatter plot (Figure 2B) shows reasonable separation between the prolifera- tive phase (blue) and the secretory phase (red). Some overlap- ping is observed which is most likely due to the fact that each woman will differ slightly between the days of the menstrual cycle and the levels of oestrogen and progesterone present. The LV1 loadings shown in Figure 2C highlight areas similar to those highlighted in the mean Raman spectra (Figure 2A). The discrimination is mainly based on glycogen (480, 937, 1381 and 1458 cm^{-1}) that is more present in the secretory samples (red) due to the higher levels of progesterone, which promotes sub-nuclear glycogen accumulation [24], and proteins (CH_2 def, 1450 cm^{-1}) and Amide I (1669 cm^{-1}) which are higher in sam- ples collected from the proliferative phase of the cycle. The pre-diction plot from the PLS-DA model (Figure 2D) shows reasonably good classification of menstrual cycle phase (proliferative phase or secretory phase) with sensitivity of 83% and specificity of 86%.

3.3 | Raman signature of postmenopausal samples

Most women are generally screened for cervical cancer up until the age of 65 years. Between the ages of 48 and 55 years, most women are said to be menopausal. Hence, it is important to determine if Pap smears collected from post-menopausal women will have a similar Raman signature to non-postmenopausal women. Mucus and cellular debris present on postmenopausal samples obscure the little cellular material that is present on the slide and make it very diffi- cult to obtain good spectra, hence the number of spectra

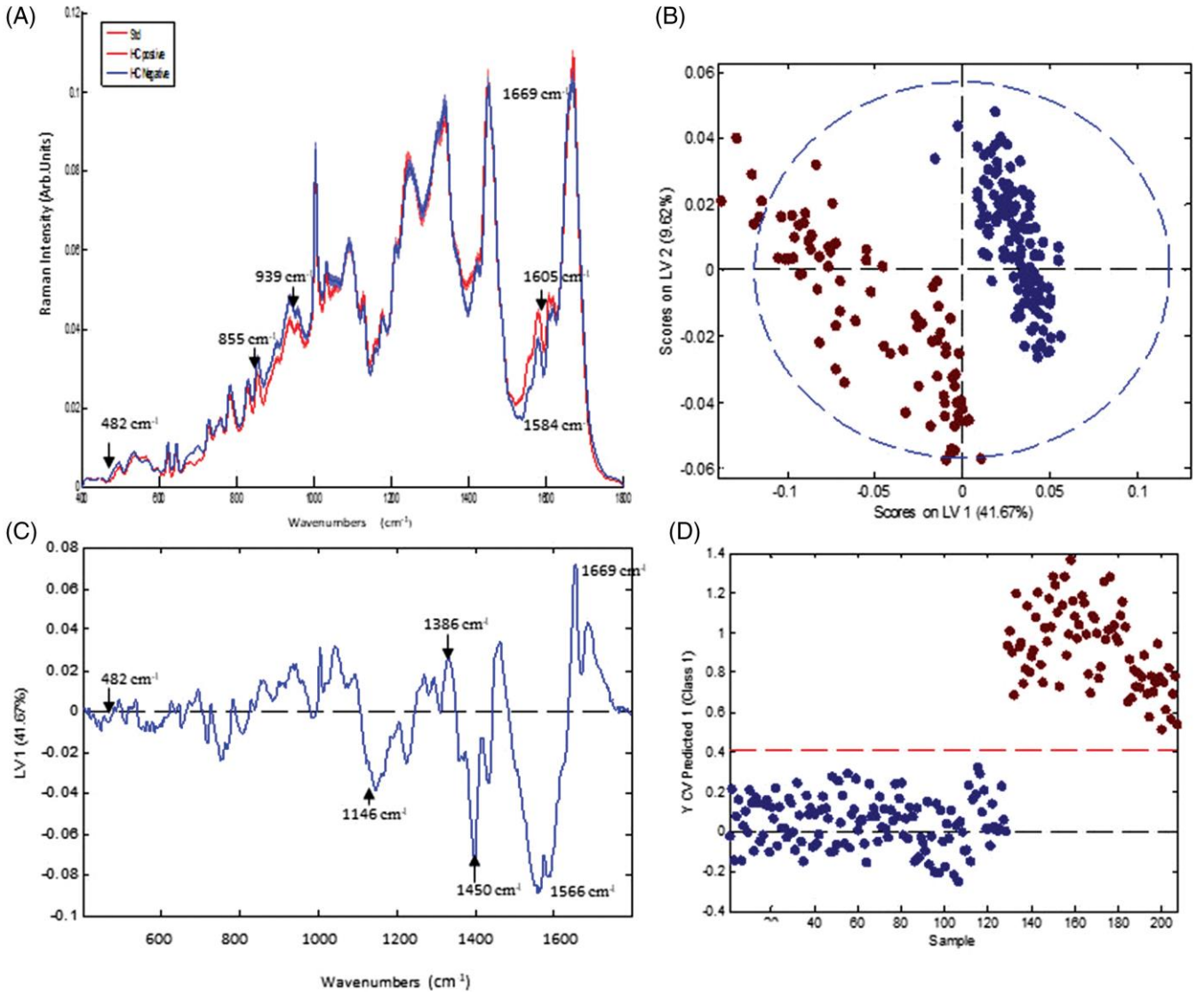

FIGURE 4 (A) Mean Raman spectra from HC positive and HC negative cells. Shading denotes the SD, (B) LV scatter scores plot of HC negative (blue) and HC positive (red), (C) LV1 loadings, (D) PLS-DA prediction plot

recorded is severely reduced and it is difficult to draw any firm conclusions. Figure 3A shows the mean and SD spectra of the 22 postmenopausal cells recorded. Figure 3B shows good discrimination between the 2 sample types. The loadings shown in Figure 3C show that the discrimination is based on glycogen (852, 1106 and 1138 cm^{-1}) and nucleic acids (781 cm^{-1}) proteins (1450 cm^{-1}) and Amide I (1669 cm^{-1}). Figure 3D shows the PLS-DA prediction plot which has a sensitivity of 100% and specificity of 95%.

Atrophic samples were not available as part of this study. No firm conclusions can be drawn from this data set except that postmenopausal samples can represent a problem for Raman-based screening based on their Pap smear presentation due to mucus, cellular debris and lack of cellular material.

3.4 | Raman signature associated with women on HC

The clinical details obtained indicated if the patient was on some form of HC. However, information on which type of contraceptive they are currently on was not included. The aim of this part of the study was to determine if Pap smears collected from women on HC will have a similar Raman signature to women who are not on HC.

Figure 4A shows that the levels of glycogen (482 and 855-939 cm^{-1}) in the HC-positive samples are lower when compared to the controls. The controls were made up of the samples collected throughout the menstrual cycle which were HC-negative. Tryptophan and Phenylalanine at peak position (1584-1605 cm^{-1}) and Amide I at peak (1669 cm^{-1}) are higher in HC samples compared to the control. The lower levels of glycogen in the HC samples could be linked to lower levels of progesterone due to its role in promoting sub-nuclear glycogen accumulation [24]. The same could be said for the higher levels of proteins detected (Phenylalanine, Tryptophan and Amide I). There is also a consistent change in the shoulder of Amide I, which is a change in Amide I protein position and folding between HC-positive and HC-negative samples. Overall, protein

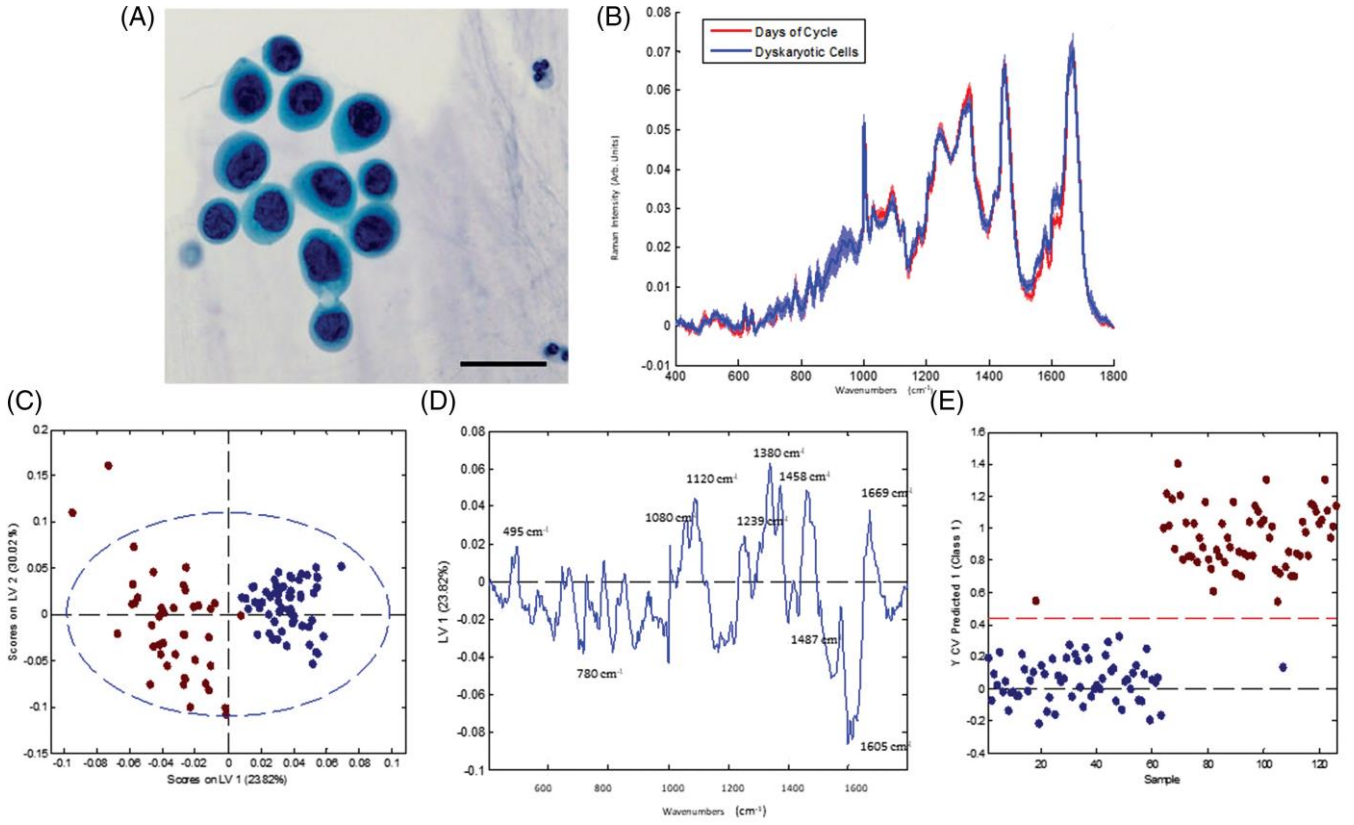

FIGURE 5 (A) Pap stained HSIL cells. Bar = 35 μm, (B) mean Raman spectra from negative samples from days 7 to 21 of the menstrual cycle (red) and spectra from HSIL samples (blue). Shading denotes the SD, (C) LV scores scatter plot of HSIL samples (red) and negative samples (blue), (D) LV1 loadings, (E) PLS-DA prediction plot

synthesis may be increased due to the constant level of hormones present.

The LV scores scatter plot (Figure 4B) shows good separation between HC-positive and HC-negative samples. There is a small amount of overlapping which could be due to a number of factors. Multiple types of contraceptive are available, which contain different types and levels of hormones, including implants, injectable contraceptive, progesterone pills, oestrogen and progesterone pills, combined oral and the patch all of which work by maintaining a constant level of hormones in the body thus preventing the rise and fall of oestrogen and progesterone. Hence, they may work differently and individual patients will also respond differently to the levels of hormones present. The loadings (Figure 4C) from LV1 show that glycogen (483 and 1386 cm^{-1}) and proteins and lipids (1146, 1450 and 1566 cm^{-1}) and Amide I (1669 cm^{-1}) are the main discriminating factors between HC-positive and HC-negative samples (Figure 4D). The PLS-DA prediction plot shows excellent classification with a sensitivity of 100% and specificity of 100%.

3.5 | Phase of menstrual cycle vs HSIL

It is important to determine if the changes observed throughout the menstrual cycle as seen in Figure 4 would affect the ability of Raman spectroscopy to discriminate HSIL from normal cells affected by the normal maturation of the cervical epithelium controlled by both the rise and fall of progesterone and oestrogen. For this part of the study, spectra from HSIL cells (Figure 5A) were recorded from 15 HPV-positive, HSIL samples and compared to an equivalent number of spectra from negative samples from days 7 to 21 of the menstrual cycle, all of which were HPV-negative. Figure 5B shows the mean spectra from neg- ative samples from days 7 to 21 of the menstrual cycle and spectra recorded from HSIL cells. The LV scores scatterplot in Figure 5C shows that HSIL cells separate well from nor- mal cells on the first LV. This shows that regardless of when a sample is taken during day 7 to 21 of the menstrual cycle, HSIL cells can still be effectively discriminated from cytology negative cells using Raman spectroscopy. Spectral changes due to the hormonal influence of oestrogen and progesterone seem to be less than the spectral changes due to the biochemical changes in the dyskaryotic cells. The loadings from LV1 in Figure 5D show that glycogen (495, 1080, 1120, 1380 and 1458 cm^{-1}), nucleic acids (780 and 1487 cm^{-1}), Amide III and Amide I proteins (1239 and 1669 cm^{-1}, respectively) and tryptophan and phenylalanine (1605 cm^{-1}) mainly contribute towards the discrimination between normal and HSIL cells. As the HSIL cells are a result of a high risk HPV infection, the

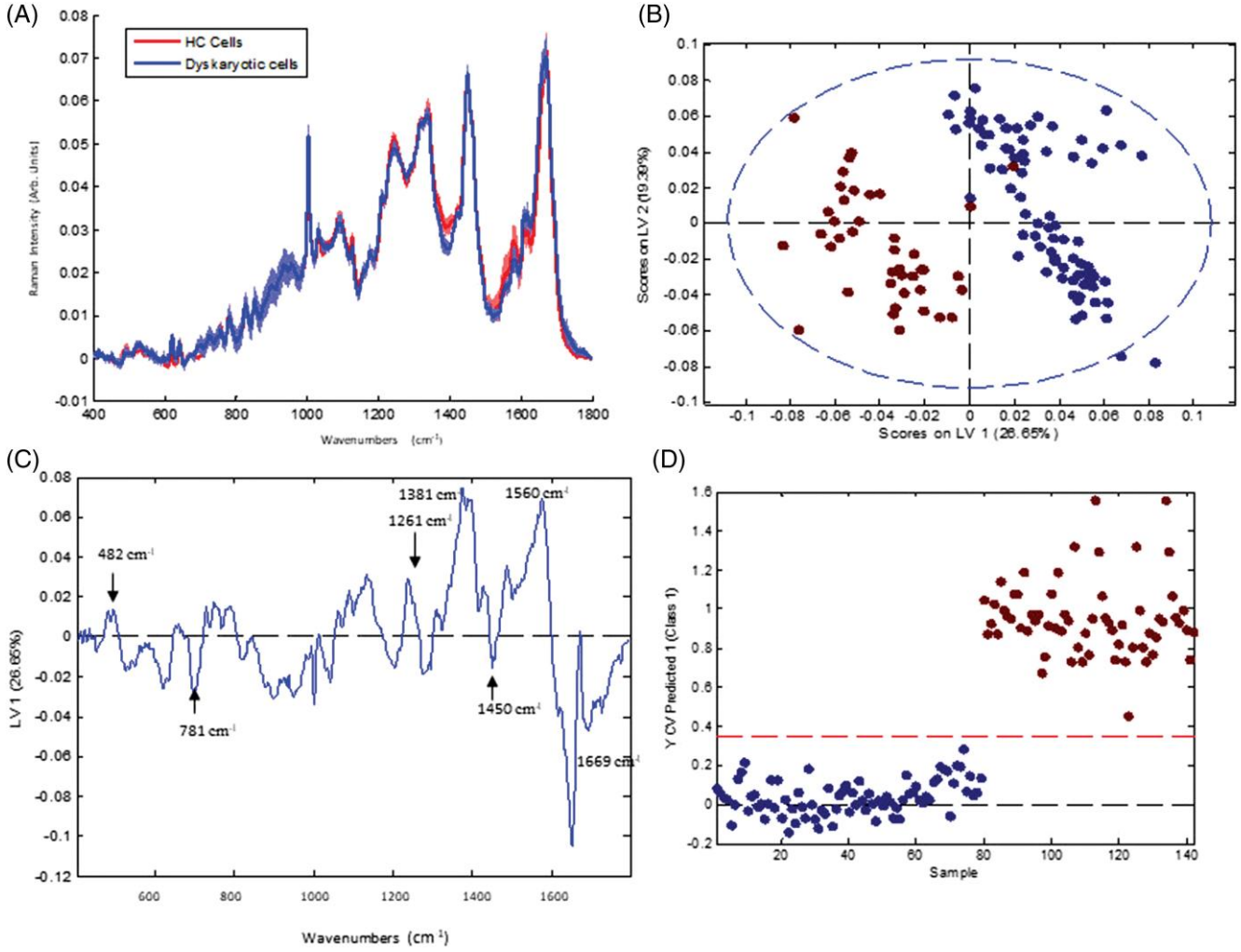

FIGURE 6 (A) Mean Raman spectra from negative HC positive samples (red) and spectra from HSIL cells (blue). Shading denotes the SD, (B) LV scores scatter plot of HSIL samples (red) and negative HC positive samples (blue), (C) LV1 loadings, (D) PLS-DA prediction plot

biochemical difference in glycogen, proteins and nucleic acids can be attributed to the downstream effects of the HPV infection. The predictions plot (Figure 5E) from the PLS-DA model shows excellent classification of the nega- tive samples (all menstrual cycle phases) and the dyskaryo- tic samples with sensitivity of 98% and a specificity of 97%.

3.6 | HC-positive samples vs HSIL

It is important to determine if the use of HC will also affect the ability of Raman spectroscopy to discriminate normal HC-positive cells from HSIL cells. Figure 6A shows the mean Raman spectra of HC-positive and HC-negative samples and spectra from HSIL cells. The LV scores scatterplot in Figure 6B shows that spectra from HC-positive samples separate from spectra from HSIL cells from HSIL samples on the first LV component with minimal overlap. Figure 6C shows the LV1 loadings which indicate that the main differences between the HC-positive cells and HSIL cells are very similar to those found for the HC negative and HSIL samples. Glycogen (482, 1261 and 1381 cm^{-1}), nucleic acids (781 cm^{-1}) and proteins (1450, 1560 and 1669 cm^{-1}) again contribute towards the discrimination. As before, it appears that the overtaking of the host cell machinery by HPV causes more of a biochemical change within the cell than the biochemical changes associated with the use of HC. The predictions plot from the PLS-DA model shows excellent classification of the negative samples (HC-positive) and the HSIL cells from HSIL samples (Figure 6D) with sensitivity of 96% and specificity of 98%.

Kanter et al. [22] showed that hormonal status influences Raman spectra from the cervix in vivo and that incorporating hormonal status into their classification algorithm increased the accuracy from 88% to 94%. However, the present study and that of Romeo et al. [20] on exfoliated cervical cells showed good discrimination between normal and abnormal samples regardless of phase of the menstrual cycle and of whether the woman was taking oral contraceptives or not.

4 | CONCLUSION

This study has shown that the day a Pap smear is taken during days 7 to 21 of the menstrual cycle will have an effect

on the spectra with regard to the level of glycogen and proteins. It should be noted, however, that this study assumes that each patient recruited follows the standard 28-day cycle, and that the patient details recorded for each sample were correct. It is possible for women have a longer or shorter cycle, hence this variation may have influenced our analysis. Postmenopausal samples represent a problem for Raman based screening due to their lack of cellular material and presence of cellular debris and mucus. The use of HC causes the most variability. Furthermore, study would be required to determine which hormone is causing the dis- crimination between HC-positive and HC-negative samples. These findings suggest that the use of oral contraceptives and the day on which the Pap smear was taken during the menstrual cycle should be incorporated into the data analy- sis to reduce variability between patient samples.

Despite this, however, the variability between days of the menstrual cycle or use of HC did not hinder the ability of Raman spectroscopy to discriminate cytology negative cells from HSIL cells. The biochemical changes induced in HSIL cells due to an active HPV infection were more pronounced than the biochemical changes due to the menstrual cycle or the use of HC. It is acknowledged that the study is limited in focussing only on HSIL samples and a further study would be required to include low-grade samples. In conclusion, this study highlights the scope of Raman spectroscopy for cervical screening despite the presence of biochemical changes associated with the menstrual cycle and the use of HC.

ACKNOWLEDGMENTS

This research was undertaken as part of CERVIVA, the Irish Cervical Screening Research Consortium and we gratefully acknowledge funding from the Health Research Board Collaborative Applied Research Grant, CARG2012/29, and Enterprise Ireland co-funded by the European Regional Development Fund (ERDF) and Ireland's EU Structural Funds Programme 2007 to 2013, CF2011 1045. We thank the Cytology staff at the Coombe Women and Infants University Hospital, Dublin, for facilitating the study and technical support staff at the FOCAS Research Institute, Dublin Institute of Technology.

CONFLICT OF INTEREST

There are no conflicts of interest.

ORCID

Damien Traynor http://orcid.org/0000-0001-6531-6653

REFERENCES

[1] L. A. Torre, F. Bray, R. L. Siegel, J. Ferlay, J. Lortet-tieulent, A. Jemal, *CA Cancer J. Clin.* 2015, *65*, 87.
[2] H. C. Kitchener, R. Blanks, H. Cubie, M. Desai, G. Dunn, R. Legood, S. Moss, *Health Technol. Assess.* 2011, *15*(3). p. 6–12.
[3] J. M. Walboomers, M. V. Jacobs, M. Manos, F. X. Bosch, J. A. Kummer, K. V. Shah, P. J. Snijders, J. Peto, C. J. Meijer, N. Munoz, *J. Pathol.* 1999, *189*, 12.
[4] G. Ronco, P. Giorgi-Rossi, F. Carozzi, M. Confortini, P. Dalla Palma, A. Del Mistro, *Lancet Oncol.* 2010, *11*, 249.
[5] J. Cuzick, L. Cadman, D. Mesher, J. Austin, L. Ashdown-Barr, L. Ho, *Br. J. Cancer* 2013, *108*, 908.
[6] M. Diem, A. Mazur, K. Lenau, J. Schubert, B. Bird, M. Miljković, C. Krafft, J. Popp, *J. Biophotonics* 2013, *6*(11–12), 855.
[7] F. Lyng, I. Ramos, O. Ibrahim, H. Byrne, *Appl. Sci.* 2015, *5*(1), 23.
[8] J. L. González-Solís, J. C. Martínez-Espinosa, L. A. Torres-González, A. Aguilar-Lemarroy, L. F. Jave-Suárez, P. Palomares-Anda, *Lasers Med. Sci.* 2014, *29*, 979.
[9] S. A. Sánchez-Rojo, B. E. Martínez-Zérega, E. F. Velázquez-Pedroza, J. C. Martínez-Espinosa, L. A. Torres-González, A. Aguilar-Lemarroy, L. F. Jave-Suárez, P. Palomares-Anda, J. L. González-Solís, *Rev. Mex. Fis.* 2016, *62*, 213.
[10] P. T. Wong, R. K. Wong, T. A. Caputo, T. A. Godwin, B. Rigas, *Proc. Natl. Acad. Sci. USA* 1991, 1991, *88*, 10988.
[11] P.T.T. Wong, M.K. Senterman, P. Jackli, R.K. Wong, S. Salib, C. E. Campbell, R. Feigel, ,W. Faught, M. Fung, Kee Fung. (2002) *Biopolymers*, *67*: 376–386 (2002).
[12] L. Chiriboga, P. Xie, V. Vigorita, D. Zarou, D. Zakim, M. Diem, *Biospectroscopy* 1998, *4*, 55.
[13] M. A. Cohenford, T. A. Godwin, F. Cahn, P. Bhandare, T. A. Caputo, B. Rigas, *Oncologia* 1997, *66*, 59.
[14] M. Diem, L. Chiriboga, P. Lasch, A. Pacifico, *Biopolymers* 2002, *67*, 349.
[15] M. J. Romeo, M. A. Quinn, F. R. Burden, D. McNaughton, *Biopolymers* 2002, *67*, 362.
[16] B. R. Wood, M. A. Quinn, B. Tait, M. Ashdown, T. Hislop, M. Romeo, D. McNaughton, *Biospectroscopy* 1998, *4*, 75.
[17] I. R. Ramos, A. D. Meade, O. Ibrahim, H. J. Byrne, M. McMenamin, M. McKenna, A. Malkin, F. M. Lyng, *Faraday Discuss.* 2016, *187*, 187.
[18] F. Bonnier, D. Traynor, P. Kearney, C. Clarke, P. Knief, C. Martin, F. Lyng, *Anal. Methods* 2014, *00*, 1.
[19] S. Rozenberg, *Eur. J. Obstet. Gynecol. Reprod. Biol.* 2001, *94*(1), 86.
[20] M. Romeo, M. J. Romeo, B. R. Wood, *Vib. Spectrosc.* 2002, *28*, 167.
[21] E. M. Kanter, S. Majumder, G. J. Kanter, E. M. Woest, A. Mahadevan-Jasen, *Arn. J. Obstet. Gynecol.* 2009, *200*(5), 1.
[22] Z. Movasaghi, S. Rehman, I. Rehman, *Appl. Spectrosc.* 2007, *42*(5), 493.
[23] P. Kearney, D. Traynor, F. Bonnier, F. Lyng, J. O'Leary, C. Martin, *J. Biomed. Opt.* 2017, *22*(10), 105008. https://doi.org/10.1117/1.JBO.22.10.105008.
[24] A. Nair, H. Taylor, *Amenorrhea. A Case Based, Clinical Guide (Genevieve Neal-Perry)*. Contemporary Endocrinology, Springer Science+ Business Media, New York, 2010, p. 23.

How to cite this article: Traynor D, Kearney P, Ramos I, Martin CM, O'Leary JJ, Lyng FM. A study of hormonal effects in cervical smear samples using Raman spectroscopy. *J. Biophotonics.* 2018; e201700240. https://doi.org/10.1002/jbio.201700240

Journal of Biomedical Optics

BiomedicalOptics.SPIEDigitalLibrary.org

Improved removal of blood contamination from ThinPrep cervical cytology samples for Raman spectroscopic analysis

Damien Traynor
Shiyamala Duraipandian
Cara M. Martin
John J. O'Leary
Fiona M. Lyng

SPIE.

Damien Traynor, Shiyamala Duraipandian, Cara M. Martin, John J. O'Leary, Fiona M. Lyng, "Improved removal of blood contamination from ThinPrep cervical cytology samples for Raman spectroscopic analysis," *J. Biomed. Opt.* 23(5), 055001 (2018), doi: 10.1117/1.JBO.23.5.055001.

Journal of Biomedical Optics 23(5), 055001 (May 2018)

Improved removal of blood contamination from ThinPrep cervical cytology samples for Raman spectroscopic analysis

Damien Traynor,[a,*] Shiyamala Duraipandian,[a] Cara M. Martin,[b] John J. O'Leary,[b] and Fiona M. Lyng[a]
[a]Dublin Institute of Technology (DIT), Focas Research Institute, DIT Centre for Radiation and Environmental Science, Dublin, Ireland
[b]Coombe Women and Infants University Hospital, Department of Pathology, Dublin, Ireland

Abstract. There is an unmet need for methods to help in the early detection of cervical precancer. Optical spectroscopy-based techniques, such as Raman spectroscopy, have shown great potential for diagnosis of different cancers, including cervical cancer. However, relatively few studies have been carried out on liquid-based cytology (LBC) pap test specimens and confounding factors, such as blood contamination, have been identified. Previous work reported a method to remove blood contamination before Raman spectroscopy by pretreatment of the slides with hydrogen peroxide. The aim of the present study was to extend this work to excessively bloody samples to see if these could be rendered suitable for Raman spectroscopy. LBC ThinPrep specimens were treated by adding hydrogen peroxide directly to the vial before slide preparation. Good quality Raman spectra were recorded from negative and high grade (HG) cytology samples with no blood contamination and with heavy blood contamination. Good classification between negative and HG cytology could be achieved for samples with no blood contamination (sensitivity 92%, specificity 93%) and heavy blood contamination (sensitivity 89%, specificity 88%) with poorer classification when samples were combined (sensitivity 82%, specificity 87%). This study demonstrates for the first time the improved potential of Raman spectroscopy for analysis of ThinPrep specimens regardless of blood contamination. [DOI: 10.1117/1.JBO.23.5.055001]

Keywords: Raman spectroscopy; cytology; ThinPrep; cervical precancer; cervical cancer; blood; blood removal.

Paper 170815R received Dec. 19, 2017; accepted for publication Apr. 16, 2018; published online May 4, 2018.

1 Introduction

Cervical cancer is the fourth most common cancer in women worldwide with an estimated 528,000 cases and 266,000 deaths in 2012.[1] The link between cervical cancer and high risk human papilloma virus (HPV) infection and the molecular control of the cell cycle is firmly established.[2] The presence of an HPV infection does not automatically mean the development of cervical cancer or precancer [cervical intraepithelial neoplasia (CIN)]. However, the HPV virus can integrate its viral DNA into the host cell's DNA located in the cell's nucleus. This integration disrupts the host cell's control of cell growth and replication and can lead to malignant transformation.[3] The most common method for cervical screening is based on the papanicolaou test (pap test), which is designed to screen for signs of precancer and cancer of the cervix. The pap test requires cells to be scraped from the cervix, fixed to a glass slide, stained, and reviewed by a trained cytologist. Cellular abnormalities are identified based on cellular morphology and staining characteristics and classified according to the degree of dysplasia. The ThinPrep liquid-based cytology (LBC) method involves the patient's cells being transferred into a specimen vial containing PreservCyt transport medium. PreservCyt is an alcohol-based solution that preserves cell morphology and breaks down biological components, such as mucin and blood. The normal smear pattern is made up of epithelial and nonepithelial components [Fig. 1(a)]. The epithelial cell components include parabasal cells, intermediate cells, superficial cells, endocervical and endometrial cells. Nonepithelial cell components include red blood cells, lymphocytes, histiocytes, polymorphs, mucus, and bacteria. Red blood cells are 7 to 8 μm in size and stain red or pink with the pap stain. They are often found in cervical samples, either due to menstruation or inflammation and their presence can also be used as an indicator of disease (precancer).[4] A patient's cervix with a high-grade (HG) lesion will often bleed on contact with the cervical brush and, as a result, the smear becomes contaminated with blood. The presence of blood in the sample will often dilute diagnostic cells, cover and surround cell groups, increase screening time, and make microscopic interpretation difficult [Fig. 1(b)]. PreservCyt contains a lysis agent for mucus and red blood cells but excessive blood in the sample vial will prevent a satisfactory smear being produced. High volumes of red blood cells will prevent the collection of epithelial cells onto the polycarbonate filter membrane during processing resulting in a ringed halo effect with red blood cells deposited mostly around the edges of the smear with very few epithelial cells present [Fig. 1(c)].

Cytology laboratories often annotate pap smears according to a blood scale index, where 0 indicates no visible evidence of blood present and 3 indicates an extremely bloody sample (Fig. 2). Samples presenting as a 2 or 3 on the blood scale are

*Address all correspondence to: Damien Traynor, E-mail: Damien.traynor@dit.ie

1083-3668/2018/$25.00 © 2018 SPIE

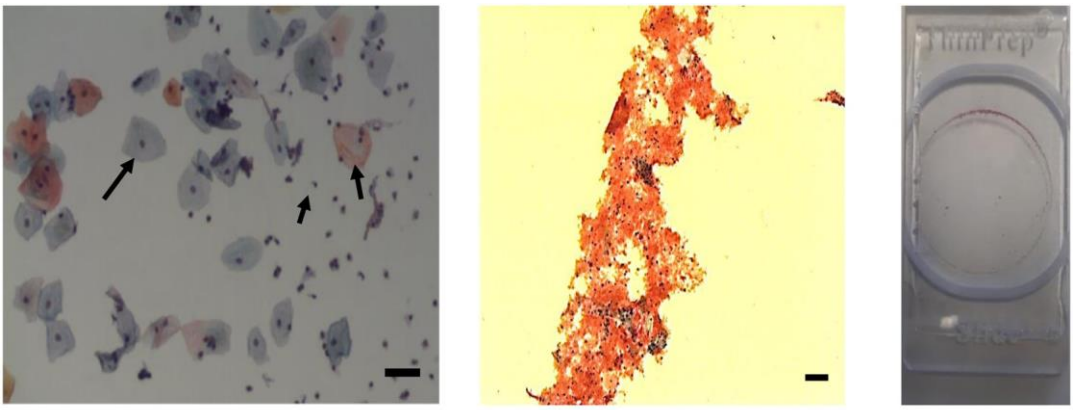

Fig. 1 (a) Pap smear after staining. Note the presence of intermediate (blue), superficial (pink) cells, and lymphocytes (indicated by arrows), (b) bloody smear pattern with red blood cells, obscuring diagnostic cells. Bar ¼ 35 μm. (c) Pap smear contaminated with blood showing ringed halo effect.

often either rejected as being unsatisfactory or treated with a wash solution to lyse more of the red blood cells to increase the number of epithelial cells present on the slide. This blood scale grading is subjective and is only based on a visual appear- ance of a sample. The advantage of the pap test is that it is a noninvasive and widely accepted screening-based test. However, despite a high specificity of 96.5%, a lower sensitivity of 85% can be due to sampling, technical and interobserver errors associated with the subjectivity of the test.[4] Over the past 20 years, Raman spectroscopy has shown potential for the diagnosis of cervical cancer both *in vivo* and *ex vivo*.[5–12] Raman spectroscopy is based on inelastic light scattering in which a sample is illuminated by monochromatic laser light and interactions between the incident photons and molecules in the sample result in the scattering of the light. The coupling of the light generates vibrations within the sample, which are characteristic of the chemical structure. The energy of the scattered light is reduced by an amount equal to the vibrational energy, which is called the Raman shift. This means that the position, peaks, and shape of the Raman bands carry information about the molecular makeup of the sample. The Raman spectrum of cells and tissues is made up of contributions from many biochemical components, including DNA, RNA, proteins, lipids, and carbohydrates.[12] To date, most likely due to confounding factors, such as blood contamination, there have been relatively few studies on Raman spectroscopy of cervical smear samples.[13–19] Rubina et al.[16] described the influence of blood on the Raman spectra of cervical cell pellets and how this might lead to false interpretations. Classification efficiency of 86% and 84% was reported for normal and abnormal samples, respectively, and this decreased to 78% and 79% after samples were treated with red blood cell lysis buffer to reduce blood contamination. A previous study by our group[17] addressed many of the issues involved in recording Raman spectra from LBC (ThinPrep) samples and described a method to remove blood contamination before Raman spectroscopy based on pretreatment of the slides with hydrogen peroxide. This was shown to minimize variability and to result in the collection of highly reproducible data with excellent discrimination between negative and HG samples. However, only blood scale 0 and blood scale 1 samples were used for this study as the treatment was not found to be effective for excessively contaminated blood scale 2 and 3 samples. Kerr et al.[20] investigated the effect of blood contamination on Raman spectra of urine cytology samples. They determined that spectra recorded from samples with a low level of blood appeared free from contamination due to the effective removal of many of the red blood cells using the lysing agent CytoLyt. However, for excessively bloody samples, several additional Raman peaks associated with blood were observed leading to the conclusion that excessively bloody samples are not suitable for diagnostics with Raman microspectroscopy. The aim of the present study was to extend our previous study[17] to samples annotated as blood scale 2 and 3 to investigate if these excessively bloody samples could be treated to render them suitable for Raman spectroscopy.

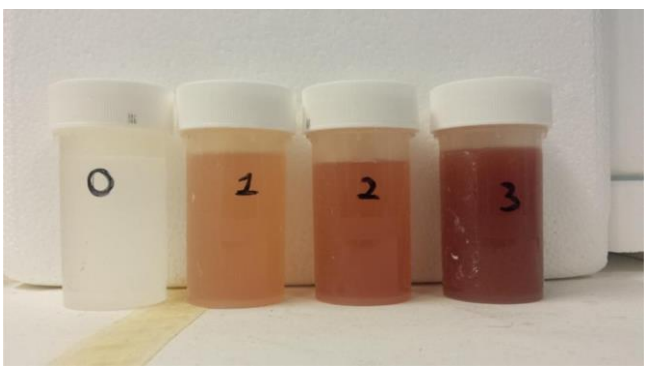

Fig. 2 ThinPrep vials graded according to the blood scale index, where 0 indicates no visible evidence of blood and 3 indicates an extremely bloody sample.

2 Materials and Methods

2.1 Samples and Blood Treatment

Cervical LBC samples were provided by Coombe Women and Infants University Hospital, Dublin, Ireland, for spectroscopic analysis with the final clinical report prepared by the cytologist and/or pathologist. This study was approved by the Research Ethics Committee at Coombe Women and Infants University Hospital. A set of 30 samples were selected, 15 HG intraepithelial neoplasia samples, which received a CIN 2 or CIN 3, result on their associated biopsy from pathology, and 15 negative samples (TN), which received a negative result from cytology. All

cytology samples were evaluated by eye according to the blood scale index and annotated as being either a grade 0, 1, 2, or 3.

HeLa cervical cancer cells were also prepared and fixed as for ThinPrep samples in PreservCyt. These samples were seeded with blood to mimic excessively bloody cytology samples. This was achieved by adding blood to the samples until they visually represented a blood scale 2 and 3 index sample.

Each ThinPrep sample vial was mixed for 3 min to break up cellular clumps. The sample was then poured into a 50-ml centrifuge tube and centrifuged for 5 min at 300 rpm. The supernatant was removed and 1 ml of H_2O_2 was added and mixed for 30 s. About 20 ml of PreservCyt was added to neutralize the H_2O_2. The sample was then centrifuged for 5 min at 600 rpm. Most of the supernatant was removed. The cell pellet was resuspended multiple times with a 1-ml pipette to break up cell clumps. The 20 ml of PreservCyt was then added and the contents poured back into the original vial.

2.2 ThinPrep Slide Preparation

The samples were then prepared using the ThinPrep 2000 processor (Hologic Inc., Marlborough, Massachusetts). The ThinPrep process begins with the patient's gynecological sample being collected by the clinician using either a cervical broom or brush. The brush/broom is then rinsed in the specimen vial containing PreservCyt transport medium (ThinPrep Pap Test; Cytyc Corporation, Boxborough, Massachusetts). The ThinPrep sample vial is then capped, labeled, and sent to the lab to be processed. The ThinPrep processor homogenizes the sample by spinning the filter and creating shear forces that breaks up any clumped material (blood, mucin, and nondiagnostic material). The cells are then transferred onto a polycarbonate filter membrane of the TransCyt filter and transferred onto a glass slide to produce a circular monolayer of cells ~20 mm in diameter. The slide is then ejected into a fixative bath of 95% ethanol.

2.3 Raman Spectroscopy

All Raman analyses was performed using a HORIBA Jobin Yvon XplorRA™ system (Villeneuve d'Ascq, France), which incorporates an Olympus microscope BX41 equipped with a ×100 objective (MPlan, Olympus, NA 0.9)¼ A 532-nm diode laser source was used. Laser power was set to 100% resulting in 16 mW at the objective. The confocal hole coupled to a slit aperture of 100 μm was set at 100 μm for all the measurements. The system was precalibrated to the 520.7 cm^{-1} spectral line for silicon. About 1200 lines/grating mm were used. The backscatter light was measured using an air-cooled CCD detector (Andor, 1024 × 256 pixels). The spectrometer was controlled by Labspec V5.0 software. Two accumulations of 30 s were performed on each cell nucleus selected. Raman spectra were acquired from the nuclei of randomly selected morphologically normal superficial and intermediate cells from each unstained pap smear.

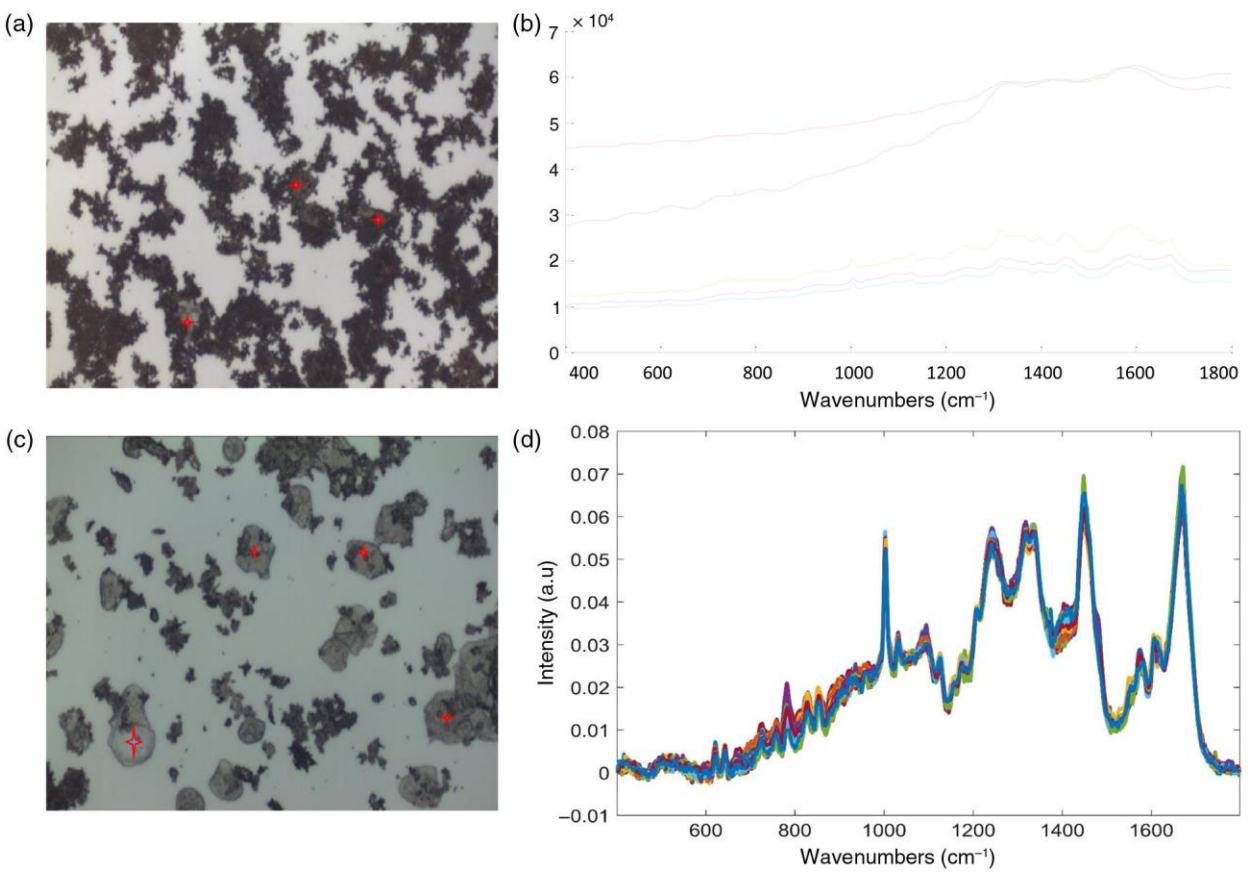

Fig. 3 (a) Untreated pap smear, blood scale 3, stars indicate recorded nuclei in field-of-view. Bar ¼ 35 μm. (b) Raman spectra recorded from untreated pap smear. (c) Treated pap smear, stars indi- cate recorded nuclei in field-of-view. Bar ¼ 35 μm. (d) Raman spectra recorded from treated pap smear.

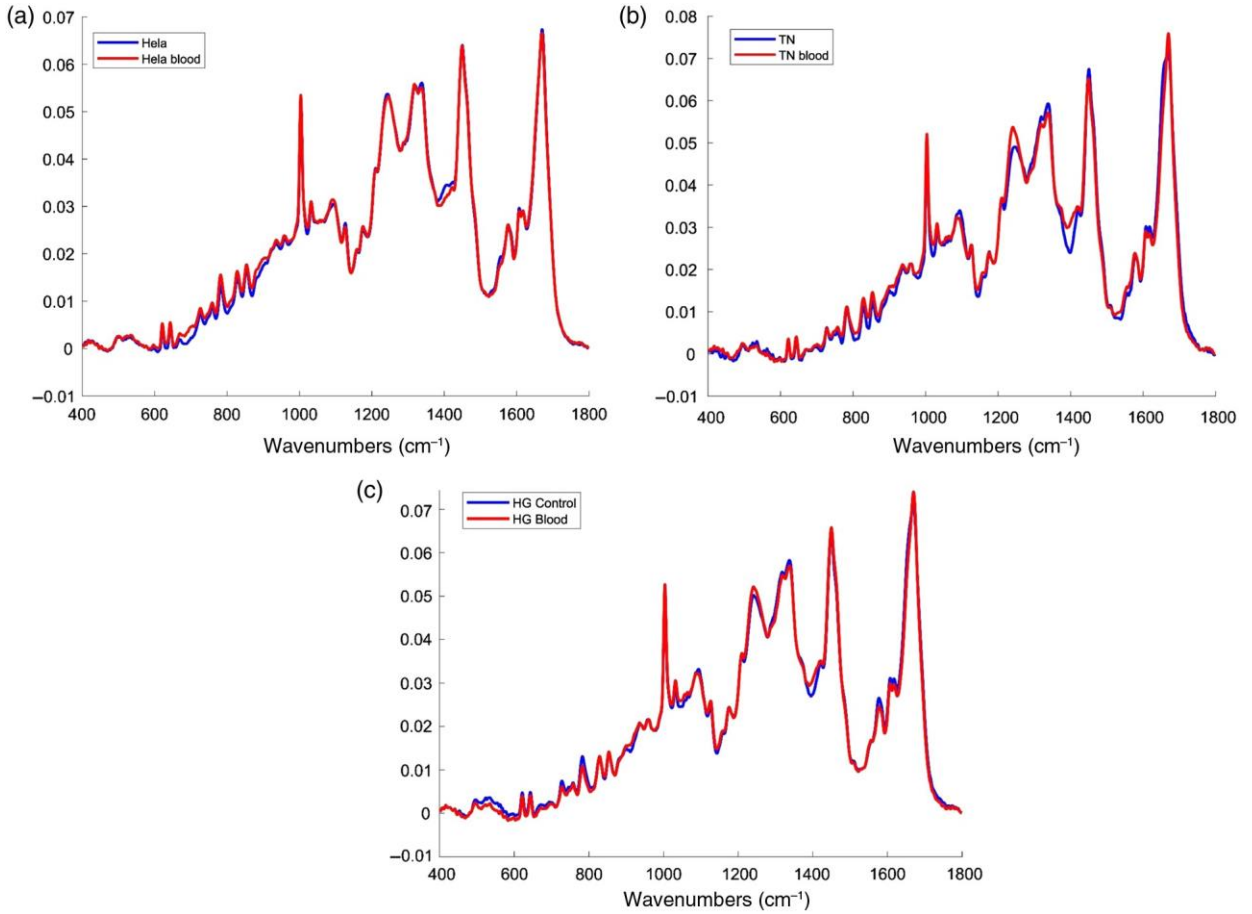

Fig. 4 (a) Mean Raman spectra of HeLa cervical cancer cells treated with blood (blood scale 2 and 3) and subsequently treated with H_2O_2 (red) and HeLa cervical cancer cells not treated with blood but treated with H_2O_2 (blue), (b) mean Raman spectra of true negative samples (TN), blood scale 2 and 3, treated with H_2O_2 (red) and blood scale 0, treated with H_2O_2, (c) mean Raman spectra of HG samples, blood scale 2 and 3 treated with H_2O_2 (red) and blood scale 0, treated with H_2O_2.

2.4 Data Preprocessing and Analysis

Data were normalized and analyzed using MATLAB software (Mathworks) and specific scripts developed and adapted for uploading of the spectra and their preprocessing, including smoothing (Savitzky–Golay K ¼ K 13), baseline correc- tion (rubberband) and vector normalization. The spectra were also corrected for the glass background using a linear least- squares method with non-negative constraints. The least-squares model was developed using spectra from the ThinPrep glass slides and selected pure biochemicals (e.g., actin, collagen, RNA, DNA, etc.) that approximate the biochemical composition of cervical cells. The data were mean centered and subjected to partial least squares discriminant analysis (PLS-DA). PLS-DA involves the creation of latent variables to maximize the cova- riation between known datasets and the response variable which they are regressed against. PLS-DA is a form of analysis that has the ability to distinguish between known classifications of sam- ples (negative, HG) and its aim is to find latent variables and directions to maximize separation in a multivariate space. To validate the method leave one patient out cross validation was performed. This involves data from one patient sample being removed from the model and the process is repeated until all samples have been left out once.

3 Results

Figure 3(a) shows an untreated Pap smear, blood scale 3. The slide was coated in blood and cellular debris. Figure 3(b) shows Raman spectra recorded from cells present on the slide. Very few cells were present and often burned on contact with the laser. A high background was observed together with Raman bands associated with blood at 754, 1311, 1374, 1398, 1588, 1640 cm^{-1}. The high background can be attributed to the cellular debris or a subunit of the oxidized hemoglobin on the surface of the cell nuclei, which has a weak fluorescence.[11] Figure 3(c) shows the same sample from Fig. 3(a) after undergoing the blood removal method. Any blood residue has been oxidized with the H_2O_2 treatment and cellular debris has been reduced allowing for high quality spectra to be recorded as demonstrated in Fig. 3(d).

In order to determine if the Raman specific method of blood removal using H_2O_2 had any effect on the spectra recorded without any external confounding factors, such as inflammation, HPV infection, etc., the protocol was performed on HeLa cervical cancer cells. HeLa cells were seeded with blood to mimic cytology samples with blood scale index 2 and 3 and HeLa cells with no added blood acted as controls. Both sample types were treated with H_2O_2 and slides prepared as for the ThinPrep

cytology samples. Figure 4(a) shows the mean Raman spectra recorded from 30 HeLa cells with and without blood contamination (blood scale 2 and 3) and treated with H_2O_2. The mean spectra display strong similarities with only minor changes at 1242 cm^{-1} (Amide III), 1350 cm^{-1} (DNA/RNA, CH def. in proteins and carbohydrates), 1430 cm^{-1} (protein, lipids), and 1669 cm^{-1} (Amide I). Figure 4(b) shows the mean Raman spectra of negative cytology samples (TN) with and without blood contamination (blood scale 2 and 3) and treated with H_2O_2. The mean spectra display strong similarities with small changes at 1242, 1350, 1430, and 1669 cm^{-1} as observed for the HeLa cells. These small changes in the spectra were consistent throughout all samples tested including the HG samples [Fig. 4(c)].

PLS-DA classification of negative cytology samples and HG cytology samples, blood scale index 0, is shown in Fig. 5. Figure 5(a) is a latent variables (LV) scores scatter plot of LV1 and LV2, which shows good discrimination along LV1. The loadings, as shown in Fig. 5(b), show that the discrimination is based around Raman peaks at 482, 851, 936, 1128, 1338, 1449, 1572, 1655, and 1669 cm^{-1}, which are mainly related to DNA, proteins, and glycogen. Figure 5(c) is a PLS-DA prediction plot showing good classification of negative and HG samples with a sensitivity of 92% and a specificity of 93% (Table 1). PLS-DA classification of TN and HG cytology samples, blood scale index 2 and 3, is shown in Fig. 6. Both negative and HG samples have undergone the Raman-specific blood removal method. Figure 6(a) is a LV scores scatter plot of treated TN and HG samples, which show overlap between the samples. The LV1 loadings, as shown in Fig. 6(b), show that the discrimination is based around Raman peaks at 482, 549, 851, 936, 1145, 1182, 1237, 1338, 1449, 1576, and 1669 cm^{-1} and are similar to the loadings shown in Fig. 5(b). The PLS-DA prediction plot is shown in Fig. 6(c) and has a sensitivity of 89% and a specificity of 88% (Table 1).

In order to determine if excessively bloody samples could be treated the same way as nonbloody samples in terms of data analysis, the Raman spectral data from the two groups (blood scale 0 and blood scale 2 and 3) were combined. Figure 7(a) shows the LV scores scatter plot, which highlights decreased discrimination between TN and HG cytology. However, the loadings shown in Fig. 7(b) remain similar to the loadings shown in Figs. 5(b) and 6(b) with Raman peaks at 482, 851, 1129, 1184, 1251, 1338, 1449, and 1669 cm^{-1}. The PLS-DA prediction plot is shown in Fig. 7(c) and has a sensitivity of 82% and a specificity of 87% (Table 1).

Interestingly, the loadings (482, 851, 936, 1149, 1338 and 1669 cm^{-1}) remain almost the same between all three datasets, blood scale 0, blood scale 2 and 3 and combined, confirming that glycogen, DNA, and proteins are the main discriminating features between negative cytology and HG cytology samples regardless of blood contamination. Similar findings have

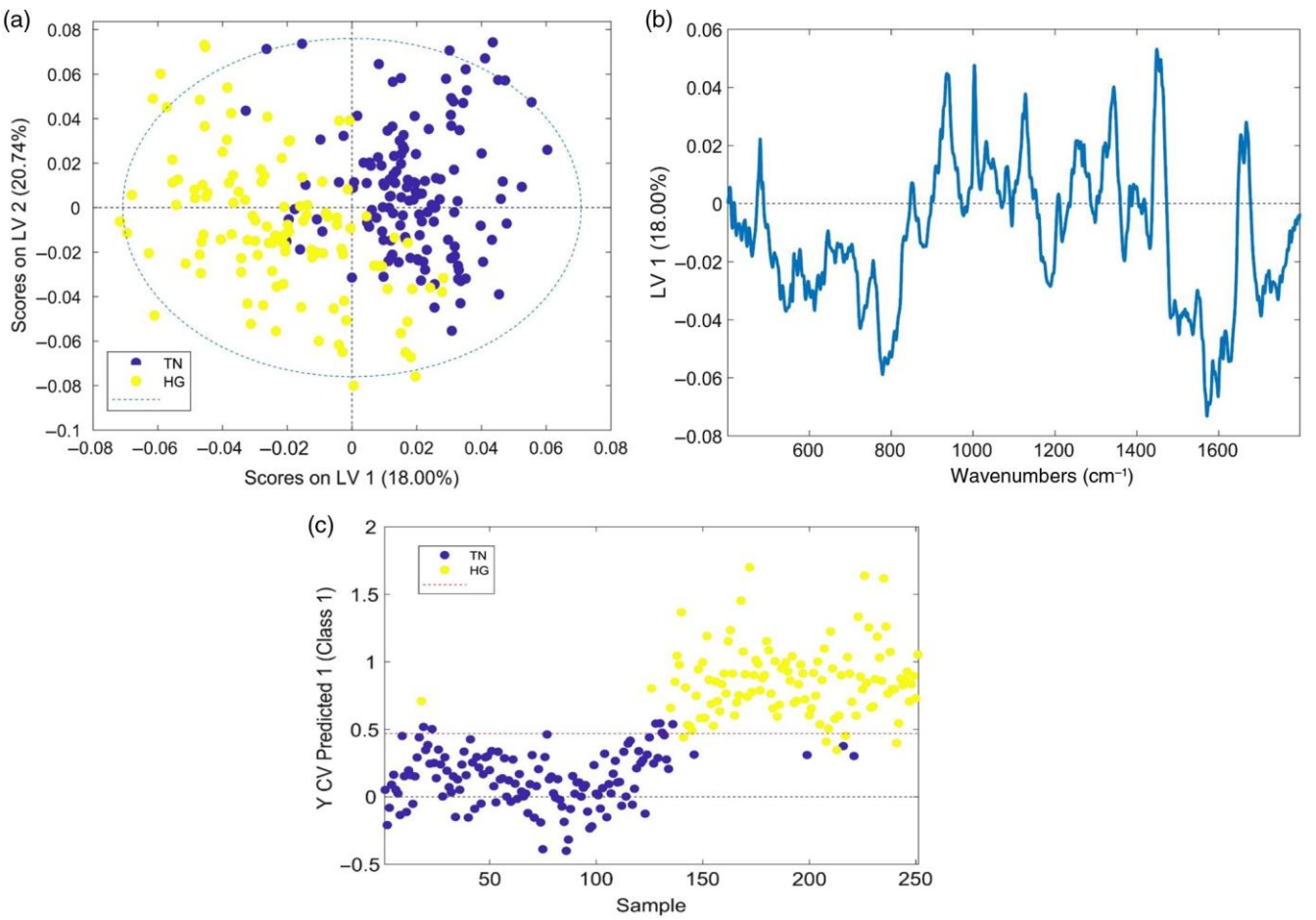

Fig. 5 (a) LV score scatter plot of Raman spectra acquired from 15 TN samples and 15 HG samples (blood scale index 0), (b) LV 1 loadings, and (c) PLS-DA prediction plot showing good discrimination between TN (blue) and HG (red) ThinPrep cytology samples.

Table 1 Sensitivity and specificity from PLS-DA classification of TN and HG cervical cytology samples with and without blood contamination and combined.

	Sensitivity (%)	Specificity (%)
Negative versus HG (blood scale 0)	92	93
Negative versus HG (blood scale 2 and 3)	89	88
Combined (blood scale 0 and 2 and 3)	82	87

been reported previously.[17,19] However, as mentioned earlier, some spectral features undergo minor changes following the blood removal method. As these features overlap with the discriminating features, this results in a reduction in classification efficiency when excessively bloody (blood scale index 2 and 3) samples and nonbloody samples (blood scale index 0) samples are combined for analysis. Comparing sensitivity and specificity of the test groups shows that blood scale 0 samples with no blood contamination performed best with a sensitivity of 92% and specificity of 93% when compared to excessively bloody blood scale 2 and 3 samples, which had a sensitivity of 89% and specificity of 88%. Combining the blood scale 0 and blood scale 2 and 3 samples for analysis resulted in a sensitivity of 82% and specificity of 87%. The high specificity indicates a good ability to accurately exclude negative samples (few false positives), however, the reduction in sensitivity indicates a reduced ability to accurately detect HG samples and an increased likelihood of false negatives.

Despite the reduction in classification efficiency, the values are higher than previously reported for samples with blood contamination. Rubina et al.[16] reported a classification efficiency of 78% and 79% for normal and abnormal bloody samples treated with red blood cell lysis buffer. In addition, Kerr et al.[20] concluded that excessively bloody samples were not suitable for diagnostics with Raman spectroscopy.

4 Conclusion

This study demonstrates for the first time that excessively bloody (blood scale 2 and 3) ThinPrep cervical smear samples can be used for diagnostics with Raman spectroscopy following a hydrogen peroxide treatment in the collection vial. However, the presence of excessive blood contamination (blood scale index 2 and 3) did result in reduced sensitivity and specificity for classification of negative and HG samples. A higher sensitivity and specificity could be achieved by keeping excessively bloody samples separate from nonbloody samples for analysis. Although this study has focused only on cervical cytology samples, thyroid, urine, and serous fluid cytology samples may also

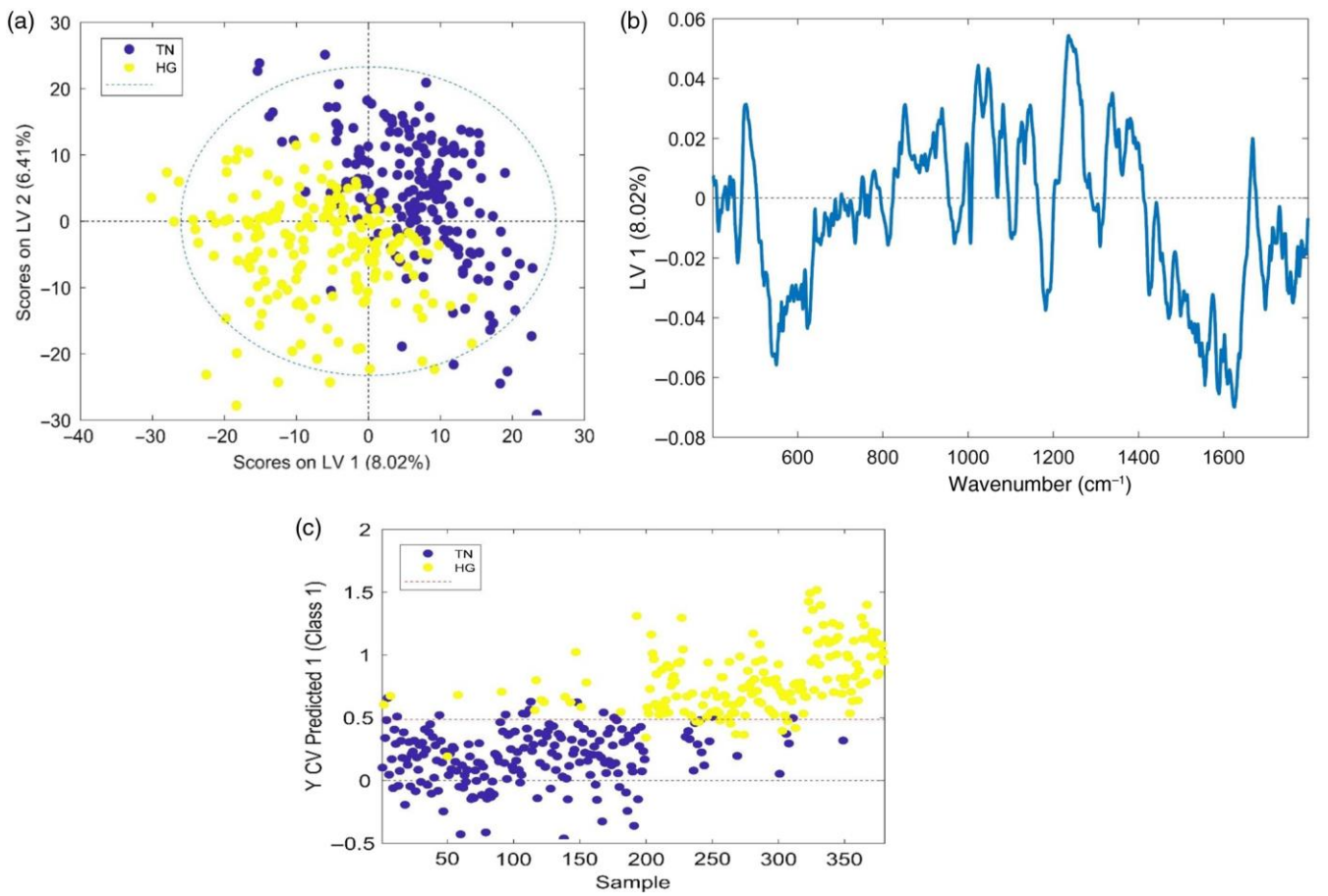

Fig. 6 (a) LV score scatter plot of Raman spectra acquired from 15 TN and 15 HG samples (blood scale index 2 and 3), (b) LV1 loadings, (c) PLS-DA prediction plot showing some discrimination between TN (blue) and HG (red) ThinPrep cytology samples, blood scale 2 and 3 and treated with H_2O_2.

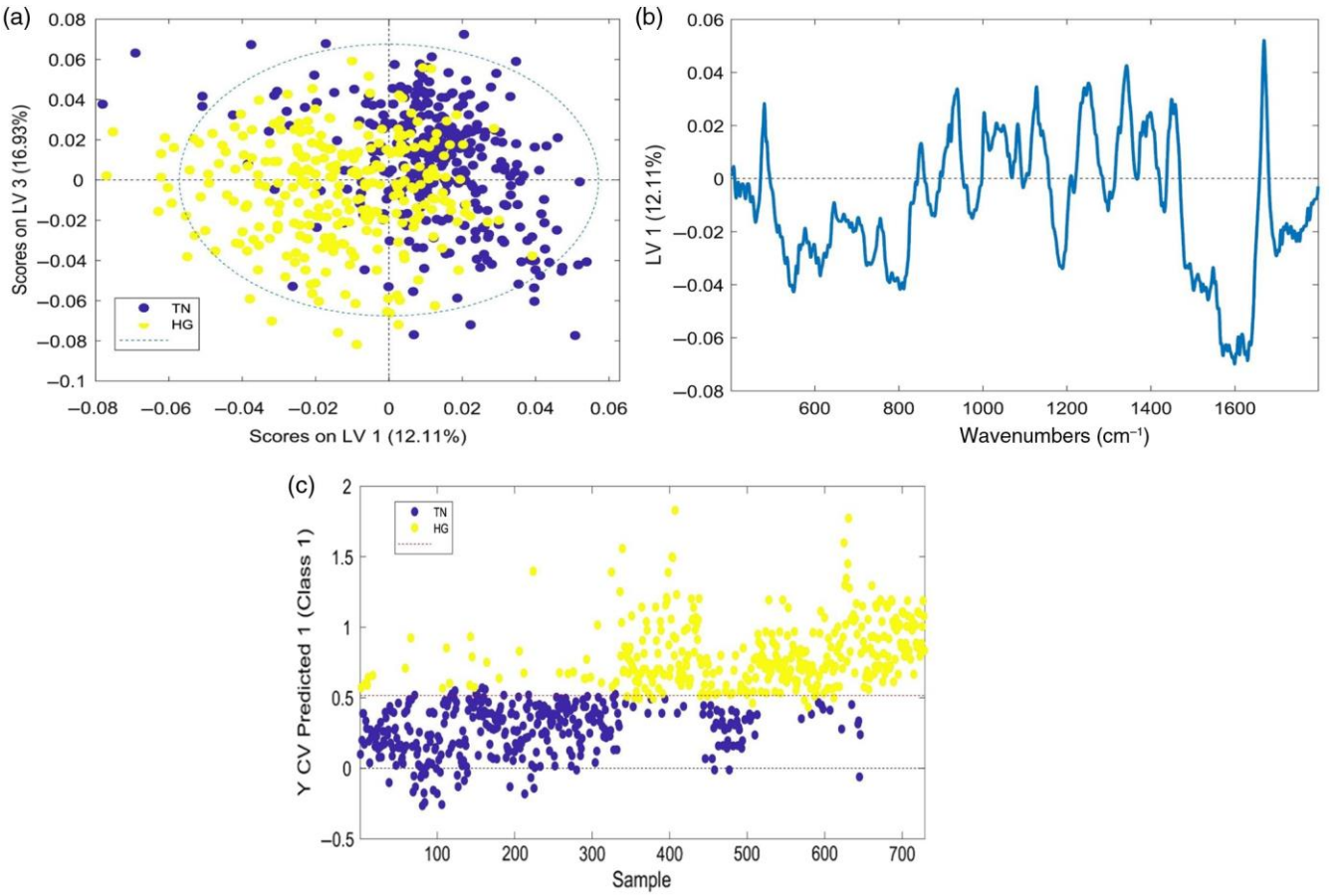

Fig. 7 (a) LV score scatter plot of Raman spectra from TN and HG samples (combined blood scale 0 and blood scale 2 and 3), (b) LV1 loadings, and (c) PLS-DA prediction plot showing some discrimination between TN (blue) and HG (red) ThinPrep cytology samples, combined blood scale 0 and blood scale 2 and 3 and treated with H_2O_2.

benefit from such an approach for Raman spectroscopic analysis. Serous fluids for cytological examination are often contaminated with a high level of blood (pericardium, pleura, and peritoneum fluids) and often require additional treatment methods, such a density gradient technique to remove red blood cells, which can result in a loss of diagnostic cellular material. The application of our blood treatment method would prevent this loss of material and allow Raman spectroscopy to be performed.

While these results are promising for the development of Raman spectroscopy for cervical cancer screening, Raman spectroscopy in its current form does not have the ability to replace cytology for cervical cancer screening and its associated benefits (e.g., detection of Herpes Simplex virus or actinomyces like organisms). However, it could be used to supplement the pap test or it could have potential as a triage test after HPV testing.

Disclosures

There are no conflicts of interest.

Acknowledgments

This research was undertaken as part of CERVIVA, the Irish Cervical Screening Research Consortium and we gratefully acknowledge funding from the Health Research Board Collaborative Applied Research Grant, CARG2012/29, and Enterprise Ireland cofunded by the European Regional Development Fund (ERDF) and Ireland's EU Structural Funds Programme 2007–2013, CF2011 1045. We thank the Cytology staff at Coombe Women and Infants University Hospital, Dublin, for facilitating the study and technical support staff at the FOCAS Research Institute, Dublin Institute of Technology.

References

1. J. Ferlay et al., "Cancer incidence and mortality worldwide: sources, methods and major patterns in GLOBOCAN 2012," *Int. J. Cancer* 136, E359–E386 (2015).
2. F. X. Bosch et al., "The causal relationship between human papillomavirus and cervical cancer," *J. Clin. Pathol.* 55, 244–265 (2002).
3. B. Shambayati, *Cytopathology*, 1st ed., pp. 88–89, Oxford University Press, Oxford (2011).
4. H. C. Kitchener et al., "MAVARIC trial study group," *Health Technol. Assess.* 15, 1–170 (2011).
5. U. Utzinger et al., "Near-infrared Raman spectroscopy for in vivo detection of cervical precancers," *Appl. Spectrosc.* 55, 955–959 (2001).
6. E. M. Kanter et al., "Effect of hormonal variation on Raman spectra for cervical disease detection," *Am. J. Obstet. Gynecol.* 200, 512.e1–512.e5 (2009).
7. E. Vargis et al., "Effect of normal variations on disease classification of Raman spectra from cervical tissue," *Analyst* 136, 2981–2987 (2011).
8. E. Vargis et al., "Sensitivity of Raman spectroscopy to normal patient variability," *J. Biomed. Opt.* 16, 117004 (2011).
9. J. Mo et al., "High wavenumber Raman spectroscopy for in vivo detection of cervical dysplasia," *Anal. Chem.* 81, 8908–8915 (2009).

10. S. Duraipandian et al., "Simultaneous fingerprint and high-wavenumber confocal Raman spectroscopy enhances early detection of cervical precancer in vivo," *Anal. Chem.* 84, 5913–5919 (2012).
11. K. Kong et al., "Raman spectroscopy for medical diagnostics—from in-vitro biofluid assays to in-vivo cancer detection," *Adv. Drug Delivery Rev.* 89, 121–134 (2015).
12. I. P. Santos et al., "Raman spectroscopy for cancer detection and cancer surgery guidance: translation to the clinics," *Analyst* 142, 3025–3047 (2017).
13. F. M. Lyng et al., "Raman spectroscopy for screening and diagnosis of cervical cancer," *Anal. Bioanal. Chem.* 407, 8279–8289 (2015).
14. M. Diem et al., "Molecular pathology via IR and Raman spectral imaging," *Biophotonics* 6, 855–886 (2013).
15. E. Vargis et al., "Near-infrared Raman microspectroscopy detects high-risk human papillomaviruses," *Transl. Oncol.* 5, 172–179 (2012).
16. S. Rubina, M. S. Vidyasagar, and C. M. Krishna, "Raman spectroscopic study on prediction of treatment response in cervical cancers," *J. Innovative Opt. Health Sci.* 6, 1350014 (2013).
17. F. Bonnier et al., "Processing ThinPrep cervical cytology samples for Raman spectroscopy analysis," *Anal. Methods* 6, 7831–7841 (2014).
18. I. Ramos, A. Malkin, and F. Lyng, "Current advances in the application of Raman spectroscopy for molecular diagnosis of cervical cancer," *BioMed Res. Int.* 9, 1–9 (2015).
19. P. Kearney et al., "Raman spectral signatures of cervical exfoliated cells from liquid-based cytology samples," *J. Biomed. Opt.* 22(10), 105008 (2017).
20. L. T. Kerr et al., "Methodologies for bladder cancer detection with Raman based urine cytology," *Anal. Methods* 8, 4991–5000 (2016).

Damien Traynor holds his BSc degree in medical and molecular cytology from the Dublin Institute of Technology (DIT). He achieved membership of the Academy of Laboratory Science in cytology in 2012 and worked as a primary screener for two years before joining DIT as a research technician. He is working on a Health Research Board funded clinical evaluation of Raman spectroscopy for the diagnosis of cervical precancer and is working on his PhD part time.

Shiyamala Duraipandian holds her BE degree in biomedical engineering from Adhiyamaan College of Engineering, Anna University. She received her PhD from the Department of Biomedical Engineering, National University of Singapore. She worked as a Marie-Curie fellow in Dublin Institute of Technology. She is working as a staff scientist in Dansk Fundamental Metrologi A/S. Her research is focused on different analytical techniques for pharm.

Cara M. Martin is an assistant professor in molecular pathology and tumor biology in the Department of Histopathology at the Trinity College Dublin. She leads the Cervical Cancer Research Group based in the Coombe Women and Infant's University Hospital. Her research program consists of translational health services-based research in female gynecological cancers. She has published 57 peer-reviewed articles and 13 book chapters, and has a *h*-index of 23 and >2500 citations.

John J. O'Leary is a professor/chair of pathology at the Trinity College Dublin and a director of pathology at the Coombe Women and Infants University Hospital, Dublin. He heads a multi-investigator team focused on the molecular characterization of several cancer systems including: ovary, cervix, prostate, thyroid, head and neck cancer, and cancer stem cell biology. He has published more than 190 peer-reviewed papers, and has a *h*-index of 49 and >9600 citations.

Fiona M. Lyng holds her BSc degree from Trinity College Dublin and her PhD from the University College Dublin. She is a head of the DIT Centre for Radiation and Environmental Science. Her research is focused on translational research for cancer diagnosis and cancer treatment. She has published over 100 peer-reviewed research papers, and has a *h*-index of 33 and >3500 citations.

Received: 4 October 2018 | Revised: 20 December 2018 | Accepted: 13 January 2019
DOI: 10.1002/jbio.201800377

JOURNAL OF BIOPHOTONICS

FULL ARTICLE

The potential of biobanked liquid based cytology samples for cervical cancer screening using Raman spectroscopy

Damien Traynor[1]* | Shiyamala Duraipandian[1] | Ramya Bhatia[2] | Kate Cuschieri[2] | Cara M. Martin[3] | John J. O'Leary[3] | Fiona M. Lyng[1]

[1]DIT Centre for Radiation and Environmental Science, Focas Research Institute, Dublin Institute of Technology (DIT), Dublin, Ireland

[2]HPV Research Group, Division of Pathology, Queens Medical Research Institute, University of Edinburgh, Edinburgh, UK

[3]Discipline of Histopathology, University of Dublin Trinity College, Dublin, Ireland

*Correspondence
Damien Traynor, DIT Centre for Radiation and Environmental Science, Focas Research Institute Dublin Institute of Technology Kevin Street Dublin 8 Ireland.
Email: damien.traynor@dit.ie

Patient samples are unique and often irreplaceable. This allows biobanks to be a valuable source of material. The aim of this study was to assess the ability of Raman spectroscopy to screen for histologically confirmed cases of Cervical Intraepithelial neoplasia (CIN) using biobanked liquid based cytology (LBC) samples. Two temperatures for long term storage were assessed; 80ºC and −25ºC. The utility of Raman spectroscopy for the detection of CIN was compared for fresh LBC samples and biobanked LBC samples. Two groups of samples were used for the study with one group associated with disease (CIN 3) and the other associated with no disease (cytology negative). The data indicates that samples stored at −80ºC are not suitable for assessment by Raman spectroscopy due to a lack of cellular material and the presence of cellular debris. However, the technology can be applied to fresh LBC samples and those stored at −25ºC and is, moreover, effective in the discrimination of negative samples from those where CIN 3 has been confirmed. Pooled fresh and biobanked samples are also amenable to the technology and achieve a similar sensitivity and specificity for CIN 3. This study demonstrates that cervical cytology samples stored within biobanks at temperatures that preclude cell lysis can act as a useful resource for Raman spectroscopy and will facilitate research and translational studies in this area.

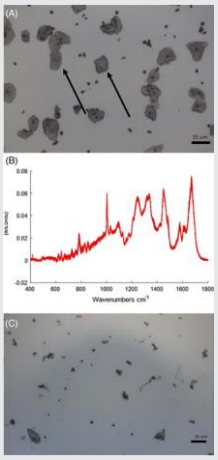

KEYWORDS
biobank, cervical cancer, cervical pre-cancer, cytology, Raman spectroscopy, ThinPrep

1 | INTRODUCTION

Every year millions of cervical Pap tests are performed throughout the world in countries for purposes of cervical screening. Most Pap tests are performed through use of liquid based cytology (LBC) where cervical cells are collected before deposition into a volume of liquid preservative. As not all the material is required for cytological assessment, the surplus, which would ordinarily be discarded, can be stored within tissue biobanks with due process of governance. Biobanks constitute a valuable source of material which may support a number of studies including those on the natural history of disease, evaluation of screening practices, vaccination effectiveness or the development of new technologies to support screening and disease management.[1–3]

There were an estimated 527 600 new cervical cancer cases and 265 700 deaths from cervical cancer worldwide in 2012.[4] This demonstrates the importance of both cervical screening to reduce the burden of disease and also

investment in research into new technologies that can improve the performance and "reach" of cervical screening Different collection media for liquid based cytology exist however one of the more common media is PreservCyt (Hologic). PreservCyt is a methanol based solution that preserves cell morphology via fixation. Fixation is routinely employed as it allows a "snapshot" of a cell's physical and biochemical state to be assessed. Methanol is an organic solvent that preserves cells through dehydration and precipitation of proteins.[5] Fixation is important given that sample collection and assessment is not performed concurrently. In addition to supporting routine screening, fixation of cells also supports longer term storage of residual material in biobanks.

The advantage of the Pap test is that it is a widely accepted screening based test with a high specificity of 95% to 98% and a sensitivity of 74% to 96%.[6] The variability in the rates of sensitivity are due to sampling technique and the variability of the cytology based screening. This can result in unnecessary gynaecological referral and patient recall. Persistent infection with high risk human papillomavirus (HPV), is accepted as the major cause of cervical pre-cancer and cancer.[7] HPV DNA testing has a higher sensitivity (>95%) but lower specificity (~84%) than the Pap test.[7] These tests are expensive, time-consuming and provide no information on cervical cytopathology.

Current methods for detection of cervical cancer and pre-cancer (CIN) are limited and there is an unmet clinical need for new screening or diagnostic tests. Recently Raman spectroscopy has shown potential as a tool for screening and diagnosis of cervical lesions and cancer.[8–10] Raman spectroscopy is based on inelastic light scattering where a sample is illuminated by a monochromatic laser light and interactions between the incident photons and molecules in the sample result in the scattering of the light. The coupling of the light generates vibrations within the sample which are characteristic of the chemical structure. This means that the position, peaks and shape of the Raman bands carry information about the molecular makeup of the sample. The Raman spectrum of cells and tissues is made up of contributions from many biochemical components including DNA, RNA, proteins, lipids and carbohydrates.[11] Raman spectroscopy can offer a label free non-destructive method for cervical cancer screening. It is an objective method, less reliant on operator performance than cytology and potentially more specific than HPV testing.

Due to confounding factors such as sample collection, blood contamination and sample variability, few studies have been performed using Raman spectroscopy on cervical cytology samples and none to our knowledge have investigated the potential of utilising biobanked LBC samples. The aim of this feasibility study was to assess the utility and performance of Raman spectroscopy for the detection of CIN using biobanked LBC samples. Samples stored at −80°C and −25°C were assessed and the ability of Raman spectra to delineate disease from no disease was determined. Additionally, Raman spectroscopy was assessed in un-banked LBC samples as a comparator.

2 | METHODS

2.1 | Sample collection

Two classes of samples were used for the study, classed as disease and no disease. Samples with no disease were defined as cytology negative and HPV negative whereas samples with disease were those associated with a histologi- cally confirmed CIN 3 with a HPV positivity according to HPV DNA and mRNA status. All samples were recruited from patients presenting at a colposcopy clinic for the first time, and had no prior history of disease. Samples were col- lected from each patient according to the standard operating procedure issued by Cervical Check Irelands national cervical cancer screening programme and the NHS Scottish cervical screening programme. Both procedures are similar and all samples were biobanked using the same methodology.

One hundred thirty-three samples were used in total for this study of which 64 were LBC biobanked samples; 32 with no disease (cytology negative) and 32 with disease (CIN 3). Biobanked samples were provided by the Scottish HPV Archive, a research tissue biobank set up to facilitate HPV associated research.

Ethical approval for use of the samples was obtained from the East of Scotland Research Ethics Service—Tayside committee. Biobanked LBC samples used for this study had been sedimented with the cellular pellet transferred into a 4.5 mL vial for long term storage in PreservCyt. After transit, samples were re-constituted to a volume of 20 mL fresh PreservCyt solution to resemble the original LBC specimen from which the sample was derived.

A further 64 non biobanked "fresh" LBC samples, 32 with no disease (cytology negative) and 32 with disease (CIN 3), were collected in PreservCyt solution from the Coombe Women and Infants University Hospital (CWIUH), Dublin, Ireland, as part of routine cytological screening. Eth- ical approval for use of anonymised samples for the study was granted by the CWIUH Research Ethics Committee (no. 28-2014). A further 5 fresh LBC samples with disease (CIN 3) were collected and split into two separate vials. One vial from each sample underwent the standard biobanking process and was stored for 3 weeks, while the other was stored at room temperature.

2.2 | ThinPrep

The samples were then prepared using the ThinPrep 2000 processor (Hologic Inc., Marlborough, Massachusetts). The ThinPrep process begins with the patient's gynaecological

sample being collected by the clinician using either a cervical broom or brush. The brush/broom is then rinsed in the specimen vial containing PreservCyt transport medium (ThinPrep Pap Test; Cytyc Corporation, Boxborough, Massachusetts). The ThinPrep sample vial is then capped, labelled and sent to the lab to be processed. The ThinPrep processor homogenises the sample by spinning the filter, creating shear forces that breaks up any clumped material (blood, mucin and non-diagnostic material). The cells are then transferred onto a polycarbonate filter membrane of the TransCyt filter and transferred onto a glass slide to produce a circular monolayer of cells ~20 mm in diameter. The slide is then ejected into a fixative bath of 95% ethanol.

2.3 | Raman spectroscopy

All Raman analysis was performed using a HORIBA Jobin Yvon XplorRA system (Villeneuve d'Ascq, France), which incorporates an Olympus microscope BX41 equipped with a ×100 objective (MPlan, Olympus, Tokyo, Japan, NA = 0.9). A 532 nm diode laser source was used. Laser power was set to 100% resulting in 16 mW at the objective. The confocal hole coupled to a slit aperture of 100 μm, was set at 100 μm, for all the measurements. The system was pre-calibrated to the 520.7 cm^{-1} spectral line for silicon. A 1200 lines per mm grating was used. The backscattered light was measured using an air-cooled CCD detector (Andor, 1024 × 256 pixels). The spectrometer was controlled by Labspec V6.0 software. Two accumulations of 30 seconds were performed on each cell nucleus selected. Raman spectra were acquired from the nuclei of 20 randomly selected morphologically normal superficial and intermediate cells from each unstained Pap smear.

2.4 | Data pre-processing and analysis

Data was normalised and analysed using Matlab software (Mathworks) and specific scripts developed and adapted for uploading of the spectra and their pre-processing, including smoothing (Savitzky-Golay K = 5, K = 13), baseline correction (Rubberband) and vector normalisation. The spectra were also corrected for the glass background using a linear least-squares method with non-negative constraints (NNLS). The least-squares model was developed using spectra from the Thinprep glass slides and selected pure biochemicals (eg, actin, glycogen, RNA, DNA, etc.) that approximate the biochemical composition of cervical cells. The data was mean centred and subjected to partial least squares discriminant analysis (PLS-DA). PLS-DA involves the creation of latent variables to maximise the co variation between known datasets and the response variable which they are regressed against. PLS-DA is a form of analysis that has the ability to distinguish between known classifications of samples and its aim is to find latent variables and directions to maximise separation in a multivariate space.[12] To validate the method, leave one patient out cross validation was performed which involved data from one patient sample being removed from the model, with this process repeated until all patient samples were left out once.

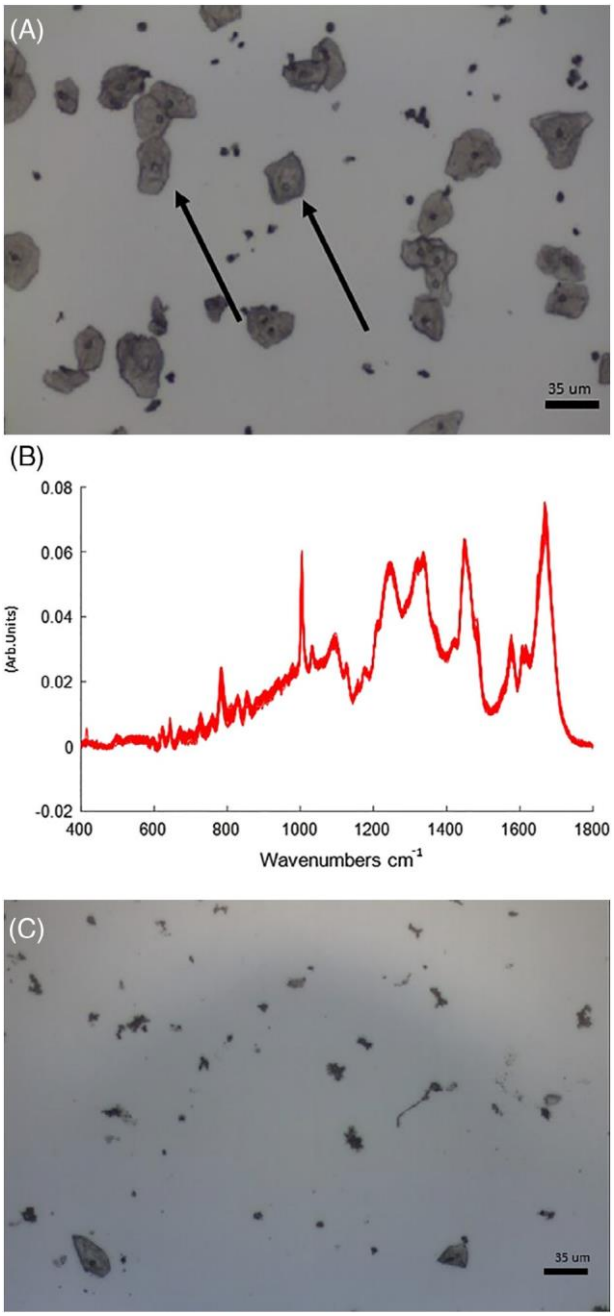

FIGURE 1 (A) LBC samples stored at −25ºC present with intact cellular morphology. Note the presence of superficial and intermediate cells on the unstained slide which were selected for Raman spectral recording. (B) High quality spectra recorded from morphologically normal intermediate and superficial cells in the spectral range 400-1800 cm^{-1}. (C) LBC samples stored at −80 ºC. Note lack of cellular material and presence of cellular debris

3 | RESULTS

3.1 | −25ºC vs −80ºC biobanked LBC samples

The samples stored at −25ºC presented with intact cellular morphology (Figure 1A) and allowed for high quality

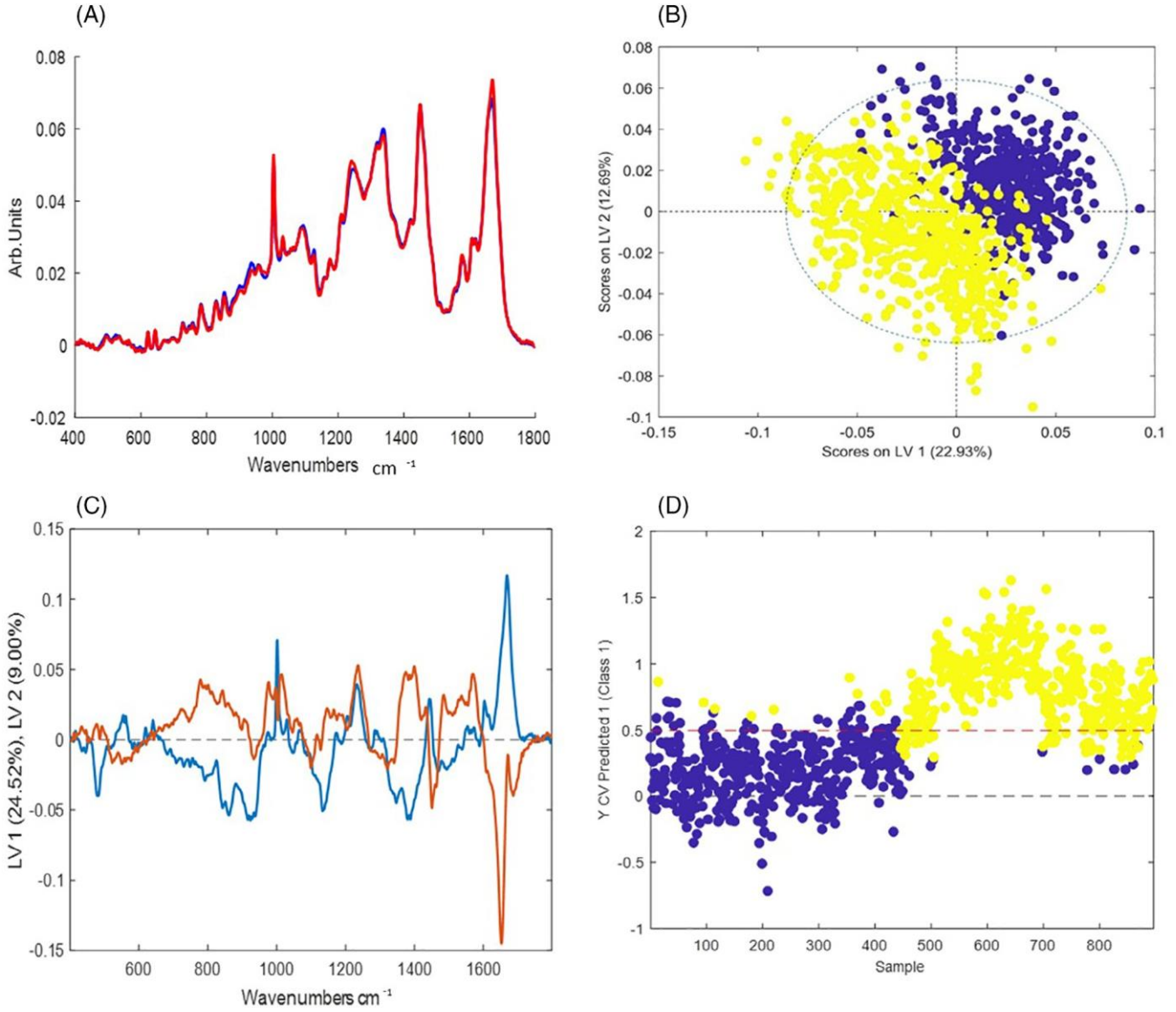

FIGURE 2 (A) mean spectra of fresh Negative (red) vs CIN 3 (blue). (B) is a latent variables (LV) scores scatter plot of LV1 and LV2, TN (yellow) vs CIN 3 (blue). (C) LV1(blue) and LV2 (orange) loadings (D) PLS_DA prediction plot CIN 3 (blue), negative (yellow)

spectra to be recorded (Figure 1B). The samples stored at −80ºC presented with cell lysis, cellular debris and very little cellular material which prevented the recording of spectra (Figure 1C). One possible explanation for this, is the freeze thaw effect which is commonly used to lyse bacteria and mammalian cells. Storing cells at −80ºC in PreservCyt without any Dimethyl Sulfoxide and bring up to room temperature can cause the cells to contract during the thawing process resulting in cell lysis. As a result, only biobanked samples previously stored at −25ºC were used for this study.

3.2 | Negative vs CIN 3 (fresh LBC samples) model

In order to determine if biobanked LBC samples could be used to discriminate no disease (cytology negative) from disease (CIN 3) using Raman spectroscopy, fresh (non biobanked) LBC samples were first examined as a control. Figure 2A shows mean spectra of Negative vs CIN 3. Figure 2B is a latent variables (LV) scores scatter plot of LV1 and LV2, which shows good discrimination along LV1 and LV2. The loadings shown in Figure 2C, show that the discrimination is based around Raman peaks at 484 (glycogen), 575 (glycogen), 881 (nucleic acids), 1004 (proteins Phenylalanine), 1139, 1238 (proteins Amide III), 1487 (proteins), 1575 (nucleic acids), 1605 (proteins) and 1669 cm^{-1} (proteins Amide I). The LV2 loadings show discrimination is based around 1238 (proteins), 1381 (glycogen), 1450 (proteins and lipids), 1642 (proteins) and 1669 cm^{-1} (proteins) (see Table 1)·[13] The PLS-DA prediction plot shown in Figure 2D and has a sensitivity of 86% and a specificity of 90% for CIN 3.

3.3 | Negative vs CIN 3 (Biobanked LBC samples) model

In order to determine if the biobanked samples can be used in a similar fashion to the fresh samples, negative and CIN

TABLE 1 Tentative peak assignments for Raman spectra of cells and tissues[13]

Raman peak position [cm^{-1}]	Proteins	Lipids	Carbohydrates	Nucleic acids
482			Glycogen	
577			Glycogen	
622	C—C twist Phe			
643	C—C twist Tyr			
727	CH2 def	C—C head		A
752	Sym br. Trp			
781				U,C,T ring br
826	Out of Plane ring br.Tyr			PO2 a.str.
851	Ring br. Tyr,C—C str. Pro			
852			Glycogen	
937			Glycogen	
985		C—C head		
1002	Sym. Ring br. Phe			
1033	C—H in plane Phe, C—C str.			
1044			Glycogen	
1060	C—N str.			
1082	C—N str.	Chain C—C str.	C—O str., Glycogen	
1096		Chain C—C str.	C—C str.	
1106			Glycogen	
1123	C—N str.	Chain C—C str.	C—O str.	
1152	C—N str.			
1207	C—C6H5 str. Phe, Trp			
1238	C—N str., Amide III			
1261			Glycogen	
1334			Glycogen	
1338	Trp			G
1366		Sym. str. CH3		
1381			Glycogen	
1450	CH2 def	CH2 def		
1458			Glycogen	
1487	CH2 def			G,A
1560	Tyr, Trp			
1575				A,G ring br
1584	C=C str., C=C bend. Trp, Phe			
1605	C=C Phe, Tyr			
1642	C=O str., C=C sym. str.			
1669	C=O str. Amide I			

3 biobanked samples were compared. Figure 3A shows the mean spectra of biobanked Negative samples vs CIN 3. Figure 3B is a latent variables (LV) scores scatter plot of LV1 and LV2 which shows good discrimination along LV1 and LV2. The loadings from LV1 are shown in Figure 3C and show that discrimination is based around Raman peaks, 622 (proteins), 640 (proteins),775 (proteins), 850 (proteins), 1122 (proteins), 1152 (proteins), 1207 (proteins), 1450 (proteins), 1560 (proteins), 1605 (proteins), 1642 (proteins) and 1669 cm^{-1} (proteins). LV2 loadings show discrimination is based on 1123 (proteins, lipids, carbohydrates), 1338 (proteins) and 1605 cm^{-1} (proteins) Raman peaks assigned to phenylalanine 1004 cm^{-1} show a slight shift between 1003 and 1004 cm^{-1} which is most likely attributed to the methanol based fixation method which suggests a change in the conformation of the phenylalanine protein.[14] The PLS-DA prediction plot shown in Figure 3D and has a sensitivity of 91% and a specificity of 92% for CIN 3.

3.4 | Biobanked vs non-Biobanked samples

Five fresh CIN 3 patient samples were split into two separate vials. One vial from each sample was frozen as described earlier and the other stored at room temperature. Figure 4A shows the mean spectra for biobanked CIN 3 samples and the same samples kept at room temperature for 3 weeks after collection. The mean spectra appear identical. There does not appear to be a difference between the fresh and

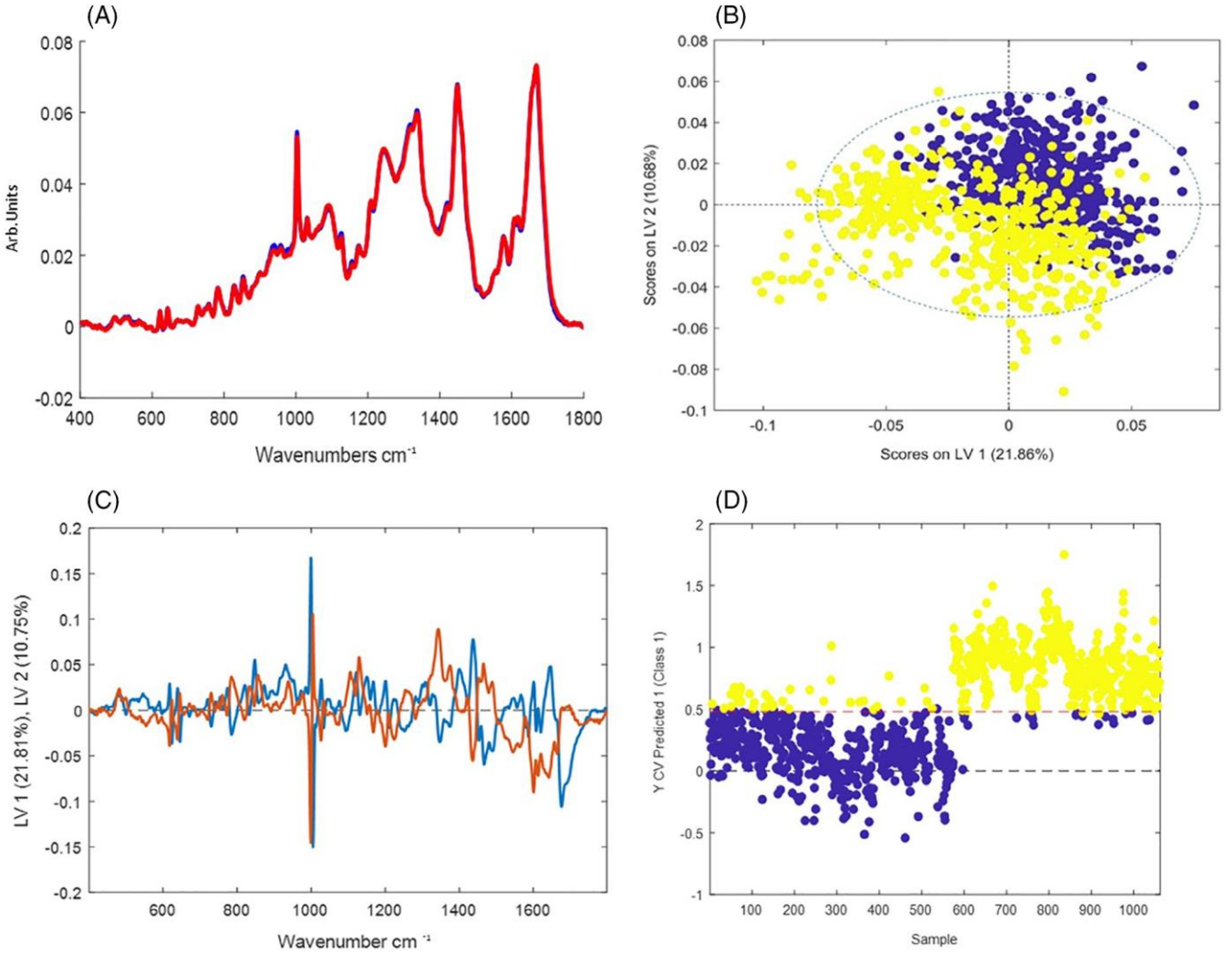

FIGURE 3 (A) mean spectra of biobanked Negative (red) vs CIN 3 (blue). (B) latent variables (LV) scores scatter plot of LV1 and LV2, TN (yellow) vs CIN 3 (blue). (C) LV1 (blue) LV2 (orange). (D) PLS_DA prediction plot CIN 3 (blue), negative (yellow)

biobanked samples. The latent variable scatter scores plot (Figure 4B) shows slight discrimination between the sample types, which is most likely due to internal sample variability [15] (LBC samples are variable by nature) and the low number of spectra recorded (60 for room temperature/biobanked). The PLS-DA prediction plot (Figure 4C) has a sensitivity of 29% and specificity of 88% for biobanked samples indicating poor discrimination between the two groups.

3.5 | Mixed model

In order to determine if we could mix fresh and biobanked samples together and still achieve a sensitivity and specificity similar to the fresh and biobanked models, 15 biobanked CIN 3 samples were mixed with 15 fresh CIN 3 samples and compared with 15 negative biobanked/ 15 fresh negative samples. Figure 5A shows the latent variable scatter scores plot of the model and we can see clear discrimination between the sample types across LV1 and LV2. The LV1 loadings (Figure 5B) show that discrimination is based on 482, (glycogen), 1443 (proteins, lipids) 1487 (proteins), 1605 (proteins) 1669 cm^{-1} (proteins) while LV2 shows the discrimination is based around 486 (glycogen), 851 (proteins), 1152 (proteins), 1381 (glycogen), 1450 (proteins/lipids), 1575 (nucleic acids) and 1669 cm^{-1} (proteins). The loadings show similarities to both the fresh and biobanked loadings, but overall show that glycogen and proteins are the main discriminating factor between negative and CIN 3 samples. PLS-DA prediction plot has a sensitivity of 94% and a specificity of 95% for CIN 3 (Figure 5C).

4 | DISCUSSION

From the results it is clear that samples biobanked at −80°C are not suitable for screening using Raman spectroscopy due to a lack of cellular material and the presence of cellular debris.

Spectral differences between fresh negative and CIN 3 samples were observed with regards to glycogen, nucleic acids and proteins. CIN 3 cells often contain little to no glycogen, hence the use of Lugol's solution to visualise abnormal cells in colposcopy [16] The discrimination associated

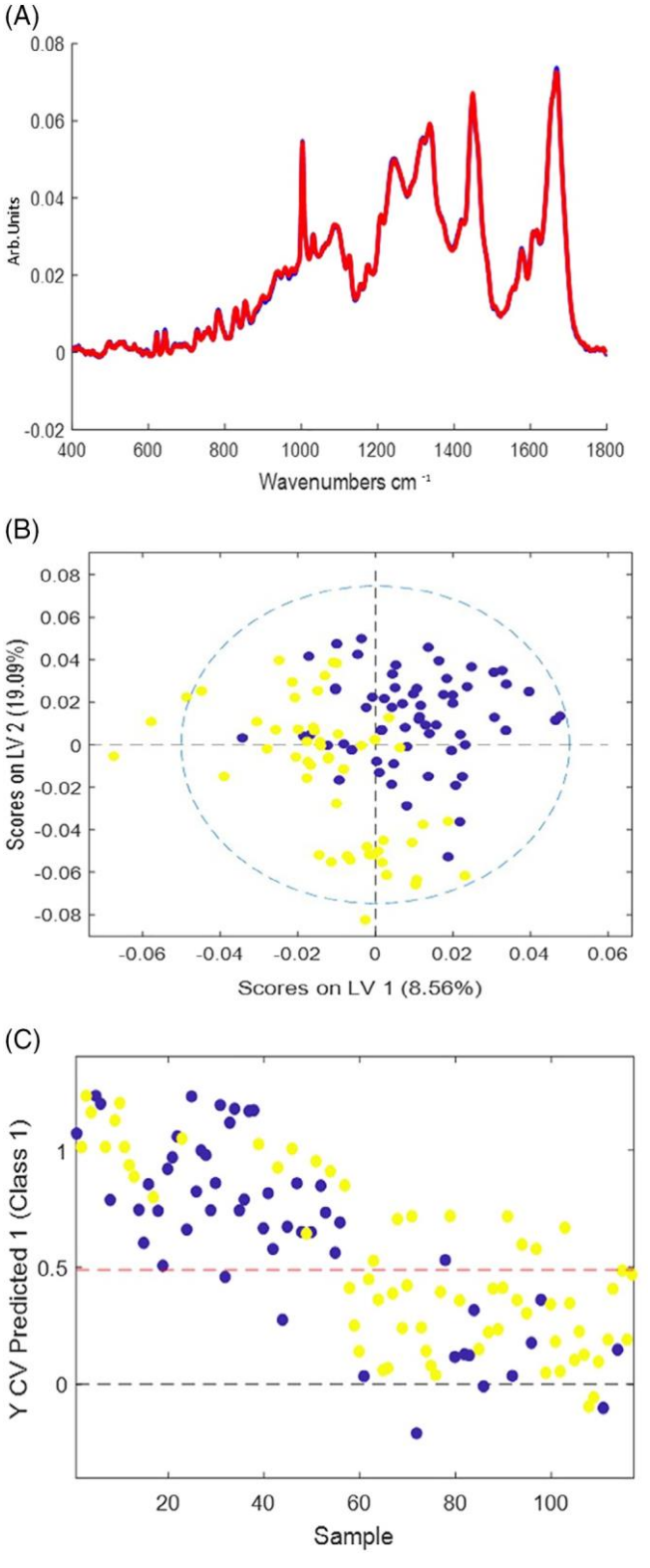

FIGURE 4 (A) mean spectra of fresh CIN 3 (blue) vs biobanked CIN 3 (red). (B) latent variables (LV) scores scatter plot of LV1 and LV2, fresh CIN 3 (yellow) vs biobanked CIN 3.(C) PLS-DA prediction plot biobanked CIN 3 (blue) vs fresh CIN 3 (yellow)

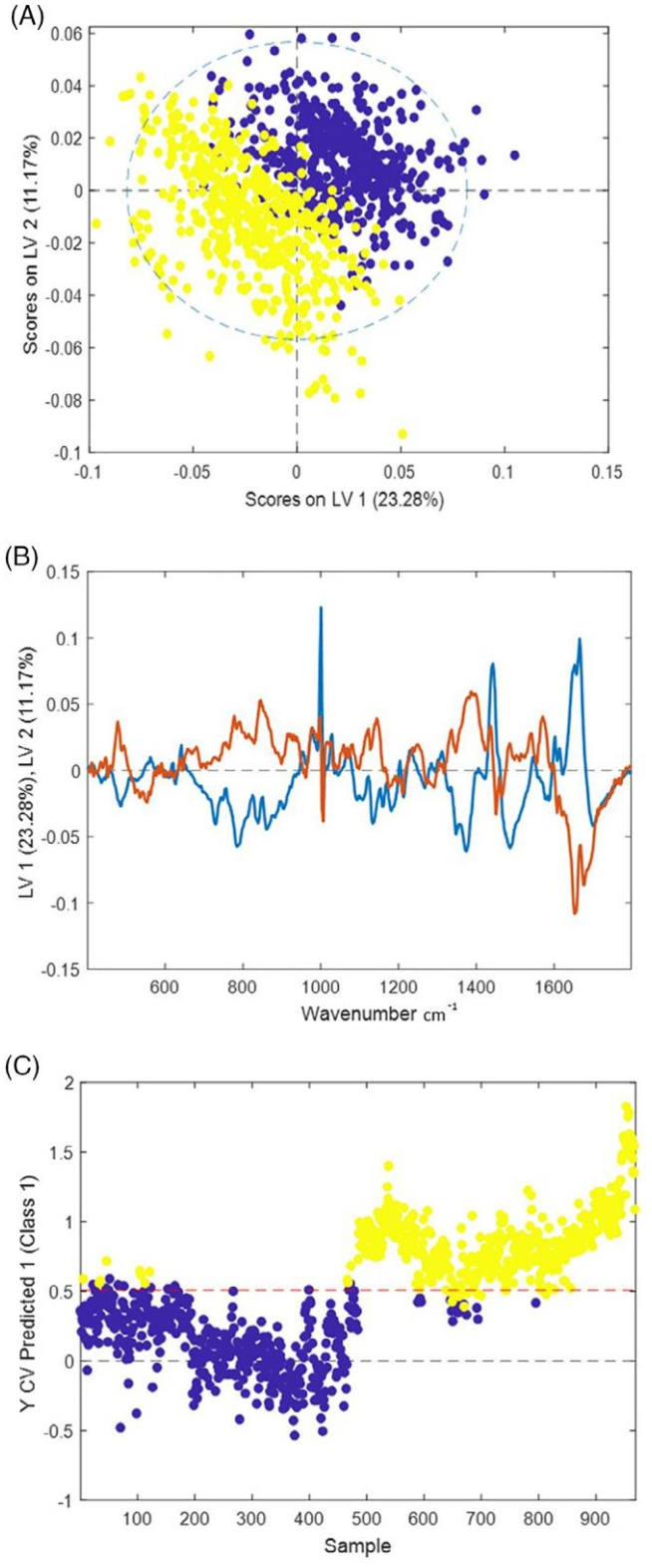

FIGURE 5 (A) latent variables (LV) scores scatter plot of LV1 and LV2, TN (yellow) vs CIN 3 (blue). (B) LV1 loadings (blue) and LV2 loadings (orange). (C) PLS-DA prediction plot CIN 3 (blue), negative (yellow)

with changes in proteins and DNA is consistent with the neoplastic changes that occur in CIN 3 supported by persistent HPV infection such as increased cell cycling with coincident increase in replication and levels of nucleic acids[15] The PLS-DA prediction plot gives a sensitivity of 86% and a specificity of 90% for CIN 3.

Negative vs CIN 3 biobanked sample results showed that discrimination was driven solely by proteins. Raman peaks associated with nucleic acids/DNA are not as strongly

present as they are in the non-biobanked samples. Long term storage of biobanked samples is likely to have led at least to an element of nucleic acids degradation which would explain why nucleic acid is not discriminatory between neg- ative and CIN 3 samples. However the PLS-DA prediction plot (Figure 3D) does show slightly higher sensitivity (91%) and specificity (92%) rates when compared to fresh samples (86% sensitivity and 90% specificity) indicating that biobanking at −20ºC does not preclude discrimination of negative and CIN 3 samples on Raman spectroscopy.

The same patient samples that had been split in two with half biobanked and the other half stored at room temperature showed no discrimination between the samples. Hence, the 3 weeks period of biobanking at −20ºC had no detrimental effects on the physical or biochemical properties of the samples. The mixed model showed that biobanked and fresh LBC samples could be combined with an improved sensitivity of 94% and specificity of 95%. A limitation of this study is the inability to use biobanked LBC samples stored at −80ºC for Raman spectroscopic analysis as most biobanks will have samples stored at -80 ºC for long term storage[3] hence, the true potential of using biobanks as a source of patient samples could be lost. Further research in this area should involve the use of different biobank specimens (bronchial and thyroid fine needle aspirations) to investigate any detrimental effects the biobanking process may have on cytological specimens[17 18].

5 | CONCLUSION

Raman spectroscopy can effectively discriminate disease free cervical LBC samples from those with disease (CIN 3) and this is possible using biobank cervical LBC samples stored at −25ºC. Pooling samples stored at −25ºC with fresh samples does not affect the sensitivity and specificity of Raman spectroscopy for the discrimination of disease. This study demonstrates that biobanks of cervical LBC samples are a useful resource for future Raman spectroscopy studies and will facilitate the further assessment of this technology which shows highly encouraging performance for the detection of cervical disease.

ORCID

Damien Traynor https://orcid.org/0000-0001-6531-6653

REFERENCES

[1] J. M. Fox, R. C. Wiggins, J. W. J. Moore, C. Brewer, B. Hunter, A. C. Andrew, F. Martin, *Cryobiology* 2017, *77*, 14. https://doi.org/10.1016/j.cryobiol.2017.06.004.
[2] L. A. Marquez-Curtis, L. E. McGann, J. A. W. Elliott, *Cryobiology* 2017, *77*, 1. https://doi.org/10.1016/j.cryobiol.2017.04.012.
[3] T. Peakman, P. Elliott, *Genome Med.* 2010, *2*(10), 2. https://doi.org/10.1186/gm193.
[4] L. A. Torre, F. Bray, R. L. Siegel, J. Ferlay, J. Lortet-Tieulent, A. Jemal, *CA: A Can J Clin* 2015, *65*(2), 87. https://doi.org/10.3322/caac.21262.
[5] N. W. Troiano, W. A. Ciovacco, M. A. Kacena, *J Histotechnol* 2009, *32* (1), 27. https://doi.org/10.1179/his.2009.32.1.27.
[6] H. C. Kitchener, R. Blanks, G. Dunn, L. Gunn, M. Desai, R. Albrow, J. Mather, D. N. Rana, H. Cubie, C. Moore, R. Legood, A. Gray, S. Moss, *Lancet Oncol* 2011, *12*(1), 56. https://doi.org/10.1016/S1470-2045(10)70264-3.
[7] G. Ronco, P. Giorgi-Rossi, F. Carozzi, M. Confortini, P. Dalla Palma, A. del Mistro, B. Ghiringhello, S. Girlando, A. Gillio-Tos, L. de Marco, C. Naldoni, P. Pierotti, R. Rizzolo, P. Schincaglia, M. Zorzi, M. Zappa, N. Segnan, J. Cuzick, New Technologies for Cervical Cancer screening (NTCC) Working Group, *Lancet Oncol.* 2010, *11*(3), 249. https://doi.org/10.1016/S1470-2045(09)70360-2.
[8] F. Lyng, D. Traynor, *Anal. Bioanal. Chem.* 2015, *407*(27), 8279.
[9] I. R. Ramos, A. D. Meade, O. Ibrahim, H. J. Byrne, M. McMenamin, M. McKenna, A. Malkin, F. M. Lyng, *Faraday Discuss* 2016, *187*, 187. https://doi.org/10.1039/C5FD00197H.
[10] S. Rubina, C. M. Krishna, *J. Cancer Res. Ther.* 2015, *11*(1), 10.
[11] I. P. Santos, E. M. Barroso, *Analyst* 2017, *142*, 3025.
[12] R. G. Brereton, G. R. Lloyd, *J. Chemometr.* 2014, *28*(4), 213. https://doi.org/10.1002/cem.2609.
[13] Z. Movasaghi, S. Rehman, I. U. Rehman, *Appl Spectrosc Rev* 2007, *42*, 493.
[14] A. Meade, *Bioanal Chem* 2010, *369*(5), 1781. https://doi.org/10.1007/s00216-009-3411-7.
[15] I. Serafín-Higuera, O. L. Garibay-Cerdenares, B. Illades-Aguiar, E. Flores-Alfaro, M. A. Jiménez-López, P. Sierra-Martínez, L. D. C. Alarcón-Romero, *Proteome Sci* 2016, *14*(1), 1. https://doi.org/10.1186/ s12953-016-0099-4.
[16] CervicalCheck. *Organisational and Clinical Guidance for Quality Assured Colposcopy Services*, CervicalCheck - The National Cervical Screening Programme, Dublin 1, 2013.
[17] M. A. Al-Abbadi, *Avicenna J Med.* 2011, *1*(1), 18.
[18] D. O'Dea, M. Bongiovanni, G. P. Sykiotis, P. G. Ziros, A. D. Meade, F. M. Lyng, A. Malkin, *Cytopathology* 2018, *30*, 51-60. https://doi.org/10.1111/cyt.12636.

How to cite this article: Traynor D, Duraipandian S, Bhatia R, et al. The potential of biobanked liquid based cytology samples for cervical cancer screening using Raman spectroscopy. *J. Biophotonics*. 2019;12: e201800377. https://doi.org/10.1002/jbio.201800377